New tools for anaerobic bacteria: metabolically engineered strains to improve energy supply, recombinant production of value-added products, and fluorescent reporter proteins

Dissertation

Submitted for the fulfillment of the requirements for the doctoral degree

Dr. rer. nat. at the Faculty of Natural Sciences,

University of Ulm

Maximilian Flaiz

from Hechingen

Ulm, 2022

The presented study was performed at the Institute of Microbiology and Biotechnology, University of Ulm, under the direction of Prof. Dr. Peter Dürre. Parts of this study were funded by the European Research Area Cofund on BioTechnologies (ERACoBioTech) within the 1st Joint Call (project BIOMETCHEM, grant 161B0609A).

Dean: Prof. Dr. Thorsten Bernhardt

1st Reviewer: Prof. Dr. Peter Dürre

2nd Reviewer: apl. Prof. Dr. Christian Riedel

Graduation date: 17.05.2022

Contents

Abstract **1**

1. Introduction **2**

1.1 Anaerobic bacteria are potent biocatalysts 2

1.2 Metabolism of various C1 carbon sources 4

1.3 Natural production of value-added biochemicals 7

1.4 Anaerobic production of hexanoate 9

1.5 Metabolic engineering of anaerobes 10

1.6 Fluorescent reporter proteins for the use in anaerobic bacteria 12

1.6.1 Oxygen-dependent fluorescent reporter proteins in *Clostridium* spp. 12

1.6.2 Flavin mononucleotide-based fluorescent proteins 13

1.6.3 Ligand-dependent self-labeling fluorescent proteins 14

1.6.4 The fluorescence-activating and absorption-shifting tag 15

1.7 Aims of this thesis 18

2. Results & Discussion **19**

2.1 Induced heterologous expression of the arginine deiminase pathway promotes growth advantages in the strict anaerobe *Acetobacterium woodii*. 19

2.2 Production of the biocommodities butanol and acetone from methanol with fluorescent FAST-tagged proteins using metabolically engineered strains of *Eubacterium limosum*. 33

2.3 Establishment of green- and red-fluorescent reporter proteins based on the fluorescence-activating and absorption-shifting tag for use in acetogenic and solventogenic anaerobes 54

2.4 *Caproicibacter fermentans* gen. nov., sp. nov., a new caproate-producing bacterium and emended description of the genus *Caproiciproducens.* 70

3. Summary **82**

4. Literature **88**

5. Abbreviations **104**

6. Publications **108**

6.1 Chronological list of publications 108

6.2 Personal contribution to the scientific publications 108

6.3 Scientific contributions on conferences 109

7. Appendix **111**

7.1 Acknowledgements 111

7.2 Curriculum vitae 112

7.3 Declaration of independent scientific work 113

Abstract

Anaerobic bacteria are promising biocatalysts for producing industrially relevant high-value chemicals from various non-food feedstocks. While solventogenic clostridia are excellent alcohol producers, acetogenic bacteria have the distinction of being able to utilize C1 carbon sources and can thus help reduce greenhouse gas emissions. While several anaerobes are genetically accessible, various genetic tools are not yet established. In this work, new molecular tools for anaerobes are presented. This includes the establishment of heterologous pathways to provide additional ATP and to produce the biocommodities butanol and acetone. Genes of the arginine deiminase pathway were heterologously expressed in *Acetobacterium woodii* to overcome energetic limitations during autotrophic growth since the conversion of arginine to ornithine, ammonia, and CO_2 provides ATP and finally boosts growth of recombinant *A. woodii* strains. The enhanced energy supply by the arginine deiminase pathway opens the door for the establishment of new recombinant pathways that require huge amounts of ATP. In addition, the application of the fluorescence-activating and absorption-shifting tag (FAST) as oxygen-independent fluorescent reporter protein further extended the molecular toolbox of anaerobes. As it turned out, FAST is perfectly suited for the construction of fluorescent FAST-tagged fusion proteins without negatively affecting the stability and functionality of the native enzyme. Both, the bifunctional aldehyde/alcohol dehydrogenase AdhE2 and the acetoacetate decarboxylase Adc from *C. acetobutylicum* were FAST-tagged and respective genes expressed in *Eubacterium limosum*. As a result, recombinant *E. limosum* strains produced 0.6 mM butanol and 1.6 mM acetone from the fluid C1 carbon source methanol, while production of FAST-tagged fusion proteins was tracked regarding fluorescence intensity during growth. In addition, the orthogonal green and red fluorescence of mutated FAST versions, greenFAST and redFAST, were evaluated and used for multicolor approaches under anaerobic conditions. Hence, the co-existence and dynamics in an anaerobic microbial co-culture consisting of two engineered *C. saccharoperbutylacetonicum* strains producing respective fluorescent proteins were monitored. Moreover, a tightly regulated inducible two-plasmid system based on the *tcdR*-P_{tcdB} promoter system of *C. difficile* was constructed. The orthogonal green and red fluorescence of greenFAST and redFAST was used to confirm the co-existence of both plasmids in *C. saccharoperbutylacetonicum* during growth at single-cell level.

1. Introduction

1.1 Anaerobic bacteria are potent biocatalysts

The reduction of greenhouse gas emissions to overcome the imminent climate change is one of the most important and simultaneously most challenging tasks that we all must face in the near future. In order to reach the goals of the Paris Agreement, which was adopted by the United Nations to limit global warming below 2 °C, and to become a net-zero emissions world until 2050, two major attempts must be made.[1,2] First, alternative processes must be developed to reduce greenhouse gas emissions, and secondly, greenhouse gases must be directly removed from the atmosphere by carbon capture technologies. To achieve these goals the use of anaerobic bacteria, especially those of the class Clostridia, is of great interest as they can convert renewable non-food carbon sources and greenhouse gases into bulk and value-added chemicals.[3,4]

Especially solventogenic and acetogenic clostridia are industrially relevant and intensively studied. Solventogenic clostridia are Gram-positive, strictly anaerobic, and spore-forming bacteria that can naturally produce biofuels such as butanol via anaerobic acetone-butanol-ethanol (ABE) fermentation.[5] All solventogenic clostridia, short solventogens, are closely related, however, can be separated into two distinct phylogenic clades (Figure 1).[6] The first clade comprises e.g. *Clostridium acetobutylicum* and *C. pasteurianum*, while the second clade includes *C. beijerinckii*, *C. saccharobutylicum,* and *C. saccharoperbutylacetonicum.* Genes for butyryl-CoA synthesis, which is the precursor of butyrate, are clustered in the butyryl-CoA synthesis (*bcs*) operon in both clades and consists of *crt*, *bcd*, *etfA/B*, and *hbd* (encoding crotonase, butyryl-CoA dehydrogenase, electron transfer flavoproteins A and B, and 3-hydroxybutyryl-CoA dehydrogenase, respectively).[7] Compared to that, the genes of the *sol* operon which are required for solvent formation, including acetone and butanol, are different within clades I and II.[6,8] In the first clade, the genes *adhE* and *ctfA/B* (encoding a bifunctional butyraldehyde/butanol dehydrogenase and acetoacetyl-CoA:acetate/butyrate-CoA transferase, respectively) are organized in the type I *sol* operon with *adc* (encoding acetoacetate decarboxylase) forming a reverse monocistronic operon. Compared to that the *sol* type II operon in solventogens of the second clade consists of *ald/bld* (encoding an NADH-dependent aldehyde dehydrogenase or butyraldehyde dehydrogenase, respectively), *ctfA/B*, and *adc*.[6,8,9] Both, acetone and butanol production via anaerobic ABE fermentation was industrially performed until the mid-1950s.[10] However, the biological synthesis from molasses

is quite expensive and the product concentration achieved was relatively low.[11] Recently, interest for acetone and butanol production via ABE fermentation has seen a new upsurge, since metabolic engineering approaches enhanced solvent production, improved substrate utilization, and robustness of cells, but most importantly solventogens can utilize non-food feedstocks including lignocellulosic biomass.[12–14] Nevertheless, fermentation using lignocellulosic biomass also faces some challenges since pretreatment is complicated, expensive, and energy-consuming.[15,16] While solventogens can make a valuable contribution for the sustainable production of bulk chemicals independent of fossil resources by applying anaerobic fermentation, acetogenic bacteria can be used for direct carbon fixation from the atmosphere.

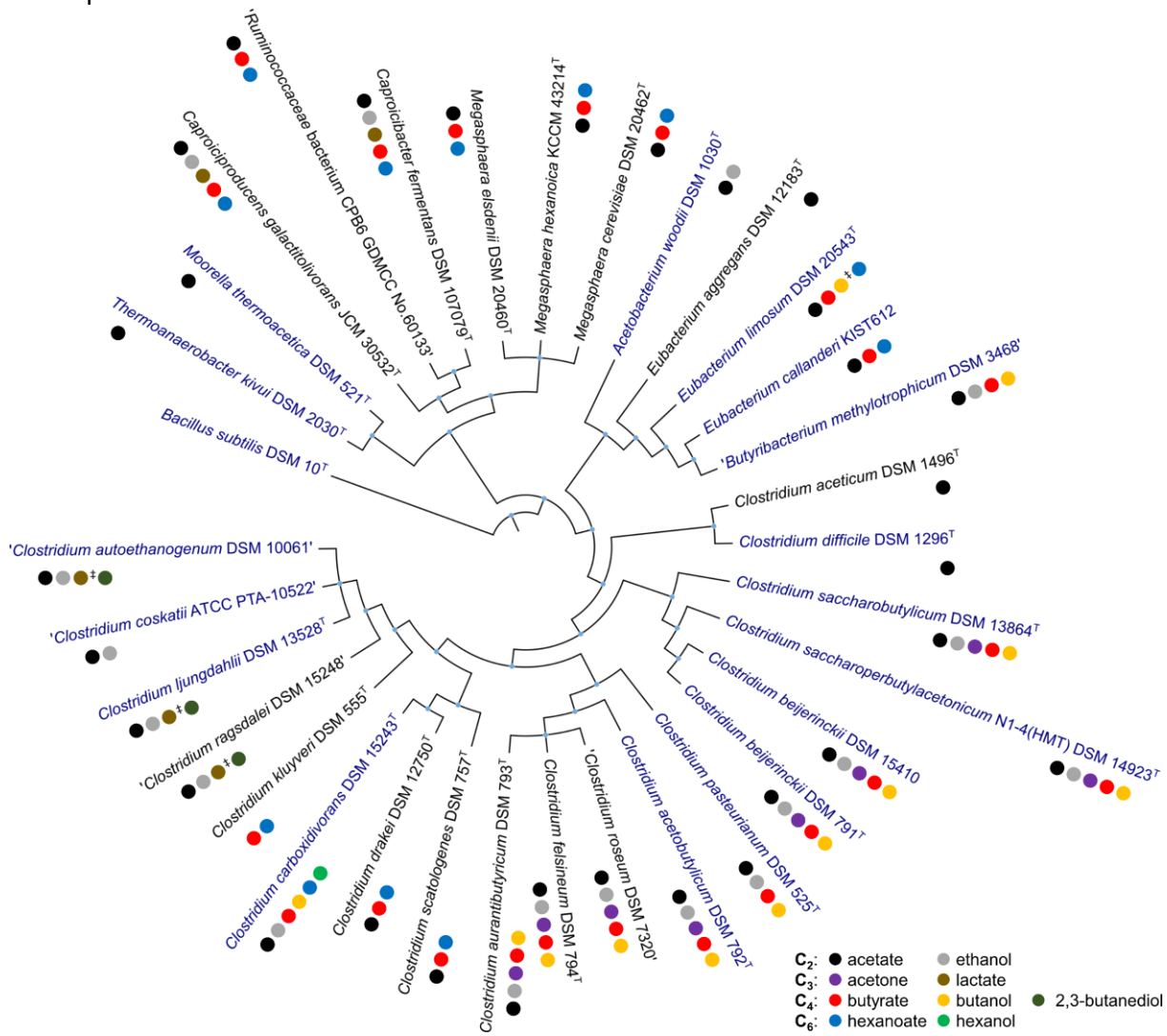

Figure 1: Phylogenetic arrangement of anaerobic bacteria relevant for this thesis based on their 16S rRNA sequence from the National Center for Biotechnology Information (NCBI, Bethesda, MD, US) database. The phylogenetic tree was rooted to *B. subtilis* DSM 10^T. Not validly described strains are marked by quotation marks. Strains that are reported to be genetically accessible are highlighted in blue. Colored dots indicate metabolic end products described in literature. Products marked with ‡ are reported to be produced in traces.[6,17–32]

Acetogenic bacteria, short acetogens, are capable of assimilating several C1 carbon sources, including industrial waste gases in form of so-called synthesis gas (syngas), carbon dioxide (CO_2), or carbon monoxide (CO), as well as methanol or formate using the Wood-Ljungdahl pathway (WLP) for energy conservation and production of the central intermediate acetyl-CoA.[33] The genera of acetogens are quite diverse including not only *Clostridium* but also *Acetobacterium*, *Eubacterium*, or *Morella* just to mention a few (Figure 1).[34] The majority of the as of yet 61 identified acetogens produce acetate as the sole metabolic end product.[17] However, an increasing number of natural products, starting from the central intermediate acetyl-CoA, including further acids but also alcohols are described in literature to be produced by various acetogens from C1 carbon sources (Figure 1).[17] Their ability to grow chemolithoautotrophically makes them perfect candidates as biocatalysts to produce several products from industrial waste gases.[35] Especially syngas is a promising substrate for acetogens since it is rich in H_2, CO_2, and CO and a steel mill off-gas, which accounts for 11 % of the total CO_2 and 7 % greenhouse gas emissions worldwide.[36] In 2018, the company LanzaTech commercialized gas fermentation in the so-called LanzaTech process.[37] They make use of acetogens to capture and re-use steel mill off-gas in form of syngas to produce fuels and chemicals and directly contribute to reducing greenhouse gas emissions.[38,39] The first reactor operates in China and produces ethanol while further plants are under construction and additional natural and recombinant products are aimed to being produced.[40,41]

1.2 Metabolism of various C1 carbon sources

The WLP is one of seven known pathways, which directly fixes CO_2 to produce biomass and ATP, and is considered to be one of the oldest known biochemical pathways.[42,43] It can be separated into two branches: the methyl and the carbonyl branch. Briefly, in the methyl branch, CO_2 is reduced to formate and bound to tetrahydrofolate (THF), which requires ATP and results in formyl-THF. This intermediate is further converted to methenyl-THF, methylene-THF, and methyl-THF. The methyl group of methyl-THF is transferred to a corrinoid iron-sulfur protein (CoFeSP) catalyzed by a methyltransferase. In the carbonyl branch, CO_2 is reduced to CO and coupled together with CoA to the methyl group of methyl-CoFeSP via CO dehydrogenase/acetyl-CoA synthase (CODH/ACS), resulting in the central intermediate acetyl-CoA. Acetyl-CoA can then be used for anabolism reactions or converted to acetyl-phosphate and acetate catalyzed by phosphotransacetylase (Pta) and acetate kinase (Ack), respectively, yielding 1 mol ATP.[44] Since the production of 1 mol acetate from two mol CO_2 requires 1 mol

ATP while only yielding 1 mol ATP, there is no net gain of ATP via the WLP[33]. However, the WLP is directly coupled to energy conservation, which is quite diverse within the different acetogenic genera.[45] A membrane integral ion-translocating protein complex (*Rhodobacter* nitrogen fixation (Rnf)- or energy-converting hydrogenase (Ech)-complex), which uses ferredoxin as the electron donor, can pump H^+ or Na^+ ions out of the cell and form a chemiosmotic gradient.[45] This gradient is then used to channel H^+ or Na^+ back into the cell by an ATPase to generate ATP. In addition, electron-bifurcating hydrogenases use electrons of H_2 yielding Fd^{2-} and NADH or NADPH. Nowadays, acetogens can be divided into those having an Rnf- or Ech-complex and regarding the ions that are used to drive the ATPase.[45] In summary, the WLP yields 0.3 mol ATP in case H_2 is used as electron donor or 1.5 mol ATP when CO is used as electron donor for each mol acetate produced.[46] Since the overall ATP gain from C1 gases is quite low, it is often stated that acetogens live at the thermodynamic limit of life.[45] This energetic limitation can complicate metabolic engineering approaches especially when synthetic pathways for heterologous production are strived to implement in which huge amounts of ATP are required.[47] Therefore, alternative ATP-generating pathways and substrates that benefit growth need to be explored. Recently, two promising strategies were examined to enhance ATP supply in acetogens including the supplementation of arginine or nitrate.[48,49] Arginine can be utilized via the arginine-deiminase (ADI) pathway, which is well described and widespread among anaerobes.[50,51] Enzymes necessary for arginine degradation include the arginine deiminase (ADI, encoded by *arcA*), which deiminates arginine and yields citrulline and ammonium, the ornithine transcarbamoylase (OTC, encoded by *arcB*) catalyzing the reaction of citrulline into ornithine and carbamoyl-phosphate, and the carbamate kinase (CK, encoded by *arcC*), which hydrolyses carbamoyl-phosphate yielding a further molecule of ammonium and CO_2 while the phosphate group is used to phosphorylate ADP to generate ATP.[52] In addition, the arginine:ornithine antiporter (ArcD) is capable of energetically independent take up arginine while exporting ornithine produced by OTC.[53] The genes encoding the ADI pathway are present and form an operon in *C. autoethanogenum* and it was already shown that cultivation of *C. autoethanogenum* using arginine as nitrogen source resulted in a growth boost and higher ATP yields.[48] Even though genes of the ADI pathway are present in the genome of other acetogens such as *A. woodii* and *E. limosum*, the genes are not clustered and *arcD* is not even annotated. Therefore, metabolic engineering approaches are essential to make use of the energy-providing ADI pathway in these acetogens.

A further attempt to overcome energetic barriers is the use of alternative non-gaseous C1 carbon sources. The process of gas fermentation in general faces some challenges since the mass transfer of gases into the liquid phase is quite poor, and therefore, limits microbial productivity.[54] One alternative to the C1 gases is the use of methanol. Methanol is liquid, completely soluble in water, and easy to store and transport.[55] The industrial and catalytic production of methanol started in 1923 by Mathias Pier at Badische Anilin- & Sodafabrik (BASF, Ludwigshafen am Rhein, Germany). The BASF-process used CO-, CO_2-, and H_2-containing syngas and operated at 300 atm and 300 – 400 °C using a zinc chromite catalyst.[56] Over the years, the methanol production process was improved by operating at lower pressure using the Imperial Chemical Industries (ICI, London, England, UK) process and development of new catalysts, which were highly selective for methanol synthesis.[56] Today, approximately 110 million tons of methanol are produced worldwide every year, of which most are produced from syngas-derived fossil resources such as natural gas and coal.[57,58] Renewable production of methanol from biomass, biogas or waste stream-stemming syngas is with 0.2 million tons per year rather low, however, would make it a sustainable carbon and energy source.[59] Several acetogens can metabolize methanol via the WLP such as *A. woodii*, *Butyribacterium methylotrophicum, E. limosum*, or *Morella thermoacetica*.[60–63] Methanol enters the WLP as methyl-THF in a reaction catalyzed by the methanol:THF-methyltransferase system (MtaABC), which consists of three proteins.[64,65] The first methyltransferase (MtaB) transfers the methyl group of methanol to the corrinoid cofactor of MtaC (a corrinoid protein (CoP)), which serves as the intermediate methyl group acceptor. The second methyltransferase (MtaA) transfers the methyl group bound to MtaC to the methyl acceptor THF.[66,67] Methyl-THF is then further oxidized to CO_2 in the reverse direction of the methyl-branch of the WLP, yielding six reducing equivalents used to reduce CO_2 to CO in the carbonyl-branch and 1 mol ATP.[68] Therefore, the conversion of methanol also requires CO_2 as electron acceptor. As described above, the methyl group of methyl-THF is transferred to CoFeSP, finally condensed with CO and CoA, catalyzed by CODH/ACS, and results in acetyl-CoA. Overall, 4 mol methanol and 2 mol CO_2 are necessary to produce 3 mol acetate. In case of *A. woodii* and *E. limosum*, methanol utilization via the WLP yields 0.83 mol ATP for each mol acetate produced and is, therefore, more efficient than cultivation with H_2 + CO_2.[67,68] In general, the utilization of methanol outperforms other C1 carbon sources, especially C1 gases, regarding energetic efficiencies.[69,70]

1.3 Natural production of value-added biochemicals

As mentioned before, acetogens can produce a variety of products from C1 carbon sources. While *A. woodii* mainly produces acetate as metabolic end product, *E. limosum* is a potent, well-known butyrate producer, especially when cultivated using methanol as a carbon source (Figures 1 and 2).[62,71] Butyrate production with *E. limosum* starts from the central WLP intermediate acetyl-CoA and is comparable to butyrate formation of solventogens, e.g. *C. acetobutylicum* (Figure 2). The genes *thl* (encoding thiolase), *hbd*, *crt*, *bcd*, and *etfA/B* form an operon in *E. limosum*, which apart from *thl*, are also part of the *bcs* operon in solventogens.[72] Therefore, respective gene products catalyze the reaction of two molecules of acetyl-CoA to butyryl-CoA. The two reactions catalyzed by Hbd and Crt are both NAD(P)H-dependent, whose supply is limited when cultivated on H_2 + CO_2 and consequently results in low or even no butyrate production.[72–74] However, since the oxidation of the methyl group during methanol cultivation yields NAD(P)H, the ratio of acetate:butyrate production shifts in favor of butyrate, which in consequence regenerates $NAD(P)^+$.[75,76] In solventogens, the formation of butyrate from butyryl-CoA is catalyzed by the enzymes phosphotransbutyrylase (Ptb) and butyrate kinase (Buk) yielding ATP (Figure 2). The genome of *E. limosum* encodes two genes coding for Ptb (Ga0213646_11734 and Ga0213646_111765). However, there is no gene annotated coding for Buk.[77,78] On the other hand, the activity of potential acetate/butyrate kinases was determined in cell-free extract of *E. limosum*, indicating that Ptb/Buk is also involved in butyrate production in *E. limosum*.[79] Overall, the formation of butyrate from methanol results in 1.5 or 2 mol ATP/butyrate, which depends on whether the methylene-THF reductase of the WLP is electron-bifurcating or not, respectively.[80] Natural butyrate production is also described for other acetogens harboring genes of the *bcs* operon in varying versions, including *B. methylotrophicum, E. aggregans, C. scatologenes, C. carboxidivorans,* and *C. drakei*.[60,81–83] *C. carboxidivorans* and CO-adapted strains of *B. methylotrophicum* can convert butyrate further to the corresponding alcohol butanol naturally (Figures 1 and 2).[84–86] Recently, native butanol production was also observed for *E. limosum* cells cultivated with methanol and formate as carbon source.[22] Albeit, just traces of butanol were produced, which might be due to an overflow metabolism similar to 2,3-butanediol production known for *C. ljungdahlii*, *C. autoethanogenum,* and *C. ragsdalei*.[22,87] Butanol is a bulk chemical and precursor from acrylate and methyl acrylate esters, which are widely used in several industrial branches. More importantly, butanol,

especially bio-based butanol, can be blended into gasoline and is, when compared to ethanol, less corrosive, has a lower vapor pressure, and a higher energy content.[11] However, compared to the industrially well-established ABE fermentation of solventogens, commercial butanol production with acetogens from C1 carbon sources was not achieved yet.[5] Besides butanol, several acetogens such as *C. ljungdahlii*, *C. autoethanogenum*, *C. ragsdalei, C. carboxidivorans, C. drakei, C. coskatii,* and *C. scatologenes* can naturally produce ethanol from C1 gases (Figure 2).[88,89] This natural alcohol production by acetogens most likely depends on the action of an aldehyde:ferredoxin oxidoreductase (Aor), since this enzyme regenerates ferredoxin needed in the WLP and therefore also maintains redox balance.[90–92] Even though different acetogens show a broad range of industrially relevant products, the product titers

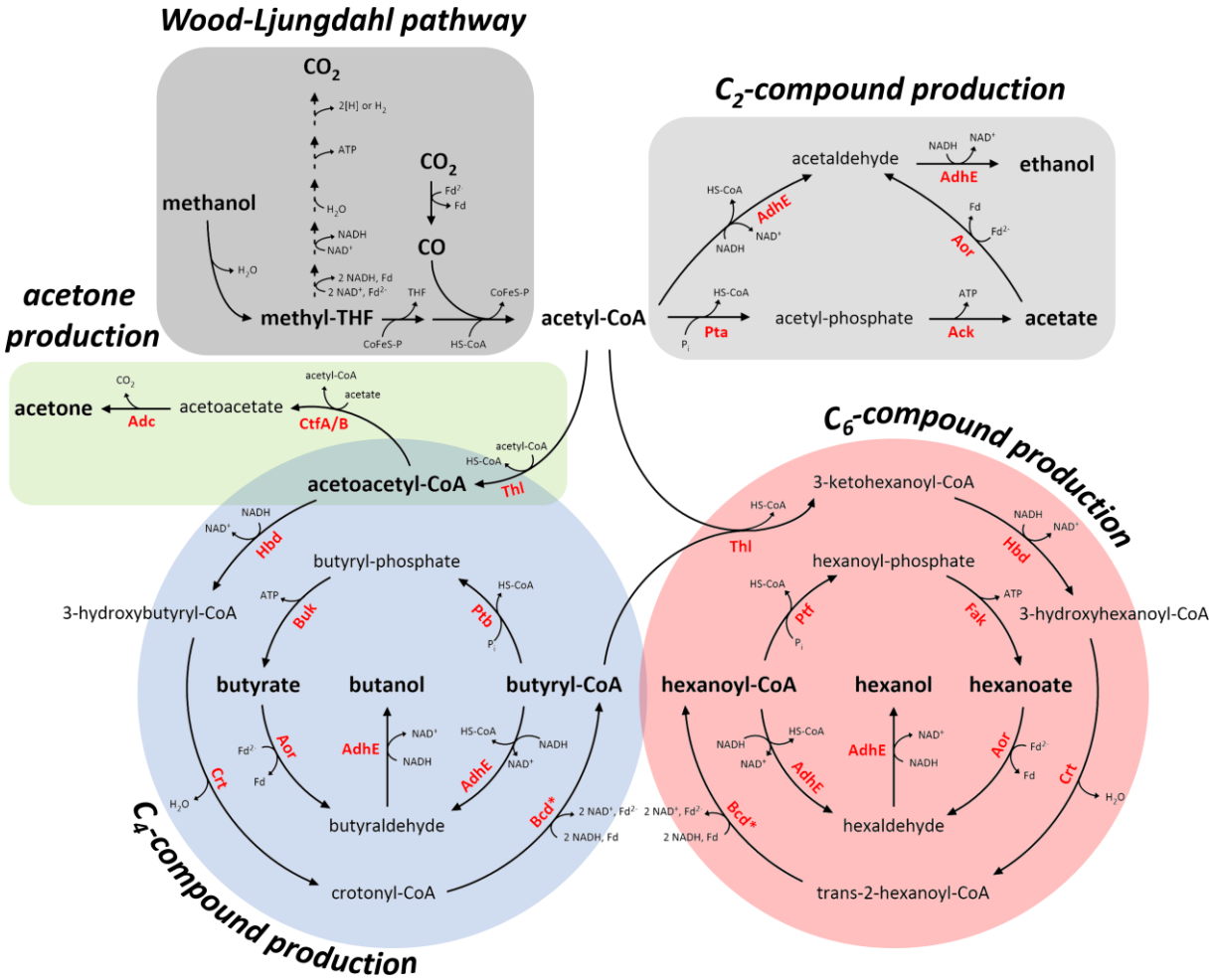

Figure 2: Schematic overview of the Wood-Ljungdahl-pathway coupled with production pathways starting from the central intermediate acetyl-CoA for the natural or recombinant formation of biocommodities. Ack, acetate kinase; Adc, acetoacetate decarboxylase; AdhE, bifunctional aldehyde/alcohol dehydrogenase; Aor, aldehyde:ferredoxin oxidoreductase ; Buk, butyrate kinase; Bcd*, butyryl-CoA dehydrogenase (*includes electron-transferring flavoproteins B and A) ; Crt, crotonase; CtfA/B, acetoacetyl-CoA:acetate/butyrate-CoA transferase; Fak, fatty acid kinase; Hbd, 3-hydroxybutyryl-CoA dehydrogenase; Pta, phosphotransacetylase; Ptb, phosphotransbutyrylase; Ptf, phosphotransferase; Thl, thiolase.

are often low and therefore not yet applicable. Other products such as acetone, which is also part of ABE fermentation of solventogens, cannot be produced naturally with acetogens. Therefore, the use of metabolic engineering to improve natural production and to establish new non-native pathways producing novel products is of great interest.

1.4 Anaerobic production of hexanoate

The interest in microbial production of the C_6 carboxylic acid hexanoate increased in recent years, since it is a versatile platform chemical in the pharmaceutical, food, and chemical industry and can be used as a precursor in biofuel production.[93] As of yet, the production of hexanoate is reported for 16 microorganisms such as *C. kluyveri*, *Caproicidiproducens galactitolivorans*, *Ruminococcaceae* bacterial strain CPB6, several species of the genus *Megasphaera*, as well as for the acetogens *E. limosum, C. scatologenes, C. drakei*, and *C. carboxidivorans*.[19–21,62,79,83,94–98] The most prominent and yet best-characterized hexanoate producer is *C. kluyveri*, which uses ethanol and acetate as electron donor and acceptor, respectively, to perform chain elongation via reverse β-oxidation.[94] However, substrates used for chain elongation can vary. Strain CPB6 uses lactate for chain elongation, growth of *Cp. galactitolivorans* and *Megaspheara* strains all depend on sugar, while acetogens produce hexanoate from C1 carbon sources.[19,20,83,95] In the acetogens, *C. scatologenes, C. drakei*, and *C. carboxidivorans* chain elongation starts from acetyl-CoA, which is converted to butyryl-CoA, and finally to hexanoyl-CoA catalyzed by the enzymes Thl, Hbd, Crt, Bcd, and EtfA/B. Since these enzymes catalyze the formation of both butyryl-CoA and hexanoyl-CoA, the operon encoding respective genes was termed hexanoyl-CoA synthesis (*hcs*) operon (Figure 2).[83] Interestingly, the only acetogen yet described that is capable to convert the C_6 carboxylic acid further to the corresponding alcohol hexanol, again most likely due to the action of Aor, is *C. carboxidivorans* (Figure 2).[83,99] Another attempt to produce hexanoate is the use of microbial mixed cultures.[97,100,101] Metagenomic analysis of such mixed cultures revealed that besides *C. kluyveri* other *Clostridium* spp. are dominant members of mixed cultures, harbor genes for chain elongation, and are capable to produce hexanoate.[102–105] Since most of these bacteria are not yet isolated in pure culture, much less validly described, efforts are made to identify new potent hexanoate producing anaerobes from such mixed cultures.

1.5 Metabolic engineering of anaerobes

The application of acetogens for new carbon capture technologies is auspicious, and therefore, the establishment of new molecular tools with different levels of possibilities for metabolic engineering is indispensable.[26] Although great efforts have been made to examine the genetic accessibility of acetogens in recent years, only for the few acetogens *A. woodii*, *C. ljungdahlii*, *C. autoethanogenum*, and *E. limosum* a suitable genetic toolbox is available. For other acetogens such as *M. thermoacetica*, *B. methylotrophicum*, *C. coskatii*, *Thermoanaerobacter kivui*, or *C. carboxidivorans*, only a few reports of engineered strains are available or are not examined in detail yet.[28,106] Overall, metabolic engineering is challenging for most acetogens.

The easiest, effective, and often used technique to transform acetogens with foreign DNA is electroporation, which can be applied for *A. woodii*, *C. ljungdahlii*, *C. autoethanogenum*, *M. thermoacetica*, *C. coskatii*, *E. limosum*, or *B. methylortrophicum*.[27,28,107–113] However, other methods are possible as well. Since restriction-modification systems are often the first barrier to transfer DNA into acetogens, conjugation can be applied since DNA is transferred from the donor, often *E. coli*, to the host strain as a single-stranded molecule. This method overcomes the restriction-modification barrier and was successfully applied to *C. autoethanogenum* and *C. carboxidivorans*.[114,115] In the case of transformation, the thermophile *T. kivui* is an exception, since this strain is the only naturally competent acetogen described so far, meaning it can take up free foreign DNA naturally.[116] The recombinant expression of native or foreign genes requires stable replicating plasmids. The stability and maintenance of such plasmids in the acetogenic host strain depend on Gram-positive origins of replication. Therefore, plasmids of the pMTL80000 series are the plasmids of choice, since several replicons such as pBP1 from *C. botulinum*, pCB102 from *C. butyricum*, and pCD6 from *C. difficile* were reported to ensure maintenance in a broad range of acetogens.[106,117] In addition, the Gram-positive replicon pIP404 from *C. perfringens* was successfully used in *A. woodii*, *C. ljungdahlii*, and *E. limosum*.[112,118,119] Combination of different origins of replication located on two different plasmids in a single cell even enables co-existence of both, which was shown for *C. autoethanogenum*.[120] Besides plasmid-based approaches, genome editing tools based on homologous recombination, CRISPR-Cas9, and CRISPR interference are reported for several acetogens.[112,113,119,121–123]

Especially, the expression of heterologous pathways in acetogens is of great interest. The first milestone was achieved with *C. ljungdahlii*, which was metabolically engineered for butanol production in a plasmid-based manner.[108] Since butanol production of the solventogen *C. acetobutylicum* is well elucidated, it is comprehensible that expression of respective genes *thl*, *crt*, *hbd*, *bcd*, *adhE*, and *bdhA* (encoding butanol dehydrogenase) in *C. ljungdahlii* caused the production of 2 mM butanol from syngas. Butanol production was further improved by gene expression of the *bcs* operon together with *thl* from *C. acetobutylicum* in both *C. ljungdahlii* and *C. autoethanogenum*, which produced 6 mM and 25.7 mM butanol, respectively, from CO-containing steel-mill waste gas.[109] A further product of the ABE fermentation, acetone, was produced from C1 gases with recombinant *C. ljungdahlii* and *A. woodii* strains.[118,124] Acetone is an important biocommodity in the chemical industry, however, production is mainly based on fossil resources and linked to phenol production.[40,125,126] As acetone is also a product of solventogenic ABE fermentation, recombinant production using acetogens was achieved by construction and heterologous expression of a synthetic acetone production operon (APO), which encodes the genes *thl*, *ctfA*/*B* (encoding acetoacetyl-CoA:acetate/butyrate-CoA transferase), and *adc* (encoding acetoacetate decarboxylase) of *C. acetobutylicum*. Starting from the central intermediate of the WLP, two molecules of acetyl-CoA are condensed to acetoacetyl-CoA catalyzed by the action of Thl. The CoA transferases CtfA/B transfer the CoA of acetoacetyl-CoA to acetate resulting in acetyl-CoA and acetoacetate. Finally, decarboxylation of acetoacetate catalyzed by Adc results in acetone (Figure 2). In *C. ljungdahlii*, acetone is further converted to isopropanol via a secondary alcohol dehydrogenase. Only with a deletion strain, in which the respective gene (CLJU_c24860) is deleted, acetone production is feasible.[127,128] Besides butanol, acetone, and isopropanol, further products were successfully recombinantly produced, such as mevalonate, isoprene, acetoin, 3-hydroxybutyrate, poly(3-hydroxybutyrate), isobutanol, or hexanoate.[27,47,83,112,119,129,130] Although the product spectrum of acetogens is growing, product yields are still low. Hence, several strategies were implemented to achieve improved production. For manipulation of gene expression levels, different promoters, including constitutive and inducible systems, have been established in several acetogens.[106] However, the activity and strength of most promoters have not been examined in detail, since enzymatic assays are time-consuming, while the use of fluorescent reporter proteins is challenging in general in anaerobes.[26] Fluorescent proteins (FPs) are

commonly used in molecular biology, however, the fluorescence of the most common FPs is oxygen-dependent or lacks brightness which limits their use in anaerobes. Therefore, the implementation of a strong-fluorescent reporter system that is functional under anaerobic conditions would expand the molecular toolbox of most of the described acetogens and solventogens.

1.6 Fluorescent reporter proteins for the use in anaerobic bacteria

1.6.1 Oxygen-dependent fluorescent reporter proteins in *Clostridium* spp.

The green fluorescent protein (GFP) from the jellyfish *Aequorea victoria* was isolated and described in 1962, not anticipating that this protein would revolutionize molecular biology.[131] The potential of GFP as a strong fluorescent reporter was firstly realized in 1994, when the respective gene was recombinantly expressed in *E. coli*.[132] From that time, GFP was used for a variety of applications in molecular biology, and Osamu Shimomura, Martin Chalfie, and Roger Y. Tsien were finally awarded with the Nobel Prize in Chemistry in 2008 “for the discovery and development of the green fluorescent protein, GFP.”

Nowadays, FPs in general are indispensable tools in molecular biology to investigate gene expression levels, protein localization and movement within the cell, protein-protein interactions, and dynamics in microbial populations.[133–140] Although the most often used FPs such as GFP and its derivates as well as proteins of the mFruit family were further developed and novel colors cover most of the spectral demands for different applications, their use is challenging under anaerobic conditions since chromophore formation is oxygen-dependent.[141,142] Still, in very few instances, FPs were used in Clostridia. In these instances, FPs were produced under anaerobic conditions and subsequently exposed to oxygen to induce the active fluorescent form. This technique is called aerobic fluorescent recovery and was first applied for *Enterobacter aerogenes*, but is only suited for aerotolerant or facultative anaerobes.[143,144] Three different oxygen-dependent FPs were examined in the pathogenic clostridia *C. perfringens* and *C. difficile*. The yellow fluorescent protein (YFP) was used in *C. perfringens* to localize a type IV pilus-associated ATPase (PilB) by constructing a YFP-PilB fusion protein. YFP-PilB was detected regarding its fluorescence after oxygen exposure and localized at cell poles of *C. perfringens*.[145] Moreover, a codon-optimized version of the cyan fluorescent protein (CFP), which is a derivate of GFP, and mCherry was used in *C. difficile*. Both reporters were used to investigate the localization of cell division proteins. Therefore, CFP or mCherry were fused to respective proteins and localized by determining their

fluorescence.[146,147] In both experiments, the fluorescent fusion proteins were produced anaerobically, and afterward, cells were fixed and exposed to oxygen overnight. Although some oxygen-dependent FPs are suitable for *C. perfringens* and *C. difficile*, real-time imaging during anaerobic growth seems impossible for most clostridial species which are strictly anaerobic. However, with the increasing relevance of anaerobic bacteria, the need for strong fluorescent reporter proteins, which are functional in a broad range of microbes in absence of oxygen, gained further importance. Fortunately, several oxygen-independent fluorescent reporters were recently developed and used in strict anaerobic *Clostridium* spp. including flavin mononucleotide-based FPs (FbFPs), self-labeling protein tags, and the fluorescence-activating and absorption-shifting tag (FAST).

1.6.2 Flavin mononucleotide-based fluorescent proteins

The most often reported FPs, which are suited for use under anaerobic conditions, are FbFPs. Initially, the blue-light photoreceptors YtvA from *Bacillus subtilis* and SB2 from *Pseudomonas putida* were engineered to develop the two FbFPs termed BsFbFP and PpFbFP, respectively.[148] In addition, the nucleotide sequence of BsFbFP was codon-optimized for usage in *E. coli* and termed EcFbFP. Moreover, further FbFPs were engineered from the blue light receptor Phot2 of *Arabidopsis thaliana* and termed iLOV and phiLOV, while the brightest of the FbFPs CreiLOV was engineered from *Chlamydomonas reinhardtii*.[149–151] The oxygen-independent fluorescence of the different FbFPs is all based on the photoactive light oxygen voltage (LOV) domain, which noncovalently binds flavin mononucleotide (FMN), and exhibits weak green fluorescence after excitation with blue light.[152] Since the synthesis of FMN does not require oxygen, the fluorescence of LOV-based FPs is oxygen-independent. Meanwhile, genes encoding BsFbFP, EcFbFP, and PpFbFP are commercially available under the brand name Everglow® and were established in different strict anaerobes for various applications. Initially, PbFbFP (everglow®-Pp1) was used in *C. cellulolyticum* and EcFbFP (everglow®-Bs2) in both *C. acetobutylicum* and *C. tyrobutyricum* to investigate promoter strength regarding their fluorescence intensity, which is the most common application for FPs in general.[153–155] In some cases, the nucleotide sequence of FbFP was codon-optimized for the desired host strain as reported for the solventogen *C. beijerinckii* or the acetogen *B. methylotrophicum*.[28,156] Besides promoter activity studies, PbFbFP was used to investigate transcriptional repression using CRISPRi in *C. acetobutylicum* and *C. pasteurianum*.[157] Moreover, the functionality of a temperature-sensitive origin of replication was investigated in *C. ljungdahlii* and

C. acetobutylicum where the plasmid loss was monitored regarding fluorescence of EcFbFP and PbFbFP producing cells.[158] Protein dynamics were investigated in *C. difficile* by using phiLOV to construct FtsZ (cytokinetic protein) and FliC (a flagellin protein) fusion proteins.[159] Moreover, phiLOV was shown to be functional in *C. sordellii* and *C. acetobutylicum*.[159] CreiLov was used to investigate inducible promoters to establish a CRISPR-Cas9 genome editing tool in *E. limosum*.[112] Interestingly, CreiLov was reported to be brighter than other LOV proteins, however, was shown to be not functional in *C. acetobutylicum*.[160]

While the different FbFP versions were successfully produced in various solventogens and acetogens, all of them feature the same weaknesses. Since the fluorescence of all described FbFPs is based on the LOV domain, they only produce cyan-green fluorescence in the range of 495 nm, which is often in the same range as autofluorescence of the host cell.[147,161] More importantly, the fluorescence signal is weak, often below the detection limit, and, therefore, indistinguishable from autofluorescence.[162] As a result, brighter and more flexible reporters, which can be adapted to the spectral needs of the experiment, are needed.

1.6.3 Ligand-dependent self-labeling fluorescent proteins

Ligand-dependent self-labeling FPs do not fluorescence on their own, but only when they covalently bind a fluorescent ligand, even in absence of oxygen. The most often used self-labeling proteins are the HaloTag, an engineered version of a haloalkane dehalogenase from *Rhodococcus rhodochrous*, the SNAP-tag, which is an engineered version of the *Homo sapiens* O^6-alkylguanine-DNA alkyltransferase, and CLIP-tag, which is a mutagenized version of the SNAP-tag.[163–165] Even though all three proteins were used for applications in anoxic environments, they were only sparsely used in *Clostridium* spp.[166] The SNAP-tag was used to study proteins involved in sporulation of *C. difficile* by constructing different fusion proteins.[167,168] Moreover, the SNAP-tag was fused to GusA and used as a bifunctional reporter in *C. acetobutylicum* to measure the strength of the constitutive P_{thl} promoter.[160] Since there are various fluorescent ligands available, the fluorescence of HaloTag and SNAP-tag can be chosen to be orthogonal to that of other FPs and therefore combined to investigate anaerobic bacterial co-cultures.[169] Although self-labeling proteins show bright fluorescence in *C. acetobutylicum* and *C. ljungdahlii*, they also harbor some major disadvantages.[170] Both, the SNAP-tag and HaloTag are considerably large with masses of 19.4 and 33 kDa, respectively, which might be problematic for the construction of fusion proteins. Moreover, both SNAP-tag and HaloTag suffer from long labeling times of 30- and 15-minutes, respectively.[169] Although

the covalent binding of the fluorogen to the self-labeling proteins is strong, and, therefore, allows in-gel fluorescence scanning of SDS-PAGE gels, the ligands are often fluorescent on their own, and cells need to be washed after incubation before scanning to prevent increased background fluorescence.[171] In addition to the ligand-dependent fluorescent proteins which bind their ligands covalently, the Bilin-binding fluorescent protein (BBFP) was recently described to be fluorescent in absence of oxygen when non-covalently bound to a ligand (bilirubin or biliverdin).[172,173] The fluorogens are cell permeable and only fluorescent when bound to BBFP and produce no backroad fluorescence. However, it has yet to be proven that BBFPs are functional in *Clostridium* spp.

1.6.4 The fluorescence-activating and absorption-shifting tag

A game-changing brightly fluorescent reporter for applications in anaerobic environments was recently developed in form of the fluorescence-activating and absorption-shifting tag (FAST, formerly Y-FAST) protein.[174] This small monomeric protein tag was engineered from the photoactive yellow protein of *Halorhodospira halophila* and is non-fluorescent on its own. Fluorescence depends on the binding of a so-called fluorogen, which are hydroxybenzylidene rhodanine derivates. Upon binding, a fluorescent FAST:fluorogen complex is formed, causing deprotonation of the fluorogen, which results in bright fluorescence of different wavelengths depending on the fluorogen used.[175] This conformational change and resulting fluorescence is completely independent of oxygen, and therefore perfectly suited for use in anoxic environments.[174] Because of its low molecular mass of 14 kDa, FAST is perfectly suited as a fluorescent tag to construct fusion proteins and track protein dynamics. Aside from that, FAST is fluorescent right after proper folding without the need for chromophore maturation time and, as a result, eminently suitable for investigating molecular processes such as protein synthesis or folding in real-time. In addition, the binding of the fluorogen is specific, rapid, and fully reversible, while unbound fluorogens are non-fluorescent and therefore do not cause undesired background fluorescence and ensure high imaging contrast.[174] Since the small FAST protein and a fluorogenic ligand forms a bipartite system, both parts were further developed and adapted to fit several different spectral demands.

The initially designed fluorogens are composed of a phenol-ring conjugated to a rhodanine heterocycle. Fluorogens with different fluorescence efficiencies and spectral properties can be designed by changing the substituents of the aromatic phenol-ring.[175] The initially described hydroxybenzylidene rhodanine derivates 4-hydroxybenzylidene-rhodanine (HBR)

and 4-hydroxy-3-methylbenzylidene-rhodanine (HMBR; ^{TF}Lime) were further developed to a whole collection of fluorogens emitting different colors.[175] Three of them are commercially available, ^{TF}Lime, ^{TF}Coral (4-hydroxy-3,5-dimethoxybenzylidene rhodanine; HBR-3,5DOM), and ^{TF}Amber (4-hydroxy-3,5-dimethylbenzylidene-rhodanine; HBR-3,5DM) resulting in green, red, or orange fluorescence, respectively, upon binding to FAST. Recently, new fluorogens were developed by replacement of rhodanine with an isosteric heterocycle resulting in variants that cover the visible spectrum from blue to red.[176] Since beforehand mentioned fluorogens are all membrane-permeable and diffuse into the cell, they are not suited to investigate cell-surface membrane proteins. Therefore, ^{TF}Amber-NP was developed harboring a carboxymethyl group, which is negatively charged, and, as a consequence, not able to cross the plasma membrane, and only labels FAST-tagged proteins exposed to the cell surface.[177,178] Besides the adaptation of the fluorogenic ligands, the FAST protein itself was engineered and optimized. The fluorescence intensity was improved by inserting a single mutation in the fluorogen binding pocket of FAST. The newly designed protein was termed FAST2 (formerly iFAST) and showed an 1.7-fold improved fluorescence intensity compared to FAST.[179] In addition, a dimerized version of FAST, as well as FAST2, resulted in 2.8-fold and 3.8-fold brighter fluorescence compared to FAST, respectively.[179] A promiscuous FAST variant termed pFAST was designed to improve binding affinities and brightness.[176] Protein interactions, including formation and dissociation, can be monitored in real-time using splitFAST.[180] This complementary system consists of two separate non-fluorescent parts, which are only fluorescent again when in proximity, and, therefore, suited to tag two possibly interacting proteins.[180] Although various fluorogens are available, which enable spectral flexibility, multicolor approaches using FAST are not possible as binding of these fluorogens is not specific, which is a major disadvantage. The color-selective FAST variants greenFAST, which only binds HMBR and, redFAST, which only binds HBR-3,5DOM, were developed to solve this problem.[181] Therefore, mutated FAST variants were designed using error-prone PCR and were screened and selected in presence of HMBR and HBR-3,5DOM regarding green and red fluorescence. The green-fluorescent reporter greenFAST harbors three mutations (G21E, P68T, G77R), which results in selective binding of HMBR. Compared to that, redFAST contains five mutations (F28L, E46Q, R52A, E81V, S99N), which improve the selectivity for the red-fluorescent dye HBR-3,5DOM.[181] Most importantly, the combination of orthogonal fluorescence emitted by greenFAST and redFAST in presence of appropriate fluorogen

concentrations opens the door for multicolor approaches in anaerobes including protein interactions or dynamics in co-cultures, which was difficult to achieve before.

While the group of Arnaud Gautier (Sorbonne University, Paris, France) focused on the establishment of their FAST variants in eukaryotic cells and *E. coli*, the group of Eleftherios Papoutsakis (University of Delaware, Newark, DE, US) showed that a codon-optimized version of FAST is functional in *Clostridium* spp. under strictly anaerobic conditions. Initially, FAST was established successfully as a reporter system in *C. acetobutylicum*.[182] The fluorescence of FAST was used to determine the strength of the thiolase (P_{thl}), acetoacetate decarboxylase (P_{adc}), and phosphotransbutyrylase (P_{ptb}) promoter from *C. acetobutylicum*. Moreover, the influence on promoter strength of a mutated version of P_{thl} termed P_{thl}^{sup} and modified ribosomal binding sites of P_{adc} and P_{ptb} were examined regarding fluorescence intensity.[182] In addition, FAST was used to localize the cell division protein ZapA of *C. acetobutylicum* by constructing a ZapA-FAST fusion protein, which was recombinantly produced and localized by fluorescence microscopy in both *C. acetobutylicum* and *C. ljungdahlii*.[169,182] Moreover, the combination of FAST with other anaerobic FPs enabled multicolor approaches. The orthogonal fluorescence of FAST, HaloTag, and SNAP-tag was combined to identify each cell type of bacterial cell mixtures containing *C. acetobutylicum* and *C. ljungdahlii.* Therefore, FAST-producing *C. acetobutylicum* cells were separated from *C. ljungdahlii* cells producing the HaloTag or SNAP-tag.[169] Moreover, *C. acetobutylicum* producing the ZapA-FAST fusion protein and *C. ljungdahlii* producing the HaloTag were used to show the exchange of cellular material of *C. acetobutylicum-C. ljungdahlii* cell fusions. Upon cell fusion, the green fluorescence of ZapA-FAST in *C. acetobutylicum* was detected in *C. ljungdahlii*, while the red fluorescence of the HaloTag was determined in *C. acetobutylicum* cells.[183]

Although FAST was established successfully for use in *C. acetobutylicum* and *C. ljungdahlii*, the potential of this system is far from exhausted and offers further exciting applications, especially in anaerobes. This includes protein production controls by tagging the protein of interest, investigating protein-protein interactions using splitFAST, or the dynamics in bacterial co-cultures by using greenFAST and redFAST.

1.7 Aims of this thesis

The use of anaerobic bacteria for the sustainable production of value-added products is outstanding but simultaneously challenging, since genetic tools are not well established for most acetogens. Therefore, the expansion of the genetic toolbox of acetogenic and solventogenic anaerobes by implementing heterologous pathways and fluorescent reporter proteins is of great interest. Since poor energy supply can negatively impact heterologous production of biocommodities, the energetic barriers of autotrophically cultivated *A. woodii* strains were investigated. The first part of this thesis hypothesized that improved ATP production by establishing the ADI pathway from *C. autoethanogenum* can boost autotrophic growth of metabolically engineered *A. woodii* strains supplemented with arginine. In the second part of the thesis, the strong and oxygen-independent fluorescent reporter protein FAST was examined for various applications in the acetogen *E. limosum*. This part of the thesis aimed to track the recombinant production of fluorescent FAST-tagged fusion proteins during cultivation of *E. limosum* by establishing elementary methods for determining the fluorescence of the whole bacterial population and at single-cell level, including the use of fluorescent microplate reader, fluorescence microscopy, and flow cytometry. In addition, the hypothesis was evaluated that the fluorescent tag has no negative impact on the stability or functionality of FAST-tagged enzymes. Finally, the production of the biocommodities butanol and acetone from the liquid C1 carbon and energy source methanol was examined. Multicolor approaches are still challenging in anaerobes due to the lack of orthogonal FPs. In the third part of the thesis, the toolbox of solventogens and acetogens was aimed to be expanded further by establishing orthogonal fluorescent reporters for such multicolor approaches. Therefore, the recombinant production of the green fluorescent protein greenFAST and the red fluorescent protein redFAST was addressed in the solventogens *C. saccharoperbutylacetonicum* and *C. acetobutylicum*, as well as in the acetogens *A. woodii* and *E. limosum*. Orthogonal fluorescence of both reporters enables the examination of dynamics in anaerobic bacterial co-cultures. Moreover, the co-existence of a tightly regulated two-plasmid system can be evaluated regarding the green and red fluorescence of metabolically engineered *C. saccharoperbutylacetonicum* strains. In the fourth part of the thesis, the isolation and valid description of a new hexanoate producer from a mixed microbial culture was realized.

2. Results & Discussion

All results acquired and interpreted during this thesis are part of the attached manuscripts.

2.1 Induced heterologous expression of the arginine deiminase pathway promotes growth advantages in the strict anaerobe *Acetobacterium woodii*.

Beck, M. H.; **Flaiz, M.;** Bengelsdorf, F. R.; Dürre, P. Induced heterologous expression of the arginine deiminase pathway promotes growth advantages in the strict anaerobe *Acetobacterium woodii*. *Appl. Microbiol. Biotechnol.* ***2020***, *104*, 687–699. https://doi.org/10.1007/s00253-019-10248-9

Rights and permissions

Reprinted with permission from Springer-Verlag GmbH Germany, part of Springer Nature 2019.

The original article can be accessed via https://doi.org/10.1007/s00253-019-10248-9

Applied Microbiology and Biotechnology (2020) 104:687–699
https://doi.org/10.1007/s00253-019-10248-9

APPLIED GENETICS AND MOLECULAR BIOTECHNOLOGY

Induced heterologous expression of the arginine deiminase pathway promotes growth advantages in the strict anaerobe *Acetobacterium woodii*

Matthias H. Beck[1] · Maximilian Flaiz[1] · Frank R. Bengelsdorf[1] · Peter Dürre[1]

Received: 19 July 2019 / Revised: 30 September 2019 / Accepted: 5 November 2019 / Published online: 6 December 2019
© Springer-Verlag GmbH Germany, part of Springer Nature 2019

Abstract
The advantage of using acetogens such as *Acetobacterium woodii* as biocatalysts converting the cheap substrate and greenhouse gas carbon dioxide (CO_2) into value-added chemicals comes together with the disadvantage of a low overall ATP gain due to the bioenergetics associated with the Wood-Ljungdahl pathway. Expanding the product spectrum of recombinant *A. woodii* strains to compounds with high ATP-demanding biosynthesis is therefore challenging. As a least invasive strategy for improved ATP generation, the exploitation of the arginine deiminase pathway (ADI) was examined under native conditions and via using heterologously expressed genes in *A. woodii*. Several promoters were analyzed for application of different gene expression levels in *A. woodii* using β-glucuronidase assays. Heterologous expression of the ADI pathway genes from *Clostridium autoethanogenum* was controlled using either the constitutive *pta-ack* promoter from *Clostridium ljungdahlii* or a tightly regulated tetracycline-inducible promoter P_{tet}. Unlike constitutive expression, only induced expression of the ADI pathway genes led to a 36% higher maximal OD_{600} when using arginine (OD_{600} 3.4) as nitrogen source and a 52% lower acetate yield per biomass compared to cells growing with yeast extract as nitrogen source (OD_{600} 2.5). In direct comparison, a 69% higher maximal OD_{600} and about 60% lower acetate yield per biomass in induced to non-induced recombinant *A. woodii* cells was noticed when using arginine. Our data suggests the application of the ADI pathway in *A. woodii* for expanding the product spectrum to compounds with high ATP-demanding biosynthesis.

Keywords Citrulline · Ornithine · Acetogens · Fumarate · Arginine · ATP

Introduction

Within the last decade, the use of and research on gas-fermenting acetogens (anaerobic bacteria employing the Wood-Ljungdahl pathway) for the production of bulk chemicals has enormously increased (Bengelsdorf et al. 2018). The key advantage of this gas fermentation technology is based on the utilization of waste gases as substrate (CO and CO_2). In contrast to other biotechnological processes, these substrates are not competing for feedstock that can also serve human nutrition (Schiel-Bengelsdorf et al. 2013). Thus, gas fermentation technology has enormous potential to reduce the greenhouse gas output. In the last decade, the company LanzaTech has developed a steel mill waste gas fermentation process, which eventually reached first commercial scale production of ethanol in 2018 (LanzaTech 2018). Acetogens can be genetically engineered to produce a variety of products such as for instance acetone, butanol, isopropanol, 3-hydroxybutyrate (3-HB), and poly(3-hydroxybutyrate) (PHB) (Bengelsdorf et al. 2018; de Souza Pinto Lemgruber et al. 2019, Flüchter et al. 2019, Woolston et al. 2018) including only a few of already possible target compounds. However, the application of acetogens is limited to products that do not require a heavy ATP biosynthesis demand as they are on the thermodynamic edge of life (Schuchmann and Müller 2014).

In *Clostridium ljungdahlii* and *Clostridium autoethanogenum*, strategies such as supplementation of arginine or nitrate have been successfully exploited to

Electronic supplementary material The online version of this article (https://doi.org/10.1007/s00253-019-10248-9) contains supplementary material, which is available to authorized users.

✉ Frank R. Bengelsdorf
frank.bengelsdorf@uni-ulm.de

[1] Institut für Mikrobiologie und Biotechnologie, Universität Ulm, Albert-Einstein-Allee 11, 89081 Ulm, Germany

688 Appl Microbiol Biotechnol (2020) 104:687–699

address this issue and to enhance ATP yield within the cells (Valgepea et al. 2017; Emerson et al. 2018). While the addition of nitrate showed promising effects such as enhancing the H_2-dependent growth and ATP yield of *C. ljungdahlii*, nitrate could not be utilized by *Acetobacterium woodii* (Emerson et al. 2018). Nevertheless, as one of the fastest CO_2-consuming acetogens, *A. woodii* is a promising candidate for biotechnological application in gas fermentation (Groher and Weuster-Botz 2016). In *C. autoethanogenum*, supplementation of arginine caused a growth boost and higher ATP yields due to the expression of the arginine deiminase (ADI) pathway (Valgepea et al. 2017). A detailed analysis of *A. woodii's* genome sequence revealed homologous genes to all genes encoding enzymes of the ADI pathway (CAETHG_3021 to CAETHG_3025) except for the gene encoding the arginine-ornithine antiporter (CAETHG_3023) from *C. autoethanogenum* (Poehlein et al. 2012; Valgepea et al. 2017). In *C. autoethanogenum*, the ADI pathway genes form an operon. However, in *A. woodii*, the respective homolog genes are scattered across the genome (Poehlein et al. 2012). This study aimed at elucidation whether *A. woodii* is capable of taking advantage of the ADI pathway either under native conditions or when the ADI operon is heterologously expressed using different promoters. Therefore, the tightly regulated promoter P_{tet} (Ransom et al. 2015) and the strong constitutive promoter $P_{pta\text{-}ack}$ (Hoffmeister et al. 2016) were used for heterologous expression of the ADI pathway genes originating from *C. autoethanogenum*. In order to investigate which promoters are suitable for different levels of expression in *A. woodii*, several promoters were analyzed using β-glucuronidase assays.

Material and methods

Bacterial strains and cultivation

Strains and plasmids used in this study are listed in Table 1. For the construction of plasmids, *Escherichia coli* DH5α was used (Thermo Fisher Scientific Inc., USA). Cultivation of *E. coli* was conducted in LB (Luria-Bertani) medium (tryptone 10 g/l, NaCl 10 g/l, yeast extract 5 g/l) at 37 °C supplemented with 15 μg/ml chloramphenicol, if necessary (Green and Sambrook 2012). *Acetobacterium woodii* DSM 1030 was cultivated under strictly anaerobic conditions at 30 °C in modified DSMZ medium 135 as described by Hoffmeister et al. (2016). The modified DSMZ medium 135 was prepared without any NH_4Cl and after autoclaving supplemented with either arginine (18 to 25 mM) or yeast extract (2 g/l) added from sterile and anaerobic stock solutions (720 mM, pH 6.0 for arginine and 100 g/l for yeast extract). The N_2 + CO_2 atmosphere was replaced by an H_2 + CO_2 atmosphere (1.1 bar overpressure) to exclude N_2 as nitrogen source. In growth experiments under autotrophic conditions, bottles were pressurized again when overpressure dropped below 0.5 bar. Subsequently, if not indicated otherwise, growth experiments with *A. woodii* strains were performed in triplicates, in 125-mL Müller-Krempel culture flasks (Müller & Krempel AG, Bülach, Switzerland) with 50 mL of the respective medium. Therefore, cells of *A. woodii* strains were obtained from DMSO stock cultures and inoculated in 5 mL modified DSMZ medium 135. These 5-mL cultures were used to inoculate pre-cultures for subsequent growth experiments. Pre-cultures were cultivated in 50 mL modified DSMZ medium 135 either with yeast extract or with arginine as nitrogen source. If applicable, fructose was added from a sterile and anaerobic stock solution (1.11 M) to a final concentration of 28 mM. Thus, respective experiments were performed under mixotrophic growth conditions. For preparation of genomic DNA, *Clostridium autoethanogenum* DSM 10061 was also taken from the laboratory culture collection and grown in modified Tanner medium (Erz 2017).

DNA manipulation and construction of plasmids for promoter assays and ADI pathway genes

Plasmid preparations from *E. coli* were performed using the Zyppy™ plasmid miniprep kit (Zymo Research, USA) according to the manufacturer's manual. For preparation of genomic DNA from *C. autoethanogenum*, the Master Pure™ Gram-positive DNA purification kit (Epicentre, USA) was used following the instructions of the manufacturer. Purification of digested plasmids from agarose gels or of PCR amplicons was performed with the NucleoSpin® gel and PCR clean-up kit (Macherey-Nagel GmbH Co. & KG, Germany). All restriction enzymes used in this study were fast digest enzymes purchased from Thermo Fisher Scientific Inc. (Waltham, USA). For all DNA amplifications, KAPA Hifi DNA polymerase (Kapa Biosystem, Sigma-Aldrich Chemie GmbH, Germany) was used except for colony PCR amplifications, which were performed using KAPA2G Robust polymerase (Kapa Biosystem, Sigma-Aldrich Chemie GmbH, Germany). All cloning work, if not indicated otherwise, was performed using standard molecular cloning techniques (Green and Sambrook 2012). All primers are listed in Table 1, all constructed plasmids are listed in Table 2, and all recombinant *A. woodii* strains constructed via electroporation are listed in Table 3. Recombinant *A. woodii* strains were obtained by preparing electrocompetent cells and following the electroporation procedure as described by Hoffmeister et al. (2016). Recombinant *A. woodii* strains were further supplemented with 25 μg/ml thiamphenicol for plasmid maintenance.

The promoters P_{bgaL}, P_{tet}, P_{fac}, $P_{ackA\text{-}theo}$, and $P_{pta\text{-}ack}$ were fused with the *gusA* reporter gene of *E. coli* to obtain a pMTL83151 *gusA* plasmid series that can be used for a

Appl Microbiol Biotechnol (2020) 104:687–699 689

Table 1 Primers used in this study

Name	Sequence (5′ to 3′)	Length (bp)
j5_gusA_fw	cgtcacgcgtccatggagatctcgagatgcatgtcgacttacgtcctgtagaaaccc	57
j5_gusA_rev	cctgcaaatgcaggcttcttatttttatgctagctcattgtttgcctccctgctgcgg	58
FW_PtetR_BamHI	catgttggatccataaaaataagaagcctgcatttg	36
RV_PtetR_XhoI	cttcatctcgagttctcctttactgcaggagctc	34
FW_PbgaL_BamHI	attgcaggatccgagatgaaaagtattagggctaatttag	40
RV_PbgaL_XhoI	tcgcatctcgagtttaccctcccaatacatttaaaataattatg	44
FW_Pfac_IPTG_XbaI	cagcattctagagcaggataaaaaaattgtag	32
RV_Pfac_IPTG_XhoI	gatatgctcgagtgcctcctaaatggggatcccc	34
FW_p83_gusA_theo	ccctgagaaggggcaacaagatgcatgtcgacttacgtcc	40
RV_p83_gusA_PackA	aataaaaaaattgctatttttttctagaggatccccgggtac	42
FW_PackA	aaaaaatagcaatttttttatttattatc	29
RV_PackA_theo	cttgttgccccttctcagggtgctgccaagggcatcaagacgatgctggtatcaccggaacctatagtgagtcgtattctatataataacagttatatatctataatacc	110
FW_Ppta-ack1L_BamHI	atcgatggatcctgcttatttgatttacattatat	35
RV_Ppta-ack1L_XhoI	agtgatctcgaggtcctcccctttaaatttaac	32
FW_CAETHG_Ptet	ctgagctcctgcagtaaaggagaactcgagatggaaactaaagttttaagaagagattcagaagttac	68
RV_CAETHG_Ptet	caaatgcaggcttcttatttttatgctagcctatatgctagcacataatactctatctgttgattttattg	71

promoter survey by determining the respective β-glucuronidase activity in *A. woodii*. Initially, the intermediate plasmid pMTL83151_gusA was constructed by amplifying the *gusA* gene from the plasmid pMDY23-Pgap (Grimm et al. 2014) using the primers j5_gusA_fw and j5_gusA_rev (Table 1). The DNA fragment was purified and ligated into the pJET 1.2/blunt cloning vector (Thermo Fisher Scientific Inc., USA) according to the manufacturer's protocol. The resulting plasmid was digested with *Xho*I and *Nhe*I, the *gusA* fragment purified, and then inserted into the *Xho*I- and *Nhe*I-digested pMTL83151. The resulting plasmid pMTL83151_gusA contained the *gusA* reporter gene without a promoter, and a ribosome-binding site upstream from *gusA* and was used for the subcloning of the aforementioned promoters.

The subcloned *bgaR*-P_{bgaL} fragment contains its native ribosomal binding site from *C. perfringens*. In contrast to Banerjee et al. (2014), the first 13 codons of the *cpe* gene were omitted. The respective DNA fragment was amplified from the plasmid pKOD_mazF using the primers FW_PbgaL_BamHI and RV_PbgaL_XhoI (Table 1), purified, and ligated into the pJET 1.2/blunt cloning vector. The resulting plasmid was digested with *Xho*I and *Bam*HI, the obtained *bgaR*-P_{bgaL} fragment purified and then inserted into the *Xho*I- and *Bam*HI-digested pMTL83151_gusA resulting in the plasmid pMTL83151_gusA_P_{bgaL}.

The *tetR*-P_{tet} fragment was amplified from the plasmid pDSW1728 using the primers FW_PtetR_BamHI and RV_PtetR_XhoI (Table 1), purified, and ligated into the pJET 1.2/blunt cloning vector. The resulting plasmid was digested with *Xho*I and *Bam*HI, the obtained *tetR*-P_{tet} fragment purified, and inserted into the *Xho*I- and *Bam*HI-digested pMTL83151_gusA plasmid, resulting in the final plasmid pMTL83151_gusA_P_{tet}. The *lacI*-P_{fac} fragment was amplified from the plasmid pMTL82251-YZ2 using the primers FW_Pfac_IPTG_XbaI and RV_Pfac_IPTG_XhoI (Table 1), purified, and then directly digested with *Xho*I and *Xba*I and inserted into the *Xho*I- and *Xba*I-digested pMTL83151_gusA, resulting in the plasmid pMTL83151_gusA_P_{fac}. The synthetic P_{ackA}-theophylline riboswitch construct contains the *ackA* promoter from *A. woodii* (Hoffmeister et al. 2016) fused with a synthetic theophylline riboswitch (Seibold and Rückert, unpublished). The respective DNA fragment was obtained by amplifying the promoter region of the *ackA* gene using genomic DNA from *A. woodii*. Therefore, the primers FW_PackA and RV_PackA_theo were used. The primer RV_PackA_theo contains the synthesized theophylline riboswitch DNA element (Table 1). The PCR amplicon was purified and inserted into an amplified pMTL83151_gusA using the primers FW_p83_gusA_theo and RV_p83_gusA_PackA (Table 1) via the In-Fusion® HD cloning kit (Takara Bio USA Inc., USA) following the manufacturer's protocol and resulting in the plasmid pMTL83151_gusA_$P_{ackA\text{-}theo}$. The *pta-ack* promoter fragment from *C. ljungdahlii* was amplified from pJIR750_$act_{pta\text{-}ack}$ using the primers FW_Ppta-ack1L_BamHI and RV_Ppta-ack1L_XhoI (Table 1), purified, then directly digested with *Xho*I and *Bam*HI, and inserted into the *Xho*I- and *Bam*HI-digested pMTL83151_gusA, resulting in the plasmid pMTL83151_gusA_$P_{pta\text{-}ack}$.

Table 2 Bacterial strains and plasmids used in this study

Bacterial strain or plasmid	Relevant features	Reference
E. coli XL1-Blue MRF′	Δ(*mcrA*)*183* Δ(*mcrCB-hsdSMR-mrr*)*173 endA1 supE44 thi-1 recA1 gyrA96 relA1 lac* [F′ *proAB lacIqZΔM15* Tn*10* (Tet^r)]	Agilent Technologies, USA
Escherichia coli DH5α	F$^-$ ϕ80d*lacI*^{q}ZΔM15 Δ(*lacZYA-argF*) U169 *recA1 endA1 hsdR*17(r_k^-, m_k^+) *phoA supE*44 λ$^-$ *thi*-1 *gyrA*96 *relA*1	Thermo Fisher Scientific Inc., Waltham MA, USA
Acetobacterium woodii DSM1030	Type strain	DSMZ GmbH, Brunswick, Germany
Clostridium autoethanogenum DSM-10061	Type strain	DSMZ GmbH, Brunswick, Germany
pJET1.2/blunt	pMB1 ori (rep); Amp^r (*bla*); *eco47IR*; P_{lacUV5}	Thermo Fisher Scientific Inc., USA
pMTL83151	Cm^r, ColE1 ori$^-$, *lacZ*, pCB102 ori$^+$, *traJ*	Heap et al. (2009)
pDSW1728	Cm^r, pMB1 ori$^-$, P_{tet}, mCherryOpt; pCD6 ori$^+$, *traJ*	Ransom et al. (2015)
pKOD_mazF	Th^r MLS^r, *ccdB repL*, ori, *bgaR* and P_{bgaL} from *Clostridium perfringens* upstream of *mazF*, DEST cassette	Al-Hinai et al. (2012)
pMTL82251-YZ2	MLS^r, ColE1 ori$^-$, pBP1 ori$^+$, *traJ, lacI,* P_{ptb}, P_{fac}	Zhang et al. (2015b); Flitsch (2016)
pJIR750_act$_{pta\text{-}ack}$	pJIR750, *adc*, *ctfA/B*, *thlA* from *Clostridium acetobutylicum*, $P_{pta\text{-}ack}$ from *C. ljungdahlii*	Hoffmeister et al. (2016)
pMTL83151_gusA	pMTL83151, *gusA* from *E. coli*	This study
pMTL83151_gusA_P_{tet}	pMTL83151_gusA; P_{tet} from pDSW1728	This study
pMTL83151_gusA_P_{fac}	pMTL83151_gusA; P_{fac} from pMTL82251-YZ2	This study
pMTL83151_gusA_$P_{ackA\text{-theo}}$	pMTL83151_gusA; P_{ackA} from *A. woodii*, theophylline riboswitch	This study (Seibold and Rückert, unpublished)
pMTL83151_gusA_P_{bgaL}	pMTL83151_gusA; P_{bgaL} from pKOD_mazF	This study
pMTL83151_gusA_$P_{pta\text{-}ack}$	pMTL83151_gusA; $P_{pta\text{-}ack}$ from *C. ljungdahlii*	This study
pMTL83151_P_{tet}_Boost	pMTL83151, P_{tet} from pDSW1728, *arcA, arcB, arcD, arcC* from *C. autoethanogenum*	This study
pMTL83151_$P_{pta\text{-}ack}$_Boost	pMTL83151, $P_{pta\text{-}ack}$ from *C. ljungdahlii, arcA, arcB, arcD, arcC* from *C. autoethanogenum*	This study

MLSr, macrolide-lincosamide-streptogramin B resistance

The ADI pathway genes (CAETHG_3021 to CAETHG_3025) were amplified using genomic DNA from *C. autoethanogenum* and the primers FW_CAETHG_Ptet and RV_CAETHG_Ptet (Table 1). The PCR amplicon was purified and inserted into an *Xho*I- and *Nhe*I-digested (excision of *gusA*) pMTL83151_gusA_P_{tet} via the In-Fusion® HD cloning kit (Takara Bio USA Inc., USA), following the manufacturer's protocol and resulting in the plasmid pMTL83151_P_{tet}_Boost. The *pta-ack* promoter sequence from *C. ljungdahlii* was excised from pMTL83151_gusA_$P_{pta\text{-}ack}$ via digestion with *Xho*I and *Bam*HI, purified, and then inserted into the *Xho*I- and *Bam*HI-digested (excision of P_{tet}) pMTL83151_P_{tet}_Boost, resulting in the plasmid pMTL83151_$P_{pta\text{-}ack}$_Boost.

Successful construction of plasmids was verified by Sanger sequencing (Eurofins Genomics GmbH, Luxemburg). Analysis of the obtained data regarding the

Table 3 Recombinant *A. woodii* strains used in this study

Recombinant strain	Plasmid	Reference
A. woodii [pMTL83151]	pMTL83151	Hoffmeister et al. 2016
A. woodii [pMTL83151_gusA]	pMTL83151_gusA	This work
A. woodii [pMTL83151_gusA_P_{tet}]	pMTL83151_gusA_P_{tet}	This work
A. woodii [pMTL83151_gusA_P_{fac}]	pMTL83151_gusA_P_{fac}	This work
A. woodii [pMTL83151_gusA_$P_{ackA\text{-theo}}$]	pMTL83151_gusA_$P_{ackA\text{-theo}}$	This work
A. woodii [pMTL83151_gusA_P_{bgaL}]	pMTL83151_gusA_P_{bgaL}	This work
A. woodii [pMTL83151_gusA_$P_{pta\text{-}ack}$]	pMTL83151_gusA_$P_{pta\text{-}ack}$	This work
A. woodii [pMTL83151_P_{tet}_Boost]	pMTL83151_P_{tet}_Boost	This work
A. woodii [pMTL83151_$P_{pta\text{-}ack}$_Boost]	pMTL83151_$P_{pta\text{-}ack}$_Boost	This work

Appl Microbiol Biotechnol (2020) 104:687–699 691

nucleic acid sequences of the *arcD* gene from *C. autoethanogenum* revealed an additional guanine nucleotide following a poly-G (4) sequence in the 3′-region of CAETHG_3023. The annotated DNA sequence would result in a stop codon. The correct sequence, however, resulted in a read-through without a translational frameshift in CAETHG_3024. Further analysis of the respective coding region by comparison with the homologous gene from the closely related *C. ljungdahlii* (CLJU_c09290) revealed an identical nucleotide sequence (aside from other *C. autoethanogenum*–specific SNPs, data not shown) (Fig. S1). Taking this into account, we concluded that the cloned genes were intact suggesting that the arginine:ornithine antiporter ArcD is encoded by one single coding sequence instead of two (CAETHG_3023 and CAETHG_3024) as in *C. ljungdahlii* (CLJU_c09290).

β-Glucuronidase assays

GusA activity was measured in cell extracts of recombinant *A. woodii* strains each harboring a plasmid of the pMTL83151_gusA series possessing promoters P_{bgaL}, P_{tet}, P_{fac}, $P_{ackA\text{-}theo}$, and $P_{pta\text{-}ack}$ (see construction of plasmids). Recombinant *A. woodii* strains were cultivated in triplicates under heterotrophic conditions (42 mM fructose), until the mid or late log phase was reached (optical density at λ = 600 nm (OD_{600}) ~ 0.40–1.3). The strain carrying the constitutive promoter $P_{pta\text{-}ack}$ from *C. ljungdahlii [pMTL83151_gusA_Ppta-ack]* was harvested and processed as described below when the late log phase was reached. Depending on the inducible promoter system encoded on the different plasmids of the pMTL83151_gusA series, cells of recombinant *A. woodii* strains were induced via the supplementation of either 200 and 400 ng/ml anhydrotetracycline (atc), 1 mM lactose, 1 mM IPTG, or 1 mM theophylline. Furthermore, respective strains were also cultivated without supplementation of an inducer. After induction, cells were further cultivated either for additional four hours or overnight. Twenty-five to 50 ml of the cell suspension was harvested (3,773 g, 4 °C, 10 min) and washed twice with cold GusA buffer (50 mM sodium phosphate, 1 mM EDTA, pH 7.0 (Zhang et al. 2015a)), and suspended in 1 ml GusA buffer. Cells were disrupted in cryotubes with glass beads (0.1-mm diameter; Carl Roth GmbH & Co. KG, Germany) using the Ribolyser Precellys24 (Bertin Instruments, France; 3 × 30 s, 6500 rpm, 4 °C) with intermediate cooling steps on ice of 1 min. To remove cell debris and glass beads, cell lysates were centrifuged for 15 min at 17,968*g* and 4 °C, transferred to fresh reaction tubes, and kept on ice until further usage. Protein concentrations were determined using the Pierce BCA protein assay kit (Thermo Fisher Scientific Inc., USA).

GusA activity of crude protein extract was measured in 96-well microplates (655900; Greiner Bio-One International GmbH, Austria) while the general procedures of the assay follow the technique reported by Zhang et al. (2015a). One hundred eighty microliters of pre-warmed (at 37 °C) MUG assay buffer (GusA buffer containing 4 mM MUG (4-methylumbelliferyl-β-D-glucuronide; Sigma-Aldrich Chemie GmbH, Germany) was added to suitable dilutions of crude protein extract (20 µl) to start the reaction. The respective fluorescence kinetic curves were recorded every 30 s for 10 min using either Infinite M200 multimode reader (Tecan Group AG, Switzerland) with a time-scan mode (λ_{ex} = 365 nm, λ_{em} = 455 nm, excitation bandwidth = 9 nm, emission bandwidth = 20 nM, gain = 100) or Synergy™ H1 microplate reader (BioTek Instruments, Inc., Winooski, USA) using the identical wavelength configurations and measuring intervals. The amount of MUG converted into 4-MU (4-methylumbelliferone, Sigma-Aldrich Chemie GmbH, Germany) was calculated using a calibration curve determined via recording the fluorescence of 180 µl of MUG assay buffer supplemented with 20 µl of respective 4-MU stock solutions (0.5 µM–100 µM) in the same way as described above. The curve slope value of produced 4-MU and the protein concentration of the respective protein extract was used to calculate the specific GusA activity.

High-performance liquid chromatography

Acetate, fumarate, and fructose from the undiluted culture supernatants were analyzed by high-performance liquid chromatography (HPLC) using the method previously described (Hoffmeister et al. 2016) with the modification of a constant column temperature of 40 °C, using the organic acid resin 150 × 8 mm column or organic acid resin 300 × 8 mm column (CS-Chromatographie-Service GmbH, Germany).

According to the methods described by Schrumpf et al. (1991), quantification of the amino acids arginine, ornithine, and citrulline was performed via derivatization followed by separation using either the Agilent LC 1100 (Agilent Technologies, USA) HPLC equipped with a fluorescence detector (FLD) or the Agilent 1260 Infinity Series HPLC system (Agilent Technologies, USA) equipped with a diode array detector (DAD). Accordingly, detection was performed either fluorometrically or by UV absorbance. After automatic pre-column derivatization with ortho-phthaldialdehyde (OPA), culture supernatants were separated using the Multohyp ODS-5µ 125 × 4 mm (CS-chromatographie-Service GmbH, Germany) or the ISAspher 100-5 C18 125 × 4 mm (ISERA GmbH, Germany) column at 40 °C. Separation was mediated with an appropriate gradient of the mobile phase using varying proportions of sodium acetate (0.1 M, pH 7.2, 15 mM sodium azide) and methanol (100%). The gradient was applied using a flow rate of 0.7–

0.8 ml/min starting with 20% methanol and increasing up to 100% methanol within 19 min of separation time. Supernatants were prepared by centrifugation (17,968*g*, 4 °C, 20 min) and aliquots of the supernatants were diluted with ddH_2O to achieve an estimated amino acid concentration between 20 and 100 μM. As an internal standard, lysine (100 μM) was added to all analyzed supernatants. Moreover, an external standard series of arginine, ornithine, and citrulline ranging between 20 and 100 μM was recorded as well for calibration purposes.

Results

Establishment of an inducible promoter system in *A. woodii*

The characteristics of the promoters P_{bgaL}, P_{tet}, P_{fac}, $P_{ackA\text{-}theo}$, and $P_{pta\text{-}ack}$ were determined to cover a broad range of specific β-glucuronidase activities expressed in microunits per milligram of protein (Fig. 1). Highest specific GusA activities of $7.8{\cdot}10^5 \pm 1.6{\cdot}10^5$ μU/mg were measured using the constitutive promoter $P_{pta\text{-}ack}$ from *C. ljungdahlii* in strain *A. woodii* [pMTL83151_gusA_$P_{pta\text{-}ack}$]. The second highest specific GusA activities were detected, when using the lactose/IPTG inducible promoter P_{fac} in induced ($5.9{\cdot}10^5 \pm 1.7{\cdot}10^5$ μU/mg) and non-induced ($2.6{\cdot}10^5 \pm 3.7{\cdot}10^3$ μU/mg) cells of the strain *A. woodii* [pMTL83151_gusA_P_{fac}]. The recombinant strain *A. woodii* [pMTL83151_gusA_P_{bgaL}] harboring the lactose-inducible promoter P_{bgaL} from *C. perfringens* exhibited slightly lower specific GusA activities of $2.2{\cdot}10^4 \pm 8.3{\cdot}10^3$ and $3.1{\cdot}10^3 \pm 2.4{\cdot}10^2$ μU/mg in induced and non-induced cells, respectively. However, tightly controlled regulation could only be observed, when *gusA* was expressed using the tetracycline-inducible promoter P_{tet} or the P_{ackA} promoter from *A. woodii* linked to the theophylline riboswitch $P_{ackA\text{-theo}}$ in the respective strains *A. woodii* [pMTL83151_gusA_P_{tet}] and *A. woodii* [pMTL83151_gusA_$P_{ackA\text{-theo}}$]. Consequently, without the supplementation of the respective inducers, only very low specific GusA activities were measured when *gusA* was controlled by P_{tet} (17 ± 35 μU/mg) or $P_{ackA\text{-theo}}$ (12 ± 18 μU/mg). Upon supplementation of the respective inducer, the specific GusA activities increased to $2.7{\cdot}10^2 \pm 48$ μU/mg using $P_{ackA\text{-theo}}$ and $1.2{\cdot}10^3 \pm 1.4{\cdot}10^2$ μU/mg with P_{tet}.

The P_{tet} promoter was chosen for the controlled expression of the ADI pathway genes from *C. autoethanogenum*. In contrast to that, the high GusA activities, which were recorded when *gusA* was expressed using $P_{pta\text{-}ack}$ without the necessity of an inducing reagent, led to the selection of $P_{pta\text{-}ack}$ as the promoter of choice for strong and constitutive expression of the ADI pathway genes.

Expression of the arginine deiminase pathway in mixotrophically growing *A. woodii*: constitutive versus tetracycline-inducible control

A fine-tuned inducible expression (P_{tet} promoter) compared to strong constitutive expression ($P_{pta\text{-}ack}$ promoter) of heterologous ADI pathway genes showed considerable differences in growth behavior and product formation of respective *A. woodii strains*. The two recombinant strains *A. woodii* [pMTL83151_P_{tet}_Boost] and *A. woodii* [pMTL83151_$P_{pta\text{-}ack}$_Boost] expressed the ADI pathway from genes originating from *C. autoethanogenum* either in a tetracycline-inducible (P_{tet}) or in a constitutive ($P_{pta\text{-}ack}$) manner. Both strains were characterized via growth experiments using either arginine or yeast extract as nitrogen source under mixotrophic conditions

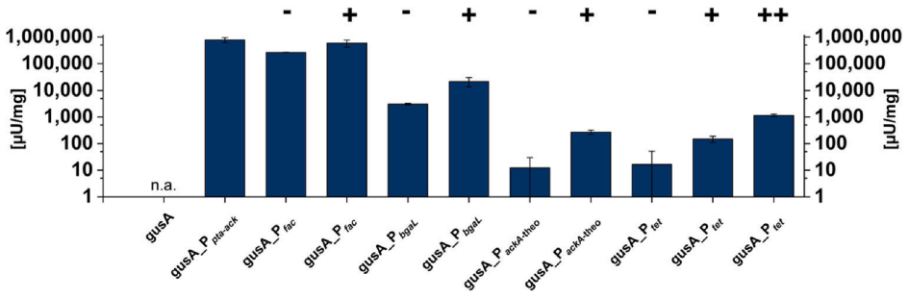

Fig. 1 Specific GusA activities in relation to the respective promoters in recombinant *A. woodii* [pMTL83151_gusA] cells. gusA, *gusA* without promoter (negative control); gusA_$P_{pta\text{-}ack}$, *gusA* under control of the constitutive $P_{pta\text{-}ack}$ promoter from *Clostridium ljungdahlii*; gusA_P_{fac}, *gusA* under control of the synthetic IPTG/lactose-inducible promoter P_{fac} without (-) and with (+) supplementation of 1 mM IPTG; gusA_P_{bgaL}, *gusA* under control of the lactose-inducible promoter P_{bgaL} from *C. perfingens* without (-) and with (+) supplementation of 1 mM lactose; gusA_$P_{ackA\text{-theo}}$, *gusA* under control of the *ackA* promoter from *A. woodii* linked downstream to a theophylline riboswitch without (-) and with (+) supplementation of 1 mM theophylline; gusA_P_{tet}, *gusA* under control of the tetracycline-inducible promoter P_{tet} without (-) and with supplementation of 200 (+) or 400 ng/ml (++) anhydrotetracycline; n.a., no activity; error bars indicate the standard deviations within biological triplicates with plotted mean values

Appl Microbiol Biotechnol (2020) 104:687–699

with fructose and CO_2 + H_2 as carbon as well as energy source. Both recombinant strains consumed arginine and produced ornithine (Figs. 2 and 3), which is a clear proof for a functional ADI pathway, since the control strains (*A. woodii* wild type and *A. woodii* [pMTL83151]) did not show such a characteristic phenotype (Fig. S2). *A. woodii* wild type and *A. woodii* [pMTL83151] grew with arginine as nitrogen

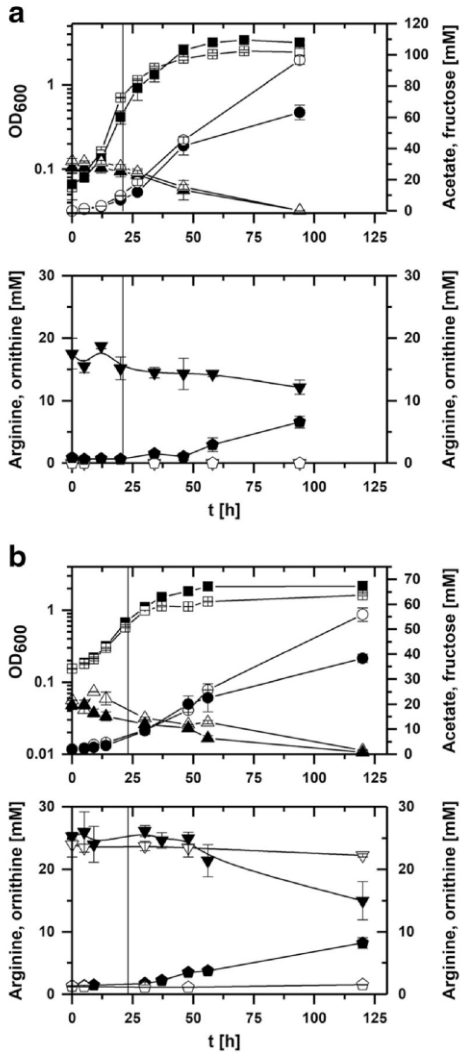

Fig. 2 Mixotrophic growth experiment with *A. woodii* [pMTL83151_P_{tet}_Boost]. **a** Induced cells (300 ng/ml atc) growing with either yeast extract (empty symbols) or arginine (filled symbols) as nitrogen source. **b** Arginine as nitrogen source, cells were either induced (filled symbols) by 300 ng/ml anhydrotetracycline or non-induced (empty symbols). Fructose and CO_2 were used as carbon, H_2 and fructose as energy sources. Monitored OD_{600}, squares (□■); fructose consumption, upward triangles (△▲); acetate production, circles (○●); arginine consumption, downward triangles (▽▼); ornithine production, pentagons (⬟); time of induction with anhydrotetracycline (300 ng/ml) is indicated by a vertical line. Error bars indicate the standard deviations within biological replicates (n = 3) with plotted mean values

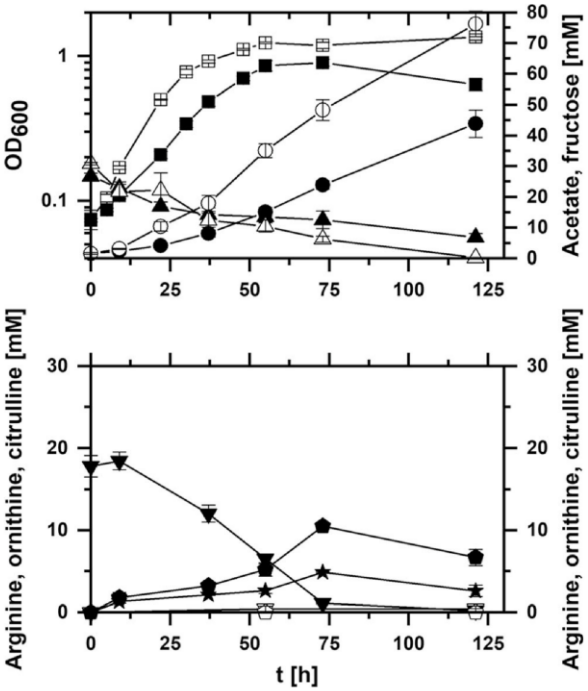

Fig. 3 Mixotrophic growth experiment with *A. woodii* [pMTL83151_$P_{pta\text{-}ack}$_Boost] growing with either yeast extract (empty symbols) or arginine (filled symbols) as nitrogen source. Fructose and CO_2 were used as carbon, H_2 and fructose as energy sources. Monitored OD_{600}, squares (□■); fructose consumption, upward triangles (△▲); acetate production, circles (○●); arginine consumption, downward triangles (▽▼); ornithine production, pentagons (⬟); citrulline production, stars (★); error bars indicate the standard deviations within biological replicates (n = 3) with plotted mean values

source (μ_{max} 0.07 1/h and 0.14 1/h) and reached maximal optical densities (OD_{600}) of 0.8 after 129 h and of 1.6 after 94 h, respectively. In a further experiment (Table 4), both strains were cultivated using yeast extract as a nitrogen source which promoted faster growth (μ_{max} of 0.14 1/h and μ_{max} of 0.2 1/h) and considerably higher maximal OD_{600} values (3.0 after 58 h and of 2.5 after 46 h). However, neither *A. woodii* wild type nor *A. woodii* [pMTL83151] produced ornithine under any condition tested (Fig. S2). Noteworthy is also the fact that only two thirds of fructose was converted into acetate in the recombinant ADI pathway-expressing strains when provided with arginine (see the Discussion section). In contrast, the control strains formed 3 moles of acetate from 1 mole of fructose (typical feature of acetogens). The data for the growth experiments are summarized in Table 4.

The *A. woodii* [pMTL83151_P_{tet}_Boost] culture, in which cells expressed the ADI pathway in the induced state, reached a maximal OD_{600} of 3.4 after 71 h with arginine as nitrogen source (Fig. 2b). The substitution of arginine with yeast extract as nitrogen source resulted in a lower maximal OD_{600} of 2.5 after 71 h (Fig. 2a). Under both conditions tested, the addition of the inducer caused a drop of the growth rate by 50% using

arginine and 77 % using yeast extract, respectively (Table 4). Besides the increase of 36% maximal OD_{600} in induced *A. woodii* [pMTL83151_P_{tet}_Boost] cells growing on arginine compared to yeast extract, another prominent difference was noticed in acetate production. While fructose consumption stayed in a similar range under tested conditions, *A. woodii* [pMTL83151_P_{tet}_Boost] produced 38.8 mM acetate per OD_{600} (97 mM total) using yeast extract and exhibited a 52% lower acetate yield (18.5 mM/OD_{600}; 63 mM total) when using arginine, respectively (Table 4). Thus, the acetate production rates were also impacted considerably since the rates dropped from 1.34 to 0.45 mM/h after induction of the ADI pathway when using arginine. The decrease of acetate production in *A. woodii* [pMTL83151_P_{tet}_Boost] was concomitant with arginine consumption and ornithine production. About 6 mM of the provided 18 mM arginine was consumed and converted into approximately 6 mM ornithine (1.8 mM/OD_{600}) at the end of the growth experiment.

To shed light on the direct impact of the P_{tet}-dependent induced expression of the heterologous ADI pathway genes in *A. woodii* [pMTL83151_P_{tet}_Boost], growth characteristics were analyzed simultaneously under induced and non-induced conditions. Figure 2b shows that the P_{tet} promoter is tightly regulated, while only induced cells notably consumed arginine and produced ornithine. The non-induced cultures reached the stationary growth phase within 30 h and a maximal OD_{600} of 1.3. The induced culture kept growing until a maximal OD_{600} of 2.2 was reached after 56 h (Fig. 2b). Besides this 69% higher final OD_{600} of the induced cultures, a further difference was noticed. The induced cultures showed about 60% lower acetate yield (17.3 mM/OD_{600} compared to 43.1 mM/OD_{600}; 38 mM compared to 56 mM total), which was also mirrored in the acetate production rates during the growth experiments (Table 4). Fructose was consumed within 120 h in the induced and non-induced cultures with similar rates (Table 4). The non-induced *A. woodii* [pMTL83151_P_{tet}_Boost] cultures showed only low arginine consumption (approximately 2 mM arginine, sufficient for growth), but did not exhibit any ornithine production. The induced cells used approximately 10 mM of arginine and produced 7 mM of ornithine (3.2 mM/OD_{600}) within the same time frame (Fig. 2b).

To address the question, if constitutive expression of the heterologous ADI pathway genes by the $P_{pta\text{-}ack}$ promoter affects the growth behavior of *A. woodii* [pMTL83151_$P_{pta\text{-}ack}$_Boost], growth characteristics were analyzed in parallel using either arginine or yeast extract as nitrogen source. When cultures were grown with yeast extract, a maximal OD_{600} of 1.2 was reached after 55 h, whereas when cultures used arginine a maximal OD_{600} of 0.8 was reached after 73 h (Fig. 3). Cultures completely metabolized fructose when growing with yeast extract, but did only consume 74% of the provided fructose when using arginine as nitrogen source. Fructose consumption rates and acetate production rates are shown in Table 4. *A. woodii* [pMTL83151_$P_{pta\text{-}ack}$_Boost] consumed all of the provided arginine (18 mM) and produced 11 mM ornithine in total with the highest detected yield of 13.8 mM/OD_{600}. Additional to ornithine, this strain produced a total of 5 mM citrulline (6.3 mM/OD_{600}), which is an intermediate of the ADI pathway.

Furthermore, fumarate was also produced by *A. woodii* [pMTL83151_$P_{pta\text{-}ack}$_Boost] to concentrations of 1.4 mM when growing using arginine, in contrast to 0.3 mM when using yeast extract as nitrogen source (Fig. S3a). Among all of the strains analyzed besides *A. woodii* [pMTL83151_$P_{pta\text{-}ack}$_Boost], only *A. woodii* [pMTL83151] produced very low amounts of fumarate (0.1 mM) when using arginine as nitrogen source (Fig. S3b).

Induced expression of the arginine deiminase pathway in autotrophically growing *A. woodii*

Analogous to the mixotrophic growth experiments, heterologous expression of the ADI pathway has been proved using *A. woodii* [pMTL83151_P_{tet}_Boost] growing autotrophically with H_2 + CO_2 as carbon and energy source. The strain (induced cells) reached similar OD_{600} values with arginine (OD_{600} 1.0) as with yeast extract (OD_{600} 0.92) as nitrogen source. Induced *A. woodii* [pMTL83151_P_{tet}_Boost] cells consumed provided arginine (16 mM) and produced a corresponding amount of ornithine. *A. woodii* [pMTL83151_P_{tet}_Boost] showed prior induction (300 ng/ml anhydrotetracycline) of the ADI pathway growth rates of 0.02 1/h (arginine) up to 0.04 1/h (yeast extract). After induction, induced cells of *A. woodii* [pMTL83151_P_{tet}_Boost] continued growing with a rate of 0.02 1/h (arginine) while growth of non-induced cells stagnated. Non-induced cells consumed about 3.5 mM arginine, however, without production of detectable amounts of ornithine. Furthermore, non-induced *A. woodii* [pMTL83151_P_{tet}_Boost] cells showed very inconsistent growth while reaching a final OD_{600} of 0.52 (Fig. 4). It has to be noted that *A. woodii* [pMTL83151_$P_{pta\text{-}ack}$_Boost] did not show detectable autotrophic growth using H_2 + CO_2 with neither arginine nor with yeast extract as nitrogen source.

Discussion

The intention of lowering energetic barriers in acetogenic metabolism becomes a challenging endeavor, especially because it is well known that these bacteria live on the thermodynamic edge of life (Schuchmann and Müller 2014). The necessity of this task becomes more and more clear since the relevance of acetogens in biotechnology is steadily increasing (Schiel-Bengelsdorf and Dürre 2012; Bengelsdorf et al. 2018; LanzaTech 2018). Valgepea et al. (2017) could demonstrate that

Table 4 Comparison of product formation and growth characteristics of mixotrophically growing (recombinant) strains of *A. woodii*

Strain and nitrogen source	Max. OD_{600}	Growth rate μ (1/h)	Fructose (mM/h)	Acetate (mM/h)	Max. amino acid excretion (mM/OD_{600})	Consumed fructose (mM)	Ornithine (mM) ≙ theoretical ATP from arginine	Acetate yield (mM/OD_{600})
A. woodii								
YE	3.0	0.14	0.61	1.80	–	24	–	26.7
ARG	0.8	0.07	0.15	0.31	–	17	–	72.5
A. woodii [pMTL83151]								
YE	2.5	0.2	0.61	2.26	–	25	–	29.2
ARG	1.6	0.14	0.18	0.98	–	23	–	51.9
A. woodii [pMTL83151_P_{tet}_Boost]								
YE (induced)	2.5	0.18[a] 0.04[b]	0.18[a]	0.38[b]	0.49[a] 1.37–1.07[b]	–	32	–	38.8
ARG (induced)	3.4	0.14[a] 0.07[b]	0.13[a]	0.34[b]	0.35[a] 1.34–0.45[b]	Ornithine, 1.8	28	6	18.5
A. woodii [pMTL83151_P_{tet}_Boost]								
ARG (induced)	2.2	0.09[a] 0.05[b]	0.26[a]	0.13[b]	0.11[a] 0.51–0.24[b]	Ornithine, 3.2	19	7	17.3
ARG (non-induced)	1.3	0.08[a] 0.04[b]	0.24[a]	0.14[b]	0.19[a] 0.62–0.47[b]	–	20	–	43.1
A. woodii [pMTL83151_$P_{pta\text{-}ack}$_Boost]								
YE	1.2	0.07	0.39[c]	0.22[d]	0.40[c] 0.67[d]	–	31	–	63.3
ARG	0.8	0.05	0.45[c]	0.10[d]	0.12[c] 0.40[d]	Ornithine, 13.8; citrulline 6.3	20	11	55.0

[a] Before time of induction

[b] After time of induction

[c] 0–22 h of cultivation

[d] 22–121 h of cultivation

– not detected

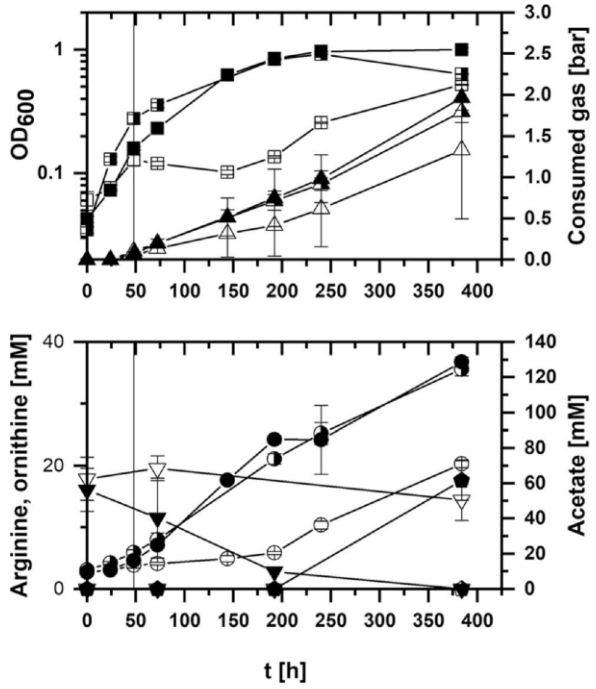

Fig. 4 *A. woodii* [pMTL83151_P_{tet}_Boost] growing autotrophically with either yeast extract (half-filled symbols; $n = 3$) or arginine (filled and empty symbols; $n = 2$) as nitrogen source. Cells growing with arginine were either induced (filled symbols) by 300 ng/ml anhydrotetracycline or non-induced (empty symbols). CO_2 was used as carbon and H_2 as energy source. Monitored OD_{600}, squares (□■◨); gas consumption (absolute value of accumulated pressure loss (bar)), upward triangles (△▲◭); acetate production, circles (○●◑); arginine consumption, downward triangles (▽▼); ornithine production, pentagons (⬟); time of induction with anhydrotetracycline (300 ng/ml) is indicated by a vertical line. Error bars indicate the standard deviations within biological replicates with plotted mean values

the ADI pathway can be exploited in *Clostridium autoethanogenum* to beneficially affect the metabolism via producing additional ATP and improving the growth of cells. So far, *A. woodii* is one of the fastest gas-consuming acetogens (Groher and Weuster-Botz 2016). The data presented in this study show that only recombinant *A. woodii* strains can make use of a heterologously expressed ADI pathway, controlled either by the P_{tet} or by the $P_{pta\text{-}ack}$ promoter, when arginine is supplemented to the medium. *A. woodii* cells are at least to some extent able to use arginine as nitrogen source, since a native arginine deiminase could cleave off ammonium and produce citrulline. Small amounts of fumarate detected in the supernatants of *A. woodii* [pMTL83151] hint to a native utilization of an urea cycle (Jackson et al. 1986), executed by the action of arginine deiminase, argininosuccinate synthetase (AS), and argininosuccinate lyase (AL), whose genes are all present in the genome of *A. woodii* and are encoded by *argA* (Awo_c08610), *argG* (Awo_c13540), and *argH* (Awo_c13530), respectively (Poehlein et al. 2012). The activity of AS and AL are responsible for the conversion of citrulline into argininosuccinate (Ratner 1954) and the subsequent cleavage to arginine and fumarate (Davison and Elliott 1952). This, however, would not result in a net gain of ammonium since the gained ammonium in the ADI reaction is eventually reinvested by the activity of argininosuccinate synthase reaction into aspartate (Ratner 1954). Puzzling, however, remains the question from where remaining nitrogen was acquired supporting the poor growth of *A. woodii* and *A. woodii* [pMTL83151] without significantly consuming provided arginine. One possibility could be the use of the amino group of cysteine hydrochloride which serves as reducing agent (1.7 mM) in the medium.

Our data showed great differences in the level of expression of the ADI pathway as well as in the determined specific GusA activities depending on whether the ADI operon or *gusA* was controlled by a constitutive or an inducible promoter. This strongly indicates that such differences in the level of (heterologous) expression very likely occur when any other gene is controlled by one of the latter promoters.

The expression on ADI genes controlled by the tetracycline-inducible promoter system P_{tet} caused beneficial effects on growth of recombinant cells consuming arginine compared to strong constitutive expression of the ADI genes using the $P_{pta\text{-}ack}$ promoter. In contrast, the strong, constitutive expression of the ADI genes in *A. woodii* [pMTL83151_$P_{pta\text{-}ack}$_Boost] led to poor or no growth in mixotrophically and autotrophically growing cells. This is surprising considering the highest theoretical ATP production from an active ADI pathway being equivalent to the ornithine excretion (Table 4). Most likely, the poor growth of *A. woodii* [pMTL83151_$P_{pta\text{-}ack}$_Boost] could be due to an excessive expression of *arcD* encoding the arginine:ornithine antiporter ArcD which is considered to be a homolog of transport membrane protein ArcD in *Lactococcus lactis* (Trip et al. 2013; Noens et al. 2015). It was shown from other membrane proteins that overexpression of the respective encoding genes can cause toxic effects to the cells (Wagner et al. 2008; O'Brien and Wright 2011). The fact that strong continuous expression in general may cause harmful effects also in other cells was shown for instance in *Saccharomyces cerevisiae* (Mumberg et al. 1994) and *E. coli* (Carrier et al. 1983). In addition, detection of citrulline in the supernatant of *A. woodii* [pMTL83151_$P_{pta\text{-}ack}$_Boost] indicates that the strong expression of the ADI genes caused an imbalance of metabolic flux of the ADI pathway. An elevated citrulline formation most likely dragged *A. woodii* [pMTL83151_$P_{pta\text{-}ack}$_Boost] cells to a further metabolic shift towards fumarate via the action of AS and AL. Citrulline excretion in relation to the ADI pathway was reported before in lactic acid bacteria with so far unknown physiological relevance (Liu and Pilone 1998; Noens and Lolkema 2017). However, it may be associated with a fast rate of citrulline formation (hydrolysis of arginine mediated by ADI) in contrast to slow removal of citrulline in the thermodynamically unfavorable ornithine carbamoyltransferase reaction (phosphorylation of citrulline

resulting in the formation of carbamyl-phosphate and ornithine) (Liu and Pilone 1998; Zúñiga et al. 2002).

On the other hand, the more moderate expression of the ADI pathway genes controlled by the P_{tet} promoter in *A. woodii* [pMTL83151_P_{tet}_Boost] cells resulted in a balanced arginine consumption and ornithine production promoting a significant growth advantage in terms of higher optical densities compared to non-induced cells as well as to cells using yeast extract as nitrogen source. This finding suggests that *A. woodii* [pMTL83151_P_{tet}_Boost] gains 1 extra mole of ATP per mole of arginine (Poolman et al. 1987; Liu and Pilone 1998) from the arginine deiminase pathway. This extra mole of ATP could be added to the theoretical amount of 4.3 moles of ATP per mole of fructose from glycolysis in combination with the Wood-Ljungdahl pathway (Schuchmann and Müller 2014), if all acetyl-CoA would be converted to acetate by the phosphotransacetylase reaction followed by substrate level phosphorylation (SLP) in the acetate kinase reaction. Remarkably, this was obviously not the case, since all recombinant strains expressing the ADI pathway showed considerably reduced acetate production yields (Table 4). The estimated fructose conversion into acetate in cells expressing the ADI pathway heterologously and consuming arginine was only two thirds compared to the respective control experiments. This is equivalent to a potential loss of 2 mol of CO_2 per fructose (or one mole of acetate) in the pyruvate:ferredoxin oxidoreductase reaction without further reduction to acetate. Thus, under the applied mixotrophic growth condition, there was presumably a downregulation of the Wood-Ljungdahl pathway. The surplus of electrons obtained from glycolysis and the pyruvate:ferredoxin oxidoreductase reaction were presumably converted into H_2 via the electron-bifurcating hydrogenase. Even if the production of hydrogen was not determined in the presented experiments, it is known that *A. woodii* is capable of H_2 production when growing chemoorganotrophically (Braun and Gottschalk 1981). The incomplete fructose conversion into acetate is an indication that less ATP was generated via SLP during the acetate kinase reaction. The loss of ATP from this reaction was more than compensated by the additional ATP gain obtained from arginine via the carbamate kinase (CK) reaction. Subsequently, the accessory acetyl-CoA has then been used for the production of biomass underlining the significant differences in final OD_{600} values. Under autotrophic growth conditions, *A. woodii* [pMTL83151_P_{tet}_Boost] cells had no detectable growth advantage when using arginine compared to yeast extract as nitrogen source (Fig. 4). However, this lack of evidence is most likely due to the very simple mode of performed batch experiments in bottles. It can be assumed that more advanced cultivation methods using gas fermentation reactor configurations will lead to a data set that allows a detailed evaluation (Grohner and Weuster-Botz 2016). Bioreactor experiments with continuous gas supply, pH control, and stirring of the culture broth usually have beneficial effects on growth and metabolism of cells compared to batch experiments in bottles. Moreover, detailed expression studies using RNA sequencing technologies can provide more insight in this matter and shed light on regulatory mechanisms as shown already for a variety of prokaryotes (Sorek and Cossart 2010). In *Lactococcus lactis*, it has been postulated that the ADI pathway (and the arginine biosynthetic operon) are both regulated by two transcriptional ArgR-type regulators (Larsen et al. 2004; Larsen et al. 2005). One of the two ArgR-type homologs (ArgR (llmg_2315)) binds to the *arcA* promoter region controlling the ADI pathway genes in an arginine-independent manner (Larsen et al. 2005). On the other hand, the second ArgR-type homolog (AhrC (llmg_1686)) represses the arginine biosynthesis and activates the expression of the ADI pathway genes only in combination of ArgR with arginine via reducing the affinity of ArgR to the operator (Larsen et al. 2005). Blastp analyses revealed that *C. autoethanogenum* as well possesses homologous proteins with 38% amino acid identity to ArgR (llmg_2315) and 58% amino acid identity to AhrC (llmg_1686) encoded in CAETHG_3019 and CAETHG_3208, respectively. A smart use of the regulators ArgR and AhrC could further improve the growth and lower energetic barriers in *A. woodii* metabolism.

The presented data show that *A. woodii* benefits from the supply of additional ATP using the recombinant ADI pathway; this might lead to an extended product range. This is in general desirable, since the current biotechnological application of acetogens is limited to a reduced amount of metabolic end products (Valgepea et al. 2017). Furthermore, the utilization of a defined medium such as the arginine-containing medium presented here, promoting optimal growth to *A. woodii* strains moderately expressing the ADI pathway, should be preferred over media containing complex ingredients such as yeast extract for the setup of precise carbon flux balances and for identification of limiting factors in growth experiments (Monod 1949). Additionally, pH regulation could be managed via sophisticated arginine supplementation in biotechnological processes minimizing the need of further addition of bases to the process, and thus lowering the production costs. Furthermore, the herein-described tetracycline-inducible promoter can be exploited as a valuable tool for general research in *A. woodii* regarding the cloning and expression of genes which cannot be accomplished using commonly used strong and constitutively active promoters (Hoffmeister et al. 2016; Bengelsdorf et al. 2018).

Acknowledgments We thank Eric Ransom and David Weiss for kindly providing plasmid pDSW1728. We thank Sophie Moormann, Julia Nothelfer, Judith Cammerer, and Lucille Exler for conducting enzymatic assays. The provision of the theophylline riboswitch sequence by Gerd Seibold and Christian Rückert is gratefully acknowledged. We thank the reviewers of this paper for constructive criticism and numerous helpful comments.

Funding information This study was funded by the ERA-IB5 program (project CO2CHEM, grant 031A566A).

Compliance with ethical standards

Conflict of interest Matthias H. Beck declares that he has no conflict of interest. Maximilian Flaiz declares that he has no conflict of interest. Frank R. Bengelsdorf declares that he has no conflict of interest. Peter Dürre declares that he has no conflict of interest.

Ethical approval This article does not contain any studies with human participants or animals performed by any of the authors.

References

Al-Hinai MA, Fast AG, Papoutsakis ET (2012) Novel system for efficient isolation of *Clostridium* double-crossover allelic exchange mutants enabling markerless chromosomal gene deletions and DNA integration. Appl Environ Microbiol 78:8112–8121. https://doi.org/10.1128/AEM.02214-12

Banerjee A, Leang C, Ueki T, Nevin KP, Lovley DR (2014) Lactose-inducible system for metabolic engineering of *Clostridium ljungdahlii*. Appl Environ Microbiol 80:2410–2416. https://doi.org/10.1128/AEM.03666-13

Bengelsdorf FR, Beck MH, Erz C, Hoffmeister S, Karl MM, Riegler P, Wirth S, Poehlein A, Weuster-Botz D, Dürre P (2018) Bacterial anaerobic synthesis gas (syngas) and CO_2 + H_2 fermentation. In: Advances in Applied Microbiology, vol 103. Elsevier, Amsterdam, pp 143–221

Braun K, Gottschalk G (1981) Effect of molecular hydrogen and carbon dioxide on chemo-organotrophic growth of *Acetobacterium woodii* and *Clostridium aceticum*. Arch Microbiol 128:294–298

Carrier MJ, Nugent ME, Tacon WCA, Primrose SB (1983) High expression of cloned genes in *E. coli* and its consequences. Trends Biotechnol 1:109–113. https://doi.org/10.1016/0167-7799(83)90033-1

Davison DC, Elliott WH (1952) Enzymic reaction between arginine and fumarate in plant and animal tissues. Nature 169:313–314. https://doi.org/10.1038/169313a0

de Souza Pinto Lemgruber R, Valgepea K, Tappel R, Behrendorff JB, Palfreyman RW, Plan M, Hodson MP, Simpson SD, Nielsen LK, Köpke M, Marcellin E (2019) Systems-level engineering and characterisation of *Clostridium autoethanogenum* through heterologous production of poly-3-hydroxybutyrate (PHB). Metab Eng 53:14–23. https://doi.org/10.1016/j.ymben.2019.01.003

Emerson DF, Woolston BM, Liu N, Donnelly M, Currie DH, Stephanopoulos G (2018) Enhancing hydrogen-dependent growth of and carbon dioxide fixation by *Clostridium ljungdahlii* through nitrate supplementation. Biotechnol Bioeng 116:294–306. https://doi.org/10.1002/bit.26847

Erz C (2017) 2,3-Butanediol production using acetogenic bacteria. PhD thesis, University of Ulm, Germany

Flitsch SK (2016) Identifikation und Charakterisierung von Regulatoren der Lösungsmittelbildung in *Clostridium acetobutylicum*. PhD thesis, University of Ulm, Germany

Flüchter S, Follonier S, Schiel-Bengelsdorf B, Bengelsdorf FR, Zinn M, Dürre P (2019) Anaerobic production of poly(3-hydroxybutyrate) and its precursor 3-hydroxybutyrate from synthesis gas by autotrophic clostridia. Biomacromolecules. https://doi.org/10.1021/acs.biomac.9b00342

Green MR, Sambrook J (2012) Molecular cloning: a laboratory manual, 4th edn. Cold Spring Harbor Laboratory Press, Cold Spring Harbor

Grimm V, Gleinser M, Neu C, Zhurina D, Riedel CU (2014) Expression of fluorescent proteins in bifidobacteria for analysis of host-microbe interactions. Appl Environ Microbiol 80:2842–2850. https://doi.org/10.1128/AEM.04261-13

Groher A, Weuster-Botz D (2016) Comparative reaction engineering analysis of different acetogenic bacteria for gas fermentation. J Biotechnol 228:82–94. https://doi.org/10.1016/j.jbiotec.2016.04.032

Heap JT, Pennington OJ, Cartman ST, Minton NP (2009) A modular system for *Clostridium* shuttle plasmids. J Microbiol Methods 78:79–85. https://doi.org/10.1016/j.mimet.2009.05.004

Hoffmeister S, Gerdom M, Bengelsdorf FR, Linder S, Flüchter S, Öztürk H, Blümke W, May A, Fischer R-J, Bahl H, Dürre P (2016) Acetone production with metabolically engineered strains of *Acetobacterium woodii*. Metab Eng 36:37–47. https://doi.org/10.1016/j.ymben.2016.03.001

Jackson MJ, Beaudet AL, O'Brien WE (1986) Mammalian urea cycle enzymes. Annu Rev Genet 20:431–464. https://doi.org/10.1146/annurev.ge.20.120186.002243

LanzaTech (2018) World's first commercial waste gas to ethanol plant starts up. https://www.lanzatech.com/2018/06/08/worlds-first-commercial-waste-gas-ethanol-plant-starts/2018/. Accessed 11 July 2019

Larsen R, Buist G, Kuipers OP, Kok J (2004) ArgR and AhrC are both required for regulation of arginine metabolism in *Lactococcus lactis*. J Bacteriol 186:1147–1157. https://doi.org/10.1128/JB.186.4.1147-1157.2004

Larsen R, Kok J, Kuipers OP (2005) Interaction between ArgR and AhrC controls regulation of arginine metabolism in *Lactococcus lactis*. J Biol Chem 280:19319–19330. https://doi.org/10.1074/jbc.M413983200

Liu S-Q, Pilone GJ (1998) A review: arginine metabolism in wine lactic acid bacteria and its practical significance. J Appl Microbiol 84:315–327. https://doi.org/10.1046/j.1365-2672.1998.00350.x

Monod J (1949) The growth of bacterial cultures. Annu Rev Microbiol 3:371–394. https://doi.org/10.1146/annurev.mi.03.100149.002103

Mumberg D, Müller R, Funk M (1994) Regulatable promoters of *Saccharomyces cerevisiae*: comparison of transcriptional activity and their use for heterologous expression. Nucleic Acids Res 22:5767–5768

Noens EEE, Lolkema JS (2017) Convergent evolution of the arginine deiminase pathway: the ArcD and ArcE arginine/ornithine exchangers. Microbiol Open 6:e00412. https://doi.org/10.1002/mbo3.412

Noens EEE, Kaczmarek MB, Żygo M, Lolkema JS (2015) ArcD1 and ArcD2 arginine/ornithine exchangers encoded in the arginine deiminase pathway gene cluster of *Lactococcus lactis*. J Bacteriol 197:3545–3553. https://doi.org/10.1128/JB.00526-15

O'Brien J, Wright GD (2011) An ecological perspective of microbial secondary metabolism. Curr Opin Biotechnol 22:552–558. https://doi.org/10.1016/j.copbio.2011.03.010

Poehlein A, Schmidt S, Kaster A-K, Goenrich M, Vollmers J, Thürmer A, Bertsch J, Schuchmann K, Voigt B, Hecker M, Daniel R, Thauer RK, Gottschalk G, Müller V (2012) An ancient pathway combining carbon dioxide fixation with the generation and utilization of a sodium ion gradient for ATP synthesis. PLoS One 7:e33439. https://doi.org/10.1371/journal.pone.0033439

Poolman B, Driessen AJ, Konings WN (1987) Regulation of arginine-ornithine exchange and the arginine deiminase pathway in *Streptococcus lactis*. J Bacteriol 169:5597–5604

Ransom EM, Ellermeier CD, Weiss DS (2015) Use of mCherry red fluorescent protein for studies of protein localization and gene expression in *Clostridium difficile*. Appl Environ Microbiol 81:1652–1660. https://doi.org/10.1128/AEM.03446-14

Ratner S (1954) Urea synthesis and metabolism of arginine and citrulline. Adv Enzymol Relat Subj Biochem 15:319–387

Schiel-Bengelsdorf B, Dürre P (2012) Pathway engineering and synthetic biology using acetogens. FEBS Lett 586:2191–2198. https://doi.org/10.1016/j.febslet.2012.04.043

Schiel-Bengelsdorf B, Montoya J, Linder S, Dürre P (2013) Butanol fermentation. Environ Technol 34:1691–1710. https://doi.org/10.1080/09593330.2013.827746

Schrumpf B, Schwarzer A, Kalinowski J, Pühler A, Eggeling L, Sahm H (1991) A functionally split pathway for lysine synthesis in *Corynebacterium glutamicum*. J Bacteriol 173:4510–4516

Schuchmann K, Müller V (2014) Autotrophy at the thermodynamic limit of life: a model for energy conservation in acetogenic bacteria. Nat Rev Microbiol 12:809–821. https://doi.org/10.1038/nrmicro3365

Sorek R, Cossart P (2010) Prokaryotic transcriptomics: a new view on regulation, physiology and pathogenicity. Nat Rev Genet 11:9–16. https://doi.org/10.1038/nrg2695

Trip H, Mulder NL, Lolkema JS (2013) Cloning, expression, and functional characterization of secondary amino acid transporters of *Lactococcus lactis*. J Bacteriol 195:340–350. https://doi.org/10.1128/JB.01948-12

Valgepea K, Loi KQ, Behrendorff JB, de Lemgruber RSP, Plan M, Hodson MP, Köpke M, Nielsen LK, Marcellin E (2017) Arginine deiminase pathway provides ATP and boosts growth of the gas-fermenting acetogen *Clostridium autoethanogenum*. Metab Eng 41:202–211. https://doi.org/10.1016/j.ymben.2017.04.007

Wagner S, Klepsch MM, Schlegel S, Appel A, Draheim R, Tarry M, Hogbom M, van Wijk KJ, Slotboom DJ, Persson JO, de Gier J-W (2008) Tuning *Escherichia coli* for membrane protein overexpression. Proc Natl Acad Sci U S A 105:14371–14376. https://doi.org/10.1073/pnas.0804090105

Woolston BM, Emerson DF, Currie DH, Stephanopoulos G (2018) Rediverting carbon flux in *Clostridium ljungdahlii* using CRISPR interference (CRISPRi). Metab Eng 48:243–253. https://doi.org/10.1016/j.ymben.2018.06.006

Zhang J, Liu Y-J, Cui G-Z, Cui Q (2015a) A novel arabinose-inducible genetic operation system developed for *Clostridium cellulolyticum*. Biotechnol Biofuels 8:36. https://doi.org/10.1186/s13068-015-0214-2

Zhang Y, Grosse-Honebrink A, Minton NP (2015b) A universal mariner transposon system for forward genetic studies in the genus *Clostridium*. PLoS One 10:e0122411. https://doi.org/10.1371/journal.pone.0122411

Zúñiga M, Pérez G, González-Candelas F (2002) Evolution of arginine deiminase (ADI) pathway genes. Mol Phylogenet Evol 25:429–444

Publisher's note Springer Nature remains neutral with regard to jurisdictional claims in published maps and institutional affiliations.

2.2 Production of the biocommodities butanol and acetone from methanol with fluorescent FAST-tagged proteins using metabolically engineered strains of *Eubacterium limosum*.

Flaiz, M.; Ludwig, G.; Bengelsdorf, F. R.; Dürre, P. Production of the biocommodities butanol and acetone from methanol with fluorescent FAST-tagged proteins using metabolically engineered strains of *Eubacterium limosum*. *Biotechnol. Biofuels* ***2021***, *14*, 117. https://doi.org/10.1186/s13068-021-01966-2

Rights and permissions

Published and reprinted under CC BY 4.0 (http://creativecommons.org/licenses/by/4.0).

The original article can be accessed via https://doi.org/10.1186/s13068-021-01966-2

Flaiz *et al. Biotechnol Biofuels* (2021) 14:117
https://doi.org/10.1186/s13068-021-01966-2

Biotechnology for Biofuels

RESEARCH Open Access

Production of the biocommodities butanol and acetone from methanol with fluorescent FAST-tagged proteins using metabolically engineered strains of *Eubacterium limosum*

Maximilian Flaiz*, Gideon Ludwig, Frank R. Bengelsdorf and Peter Dürre

Abstract

Background: The interest in using methanol as a substrate to cultivate acetogens increased in recent years since it can be sustainably produced from syngas and has the additional benefit of reducing greenhouse gas emissions. *Eubacterium limosum* is one of the few acetogens that can utilize methanol, is genetically accessible and, therefore, a promising candidate for the recombinant production of biocommodities from this C1 carbon source. Although several genetic tools are already available for certain acetogens including *E. limosum*, the use of brightly fluorescent reporter proteins is still limited.

Results: In this study, we expanded the genetic toolbox of *E. limosum* by implementing the fluorescence-activating and absorption shifting tag (FAST) as a fluorescent reporter protein. Recombinant *E. limosum* strains that expressed the gene encoding FAST in an inducible and constitutive manner were constructed. Cultivation of these recombinant strains resulted in brightly fluorescent cells even under anaerobic conditions. Moreover, we produced the biocommodities butanol and acetone from methanol with recombinant *E. limosum* strains. Therefore, we used *E. limosum* cultures that produced FAST-tagged fusion proteins of the bifunctional acetaldehyde/alcohol dehydrogenase or the acetoacetate decarboxylase, respectively, and determined the fluorescence intensity and product concentrations during growth.

Conclusions: The addition of FAST as an oxygen-independent fluorescent reporter protein expands the genetic toolbox of *E. limosum*. Moreover, our results show that FAST-tagged fusion proteins can be constructed without negatively impacting the stability, functionality, and productivity of the resulting enzyme. Finally, butanol and acetone can be produced from methanol using recombinant *E. limosum* strains expressing genes encoding fluorescent FAST-tagged fusion proteins.

Keywords: Acetogens, Anaerobes, C1-substrates, Fluorescence-activating and absorption shifting tag, Fluorescence reporter system, Fusion protein

Background

Acetogens are promising biocatalysts for the sustainable production of biocommodities since their ability to use carbon dioxide (CO_2)- and carbon monoxide (CO)-containing industrial waste gases as feedstock contributes to the reduction of greenhouse gas emissions. Nevertheless, the fermentation of such synthesis gas (syngas)

*Correspondence: maximilian.flaiz@uni-ulm.de
Institute of Microbiology and Biotechnology, Ulm University, Albert-Einstein-Allee 11, 89081 Ulm, Germany

© The Author(s) 2021. This article is licensed under a Creative Commons Attribution 4.0 International License, which permits use, sharing, adaptation, distribution and reproduction in any medium or format, as long as you give appropriate credit to the original author(s) and the source, provide a link to the Creative Commons licence, and indicate if changes were made. The images or other third party material in this article are included in the article's Creative Commons licence, unless indicated otherwise in a credit line to the material. If material is not included in the article's Creative Commons licence and your intended use is not permitted by statutory regulation or exceeds the permitted use, you will need to obtain permission directly from the copyright holder. To view a copy of this licence, visit http://creativecommons.org/licenses/by/4.0/. The Creative Commons Public Domain Dedication waiver (http://creativecommons.org/publicdomain/zero/1.0/) applies to the data made available in this article, unless otherwise stated in a credit line to the data.

faces technical challenges as the mass transfer of gases into the liquid state of media is quite poor and consequently limits microbial productivity [1]. An alternative to the C1 gases as a substrate is the use of methanol, since it bears the advantage of easy transport, storage, and is completely soluble in water, and does, therefore, not suffer from mass transfer issues [2]. Methanol can be produced from CO-, CO_2-, and H_2-containing syngas [3] and is a cheap, sustainable, and relatively pure feedstock for a variety of bacteria [4–7]. Several acetogens can utilize methanol via the Wood–Ljungdahl pathway [8], which has been elucidated in detail for *Acetobacterium woodii* [9]. Since the production of chemicals with methanol-utilizing acetogens seems to be auspicious, it is also of great interest to expand their molecular toolbox. Molecular tools with different levels of possibilities for metabolic engineering are available for acetogens such as *A. woodii*, *Clostridium ljungdahlii*, *C. autoethanogenum*, and *E. limosum.* That includes, e.g., genomic editing tools [10–14] and the expression of recombinant pathways to produce biocommodities such as butanol [15, 16], acetone [17–19], isopropanol [20], 3-hydroxybutyrate [21], or poly(3-hydroxybutyrate) [22]. However, fluorescent reporter systems which are well-established and often used tools in molecular biology to study gene expression [23, 24], promoter activities [25, 26], or the dynamics in microbial populations and co-cultures [27–29] are still restricted for acetogens, basically due to the lack of proteins that show bright fluorescence under anaerobic conditions. Recently, the fluorescence-activating and absorption shifting tag (FAST) [30] was established in *C. acetobutylicum* [31] and *C. ljungdahlii* [32] and opened the door for application in other anaerobic bacteria, since its fluorescence is bright and independent of oxygen. FAST is a small-sized protein with a mass of 14 kDa that only shows fluorescence when it forms a non-covalent reversible complex with a fluorogenic ligand, a so-called fluorogen [30, 33]. Those fluorogens are hydroxybenzylidene rhodanine derivatives that are non-fluorescent by themselves and only show fluorescence when bound to FAST [30]. Due to the small size, FAST is perfectly suited for genetic fusion to any protein of interest (POI) [30]. Such fusion proteins enable investigations of protein localization and intracellular dynamics [31, 34–36].

In this study, we aimed to expand the genetic toolbox of the Gram-positive, methanol-utilizing acetogen *E. limosum* [37], which is one of the few acetogens that is genetically accessible [13, 38], by establishing FAST as a fluorescent reporter system. We used FAST to construct FAST-tagged fusion proteins. As an initial approach, the bifunctional acetaldehyde/alcohol dehydrogenase (AdhE2) from *C. acetobutylicum*, which mediates the reaction from butyryl-CoA to butanol [39], was tagged with FAST and the respective gene expressed in recombinant *E. limosum* strains (Fig. 1). Since *E. limosum* produces butyryl-CoA naturally [40], the heterologous expression of the gene encoding the FAST-tagged AdhE2 fusion protein is sufficient to produce butanol. As a second approach, the acetoacetate decarboxylase (Adc) originating from *C. acetobutylicum* was FAST-tagged and the respective gene used to assemble an artificial acetone production operon (APO) also including the genes *thlA* and *ctfA/B* (encoding thiolase and acetoacetyl-CoA: acetate/butyrate-CoA transferase) originating from *C. acetobutylicum* [41, 42]. Thus, acetone production can be achieved by expression of the APO using recombinant *E. limosum* strains (Fig. 1). Evidence for heterologous production of the FAST-tagged AdhE2 and Adc fusion proteins within *E. limosum* mutants was provided by the determination of the fluorescence intensity of the respective bacterial populations producing the FAST-tagged fusion proteins during growth. Moreover, a comparison of production patterns of the biocommodities butanol and acetone using the C1 carbon source methanol provides first insight regarding stability, functionality, and productivity of the AdhE2 and Adc FAST-tagged fusion proteins.

Results

Growth of *E. limosum* using different carbon sources

E. limosum NG-6894 was cultivated heterotrophically using glucose or methanol as well as autotrophically using $H_2 + CO_2$ and syngas as carbon and energy source. Heterotrophically cultivated cells using glucose reached a maximal optical density (OD_{600}) of 2.83 with a growth rate of 0.23 h^{-1}. Cell cultures grown on various methanol concentrations of 50, 100, and 200 mM showed maximal OD_{600} values of 1.4, 2, and 2.6, respectively, while having a similar growth rate of about 0.09 h^{-1} (Fig. 2a and Table 1). Autotrophically grown cells using $H_2 + CO_2$ showed the lowest growth rate of 0.02 h^{-1} and a maximal OD_{600} value of 0.6. Cultivation using syngas resulted in a maximal OD_{600} of 2.9 and a growth rate of 0.06 h^{-1} (Fig. 2b and Table 1). *E. limosum* NG-6894 produced acetate and butyrate under heterotrophic as well as under autotrophic growth conditions, while the ratio between these products varied depending on the substrates used. Acetate and butyrate production started at the end of the exponential growth phase and reached their maximum in the stationary growth phase after the substrate was consumed completely. Heterotrophically grown cells using glucose showed a product ratio of acetate:butyrate of 6:1, which shifted to 2:1 when cells were cultivated with methanol, independent of the used amount of methanol (Table 1). *E. limosum* NG-6894 cells cultivated autotrophically using $H_2 + CO_2$ produced

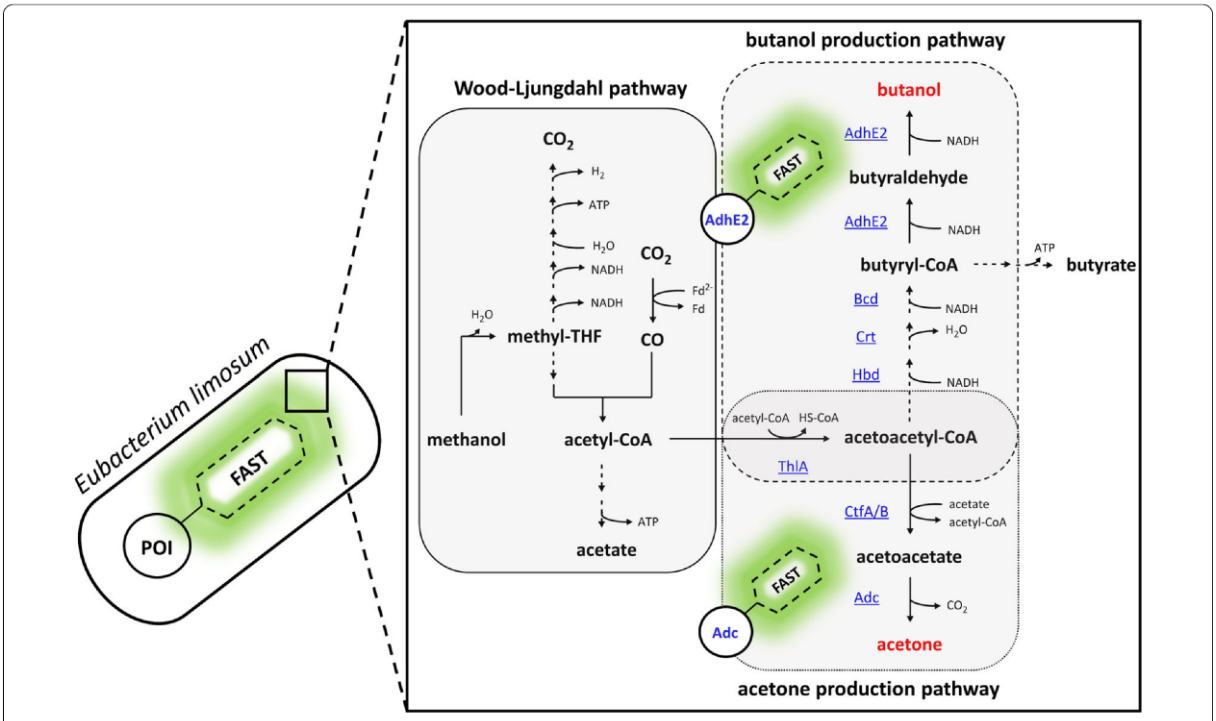

Fig. 1 Schematic overview of the WLP based on Kremp *et al*. [9] coupled with the recombinant butanol and acetone production pathway in *E. limosum*. Butanol and acetone production can be achieved with FAST-tagged AdhE2 and Adc fusion proteins, respectively. ThlA, thiolase; CtfA/B, acetoacetyl-CoA:acetate/butyrate-CoA transferase; Adc, acetoacetate decarboxylase; Hbd, 3-hydroxybutyryl-CoA dehydrogenase; Crt, crotonase; Bcd, butyryl-CoA dehydrogenase; AdhE2, bifunctional acetaldehyde/alcohol dehydrogenase

the highest amounts of acetate (85 mM) and only low amounts of butyrate (2.4 mM), which resulted in a product ratio of 36:1. Cells grown using syngas achieved an acetate:butyrate ratio of 9:2 (Table 1). As a control, cells cultivated without the addition of a defined carbon source except for the standard medium components carbonate and yeast extract accomplished only one doubling and produced traces of acetate (2.2–6 mM).

Engineering of the fluorescence activation and absorption shifting tag in *E. limosum*

After transformation, the recombinant *E. limosum* [pMTL83251_P_{bgaL}_FAST] expressed the FAST-encoding gene (*feg*) controlled by the lactose-inducible *bgaR*-P_{bgaL} promoter. Cells of that strain showed bright fluorescence during growth only in the presence of the fluorogen ^{TF}Lime after induction of gene expression (Fig. 3). *E. limosum* [pMTL83251_P_{bgaL}_FAST] was cultivated on glucose and reached a 26-fold higher maximum fluorescence intensity after 48 h of cultivation compared to the non-induced strain. Cells of the non-induced strain did not show any fluorescence except autofluorescence in the presence of ^{TF}Lime. Both, the induced and the non-induced strain reached similar maximal OD_{600} values of 3 and 3.1 after 24 h of cultivation, respectively. The empty vector control *E. limosum* [pMTL83251] reached an OD_{600} of 2.7 and showed only autofluorescence when supplemented with ^{TF}Lime (Fig. 3a). Fluorescence microscopy was used to image fluorescent cells (Fig. 3b). The resulting micrographs show brightly fluorescent cells of *E. limosum* [pMTL83251_P_{bgaL}_FAST] with induced gene expression. Non-induced as well as cells of the empty vector control *E. limosum* [pMTL83251] did not show any fluorescence. Nevertheless, fluorescence microscopy revealed an inhomogeneous population of fluorescent and non-fluorescent *E. limosum* [pMTL83251_P_{bgaL}_FAST] cells. *E. limosum* [pMTL83251_P_{bgaL}_FAST] cells expressing *feg* and cultivated under equal growth conditions were analyzed at single cell level using flow cytometry (Fig. 3c). Initial autofluorescence of cells of the empty vector control strain *E. limosum* [pMTL83251] was determined and gated as non-fluorescent events. Cells of the strain *E. limosum* [pMTL83251_P_{bgaL}_FAST] with lactose-induced *feg* expression resulted in a clear shift showing a population with green fluorescence and confirming the results obtained by fluorescence microscopy. Flow cytometry data revealed that in the late exponential growth phase

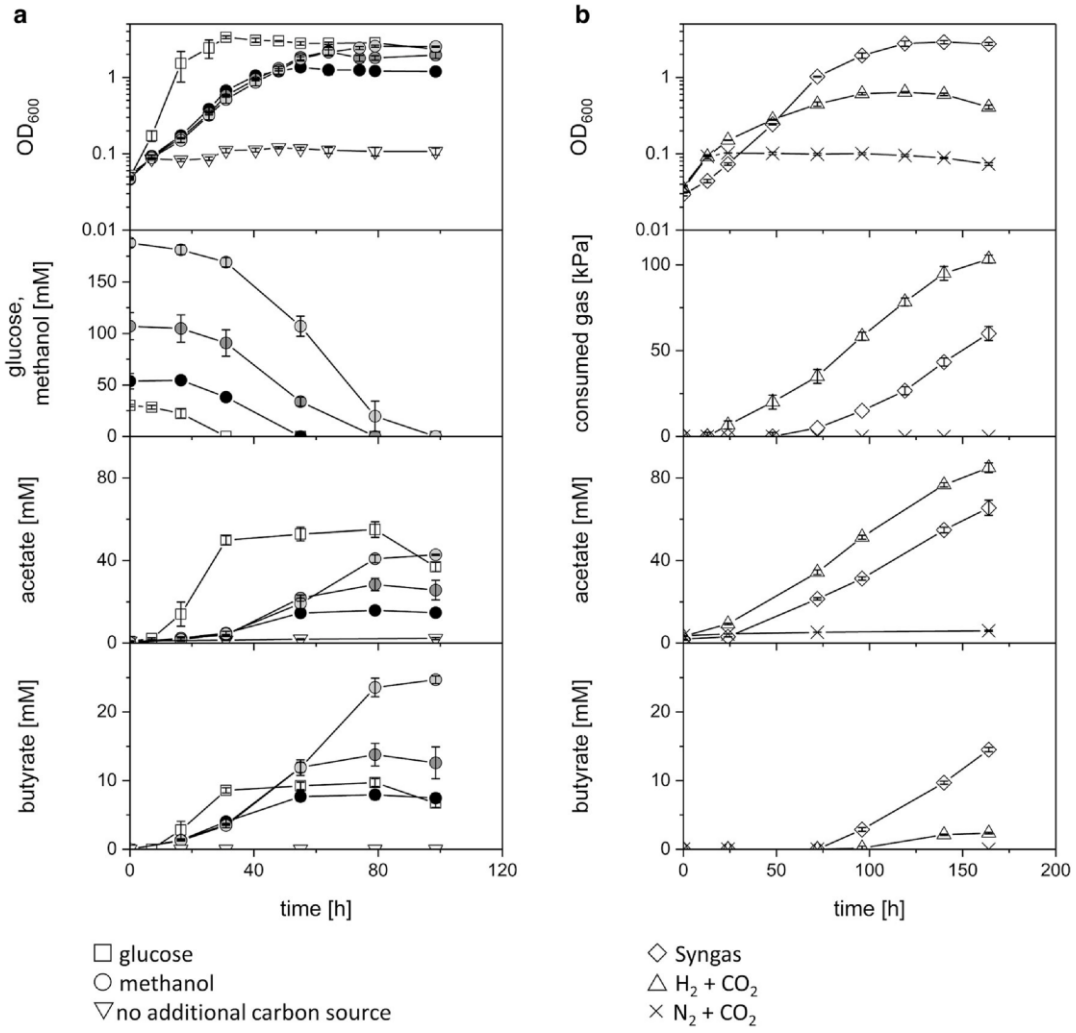

Fig. 2 **a** Heterotrophic and **b** autotrophic growth experiments using *E. limosum* NG-6894 cultivated on different carbon and energy sources. *E. limosum* was cultivated with 30 mM glucose (white); 50 (black), 100 (dark gray), or 200 mM (gray) methanol; without additional carbon source; Syngas; $H_2 + CO_2$; $N_2 + CO_2$. OD_{600}, glucose, methanol, and gas consumption (absolute value of accumulated pressure loss) as well as acetate and butyrate production were monitored. Error bars indicate standard deviations. n = 3

62% of induced *E. limosum* [pMTL83251_P_{bgaL}_FAST] cells were fluorescent, while 38% of them were non-fluorescent. The number of fluorescent cells increased in the stationary growth phase up to 72%. In the late stationary growth phase, after 72 h of cultivation, the number of fluorescent cells decreased to 59%. The population of the non-induced cells showed no shift and were non-fluorescent during all determined time points (Fig. 3d).

Furthermore, the fluorescence of FAST-producing cells cultivated with methanol as carbon and energy source was examined. In addition to *E. limosum* [pMTL83251_P_{bgaL}_FAST] a strain termed *E. limosum* [pMTL83251_P_{thlA}_FAST] was constructed that expressed *feg* under the control of the constitutive P_{thlA} promoter. *E. limosum* [pMTL83251] harboring the empty vector control showed only autofluorescence when the fluorogen ^{TF}Lime was supplemented (Fig. 4a). The constitutive expression of *feg* by *E. limosum* [pMTL83251_P_{thlA}_FAST] caused a clear and increasing fluorescence during growth and a maximum intensity during the stationary stage (Fig. 4b). The fluorescence intensity of cells that produced FAST constitutively was 5.1-fold higher compared to the autofluorescence of *E. limosum* [pMTL83251]. The lactose-induced expression of *feg* by

Table 1 Comparison of growth characteristics and products of *E. limosum* NG-6894 cultivated using various carbon and energy sources

Substrate	Max. OD_{600}	Growth rate (h^{-1})	Doubling time (h)	Products (mM)		Products (mol/100 mol substrate)		Product ratio (acetate:butyrate)[a]
				Acetate	Butyrate	Acetate	Butyrate	
Glucose								
30 mM	2.8	0.23	3	55	9.7	183.2	32.4	6:1
Methanol								
50 mM	1.4	0.09	7.7	15.8	8	29.5	14.8	2:1
100 mM	2	0.09	7.7	28.4	13.8	26.6	12.9	2:1
200 mM	2.6	0.09	7.7	42.8	24.7	22.8	13.1	2:1
Gases								
$H_2 + CO_2$	0.6	0.02	34.7	85	2.4	n.d.	n.d.	36:1
Syngas	2.9	0.06	11.6	65.5	14.5	n.d.	n.d.	9:2

[a] Product ratios were calculated for products in (mM) and (mol/100 mol substrate)

n.d. not determined

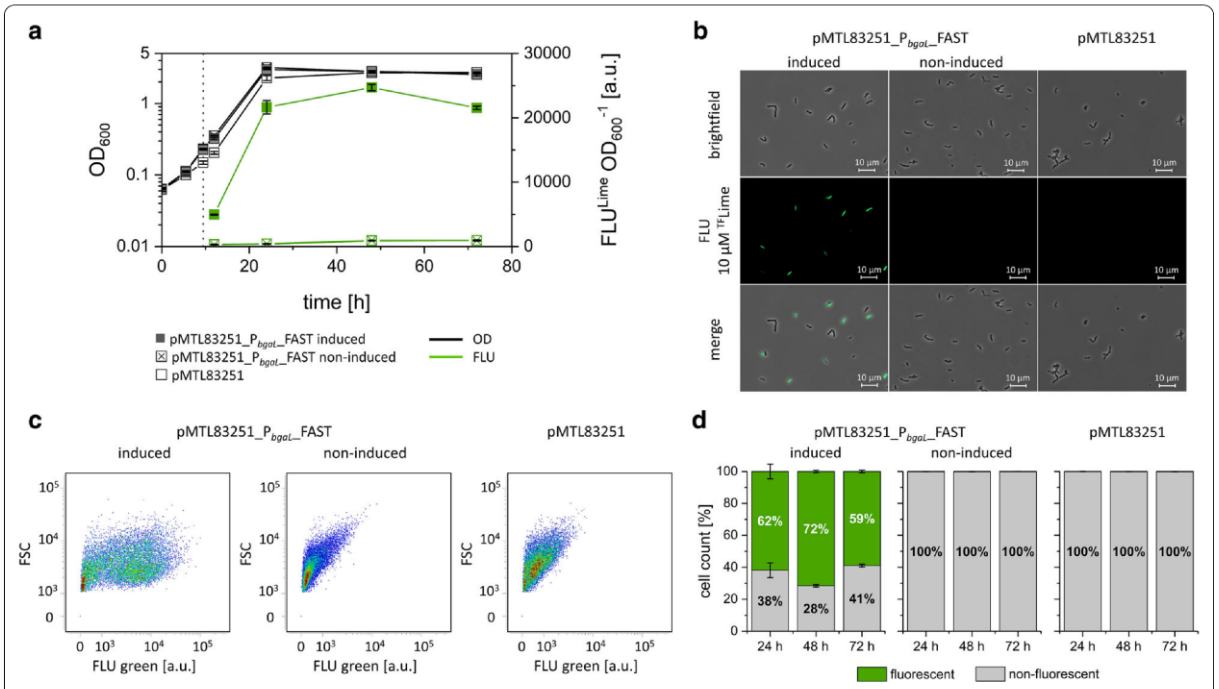

Fig. 3 **a** Fluorescence intensity of recombinant *E. limosum* strains during growth in presence of the fluorogen ^{TF}Lime. Cells were cultivated using 30 mM glucose. Monitored were OD_{600} and fluorescence intensity of *E. limosum* [pMTL83251_P_{bgaL}_FAST] with induced and non-induced gene expression as well as *E. limosum* [pMTL83251]. **b** Micrographs of *E. limosum* [pMTL83251_P_{bgaL}_FAST] and *E. limosum* [pMTL83251] after 72 h of incubation. Gene expression of cells was either induced or non-induced. **c** Density plots of *E. limosum* [pMTL83251_P_{bgaL}_FAST] and *E. limosum* [pMTL83251] after 72 h of incubation. Gene expression of cells was either induced or non-induced. **d** Number of fluorescent *E. limosum* cells determined after 24 h, 48 h, and 72 h cultivation. n = 3

E. limosum [pMTL83251_P_{bgaL}_FAST] caused clear fluorescence during cultivation and reached a maximum at 114 h in the stationary growth phase (Fig. 4c). Non-induced cells only showed autofluorescence in the same order of magnitude as cells of the empty vector control *E. limosum* [pMTL83251]. The fluorescence intensity of lactose-induced cells was 3.5- and 3.3-fold higher compared to non-induced cells and those of the empty

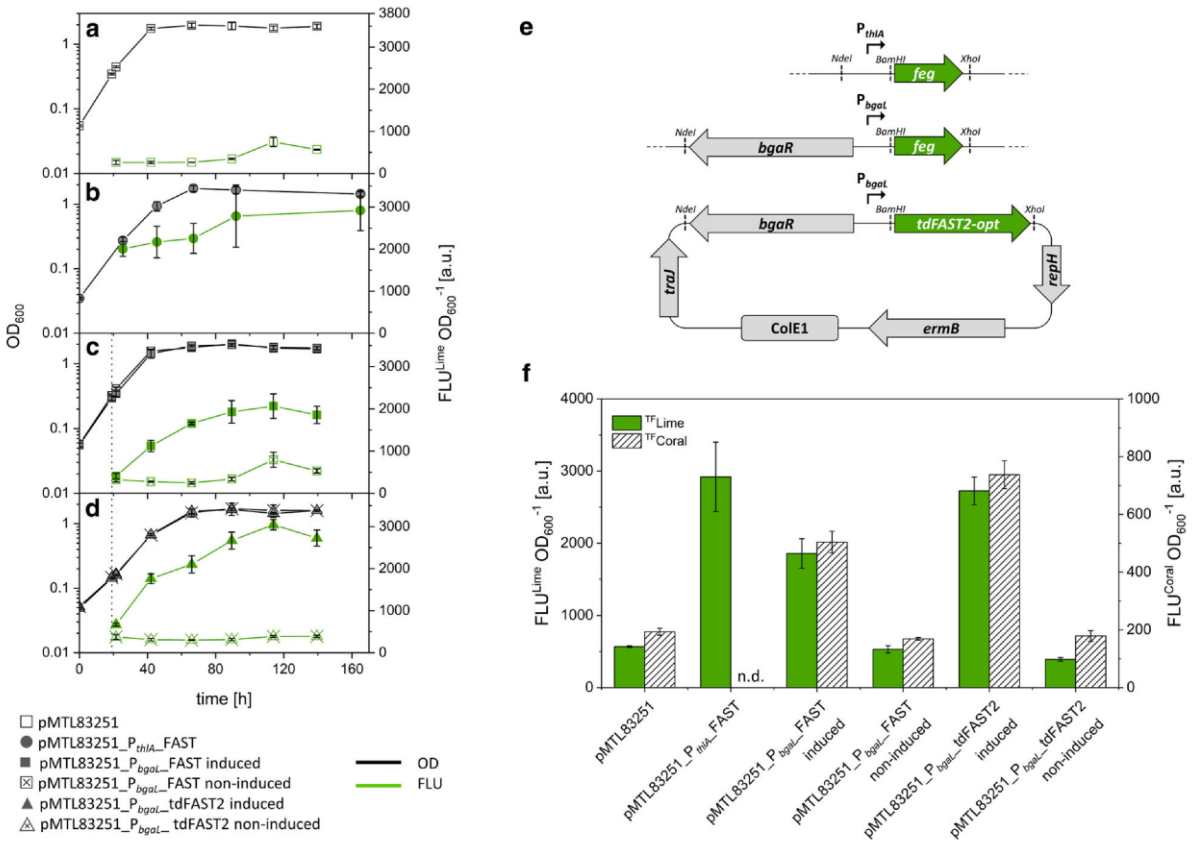

Fig. 4 Fluorescence intensity of recombinant *E. limosum* strains grown on methanol (100 mM) in presence of the fluorogen ^{TF}Lime. **a** OD_{600} and fluorescence intensity of *E. limosum* [pMTL83251], **b** *E. limosum* [pMTL83251_P_{thlA}_FAST], **c** *E. limosum* [pMTL83251_P_{bgaL}_FAST], and **d** *E. limosum* [pMTL83251_P_{bgaL}_tdFAST2] were monitored. Gene expression of *E. limosum* [pMTL83251_P_{bgaL}_FAST] and *E. limosum* [pMTL83251_P_{bgaL}_tdFAST2] was either induced by lactose or non-induced. Time of induction with lactose is indicated with the vertical dotted line. n=3, error bars show standard deviation. **e** Genetic maps of plasmids representing pMTL83251_P_{thlA}_FAST (top), pMTL83251_P_{bgaL}_FAST (middle), and pMTL83251_P_{bgaL}_tdFAST2 (bottom). Fluorescence during growth of cells harboring respective plasmids are shown in panel b, c, and d, respectively. **f** Maximal fluorescence intensity of recombinant *E. limosum* strains in the presence of the fluorogen ^{TF}Lime or ^{TF}Coral. Mean fluorescence was determined during stationary growth phase at an OD_{600} of ~ 1.5, n = 3, error bars show standard deviation. n = 3

vector control respectively. *E. limosum* [pMTL83251_P_{thlA}_FAST] producing FAST constitutively showed a 1.6-fold higher fluorescence intensity comparing to that of cells with induced *feg* gene expression (Fig. 4f). Although cultivation of *E. limosum* [pMTL83251_P_{bgaL}_FAST] resulted in fluorescence, cells cultivated using glucose led to a 13.3-fold enhanced fluorescence intensity compared to cells cultivated on methanol.

Also, tdFAST2 was codon optimized for *E. limosum* and the respective gene used to construct the plasmid pMTL83251_P_{bgaL}_tdFAST2 harboring the gene *tdFAST2-opt* under the control of the *bgaR*-P_{bgal} lactose-inducible promoter (Fig. 4e). The induced expression of the codon-optimized *tdFAST2-opt* gene with *E. limosum* [pMTL83251_P_{bgaL}_tdFAST2] resulted in a 1.5-fold improved fluorescence compared to *E. limosum* [pMTL83251_P_{bgaL}_FAST] expressing *feg* controlled by the same promoter (Fig. 4f). The non-induced cells of *E. limosum* [pMTL83251_P_{bgaL}_tdFAST2] only showed autofluorescence.

Moreover, the fluorescence intensity of recombinant *E. limosum* strains expressing *feg* or *tdFAST2-opt* was examined when supplemented with the red fluorescent dye ^{TF}Coral after excitation at 516 nm (Fig. 4f). The use of the fluorogen ^{TF}Coral caused clear fluorescence of *E. limosum* [pMTL83251_P_{bgaL}_FAST] after induction of *feg* gene expression and showed 3- and 2.6-fold higher intensities compared to non-induced cells and those harboring the empty vector control, respectively. Furthermore, induced *E. limosum* [pMTL83251_P_{bgaL}_tdFAST2] cells

showed a 1.5-fold higher fluorescent intensity compared to induced cells of *E. limosum* [pMTL83251_P_{bgaL}_FAST] in presence of ^{TF}Coral. Non-induced as well as cells of the empty vector control showed autofluorescence only.

Butanol production using FAST-tagged AdhE2 fusion proteins by recombinant *E. limosum* strains

FAST was fused to the C- or the N-terminus of AdhE2 (CA_P0035) using a flexible glycine linker. The resulting fusion proteins were used to examine the impact of the fluorescent FAST tag on functionality and productivity of AdhE2. Both AdhE2 fusion proteins were heterologously produced using the strains *E. limosum* [pMTL83251_P_{bgaL}_C-FAST-AdhE2] (C-terminal tag) and *E. limosum* [pMTL83251_P_{bgaL}_N-FAST-AdhE2] (N-terminal tag). *E. limosum* [pMTL83251_P_{bgaL}_AdhE2] produced the native AdhE2 from *C. acetobutylicum* and was constructed and served as a control for butanol production using glucose or methanol as a carbon source.

Cultivation of *E. limosum* [pMTL83251_P_{bgaL}_C-FAST-AdhE2] using glucose as a carbon source and induced gene expression resulted in a maximal OD_{600} of 2.5 and a growth rate of 0.16 h^{-1}. Non-induced cells reached an OD_{600} of 3 with a growth rate of 0.17 h^{-1}. Clear fluorescence was observed after induction of gene expression, proving production of the C-terminal FAST-tagged AdhE2 fusion protein. Fluorescence increased during growth and reached a maximum in the late exponential growth phase. Non-induced cells showed only autofluorescence. The acetate:butyrate ratio was 10:1 and 8:1 for induced and non-induced cells, respectively. Butanol and ethanol were produced after induction of gene expression of the gene encoding the C-terminal FAST-tagged AdhE2 fusion protein. Induced cells produced up to 1 mM ethanol and 0.6 mM butanol at the end of the exponential growth phase. Non-induced cells produced traces of ethanol (0.3 mM), while no butanol was detected (Fig. 5a, Table 2, and Additional file 1: Table S1).

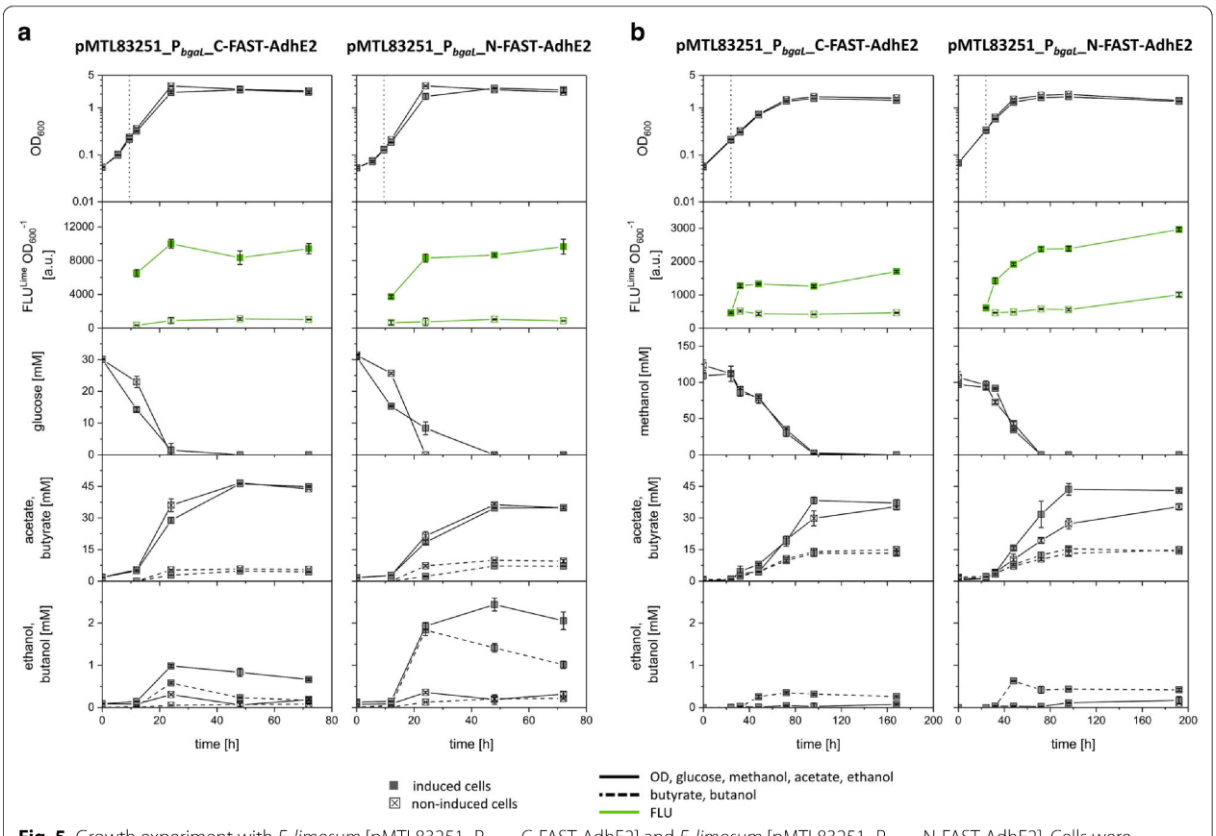

Fig. 5 Growth experiment with *E. limosum* [pMTL83251_P_{bgaL}_C-FAST-AdhE2] and *E. limosum* [pMTL83251_P_{bgaL}_N-FAST-AdhE2]. Cells were cultivated using **a** 30 mM glucose or **b** 100 mM methanol. Gene expression of cells was either induced by lactose or non-induced. Time of induction with lactose is indicated with the vertical dotted line. OD_{600}, fluorescence intensity in presence of ^{TF}Lime, glucose or methanol consumption as well as acetate, butyrate, ethanol, and butanol production were monitored. Error bars indicate standard deviations. n = 3

Table 2 Growth characteristics, ethanol, and butanol production of recombinant *E. limosum* strains characterized in growth experiments using glucose as carbon source

Recombinant *E. limosum* strains	OD_{max}	Growth rate (h^{-1})	Ethanol (mM)	Butanol (mM)
pMTL83251_P_{bgaL}_AdhE2				
Induced	2.5	0.17	1.9	1.6
Non-induced	2.8	0.2	0.3	0.3
pMTL83251_P_{bgaL}_C-FAST-AdhE2				
Induced	2.5	0.16	1	0.6
Non-induced	3	0.17	0.3	0
pMTL83251_P_{bgaL}_N-FAST-AdhE2				
Induced	2.7	0.18	2.4	1.8
Non-induced	3	0.22	0.4	0.2

Table 3 Growth characteristics, ethanol, and butanol production of recombinant *E. limosum* strains characterized in growth experiments using methanol as carbon source

Recombinant *E. limosum* strains	OD_{max}	Growth rate (h^{-1})	Ethanol (mM)	Butanol (mM)
pMTL83251_P_{bgaL}_AdhE2				
Induced	1.5	0.05	0.1	0.6
Non-induced	1.7	0.05	0	0
pMTL83251_P_{bgaL}_C-FAST-AdhE2				
Induced	1.6	0.05	0.1	0.4
Non-induced	1.8	0.05	0	0
pMTL83251_P_{bgaL}_N-FAST-AdhE2				
Induced	1.7	0.06	0.2	0.6
Non-induced	2	0.06	0	0

E. limosum [pMTL83251_P_{bgaL}_C-FAST-AdhE2] cultivated using methanol as a carbon source showed a growth rate of 0.05 h^{-1} with induced and non-induced gene expression and reached OD_{600} values of 1.6 and 1.8, respectively. Clear fluorescence was determined after induction of gene expression that caused production of the FAST-tagged AdhE2 fusion protein and resulted in a 3.7-fold higher intensity compared to autofluorescence of non-induced cells. The induced culture showed an acetate:butyrate ratio of 3:1, while the non-induced culture showed a ratio of 2:1. Only the induced culture of *E. limosum* [pMTL83251_P_{bgaL}_C-FAST-AdhE2] produced traces of ethanol (0.1 mM) and up to 0.4 mM butanol from methanol at the end of the exponential growth phase. Non-induced strains did not produce any alcohols (Fig. 5c, Table 3, and Additional file 1: Table S2).

E. limosum [pMTL83251_P_{bgaL}_N-FAST-AdhE2] cells producing the N-terminal FAST-tagged AdhE2 fusion protein, showed distinct fluorescence after induction of gene expression when cultivated with glucose, and reached a maximal OD_{600} of 2.7 with a growth rate of 0.18 h^{-1}. Non-induced cells showed autofluorescence only and reached a maximal OD_{600} of 3 with a growth rate of 0.22 h^{-1}. Fluorescence intensities were comparable to those determined for *E. limosum* [pMTL83251_P_{bgaL}_C-FAST-AdhE2] cultivated using glucose. An acetate:butyrate ratio of 5:1 was determined for induced and 4:1 for non-induced cells. Up to 2.4 mM ethanol and 1.8 mM butanol were produced at the end of the exponential growth phase with cells that expressed the gene encoding the N-terminal FAST-tagged AdhE2 fusion protein. Moreover, the uninduced cells produced up to 0.4 mM ethanol and 0.2 mM butanol (Fig. 5b, Table 2, and Additional file 1: Table S1).

E. limosum [pMTL83251_P_{bgaL}_N-FAST-AdhE2] cultivated using methanol showed a growth rate of 0.06 h^{-1}, while the induced and non-induced cells reached an OD_{600} of 1.7 and 2, respectively. Induced cells produced the N-terminal FAST-tagged AdhE2 fusion protein after induction of gene expression and showed distinct fluorescence during growth with a maximum at the early stationary stage. Non-induced cells only showed autofluorescence. The acetate:butyrate ratio shifted from 3:1 to 2:1 for the induced and non-induced cells, respectively. Consequently, that strain produced 0.2 mM of ethanol and 0.6 mM of butanol at the end of the exponential growth phase. Non-induced cells again did not produce any alcohols (Fig. 5d, Table 3, and Additional file 1: Table S2). Finally, the strain that produced the N-terminal tagged version of AdhE2 showed a 1.4-fold higher fluorescence intensity compared to the strain that produced the C-terminal tagged version.

The control culture *E. limosum* [pMTL83251_P_{bgaL}_AdhE2] that produced the non-tagged version of AdhE2 showed similar characteristics regarding growth rate and production patterns. Cells were grown with glucose as a carbon source and reached a maximal OD_{600} of 2.5 with a growth rate of 0.17 h^{-1} when *adhE2* gene expression was induced. Non-induced cells showed improved growth with a maximal OD_{600} of 2.8 and a growth rate of 0.2 h^{-1}. The acetate:butyrate ratio was 6:1 in the case of the induced and 5:1 in the case of the non-induced cells. Gene expression of *adhE2* in an inducible manner resulted in the production of up to 1.9 mM ethanol and 1.6 mM butanol at the end of the exponential growth phase. Non-induced cells only produced traces of ethanol and butanol (0.3 mM) (Additional file 1: Fig. S1A, Table S1, Table 2). Both, the induced as well as the non-induced cells of *E. limosum* [pMTL83251_P_{bgaL}_AdhE2] were cultivated with methanol and showed a growth rate of 0.05 h^{-1} with maximal OD_{600} values of 1.5 and 1.7, respectively. The acetate:butyrate ratio shifted to 3:1 for the induced and 2:1 for the non-induced cells. Induced

expression of *adhE2* caused production of 0.6 mM butanol and traces of ethanol (0.1 mM) in the late exponential growth phase during these batch experiments. The non-induced cells produced no alcohols from methanol (Additional file 1: Fig. S1B, Table S2, Table 3).

Acetone production with FAST-tagged Adc fusion proteins using recombinant *E. limosum* strains

The fluorescent FAST tag had no obvious negative effect on the catalytic properties of AdhE2. Subsequently, *feg* was fused to *adc* and the respective gene was expressed constitutively, together with the remaining genes of the APO, using the promoter P_{thlA}. Thus, the two strains designated *E. limosum* [pMTL83251_P_{thlA}_C-FAST-Adc] and *E. limosum* [pMTL83251_P_{thlA}_N-FAST-Adc] were constructed that produced either the C- or N-terminal FAST-tagged Adc fusion protein, respectively. Those constructed strains were used to perform growth experiments to prove the functionality and productivity of the FAST-tagged Adc fusion proteins.

E. limosum [pMTL83251_P_{thlA}_C-FAST-Adc] and *E. limosum* [pMTL83251_P_{thlA}_N-FAST-Adc] were cultivated with glucose and showed growth rates of about 0.15 h^{-1} while reaching maximal OD_{600} values of 3.3 and 3.1, respectively (Fig. 6a and Table 4). Both strains produced acetone, acetate, and butyrate as metabolic end products (Additional file 1: Table S1 and Table 4). *E. limosum* [pMTL83251_P_{thlA}_C-FAST-Adc] cells that constitutively expressed the APO genes produced 0.8 mM of acetone, while fluorescence intensity was 2.3-fold higher compared to the autofluorescence of the empty vector control strain. *E. limosum* [pMTL83251_P_{thlA}_N-FAST-Adc] cells that expressed the gene encoding the N-terminal FAST-tagged Adc fusion protein produced only traces of acetone (0.1 mM) and exhibited 1.5-fold higher fluorescence compared to the autofluorescence of the empty vector control strain (Fig. 6b and Table 4). The control strain *E. limosum* [pMTL83251_P_{thlA}_act], expressing the non-FAST-tagged native genes of the APO controlled by the P_{thlA} promoter, reached an OD_{600} of 3, had a growth rate of 0.15 h^{-1}, and produced acetate, butyrate as well as

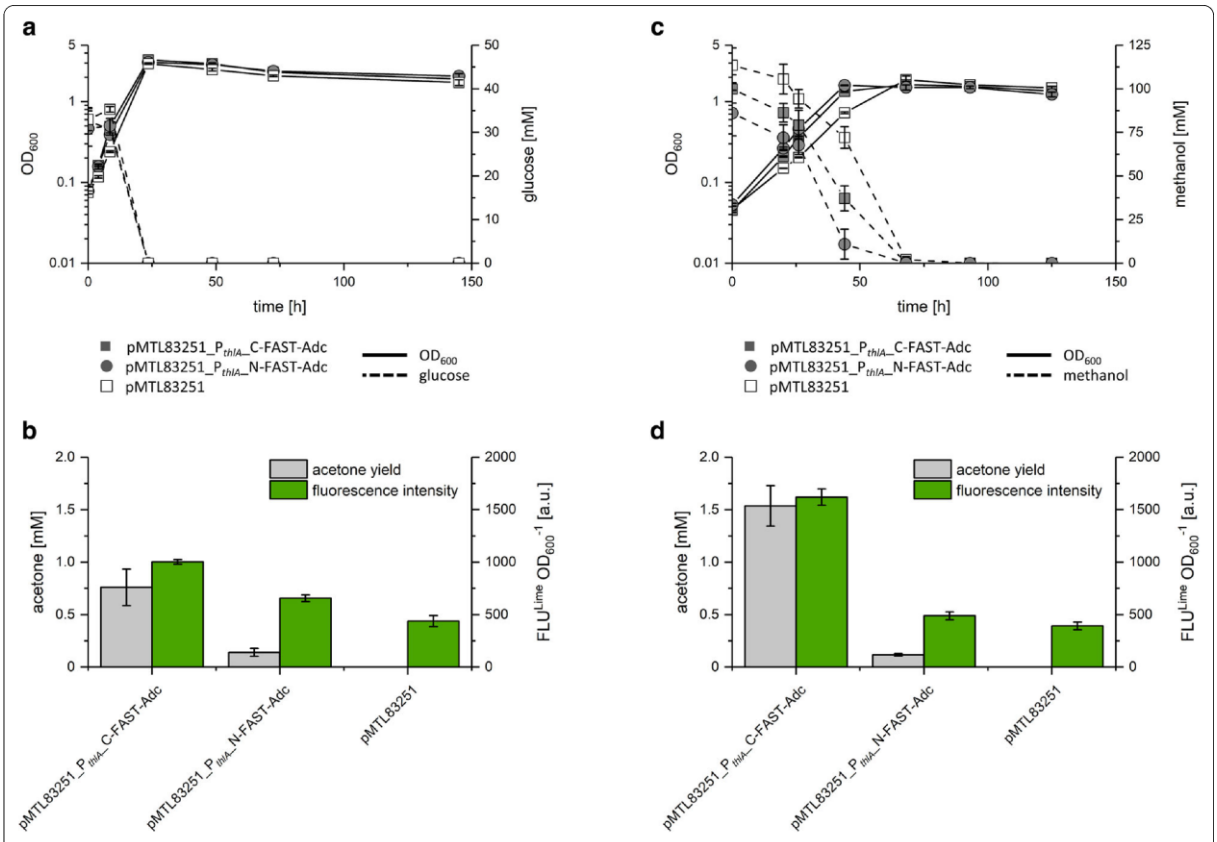

Fig. 6 Growth experiment using *E. limosum* [pMTL83251_P_{thlA}_C-FAST-Adc], *E. limosum* [pMTL83251_P_{thlA}_N-FAST-Adc], and *E. limosum* [pMTL83251]. Cells were cultivated using **a**, **b** 30 mM glucose or **c**, **d** 100 mM methanol as carbon source. Displayed are **a**, **c** OD_{600} and substrate consumption as well as **b**, **d** maximal acetone concentrations and fluorescence intensities. Error bars indicate standard deviations. n = 3

Table 4 Growth characteristics and acetone production of recombinant *E. limosum* strains characterized in growth experiments using glucose or methanol as carbon source

Recombinant *E. limosum* strains	Cultivated using glucose			Cultivated using methanol		
	OD_{max}	Growth rate (h^{-1})	Acetone (mM)	OD_{max}	Growth rate (h^{-1})	Acetone (mM)
pMTL83251_P_{thlA}_act	3	0.15	0.8	1.7	0.06	0.3
pMTL83251_P_{thlA}_C-FAST-Adc	3.3	0.15	0.8	1.6	0.08	1.6
pMTL83251_P_{thlA}_N-FAST-Adc	3.1	0.15	0.1	1.6	0.07	0.1

0.8 mM acetone (Additional file 1: Fig. S2A and Table 4). The empty vector control *E. limosum* [pMTL83251] had a maximal growth rate of 0.17 h^{-1}, reached a maximal OD_{600} of 2.5, showed only autofluorescence, and did not produce any acetone.

Cultivation of *E. limosum* [pMTL83251_P_{thlA}_C-FAST-Adc] and *E. limosum* [pMTL83251_P_{thlA}_N-FAST-Adc] using methanol as a carbon source resulted in maximal growth rates of 0.08 and 0.07 h^{-1}, respectively (Fig. 6c and Table 4). Both cultures reached a maximal OD_{600} of 1.6 and produced acetate, butyrate, and acetone (Additional file 1: Table S2 and Table 4). *E. limosum* [pMTL83251_P_{thlA}_C-FAST-Adc] produced the highest amount of acetone (1.6 mM) cultivated using methanol, while the strain *E. limosum* [pMTL83251_P_{thlA}_N-FAST-Adc] expressing the gene encoding N-terminal tagged Adc fusion protein only produced 0.1 mM acetone. Fluorescence intensity of *E. limosum* [pMTL83251_P_{thlA}_C-FAST-Adc] was four- and three-fold higher compared to the fluorescence of *E. limosum* [pMTL83251] and *E. limosum* [pMTL83251_P_{thlA}_N-FAST-Adc], respectively (Fig. 6d). *E. limosum* [pMTL83251_P_{thlA}_C-FAST-Adc] cultivated using methanol showed a twofold higher acetone production as well as fluorescence intensity when compared to the cells cultivated using glucose. *E. limosum* [pMTL83251_P_{thlA}_N-FAST-Adc] showed minor fluorescence and low amounts of acetone under both conditions tested. *E. limosum* [pMTL83251_P_{thlA}_act] cultivated using methanol reached an OD_{600} of 1.7, had a growth rate of 0.6 h^{-1}, and produced acetate and butyrate in a ratio of 2:1 and 0.3 mM acetone (Additional file 1: Fig S2B, Table 4). The empty vector control *E. limosum* [pMTL83251] reached a maximal OD_{600} of 1.9 with a growth rate of 0.07 h^{-1}, did not produce any acetone, and only showed autofluorescence in the presence of ^{TF}Lime.

Discussion

Methanol promotes butyrate production in *E. limosum*

Since we are aiming to produce butanol and acetone using recombinant *E. limosum* strains, different carbon sources were investigated as alternatives to commonly used sugars. Therefore, we focused on non-food feedstock-derived C1 carbon sources such as methanol, H_2 + CO_2, and CO containing syngas and their impact on growth behavior and product spectrum of *E. limosum*. Cultivation of *E. limosum* using methanol resulted in higher growth rates compared to cells cultivated with the C1 gases as reported before [43, 44]. The C1 carbon sources clearly influenced the product spectrum of *E. limosum*, since high amounts of methanol (200 mM) resulted in improved butyrate production titers. Methanol is oxidized to CO_2 via the WLP which provides three mol NAD(P)H per methyl group oxidized [45, 47]. The NAD(P)H-$NAD(P)^+$ balance is regulated during butyrate production since the reactions catalyzed by 3-hydroxybutyryl-CoA dehydrogenase and crotonase are NADH dependent and, therefore, regenerate $NAD(P)^+$. Thus, the acetate:butyrate ratio shifts in favor of butyrate when cells grow on methanol [46]. Moreover, the utilization of methanol yields 1.83 ATP/butyrate, while H_2 + CO_2 utilization only yields 1 ATP/butyrate [47]. As shown for *C. autoethanogenum* and *A. woodii* mutants, improved ATP supply benefits fast growth and abolishes acetate production [48, 49]. In general, cultivation with methanol results in high efficiencies of bioproduction compared to the cultivation with the C1 gases [50, 51]. High amounts of methanol (200 mM) had no clear negative impact on the growth of *E. limosum*. Thus, sustainably produced methanol could be a promising substitute for glucose and C1 gases as substrate. During our experiments, the wild-type strain *E. limosum* NG-6894 did not produce any butanol. However, *E. callanderi* KIST612 (former *E. limosum* KIST612) produces low amounts of butyrate from methanol [52] as well as traces of butanol from CO [53]. Natural butanol production from C1 gases is reported for the methanol-utilizing acetogen *Butyribacterium methylotrophicum,* which is closely related to *E. limosum* [54]. In *B. methylotrophicum*, the production of one mol butanol from methanol requires six reducing equivalents and yields 1.5 ATP/butanol [47].

Establishment of FAST as fluorescent reporter in *E. limosum*

We established FAST as a fluorescent reporter protein for *E. limosum* and determined the fluorescence of *feg* expressing cells using a microplate reader, fluorescence microscopy, and flow cytometry. Lactose-induced expression of *feg* caused bright fluorescence of respective *E. limosum* cells, no matter if fluorescence analytics were carried out under aerobic or anaerobic conditions. Interestingly, the *bgaR*-P_{bgaL} lactose-inducible system originating from *C. perfringens* was tightly regulated in *E. limosum*, since only cells with induced *feg* expression showed bright fluorescent cells. This tightly regulated expression of the *bgaR*-P_{bgaL} promoter was also reported for *C. perfringens* [55] *C. acetobutylicum* [56], and *C. ljungdahlii* [17], while gene expression was found to be leaky in *A. woodii* [49]. Moreover, we also showed constitutive FAST production with the P_{thlA} promoter from *C. acetobutylicum*. This constitutive expression caused improved fluorescence of cells compared to the lactose-induced *feg* expression. As of yet, only a very limited number of fluorescent proteins were shown to be somewhat functional in anaerobes, since the fluorescence of the most common fluorescent reporters including GFP and its derivatives is oxygen dependent [57]. Mostly, the flavin mononucleotide-based fluorescent proteins (FbFPs) [58] were used in anaerobes as fluorescent reporters as reported for *Clostridium cellulolyticum* [26], *Clostridioides difficile, Clostridium acetobutylicum, Clostridium sordellii* [35], *C. ljungdahlii* [59], *Clostridium beijerinckii* [60], and *Clostridium tyrobutyricum* [61]. Moreover, Shin *et al.* [13] established an engineered FbFP version (CreiLOV) as a reporter gene in *E. limosum* ATCC8486. Although FbFPs are functional under anoxic conditions, they show a fairly low brightness compared to control strains that do not express the respective fluorescent protein. In contrast, the FAST system was recently established in *C. acetobutylicum* and *C. ljungdahlii* and showed a clear and obvious fluorescence [31, 32, 62]. The fluorescence of recombinant *E. limosum* strains expressing *feg* constructed in this work is up to 26-fold improved compared to the control strain. Thus, FAST seems to be perfectly suited as a fluorescent reporter for anaerobic bacteria. An alternative to FAST could be the SNAP- and the Halo-Tag, which were shown to be functional in *C. acetobutylicum* and *C. ljungdahlii* [32]. Both tags show oxygen-independent bright fluorescence when covalently bound to a fluorogenic ligand. However, both tags require a quite long labeling time. Moreover, compared to the 14 kDa of FAST the SNAP- and Halo-Tag are larger proteins with a mass of 19.4 and 33 kDa respectively. In sum, FAST seems to be best suited for the construction of fusion proteins.

As dimerized fluorescent proteins can result in brighter fluorescence [63], we used tdFAST2 to improve fluorescence brightness with *E. limosum*. Compared to cells producing FAST, Tebo et al. [64] could show a 3.8-fold brighter fluorescence of tdFAST2-producing HEK 293 T cells. Here, we achieved a 1.5-fold improved fluorescence by expressing the codon-optimized gene encoding tdFAST2 in *E. limosum* confirming the findings of Tebo et al. [64] that production of tdFAST2 improves fluorescence brightness. With approx. 28 kDa, the molecular mass of tdFAST2 is comparable to the mass of EGFP or mCherry [65]. The improved brightness of tdFAST2 also improves the detection limit of tdFAST2-tagged proteins which might be important especially for protein localization experiments [66]. As we only showed a 1.5-fold improved fluorescence of tdFAST2, we chose the less bright but smaller FAST for the construction of AdhE2 and Adc fusion proteins.

Fluorescence microscopy of FAST-producing *E. limosum* cells revealed that plasmid-based induced expression of *feg* caused bright fluorescent *E. limosum* cells showing an inhomogeneous population. This finding was confirmed by respective flow cytometry experiments which revealed that the number of fluorescent cells varies between 72 and 59%. Such a phenotypic heterogeneity of bacterial populations with plasmid-based induced gene expression was previously reported [67–69]. One possible reason that might cause these heterogeneous populations is the usage of the lactose-inducible promoter system. The resulting *feg* gene expression may not only depend on the amount of inducer, but also on the uptake mechanism of the inducer molecule [68]. The lactose-inducible *bgaR*-P_{bgaL} system was also used in *C. perfringens* to express the gene *yfp-pilB* which encodes a yellow fluorescent protein-tagged fusion protein and caused an inhomogeneous fluorescent population [55]. In this experiment, Hartman et al. [55] reported that YFP-PilB was detected in 73% of the cells. Moreover, the inhomogeneous population might be caused by plasmid instability or even the loss of the plasmid encoding the reporter gene [67]. Siebert et al. [69] reported an inhomogeneous population of *Oligotropha carboxidovorans* which expressed the gene encoding mCherry in a plasmid-based manner. The reported inhomogeneity was overcome by the genomic integration of the respective gene encoding mCherry into the genome of *Oligotropha carboxidovorans*. Genomic integration of *feg* into *E. limosum* should be possible using the CRISPR-Cas9 genome editing tool [13].

Five different fluorogens are commercially available at The Twinkle Factory which can bind FAST and its variants to form the fluorescent FAST:fluorogen complex [33, 70]. Expression of *feg* or the gene encoding tdFAST2

resulted in green or red fluorescence when ^{TF}Lime or ^{TF}Coral was used, respectively. As different bacteria and proteins show autofluorescence upon excitation with different wavelength [34, 71, 72], FAST should be considered as a fluorescent reporter protein in a large variety of bacteria as the choice of the fluorogen can be adapted to the spectral conditions needed for the study. Recently, Tebo *et al.* [73] reported two engineered FAST versions termed greenFAST and redFAST. While greenFAST binds ^{TF}Lime, redFAST only binds ^{TF}Coral, which we showed can both be used in *E. limosum.* These two FAST variants augmented the FAST system and facilitate applications including two-color or even mixed culture imaging in anoxic environments.

C- and N-terminally tagged AdhE2 and Adc fusion protein construction

In this study, we designed AdhE2 and Adc FAST-tagged fusion proteins and expressed respective genes in recombinant *E. limosum* strains. The X-ray crystal structure of Adc (3BH2) originating from *C. acetobutylicum* was provided by Ho et al. [74], but to our knowledge there is none for AdhE2 from *C. acetobutylicum*. Based on the crystal structure, first hints can be derived if either the C- or N-terminal end of the protein should be tagged without causing negative impacts regarding the folding, activity, and productivity of the enzyme. The probability of creating a functional fusion protein was maximized as both the C- and N- terminal tagged versions of both Adc and AdhE2 were constructed [75]. This approach diminishes the risk of constructing non-functional fusion proteins since the interactions of the C- and N- terminal end with other structures within the enzyme are unpredictable, especially for AdhE2. We further used a flexible GS linker as it was shown to promote proper folding of the enzyme and improves the stability of fusion proteins [76]. We cloned the native genes and genes encoding the FAST-tagged fusion proteins without affecting non-coding regions including promoters. As a result, the native genes as well as the genes encoding the FAST-tagged fusion proteins were expressed under the control of the same promoter. We consequently assume that native and tagged genes are transcribed at comparable levels.

The increasing fluorescence of *E. limosum* [pMTL83251_P_{bgaL}_C-FAST-AdhE2] and *E. limosum* [pMTL83251_P_{bgaL}_N-FAST-AdhE2] during growth proves the production of the C- and N-terminal tagged AdhE2 fusion proteins after induction of gene expression. Butanol production with strains producing the C- and N-terminal tagged AdhE2 fusion proteins prove that AdhE2 is still functional even with the fluorescent tag. The functionality of the N-terminal tagged version of AdhE2 seems not to be affected since the respective strain produced similar amounts of alcohols as the strain expressing the non-tagged native *adhE2* of *C. acetobutylicum*. However, the productivity of the C-terminal tagged version seems slightly reduced since less alcohol was produced compared to the strains just expressing *adhE2*. In addition to butanol, ethanol was produced, since AdhE2 converts not only butyryl-CoA to butanol but also acetyl-CoA to ethanol via the respective aldehyde [77]. Interestingly, if cells of both strains were cultivated with glucose as carbon source, fluorescence of the N- and C-terminal tagged fusion proteins was improved compared to cultivation on methanol. This also indicates an improved production of the fusion proteins. Moreover, both strains cultivated on glucose produced more butanol as well as ethanol compared to the cells of the respective strain cultivated using methanol. This finding indicates a coherence between the fluorescence of cells expressing genes encoding *adhE2* fusion proteins and the amount of recombinantly produced product.

In the case of the constitutive production of FAST-tagged Adc fusion proteins, only the C-terminal FAST-tagged version of Adc produced by *E. limosum* [pMTL83251_P_{thlA}_C-FAST-Adc] showed clear fluorescence. The strain *E. limosum* [pMTL83251_P_{thlA}_N-FAST-Adc] producing the N-terminal tagged version of Adc only showed a low fluorescence intensity and acetone productivity. Several factors might affect the fluorescence brightness of fluorescent fusion proteins including intrinsic brightness, folding efficiency, and translation efficiency [78]. Adc itself forms a homododecameric complex with a total mass of 365 kDa [74]. We assume, based on the X-ray structure, that the free C-terminal end of the non-tagged Adc subunits is not interfering with any residues of the protein and, therefore, not harming folding efficiency. However, the N-terminal end of Adc seems to form hydrogen bonds with LYS45, ARG44, VAL47, and GLU49 of the closest subunit. Therefore, the fusion of FAST with the sterically hindered N-terminal end might indeed affect the folding efficiency of the fusion protein or even prevents the formation of the homododecameric complex [79]. In contrast, the folding efficiency of the C-terminal FAST-tagged Adc does not seem to be affected as cells producing the respective fusion protein are fluorescent. Heterologous expression of *adc* originating from *C. acetobutylicum* and the FAST-tagged variants with *E. limosum* might result in inefficient translation regarding their different codon usage [80]. Adapting *adc* as well as genes encoding respective FAST-tagged Adc fusion proteins to the codon usage of *E. limosum* might improve translation efficiency causing enhanced protein production and improved fluorescence brightness. Nevertheless, *E. limosum* [pMTL83251_P_{thlA}_C-FAST-Adc] produced up

to 0.8 mM acetone when cultivated with glucose and 1.6 mM from methanol providing evidence that the C-terminal tagged Adc fusion protein is functional and forms the catalytically active homododecameric Adc complex. *E. limosum* [pMTL83251_P_{thlA}_act] expressing the native genes of the APO produced 0.8 mM and 0.3 mM acetone when cultivated with glucose or methanol, respectively. This finding shows that the productivity of the C-terminal tagged Adc fusion protein is not negatively affected. To our knowledge, acetone was neither produced with *E. limosum* nor from the sustainable C1 carbon source methanol before. Although acetone production from methanol seems to be promising, several improvements of this recombinant pathway must be performed including codon harmonization, genomic integration, and bioreactor experiments which usually show a beneficial effect on bioproduction.

Conclusions

In this study, we implemented the fluorescent activating and absorption shifting tag as an oxygen-independent fluorescent reporter protein in *E. limosum*. We showed that this reporter protein is functional under various growth conditions and can be adapted to the natural spectral properties of the organism using different fluorogens. We showed that the fluorescence of *feg*-expressing cells can be determined using a microplate reader, fluorescence microscopy, or flow cytometry. Butanol, as well as acetone, was produced by expressing the native genes of *C. acetobutylicum* and genes encoding fluorescent FAST-tagged fusion proteins. The expression of the genes encoding the fluorescent FAST-tagged fusion proteins enabled to monitor protein production during growth. We showed that those fusion proteins are functional and that the productivity is not negatively affected, however, dependent on which end the protein was tagged. The use of FAST as a fluorescence reporter not only expands the molecular toolbox of *E. limosum* but also is a promising reporter tool for other anaerobic bacteria as well. For the first time, we could show the production of the biocommodities acetone and butanol from methanol with recombinant *E. limosum* strains.

Methods

Strains, medium, and cultivation

The strains used in this study are listed in Table 5. *E. coli* DH5α was used for plasmid cloning and cultivated in liquid modified lysogeny broth (1% tryptone, 1% NaCl, 0.5% yeast extract) [81] while shaking or on respective agar plates at 37 °C. When required medium was supplemented with 250 µg mL^{-1} erythromycin. *E. limosum* NG-6894 was cultivated in modified DSM 135 medium under strictly anaerobic conditions at 37 °C. The modified DSM 135 medium contained 12.9 mM KH_2PO_4, 48.5 mM K_2HPO_4, 18.7 mM NH_4Cl, 49.6 mM NaCl, 58.9 mM $KHCO_3$, 2.8 mM L-cysteine-HCl, 1.5 mM $MgSO_4$, 4.4 µM resazurin, 0.2% (wt/vol) yeast extract, 0.1% (vol/vol) trace element solution SL-9 [82], 0.1% (vol/vol) selenite-tungstate solution [82], and 0.2% (vol/vol) vitamin solution DSM 141. If necessary, the medium was supplemented with antibiotics (5 µg mL^{-1} clarithromycin) after autoclaving. Heterotrophic cultivations of *E. limosum* was carried out in 50 mL medium in 125 mL Müller–Krempel flasks and were supplemented with 30 mM glucose or 50, 100 or 200mM methanol. Autotrophic cultivations were also carried out in 50 mL medium in 500 mL Müller–Krempel flasks, which were pressurized to 1.1 bar overpressure with $H_2 + CO_2$ (67% H_2 + 33% CO_2) or syngas (10% CO_2, 40% CO, 10% N_2, 40% H_2) and repressured when below 0.5 bar. Before growth experiments were carried out, cells were grown from DMSO stock cultures in 5 mL of the respective medium. These 5 mL cultures were used to prepare 50 mL precultures supplemented with glucose or methanol for subsequent growth experiments. For autotrophic growth experiments, cells from 5 mL cultures were adapted to growth conditions by transferring them two times to fresh 50 mL medium in 500 mL Müller–Krempel culture flasks with the respective gas atmosphere.

Plasmid construction

All plasmids and primers used in this study are listed in Tables 6 and 7, respectively. DNA fragments for cloning purposes were amplified using the KAPA Hifi

Table 5 Strains used in this study

Strain	Description	Source
E. coli DH5α	*E. coli* for plasmid construction	Thermo Fisher Scientific Inc., Waltham, MA, USA
E. limosum NG-6894	This strain grows on a defined medium (without any yeast extract) and does not produce any sticky polymers	Prof. Philippe Soucaille, INSA, University of Toulouse, France

polymerase (Kapa Biosystem, Sigma-Aldrich Chemie GmbH, Munich, Germany). Primers used in this study were synthesized by biomers.net GmbH (Ulm, Germany) and designed to have a 15–25 nucleotide overlap with the respective vector DNA. Vector DNA for cloning purposes was linearized using Fast digest enzymes (Thermo Fisher Scientific Inc., Waltham, USA). PCR and digested vector DNA fragments were purified using the NucleoSpin® Gel and PCR clean-up kit (Macherey-Nagel GmbH & Co. KG, Düren, Germany). All plasmids were constructed by assembling PCR and vector DNA fragments using the NEBuilder Hifi DNA Assembly Cloning Kit according to the manufacturer's protocol (New England Biolabs, Ipswich, MA, USA). Assembled plasmids were used for the transformation of chemically competent *E. coli* DH5α cells and verified via Sanger sequencing (Eurofins Genomics GmbH, Luxemburg).

To establish FAST as a reporter protein in *E. limosum*, plasmids harboring *feg* were constructed. Therefore, *feg* was amplified together with the promoter P_{thl}^{sup} from plasmid p95thl^{sup}FAST [31] using primers FW_Pthlsup_FAST_NdeI and RV_Pthlsup_FAST_XhoI (Table 7). The amplified PCR fragment was cloned via *Nde*I and *Xho*I recognition sites into vector pMTL83251 resulting in the plasmid pMTL83251_P_{thl}^{sup}_FAST. The promoter region of P_{thl}^{sup} from plasmid pMTL83251_P_{thl}^{sup}_FAST was further exchanged with the lactose-inducible *bgaR*-P_{bgaL} system from *C. perfringens* [55] and P_{thlA} from *C. acetobutylicum* [18]. Therefore, the *bgaR*-P*bgaL*-encoding DNA fragment was amplified from plasmid pMTL83151_gusA_P_{bgaL} [49] using the primers FW_PbgaL_NdeI and RV_PbgaL_BamHI. The DNA fragment containing the promoter region of P_{thlA} was amplified from plasmid pJIR750_act [18] using primers FW_Pthl_NdeI and RV_Pthl_BamHI (Table 7). Both promoter containing DNA fragments were assembled with pMTL83251_P_{thl}^{sup}_FAST (excision of P_{thl}^{sup}) resulting in plasmids pMTL83251_P_{thlA}_FAST and pMTL83251_P_{bgaL}_FAST.

The gene *feg* of pMTL83251_P_{bgaL}_FAST was exchanged with the gene encoding tdFAST2. The sequence of tdFAST2 was obtained from Tebo et al. [64] and codon optimized for *E. limosum* using the GENEius tool (Eurofins Genomics GmbH, Luxemburg) and synthesized by Eurofins Genomics Germany GmbH (Ebersberg, Germany). The gene *tdFAST2-opt* was amplified from the delivered plasmid pEX-A128_tdFAST2-opt using the primers FW_tdFAST2-opt_BamHI and RV_tdFAST2-opt_XhoI (Table 7) and ligated with *Bam*HI and *Xho*I digested pMTL83251_P_{bgaL}_FAST (excision of *feg*) vector DNA resulting in plasmid pMTL83251_P_{bgaL}_tdFAST2.

For butanol production with *E. limosum,* the plasmid pMTL83251_P_{bgaL}_AdhE2 was constructed. The gene *adhE2* was amplified from genomic DNA of *C. acetobutylicum* using primers FW_C1_adhe2 and RV_N2_adhE2 (Table 7). The gene was assembled under the control of the lactose-inducible *bgaR*-P_{bgaL} promoter using the plasmid DNA of pMTL83251_P_{bgaL}_FAST, which was digested using *Bam*HI and *Xho*I (excision of *feg*).

For acetone production with *E. limosum,* the plasmid pMTL83251_P_{thlA}_act was constructed encoding the genes of the APO under the control of promoter P_{thlA}. The origin of these genes as well as their locus tags are listed in Table 6. These genes as well as the DNA fragment containing the promoter region of P_{thlA} were amplified from plasmids pJIR750_act using primers FW_act_NdeI and RV_act_XhoI (Table 7). The amplified PCR fragments were cloned via the *Nde*I and *Xho*I restriction sites of pMTL83251 resulting in the plasmids pMTL83251_P_{thlA}_act.

Moreover, plasmids were constructed to produce C- and N- terminal FAST-tagged fusion proteins of AdhE2 and Adc. FAST was C- and N-terminal fused to AdhE2 or Adc using a glycine linker (GGGGS) with the sequence ggtggtggtggttct. For the construction of C-terminal tagged fusion proteins, the 3' end of the gene of interest was fused to the 5' end of *feg.* Therefore, the gene of interest was amplified without its stop codon while *feg* was amplified without its start codon. To construct N-terminal FAST-tagged fusion proteins, the 3′ end of *feg* was fused to the 5′ end of the gene of interest. The gene of interest was amplified without its start codon, while *feg* was amplified without its stop codon.

The plasmid pMTL83251_P_{bgaL}_C-FAST-AdhE2 was constructed to produce the C-terminal FAST-tagged AdhE2 fusion protein. *adhE2* was amplified from plasmid pMTL83251_P_{bgaL}_AdhE2 using primers FW_C1_adhE2 and RV_C1_adhE2-FAST (Table 7), *feg* was amplified from plasmid pMTL83251_P_{bgaL}_FAST using primers FW_C2_adhE2-FAST and RV_C2_FAST (Table 7). Primers RV_C1_adhE2-FAST and FW_C2_adhE2-FAST contain the sequence for the glycine-linker. The plasmid pMTL83251_P_{bgaL}_N-FAST-AdhE2 was constructed to produce the N-terminal FAST-tagged AdhE2 fusion protein. *adhE2* was amplified from plasmid pMTL83251_P_{bgaL}_AdhE2 using primers FW_N1_adhE2 and RV_N1_FAST-adhE2 while *feg* was amplified from plasmid pMTL83251_P_{bgaL}_FAST using primers FW_N2_FAST-adhE2 and RV_N2_adhE2 (Table 7). Primers RV_N1_FAST-adhE2 and FW_N2_FAST-adhE2 contain the sequence for the glycine linker.

The plasmid pMTL83251_P_{thlA}_C-FAST-Adc was constructed to produce the C-terminal FAST-tagged Adc fusion protein. *adc* was amplified from plasmid pMTL83251_P_{thlA}_act using primers FW_C1_adc and RV_C1_adc-FAST, and *feg* was amplified from plasmid

Table 6 Plasmids used in this study

Plasmid	Description	Source
pMTL83251	ColE1 ori$^-$, pCB102 ori$^+$, Em^r, *traJ*, *lacZ*	[83]
pMTL83151_gusA_P_{bgaL}	ColE1 ori$^-$, pCB102 ori$^+$, Cm^r, *traJ*, *lacZ*, *gusA* from *E. coli*, *bgaR*-P_{bgaL} from *C. perfringens*	[49]
pJIR750_act	pJIR750; P_{thl}, *thlA* (CAC2873), *ctfA/B* (CA_P0163/P0164), *adc* (CA_P0165) from *C. acetobutylicum*	[18]
p95thl^{sup}FAST	ColE1 ori$^-$, *repL* ori$^+$, Amp^r, Em^r, *lacZ*, P_{thl}^{sup}, *feg*	[31]
pMTL83251_P_{thl}^{sup}_FAST	pMTL83251; P_{thl}^{sup}, *feg* from p95thl^{sup}FAST	This work
pMTL83251_P_{thlA}_FAST	pMTL83251; P_{thlA}, from pMTL83251_P_{thlA}_act; *feg* from p95thl^{sup}FAST	This work
pMTL83251_P_{bgaL}_FAST	pMTL83251; *bgaR*-P_{bgaL} from *C. perfringens*; *feg* from p95thl^{sup}FAST	This work
pEX-A128_tdFAST2-opt	pUC ori$^-$, Amp^r, MSC, gene encoding tdFAST2 codon optimized for *E. limosum*	Eurofins Genomics Germany GmbH, Ebersberg, Germany
pMTL83251_P_{bgaL}_tdFAST2	pMTL83251; *bgaR*-P_{bgaL} from *C. perfringens*; gene encoding tdFAST2 codon optimized for *E. limosum*	This work
pMTL83251_P_{bgaL}_AdhE2	pMTL83251; *bgaR*-P_{bgaL} from *C. perfringens*; *adhE2* from *C. acetobutylicum*	This work
pMTL83251_P_{bgaL}_C-FAST-AdhE2	pMTL83251; *bgaR*-P_{bgaL} from *C. perfringens*; *adhE2* from *C. acetobutylicum* C-terminal tagged with *feg* from p95thl^{sup}FAST	This work
pMTL83251_P_{bgaL}_N-FAST-AdhE2	pMTL83251; *bgaR*-P_{bgaL} from *C. perfringens*; *adhE2* from *C. acetobutylicum* N-terminal tagged with *feg* from p95thl^{sup}FAST	This work
pMTL83251_P_{thlA}_act	pMTL83251; P_{thl}, *thlA*, *ctfA/B*, *adc* from pJIR_act	This work
pMTL83251_P_{thlA}_C-FAST-Adc	pMTL83251; P_{thlA}, *thlA*, *ctfA/B*, from pJIR_act; *adc* from *C. acetobutylicum* C-terminal tagged with *feg* from p95thl^{sup}FAST	This work
pMTL83251_P_{thlA}_N-FAST-Adc	pMTL83251; P_{thlA}, *thlA*, *ctfA/B*, from pJIR_act; *adc* from *C. acetobutylicum* N-terminal tagged with *feg* from p95thl^{sup}FAST	This work

pMTL83251_P_{bgaL}_FAST using primers FW_C2_adc-FAST and RV_C2_FAST (Table 7). Primers RV_C1_adc-FAST and FW_C2_adc-FAST contain the sequence for the glycine linker. The plasmid pMTL83251_P_{thlA}_N-FAST-Adc was constructed to produce the N-terminal FAST-tagged Adc fusion protein. The gene *adc* was amplified from plasmid pMTL83251_P_{thlA}_act using primers FW_N1_adc-FAST and RV_N1_FAST-adc and *feg* was amplified from plasmid pMTL83251_P_{bgaL}_FAST using primers FW_N2_FAST-adc and RV_N2_adc (Table 7). Primers RV_N1_FAST-adc and FW_N2_FAST-adc contain the sequence for the glycine linker.

Transformation

Electroporation and preparation of electrocompetent *E. limosum* cells were performed according to the protocol of Leang *et al.* [84] with several modifications. All steps were carried out under anaerobic conditions in an anaerobic chamber (gas atmosphere 95% N_2 and 5% H_2). Plastic materials were placed 24 h before use into the anaerobic chamber to remove any traces of oxygen. For the preparation of electrocompetent cells, *E. limosum* was cultivated at 37 °C in 100 mL modified DSM 135 medium supplemented with 100 mM methanol and 40 mM DL-Threonine. Cells were cultivated until the early exponential growth phase (OD_{600} 0.3–0.5) and harvested by centrifugation at 7690×*g* for 10 min at 4 °C. Subsequently, cells were washed two times with anaerobic SMP buffer (270 mM sucrose, 1 mM $MgCl_2$, 7 mM NaH_2PO_4, pH 6) by centrifugation at 7.690×*g* for 10 min at 4 °C. Afterwards, the cell pellet was suspended in 648 µL SMP buffer and 72 µL DMSO, distributed into cryotubes, and stored at − 80 °C until use.

Transformation of *E. limosum* cells was performed using 3–5 µg plasmid DNA, which were added to 25 µL of electrocompetent cells into a pre-cooled 1 mm electroporation cuvette (Biozym Scientific GmbH, Oldendorf, Germany). Cells were pulsed (625 V, 25 µF, 600 Ω; Gene Pulser Xcell^{TM}, Bio-Rad Laboratories GmbH, Munich, Germany) and immediately transferred into 5 mL fresh medium. *E. limosum* cells were recovered at 37 °C in 5 mL modified DSM 135 medium supplemented with 100 mM methanol. The OD_{600} of transformed cells was monitored. After one or two doublings, 5 µg mL^{-1} clarithromycin was added to the medium for selection of recombinant strains. After a further increase of the OD_{600}, which indicates a successful transformation, cells were transferred two more times into fresh medium supplemented with 5 µg mL^{-1} of clarithromycin. Successfully transformed cells were verified by isolation of plasmid DNA using the Zyppy^{TM} Plasmid Miniprep Kit (Zymo Research, Irvine, CA, USA). This preparation was used to transform chemically competent *E. coli* DH5α cells

Table 7 Primers used in this study

Primer	Sequence 5′–3′	Length (bp)
FW_C1_adhE2	ttaaatgtattgggagggtggatccatgaaagttacaaatcaaaaagaac	50
RV_N2_adhE2	agcttgcatgtctgcaggcctcgagttaaaatgattttatatagatatccttaagttc	58
FW_act_NdeI	gaccgcggccgctgtatccatatgtcaagaagaggcac	38
RV_act_XhoI	agcttgcatgtctgcaggcctcgagttacttaagataatcatatatatacttcag	54
FW_PthIsup_FAST_NdeI	atgaccgcggccgctgtatccatatgtttttaacaaaaagtattgaaatttg	52
RV_PthIsup_FAST_XhoI	aagcttgcatgtctgcaggcctcgagtcataccctcttaac	41
FW_PbgaL_NdeI	gaccgcggccgctgtatccatatgtaatttagatattaattctaaattaagtgaaattaatatag	65
RV_PbgaL_BamHI	caaatgctacgtgttccatggatccaccctcccaatacatttaaaataattatg	54
FW_PthI_NdeI	gaccgcggccgctgtatccatatgtcaagaagaggcacctcatc	44
RV_PthI_BamHI	caaatgctacgtgttccatggatcctaacctcctaaattttgatacgg	48
FW_tdFAST2-opt_BamHI	ttaaatgtattgggagggtggatccatggagcatgtagcttttg	44
RV_tdFAST2-opt_XhoI	agcttgcatgtctgcaggcctcgagtcaaacccgtttgacgaag	44
RV_C1_adhE2-FAST	ctacgtgttcagaaccaccaccaccaaatgattttatatagatatccttaagttc	55
FW_C2_adhE2-FAST	aaaatcatttggtggtggtggttctgaacacgtagcatttggaag	45
RV_C2_FAST	agcttgcatgtctgcaggcctcgagtcataccctcttaacgaaaac	46
FW_N1_FAST	ttaaatgtattgggagggtggatccatggaacacgtagcatttg	44
RV_N1_FAST-adhE2	ttgtaactttagaaccaccaccacctaccctcttaacgaaaac	43
FW_N2_FAST-adhE2	taagagggtaggtggtggtggttctaaagttacaaatcaaaaagaactaaaac	53
FW_C1_adc	acccatggctgtttaggtacctttatgttaaaggatgaagtaattaaac	50
RV_C1_adc-FAST	ctacgtgttcagaaccaccaccaccttaagataatcatatatatacttcagc	52
FW_C2_adc-FAST	ttatcttaagggtggtggtggttctgaacacgtagcatttggaag	45
FW_N1_FAST-adc	acccatggctgtttaggtacctttatggaacacgtagcatttg	44
RV_N1_FAST-adc	catcctttaaagaaccaccaccacctaccctcttaacgaaaac	43
FW_N2_FAST-adc	taagagggtaggtggtggtggttctttaaaggatgaagtaattaaacaaattag	54
RV_N2_adc	agcttgcatgtctgcaggcctcgagttacttaagataatcatatataacttcag	54

to amplify the plasmids. After transformation, plasmids were isolated and checked by restriction analysis. Recombinant strains were stored in cryotubes with 10% DMSO at − 80 °C. All recombinant strains constructed in this study are listed in Table 8.

Fluorescence determination

Fluorescence of FAST and FAST-tagged fusion protein-producing recombinant *E. limosum* strains, cultivated anaerobically until the stationary growth phase, were determined using a microplate reader, fluorescence microscopy, or flow cytometry. Therefore, 2 mL culture broth was taken anaerobically during growth and

Table 8 Recombinant strains used in this study

Recombinant strain	Plasmid	Reference
E. limosum [pMTL83251]	pMTL83251	This work
E. limosum [pMTL83251_P_{thlA}_FAST]	pMTL83251_P_{thlA}_FAST	This work
E. limosum [pMTL83251_P_{bgaL}_FAST]	pMTL83251_P_{bgaL}_FAST	This work
E. limosum [pMTL83251_P_{bgaL}_tdFAST2]	pMTL83251_P_{bgaL}_tdFAST2	This work
E. limosum [pMTL83251_P_{bgaL}_AdhE2]	pMTL83251_P_{bgaL}_AdhE2	This work
E. limosum [pMTL83251_P_{bgaL}_C-FAST-AdhE2]	pMTL83251_P_{bgaL}_C-FAST-AdhE2	This work
E. limosum [pMTL83251_P_{bgaL}_N-FAST-AdhE2]	pMTL83251_P_{bgaL}_N-FAST-AdhE2	This work
E. limosum [pMTL83251_P_{thlA}_act]	pMTL83251_P_{thlA}_act	This work
E. limosum [pMTL83251_P_{thlA}_C-FAST-Adc]	pMTL83251_P_{thlA}_C-FAST-Adc	This work
E. limosum [pMTL83251_P_{thlA}_N-FAST-Adc]	pMTL83251_P_{thlA}_N-FAST-Adc	This work

harvested by centrifugation at 7711×*g* for 15 minutes at 4°C. The supernatant was discarded and harvested cells were washed with anaerobic PBS buffer (137 mM NaCl, 2.7 mM KCl, 10 mM Na_2HPO_4, 1.8 mM KH_2PO_4) followed by centrifugation at 7711×*g* for 15 minutes at 4°C. Cell pellets were suspended in anaerobic PBS buffer (end OD_{600} 1).

Microplate reader

100 µL of suspended cells was transferred to black flat-bottomed 96-well microtiter plates (Greiner Bio-One GmbH, Frickenhausen, Deutschland) and supplemented with 10 µM fluorogen of the green dye ^{TF}Lime (ex. 480/em. 541) or the red dye ^{TF}Coral (ex. 516/em. 600) (The Twinkle Factory, France, Paris). Excitation and emission wavelengths both correspond to the respective maximum of the fluorogen. Fluorescence intensities of the whole population were determined using the SYNERGY H1 microplate reader (BioTek, Bad Friedrichshall, Germany) located in an anaerobic chamber and finally normalized to the OD_{600} of PBS-washed cells.

Fluorescence microscopy

Washed cells were stained with 10 µM ^{TF}Lime and transferred onto an 1% agarose pad on a microscopy slide, covered with a glass coverslip, and sealed with nail polish. Cells were viewed with a 63x objective, using a Zeiss Axio Observer Z1 (Zeiss, Oberkochen, Germany). Green fluorescence of the FAST:fluorogen complex was detected using the Zeiss filter set 38 HE (ex. BP 470/40, em. BP 525/50). Data were analyzed using the Zeiss Zen 2.6 blue edition software.

Flow cytometry

Washed cells were stained with 10 µM ^{TF}Lime diluted in PBS buffer (end OD_{600}: 0.01). Green fluorescence of the FAST:fluorogen complex was assessed using an excitation wavelength of 488 nm and a 528/46 nm emission filter. For analysis, at least 10,000 events were recorded using an Amnis® CellStream® flow cytometer (Luminex Corporation, Austin, TX, USA). Acquired data were analyzed using the CellStreamTM Analysis tool version 1.2.152 (Luminex Corporation, Austin, TX, USA).

Analytics

2 mL samples were withdrawn from cell cultures during the growth of *E. limosum* to analyze OD_{600}, product spectrum as well as substrate consumption. After OD_{600} of the withdrawn culture broth was determined at 600 nm using the GENESYS 10vis photometer (Thermo Scientific, Waltham, MA, USA), the remaining culture was centrifuged at 17,968×*g* for 20 minutes at 4 °C to remove cell debris. The supernatant was used for HPLC and GC analysis.

High-performance liquid chromatography

The concentration of glucose, acetate, and butyrate from culture supernatant was determined using the Agilent 1260 Infinity II HPLC system (Agilent Technologies, Santa Clara, CA, USA), equipped with a diode array detector and a refractive index detector. To achieve separation, 20 µL of the supernatant was injected into the organic acid resin 150 x 8 mm column (CS-chromatographie-Service GmbH, Langerwehe, Germany) packed with polystyrene divinylbenzene copolymer operating at a constant temperature of 40 °C. As mobile phase, 5 mM H_2SO_4 was used with a flow rate of 0.7 mL min^{-1}. The software OpenLAB CDS ChemStation Edition A.01.03 (Agilent Technologies, Santa Clara, CA, USA) was used for data analysis.

Gas chromatography

The concentration of methanol, ethanol, butanol, and acetone in the culture broth was analyzed via gas chromatography. A PerkinElmer Clarus 680 GC system (Perkin Elmer LAS GmbH, Waltham, MA, USA) equipped with an Elite-FFAP capillary column (length 30 m x inner diameter 0.32 mm, film thickness 0.25 µm) (Perkin Elmer LAS GmbH, Waltham, MA, USA) and FID detector was used. Supernatants were acidified with 2 M HCL. H_2 was used as the carrier gas. The injector and detector were operated at 225 and 300 °C, respectively. 0.5 µL of the culture broth was injected into the gas chromatograph and analyzed using the following temperature profile: 40 °C for 2.5 minutes; 40 °C–250 °C with 40 °C min^{-1}; 250 °C for 2 minutes.

Abbreviations

Adc: Acetoacetate decarboxylase; AdhE2: Bifunctional acetaldehyde/alcohol dehydrogenase; APO: Acetone production operon; FAST: Fluorescence-activating and absorption shifting tag; OD_{600}: Optical density; POI: Protein of interest.

Supplementary Information

The online version contains supplementary material available at https://doi.org/10.1186/s13068-021-01966-2.

Additional file 1. Fig. S1. Growth experiment with *E. limosum* [pMTL83251_P_{bgaL}_AdhE2] and *E. limosum* [pMTL83251]. Strains were cultivated using 30 mM glucose (A) or 100 mM methanol (B) as carbon source. Gene expression of cells was either induced by lactose or non-induced. Induction with lactose is indicated with the vertical dotted line. Monitored are OD_{600}, methanol consumption, as well as acetate, butyrate, ethanol, and butanol production. Error bars indicate standard deviations. n = 3. **Fig. S2.** Growth experiment with *E. limosum* [pMTL83251_P_{thlA}_act] and *E. limosum* [pMTL83251]. Strains were cultivated using 30 mM glucose (A) or 100 mM methanol (B) as carbon source. Monitored are OD_{600}, glucose and methanol consumption, as well as acetate, butyrate,

and acetone production. Error bars indicate standard deviations. n = 3. **Table S1.** Growth characteristics and product formation of recombinant *E. limosum* strains characterized in growth experiments using glucose as carbon source. **Table S2.** Growth characteristics and product formation of recombinant *E. limosum* strains characterized in growth experiments using methanol as carbon source.

Acknowledgements
We thank Eleftherios (Terry) Papoutsakis (Delaware Biotechnology Institute, University of Delaware, Newark, DE, USA) for kindly providing the plasmid p95thl^{sup}FAST. We further thank Philippe Soucaille (INSA, University of Toulouse, Toulouse, France) for providing the strain *E. limosum* NG-6894.

Authors' contributions
MF, FRB, and PD designed the experiments. MF and GL performed the experiments. MF analyzed the data and wrote the manuscript. FRB and PD participated in writing the manuscript and revised the paper. All authors read and approved the final manuscript.

Funding
Open Access funding enabled and organized by Projekt DEAL. This research was funded by the European Research Area Cofund on BioTechnologies (ERA-CoBioTech) within the 1st Joint Call (project BIOMETCHEM, grant 161B0609A).

Availability of data and materials
All data generated during this study are included in this article and the additional files. Raw data are available on reasonable request.

Declarations

Ethics approval and consent to participate
Not applicable.

Consent for publication
Not applicable.

Competing interests
The authors declare that they have no competing interests.

Received: 27 January 2021 Accepted: 29 April 2021
Published online: 10 May 2021

References

1. Acharya B, Roy P, Dutta A. Review of syngas fermentation processes for bioethanol. Biofuels. 2014;5:551–64. https://doi.org/10.1080/17597269.2014.1002996.
2. Bertau M, Offermanns H, Plass L, Schmidt F, Wernicke HJ. Methanol: the basic chemical and energy feedstock of the future. Heidelberg: Springer; 2014.
3. Sheldon D. Methanol production—a technical history. Johns Matthey Technol Rev. 2017;61:172–82. https://doi.org/10.1595/205651317X695622.
4. Bengelsdorf FR, Beck MH, Erz C, Hoffmeister S, Karl MM, Riegler P, et al. Bacterial anaerobic synthesis gas (syngas) and $CO_2 + H_2$ fermentation. In: Advances in Applied Microbiology. Elsevier; 2018. p. 143–221. https://doi.org/https://doi.org/10.1016/bs.aambs.2018.01.002.
5. Pfeifenschneider J, Brautaset T, Wendisch VF. Methanol as carbon substrate in the bio-economy: metabolic engineering of aerobic methylotrophic bacteria for production of value-added chemicals. Biofuel Bioprod Bior. 2017;11:719–31. https://doi.org/10.1002/bbb.1773.
6. Schrader J, Schilling M, Holtmann D, Sell D, Filho MV, Marx A, et al. Methanol-based industrial biotechnology: current status and future perspectives of methylotrophic bacteria. Trends Biotechnol. 2009;27:107–15. https://doi.org/10.1016/j.tibtech.2008.10.009.
7. Weijma J, Stams AJM. Methanol conversion in high-rate anaerobic reactors. Water Sci Technol. 2001;44:7–14. https://doi.org/10.2166/wst.2001.0452.
8. Bache R, Pfennig N. Selective isolation of *Acetobacterium woodii* on methoxylated aromatic acids and determination of growth yields. Arch Microbiol. 1981;130:255–61. https://doi.org/10.1007/BF00459530.
9. Kremp F, Poehlein A, Daniel R, Müller V. Methanol metabolism in the acetogenic bacterium *Acetobacterium woodii*. Environ Microbiol. 2018;20:4369–84. https://doi.org/10.1111/1462-2920.14356.
10. Mueller AP, Köpke M. Recombinant microorganisms and uses therefor. Washington, DC; US 2013/03300809 A1, 2013.
11. Huang H, Chai C, Li N, Rowe P, Minton NP, Yang S, et al. CRISPR/Cas9-based efficient genome editing in Clostridium ljungdahlii, an autotrophic gas-fermenting bacterium. ACS Synth Biol. 2016;5:1355–61. https://doi.org/10.1021/acssynbio.6b00044.
12. Nagaraju S, Davies NK, Walker DJF, Köpke M, Simpson SD. Genome editing of *Clostridium autoethanogenum* using CRISPR/Cas9. Biotechnol Biofuels. 2016;9:15. https://doi.org/10.1186/s13068-016-0638-3.
13. Shin J, Kang S, Song Y, Jin S, Lee JS, Lee J-K, et al. Genome engineering of *Eubacterium limosum* using expanded genetic tools and the CRISPR-Cas9 system. ACS Synth Biol. 2019;8:2059–68. https://doi.org/10.1021/acssynbio.9b00150.
14. Jin S, Bae J, Song Y, Pearcy N, Shin J, Kang S, et al. Synthetic biology on acetogenic bacteria for highly efficient conversion of C1 gases to biochemicals. Int J Mol Sci. 2020;21:7639. https://doi.org/10.3390/ijms21207639.
15. Köpke M, Held C, Hujer S, Liesegang H, Wiezer A, Wollherr A, et al. *Clostridium ljungdahlii* represents a microbial production platform based on syngas. Proc Natl Acad Sci USA. 2010;107:13087–92. https://doi.org/10.1073/pnas.1004716107.
16. Köpke M, Liew F. Production of butanol from carbon monoxide by a recombinant microorganism. Washington, DC; US 2011/0236941, 2011.
17. Banerjee A, Leang C, Ueki T, Nevin KP, Lovley DR. Lactose-inducible system for metabolic engineering of *Clostridium ljungdahlii*. Appl Environ Microbiol. 2014;80:2410–6. https://doi.org/10.1128/AEM.03666-13.
18. Hoffmeister S, Gerdom M, Bengelsdorf FR, Linder S, Flüchter S, Öztürk H, et al. Acetone production with metabolically engineered strains of *Acetobacterium woodii*. Metab Eng. 2016;36:37–47. https://doi.org/10.1016/j.ymben.2016.03.001.
19. Jones SW, Fast AG, Carlson ED, Wiedel CA, Au J, Antoniewicz MR, et al. CO_2 fixation by anaerobic non-photosynthetic mixotrophy for improved carbon conversion. Nat Commun. 2016;7:12800. https://doi.org/10.1038/ncomms12800.
20. Bengelsdorf FR, Poehlein A, Linder S, Erz C, Hummel T, Hoffmeister S, et al. Industrial acetogenic biocatalysts: a comparative metabolic and genomic analysis. Front Microbiol. 2016;7:5. https://doi.org/10.3389/fmicb.2016.01036.
21. Woolston BM, Emerson DF, Currie DH, Stephanopoulos G. Rediverting carbon flux in *Clostridium ljungdahlii* using CRISPR interference (CRISPRi). Metab Eng. 2018;48:243–53. https://doi.org/10.1016/j.ymben.2018.06.006.
22. Flüchter S, Follonier S, Schiel-Bengelsdorf B, Bengelsdorf FR, Zinn M, Dürre P. Anaerobic production of poly(3-hydroxybutyrate) and its precursor 3-hydroxybutyrate from synthesis gas by autotrophic clostridia. Biomacromolecules. 2019;20:3271–82. https://doi.org/10.1021/acs.biomac.9b00342.
23. Chalfie M, Tu Y, Euskirchen G, Ward W, Prasher D. Green fluorescent protein as a marker for gene expression. Science. 1994;263:802–5. https://doi.org/10.1126/science.8303295.
24. Landete JM, Medina M, Arqués JL. Fluorescent reporter systems for tracking probiotic lactic acid bacteria and bifidobacteria. World J Microbiol Biotechnol. 2016;32:119. https://doi.org/10.1007/s11274-016-2077-5.
25. Changsen C, Franzblau SG, Palittapongarnpim P. Improved green fluorescent protein reporter gene-based microplate screening for antituberculosis compounds by utilizing an acetamidase promoter. Antimicrob Agents Chemother. 2003;47:3682–7. https://doi.org/10.1128/AAC.47.12.3682-3687.2003.
26. Teng L, Wang K, Xu J, Xu C. Flavin mononucleotide (FMN)-based fluorescent protein (FbFP) as reporter for promoter screening in *Clostridium cellulolyticum*. J Microbiol Methods. 2015;119:37–43. https://doi.org/10.1016/j.mimet.2015.09.018.

27. Bloemberg GV, O'Toole GA, Lugtenberg BJJ, Kolter R. Green fluorescent protein as a marker for *Pseudomonas* spp. Appl Environ Microbiol. 1997;63:4543–51. https://doi.org/10.1128/AEM.63.11.4543-4551.1997.
28. Southward CM, Surette MG. The dynamic microbe: green fluorescent protein brings bacteria to light: monitoring microbial dynamics with GFP. Mol Microbiol. 2002;45:1191–6. https://doi.org/10.1046/j.1365-2958.2002.03089.x.
29. Charubin K, Bennett RK, Fast AG, Papoutsakis ET. Engineering *Clostridium* organisms as microbial cell-factories: challenges & opportunities. Metab Eng. 2018;50:173–91. https://doi.org/10.1016/j.ymben.2018.07.012.
30. Plamont M-A, Billon-Denis E, Maurin S, Gauron C, Pimenta FM, Specht CG, et al. Small fluorescence-activating and absorption-shifting tag for tunable protein imaging in vivo. Proc Natl Acad Sci USA. 2016;113:497–502. https://doi.org/10.1073/pnas.1513094113.
31. Streett HE, Kalis KM, Papoutsakis ET. A strongly fluorescing anaerobic reporter and protein-tagging system for *Clostridium* organisms based on the fluorescence-activating and absorption-shifting tag protein (FAST). Appl Environ Microbiol. 2019;85:e00622-19. https://doi.org/10.1128/AEM.00622-19.
32. Charubin K, Streett H, Papoutsakis ET. Development of strong anaerobic fluorescent reporters for *Clostridium acetobutylicum* and *Clostridium ljungdahlii* using HaloTag and SNAP-tag proteins. Appl Environ Microbiol. 2020;86:e01271-20. https://doi.org/10.1128/AEM.01271-20.
33. Li C, Plamont M-A, Sladitschek HL, Rodrigues V, Aujard I, Neveu P, et al. Dynamic multicolor protein labeling in living cells. Chem Sci. 2017;8:5598–605. https://doi.org/10.1039/C7SC01364G.
34. Ransom EM, Ellermeier CD, Weiss DS. Use of mCherry red fluorescent protein for studies of protein localization and gene expression in Clostridium difficile. Appl Environ Microbiol. 2015;81:1652–60. https://doi.org/10.1128/AEM.03446-14.
35. Buckley AM, Jukes C, Candlish D, Irvine JJ, Spencer J, Fagan RP, et al. Lighting up *Clostridium difficile*: reporting gene expression using fluorescent Lov domains. Sci Rep. 2016;6:23463. https://doi.org/10.1038/srep23463.
36. Stockmar I, Feddersen H, Cramer K, Gruber S, Jung K, Bramkamp M, et al. Optimization of sample preparation and green color imaging using the mNeonGreen fluorescent protein in bacterial cells for photoactivated localization microscopy. Sci Rep. 2018;8:10137. https://doi.org/10.1038/s41598-018-28472-0.
37. Sharak Genthner BR, Davis CL, Bryant MP. Features of rumen and sewage sludge strains of *Eubacterium limosum*, a methanol- and H_2-CO_2-utilizing species. Appl Environ Microbiol. 1981;42:12–9. https://doi.org/10.1128/AEM.42.1.12-19.1981.
38. Kang S, Song Y, Jin S, Shin J, Bae J, Kim DR, et al. Adaptive laboratory evolution of *Eubacterium limosum* ATCC 8486 on carbon monoxide. Front Microbiol. 2020;11:402. https://doi.org/10.3389/fmicb.2020.00402.
39. Fontaine L, Meynial-Salles I, Girbal L, Yang X, Croux C, Soucaille P. Molecular characterization and transcriptional analysis of adhE2, the gene encoding the NADH-dependent aldehyde/alcohol dehydrogenase responsible for butanol production in alcohologenic cultures of *Clostridium acetobutylicum* ATCC 824. J Bacteriol. 2002;184:821–30. https://doi.org/10.1128/JB.184.3.821-830.2002.
40. Lindley ND, Loubiere P, Pacaud S, Mariotto C, Goma G. Novel products of the acidogenic fermentation of methanol during growth of *Eubacterium limosum* in the presence of high concentrations of organic acids. Microbiology. 1987;133:3557–63. https://doi.org/10.1099/00221287-133-12-3557.
41. Wiesenborn DP, Rudolph FB, Papoutsakis ET. Thiolase from *Clostridium acetobutylicum* ATCC 824 and its role in the synthesis of acids and solvents. Appl Environ Microbiol. 1988;54:2717–22. https://doi.org/10.1128/AEM.54.11.2717-2722.1988.
42. Cornillot E, Nair RV, Papoutsakis ET, Soucaille P. The genes for butanol and acetone formation in *Clostridium acetobutylicum* ATCC 824 reside on a large plasmid whose loss leads to degeneration of the strain. J Bacteriol. 1997;179:5442–7. https://doi.org/10.1128/jb.179.17.5442-5447.1997.
43. Sharak Genthner BR, Bryant MP. Additional characteristics of one-carbon-compound utilization by *Eubacterium limosum* and *Acetobacterium woodii*. Appl Environ Microbiol. 1987;53:471–6. https://doi.org/10.1128/AEM.53.3.471-476.1987.
44. Loubiere P, Gros E, Paquet V, Lindley ND. Kinetics and physiological implications of the growth behaviour of *Eubacterium limosum* on glucose/methanol mixtures. J Gen Microbiol. 1992;138:979–85. https://doi.org/10.1099/00221287-138-5-979.
45. Pacaud S, Loubiere P, Goma G, Lindley ND. Effects of various organic acid supplements on growth rates of *Eubacterium limosum* B2 on methanol. Appl Microbiol Biotechnol. 1986;24:7. https://doi.org/10.1007/BF00266289.
46. Pacaud S, Loubiere P, Goma G. Methanol metabolism by *Eubacterium limosum* B2: effects of pH and carbon dioxide on growth and organic acid production. Curr Microbiol. 1985;12:245–50. https://doi.org/10.1007/BF01567972.
47. Kremp F, Müller V. Methanol and methyl group conversion in acetogenic bacteria: biochemistry, physiology and application. FEMS Microbiol Rev. 2020. https://doi.org/10.1093/femsre/fuaa040.
48. Valgepea K, Loi KQ, Behrendorff JB, Lemgruber R, Plan M, Hodson MP, et al. Arginine deiminase pathway provides ATP and boosts growth of the gas-fermenting acetogen *Clostridium autoethanogenum*. Metab Eng. 2017;41:202–11. https://doi.org/10.1016/j.ymben.2017.04.007.
49. Beck MH, Flaiz M, Bengelsdorf FR, Dürre P. Induced heterologous expression of the arginine deiminase pathway promotes growth advantages in the strict anaerobe *Acetobacterium woodii*. Appl Microbiol Biotechnol. 2020;104:687–99. https://doi.org/10.1007/s00253-019-10248-9.
50. Claassens NJ, Cotton CAR, Kopljar D, Bar-Even A. Making quantitative sense of electromicrobial production. Nat Catal. 2019;2:437–47. https://doi.org/10.1038/s41929-019-0272-0.
51. Cotton CAR, Claassens NJ, Benito-Vaquerizo S, Bar-Even A. Renewable methanol and formate as microbial feedstocks. Curr Opin Biotechnol. 2020;62:168–80. https://doi.org/10.1016/j.copbio.2019.10.002.
52. Litty D, Müller V. Butyrate production in the acetogen *Eubacterium limosum* is dependent on the carbon and energy source. Microb Biotechnol. 2021. https://doi.org/10.1111/1751-7915.13779.
53. Park S, Yasin M, Jeong J, Cha M, Kang H, Jang N, et al. Acetate-assisted increase of butyrate production by *Eubacterium limosum* KIST612 during carbon monoxide fermentation. Bioresour Technol. 2017;245:560–6. https://doi.org/10.1016/j.biortech.2017.08.132.
54. Grethlein AJ, Worden RM, Jain MK, Datta R. Evidence for production of n-butanol from carbon monoxide by *Butyribacterium methylotrophicum*. J Ferment Bioeng. 1991;72:58–60. https://doi.org/10.1016/0922-338X(91)90147-9.
55. Hartman AH, Liu H, Melville SB. Construction and characterization of a lactose-Inducible promoter system for controlled gene expression in *Clostridium perfringens*. Appl Environ Microbiol. 2011;77:471–8. https://doi.org/10.1128/AEM.01536-10.
56. Al-Hinai MA, Fast AG, Papoutsakis ET. Novel system for efficient isolation of *Clostridium* double-crossover allelic exchange mutants enabling markerless chromosomal gene deletions and DNA integration. Appl Environ Microbiol. 2012;78:8112–21. https://doi.org/10.1128/AEM.02214-12.
57. Zimmer M. Green Fluorescent Protein (GFP): applications, structure, and related photophysical behavior. Chem Rev. 2002;102:759–82. https://doi.org/10.1021/cr010142r.
58. Drepper T, Eggert T, Circolone F, Heck A, Krauß U, Guterl J-K, et al. Reporter proteins for in vivo fluorescence without oxygen. Nat Biotechnol. 2007;25:443–5. https://doi.org/10.1038/nbt1293.
59. Molitor B, Kirchner K, Henrich AW, Schmitz S, Rosenbaum MA. Expanding the molecular toolkit for the homoacetogen *Clostridium ljungdahlii*. Sci Rep. 2016;6:31518. https://doi.org/10.1038/srep31518.
60. Seo S-O, Lu T, Jin Y-S, Blaschek HP. Development of an oxygen-independent flavin mononucleotide-based fluorescent reporter system in *Clostridium beijerinckii* and its potential applications. J Biotechnol. 2018;265:119–26. https://doi.org/10.1016/j.jbiotec.2017.11.003.
61. Cheng C, Lin M, Jiang W, Zhao J, Li W, Yang S-T. Development of an in vivo fluorescence based gene expression reporter system for *Clostridium tyrobutyricum*. J Biotechnol. 2019;305:18–22. https://doi.org/10.1016/j.jbiotec.2019.08.019.
62. Charubin K, Modla S, Caplan JL, Papoutsakis ET. Interspecies microbial fusion and large-scale exchange of cytoplasmic proteins and RNA in a syntrophic *Clostridium* coculture. mBio. 2020;11:e02030-20. https://doi.org/10.1128/mBio.02030-20.
63. Shaner NC, Campbell RE, Steinbach PA, Giepmans BNG, Palmer AE, Tsien RY. Improved monomeric red, orange and yellow fluorescent proteins derived from *Discosoma* sp. red fluorescent protein. Nat Biotechnol. 2004;22:1567–72. https://doi.org/10.1038/nbt1037.

64. Tebo AG, Pimenta FM, Zhang Y, Gautier A. Improved chemical-genetic fluorescent markers for live cell microscopy. Biochemistry. 2018;57:5648–53. https://doi.org/10.1021/acs.biochem.8b00649.
65. Day RN, Davidson MW. The fluorescent protein palette: tools for cellular imaging. Chem Soc Rev. 2009;38:2887. https://doi.org/10.1039/b901966a.
66. Tanenbaum ME, Gilbert LA, Qi LS, Weissman JS, Vale RD. A protein-tagging system for signal amplification in gene expression and fluorescence imaging. Cell. 2014;159:635–46. https://doi.org/10.1016/j.cell.2014.09.039.
67. Siegele DA, Hu JC. Gene expression from plasmids containing the *araBAD* promoter at subsaturating inducer concentrations represents mixed populations. Proc Natl Acad Sci USA. 1997;94:8168–72. https://doi.org/10.1073/pnas.94.15.8168.
68. Binder D, Probst C, Grünberger A, Hilgers F, Loeschcke A, Jaeger KE, et al. Comparative single-cell analysis of different *E. coli* expression systems during microfluidic cultivation. PLoS ONE. 2016;11:e0160711. https://doi.org/10.1371/journal.pone.0160711.
69. Siebert D, Busche T, Metz AY, Smaili M, Queck BAW, Kalinowski J, et al. Genetic engineering of *Oligotropha carboxidovorans* strain OM5—a promising candidate for the aerobic utilization of synthesis gas. ACS Synth Biol. 2020;9:1426–40. https://doi.org/10.1021/acssynbio.0c00098.
70. Li C, Tebo AG, Thauvin M, Plamont M, Volovitch M, Morin X, et al. A far-red emitting fluorescent chemogenetic reporter for in vivo molecular imaging. Angew Chem Int Ed. 2020;59:17917–23. https://doi.org/10.1002/ange.202006576.
71. Mihalcescu I, Van-Melle Gateau M, Chelli B, Pinel C, Ravanat J-L. Green autofluorescence, a double edged monitoring tool for bacterial growth and activity in micro-plates. Phys Biol. 2015;12:066016. https://doi.org/10.1088/1478-3975/12/6/066016.
72. Surre J, Saint-Ruf C, Collin V, Orenga S, Ramjeet M, Matic I. Strong increase in the autofluorescence of cells signals struggle for survival. Sci Rep. 2018;8:12088. https://doi.org/10.1038/s41598-018-30623-2.
73. Tebo AG, Moeyaert B, Thauvin M, Carlon-Andres I, Böken D, Volovitch M, et al. Orthogonal fluorescent chemogenetic reporters for multicolor imaging. bioRxiv. 2020. https://doi.org/10.1038/s41589-020-0611-0.
74. Ho M-C, Ménétret J-F, Tsuruta H, Allen KN. The origin of the electrostatic perturbation in acetoacetate decarboxylase. Nature. 2009;459:393–7. https://doi.org/10.1038/nature07938.
75. Snapp E. Design and use of fluorescent fusion proteins in cell biology. Curr Protoc Cell Biol. 2005;27:1–13. https://doi.org/10.1002/0471143030.cb2104s27.
76. Chen X, Zaro JL, Shen W-C. Fusion protein linkers: property, design and functionality. Adv Drug Deliv Rev. 2013;65:1357–69. https://doi.org/10.1016/j.addr.2012.09.039.
77. Yoo M, Croux C, Meynial-Salles I, Soucaille P. Elucidation of the roles of adhE1 and adhE2 in the primary metabolism of Clostridium acetobutylicum by combining in-frame gene deletion and a quantitative system-scale approach. Biotechnol Biofuels. 2016;9:92. https://doi.org/10.1186/s13068-016-0507-0.
78. Sheff MA, Thorn KS. Optimized cassettes for fluorescent protein tagging in *Saccharomyces cerevisiae*. Yeast. 2004;21:661–70. https://doi.org/10.1002/yea.1130.
79. Specht EA, Braselmann E, Palmer AE. A critical and comparative review of fluorescent tools for live-cell Imaging. Annu Rev Physiol. 2017;79:93–117. https://doi.org/10.1146/annurev-physiol-022516-034055.
80. Nieuwkoop T, Finger-Bou M, van der Oost J, Claassens NJ. The ongoing quest to crack the genetic code for protein production. Mol Cell. 2020;80:193–209. https://doi.org/10.1016/j.molcel.2020.09.014.
81. Bertani G. Studies on lysogenesis I. The mode of phage liberation by lysogenic *Escherichia coli*. J Bacteriol. 1951;62:293–300. https://doi.org/10.1128/JB.62.3.293-300.1951.
82. Tschech A, Pfennig N. Growth yield increase linked to caffeate reduction in *Acetobacterium woodii*. Arch Microbiol. 1984;137:163–7. https://doi.org/10.1007/BF00414460.
83. Heap JT, Pennington OJ, Cartman ST, Minton NP. A modular system for *Clostridium* shuttle plasmids. J Microbiol Methods. 2009;78:79–85. https://doi.org/10.1016/j.mimet.2009.05.004.
84. Leang C, Ueki T, Nevin KP, Lovley DR. A genetic system for *Clostridium ljungdahlii*: a chassis for autotrophic production of biocommodities and a model homoacetogen. Appl Environ Microbiol. 2013;79:1102–9. https://doi.org/10.1128/AEM.02891-12.

Publisher's Note

Springer Nature remains neutral with regard to jurisdictional claims in published maps and institutional affiliations.

Ready to submit your research? Choose BMC and benefit from:

- fast, convenient online submission
- thorough peer review by experienced researchers in your field
- rapid publication on acceptance
- support for research data, including large and complex data types
- gold Open Access which fosters wider collaboration and increased citations
- maximum visibility for your research: over 100M website views per year

At BMC, research is always in progress.

Learn more biomedcentral.com/submissions

BMC

2.3 Establishment of green- and red-fluorescent reporter proteins based on the fluorescence-activating and absorption-shifting tag for use in acetogenic and solventogenic anaerobes

Flaiz, M.; Baur, T.; Gaibler, J.; Kröly, C.; Dürre, P. Establishment of green- and red-fluorescent reporter proteins based on the fluorescence-activating and absorption-shifting tag for use in acetogenic and solventogenic anaerobes. *ACS Synth. Biol. 2022, 11,* 953-967.

Rights and permissions

Reprinted with permission from *ACS Synth. Biol. 2022*, 11, 2, 953–967. Copyright 2022 American Chemical Society.

The original article can be accessed via https://doi.org/10.1021/acssynbio.1c00554

ACS SyntheticBiology

pubs.acs.org/synthbio Research Article

Establishment of Green- and Red-Fluorescent Reporter Proteins Based on the Fluorescence-Activating and Absorption-Shifting Tag for Use in Acetogenic and Solventogenic Anaerobes

Maximilian Flaiz,* Tina Baur, Jana Gaibler, Christian Kröly, and Peter Dürre

Cite This: ACS Synth. Biol. 2022, 11, 953−967 Read Online

ACCESS | Metrics & More | Article Recommendations | Supporting Information

ABSTRACT: Anaerobic bacteria are promising biocatalysts to produce industrially relevant products from nonfood feedstocks. Several anaerobes are genetically accessible, and various molecular tools for metabolic engineering are available. Still, the use of bright fluorescent reporters, which are commonly used in molecular biological approaches is limited under anaerobic conditions. Therefore, the establishment of different anaerobic fluorescent reporter proteins is of great interest. Here, we present the establishment of the green- and red-fluorescent reporter proteins greenFAST and redFAST for use in different solventogenic and acetogenic bacteria. Green fluorescence of greenFAST was bright in *Clostridium saccharoperbutylacetonicum*, *Clostridium acetobutylicum*, *Acetobacterium woodii*, and *Eubacterium limosum*, while only *C. saccharoperbutylacetonicum* showed bright red fluorescence when producing redFAST. We used both reporter proteins in *C. saccharoperbutylacetonicum* for multicolor approaches. These include the investigation of the co-culture dynamics of metabolically engineered strains. Moreover, we established a tightly regulated inducible two-plasmid system and used greenFAST and redFAST to track the coexistence and interaction of both plasmids under anaerobic conditions in *C. saccharoperbutylacetonicum*. The establishment of greenFAST and redFAST as fluorescent reporters opens the door for further multicolor approaches to investigate cell dynamics, gene expression, or protein localization under anaerobic conditions.

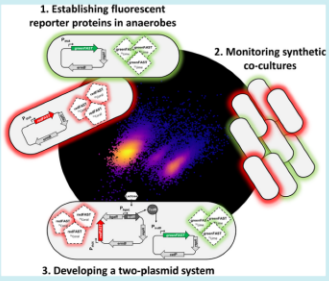

KEYWORDS: *Acetobacterium woodii, Clostridium acetobutylicum, Clostridium saccharoperbutylacetonicum, Eubacterium limosum, fluorescent reporter proteins, synthetic co-cultures, two-plasmid system*

Downloaded via UNIV ULM on May 30, 2022 at 12:05:51 (UTC).
See https://pubs.acs.org/sharingguidelines for options on how to legitimately share published articles.

INTRODUCTION

The interest in anaerobic solventogenic and acetogenic microbes increased in recent years since they can be used to produce chemicals from renewable nonfood carbon sources and greenhouse gases. Solventogenic clostridia perform acetone−butanol−ethanol fermentation to produce industrially relevant alcohols from lignocellulosic biomass and can be divided into two distinct phylogenetic clades.[1,2] The first clade, which includes *Clostridium acetobutylicum*, harbors the type I *sol* operon, consisting of *adhE* (encoding a bifunctional butyraldehyde/butanol dehydrogenase), *ctfA/B* (encoding the two subunits of a CoA-transferase), and a separate *adc* (encoding an acetoacetate decarboxylase) operon. Strains of the second clade, including *Clostridium beijerinckii* and *Clostridium saccharoperbutylacetonicum*, harbor the type II *sol* operon consisting of the genes *ald* or *bld* (encoding an NADH-dependent aldehyde dehydrogenase or a butyraldehyde dehydrogenase, respectively), *ctfA/B*, and *adc*.[3] Compared to solventogenic clostridia, acetogens such as *Acetobacterium woodii* or *Eubacterium limosum* are of great interest since they can utilize C_1-carbon sources, e.g., CO, $CO_2 + H_2$, methanol, or formate and industrial waste gases, which can contribute to the reduction of greenhouse gas emissions while producing industrially relevant products.[4]

Several solventogens and acetogens are genetically accessible, and molecular tools for genome editing or to express recombinant pathways were already established.[5−7] However, the use of strong fluorescent reporter proteins, which are commonly used in molecular biology, is still limited in anaerobes. In the case of the green-fluorescent protein (GFP) and its derivates, oxygen is needed for chromophore maturation,[8] while the use of FMN-binding fluorescent proteins (FbFPs) only results in poor cyan-green fluorescence.[9] Recently, the fluorescence-activating and absorption-shifting tag (FAST) protein was established as an anaerobic fluorescent reporter in the solventogen *C. acetobutylicum*,[10] and the acetogens *C. ljungdahlii*[11] and *E. limosum*.[12] FAST is a fluorescence-activating protein that shows bright fluorescence when bound to a fluorogenic ligand and can be used to study gene expression

Received: November 2, 2021
Published: January 27, 2022



ACS Publications © 2022 The Authors. Published by American Chemical Society

https://doi.org/10.1021/acssynbio.1c00554
ACS Synth. Biol. 2022, 11, 953−967

ACS Synthetic Biology pubs.acs.org/synthbio Research Article

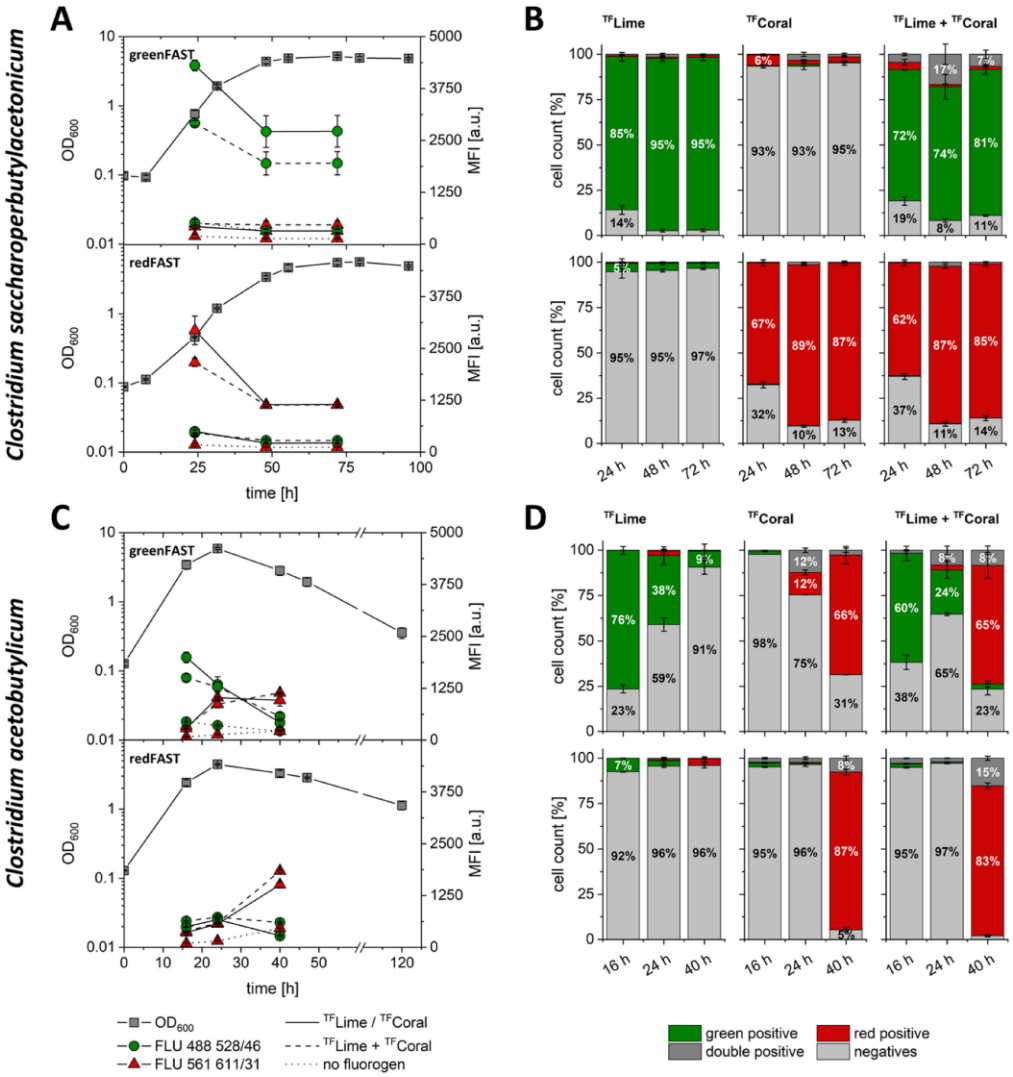

Figure 1. greenFAST and redFAST as fluorescent reporters in solventogenic anaerobes. (A) Growth, mean fluorescence intensity (MFI), and (B) number of green- or red-fluorescent cells of *C. saccharoperbutylacetonicum* [pMTL83251_P_{thlA}_greenFAST] (top) and *C. saccharoperbutylacetonicum* [pMTL83251_P_{thlA}_redFAST] (bottom). MFI of the whole population was determined after 24, 48, and 72 h of cultivation ($n = 3$). (C) Growth, MFI, and (D) number of green- or red-fluorescent cells of *C. acetobutylicum* [pMTL83251_P_{thlA}_greenFAST] (top) and *C. acetobutylicum* [pMTL83251_P_{thlA}_redFAST] (bottom). MFI of the whole population was determined after 16, 24, and 40 h of cultivation ($n = 3$). The cells were labeled using 5 μM ^{TF}Lime, 10 μM ^{TF}Coral, or a mixture of both fluorogens.

and promoter activities or to construct fluorescent fusion proteins to investigate their production, localization, and dynamics.[13−15] Several fluorogens are available, including the green-fluorescent dye 4-hydroxy-3-methylbenzylidene rhodanine (HMBR; ^{TF}Lime) and the red-fluorescent dye 4-hydroxy-3,5-dimethoxybenzylidene rhodanine (HBR-3,5-DOM; ^{TF}Coral).[16] However, since both fluorogens bind nonselective to FAST, multicolor approaches are not possible. To overcome this issue, Tebo et al. constructed greenFAST and redFAST, which are mutated FAST versions that selectively bind HMBR and HBR-3,5-DOM, respectively, causing bright green or red fluorescence.[17] This breakthrough enables the combination of greenFAST and redFAST and use them as multicolor-fluorescence reporters to investigate intracellular dynamics or the dynamics in anaerobic microbial populations and co-cultures.

Such bacterial co-cultures can be categorized into natural, enriched natural, artificial, and synthetic co-cultures.[18] While artificial co-cultures are defined and consist of two or more identified wild-type species, synthetic co-cultures contain at least one genetically modified strain. The use of synthetic co-cultures to produce industrially relevant products is of great interest, however, also faces several challenges. First, the coexistence of the bacterial strains has to be ensured and maintained during fermentation while fluctuation in the populations has to be minimized.[19] Second, to yield the maximal amount of desired product with separated synthetic metabolic pathways, not only the strain-to-strain ratio but also the dynamics and the number of producing cells must be balanced and tracked during

https://doi.org/10.1021/acssynbio.1c00554
ACS Synth. Biol. 2022, 11, 953−967

ACS Synthetic Biology pubs.acs.org/synthbio Research Article

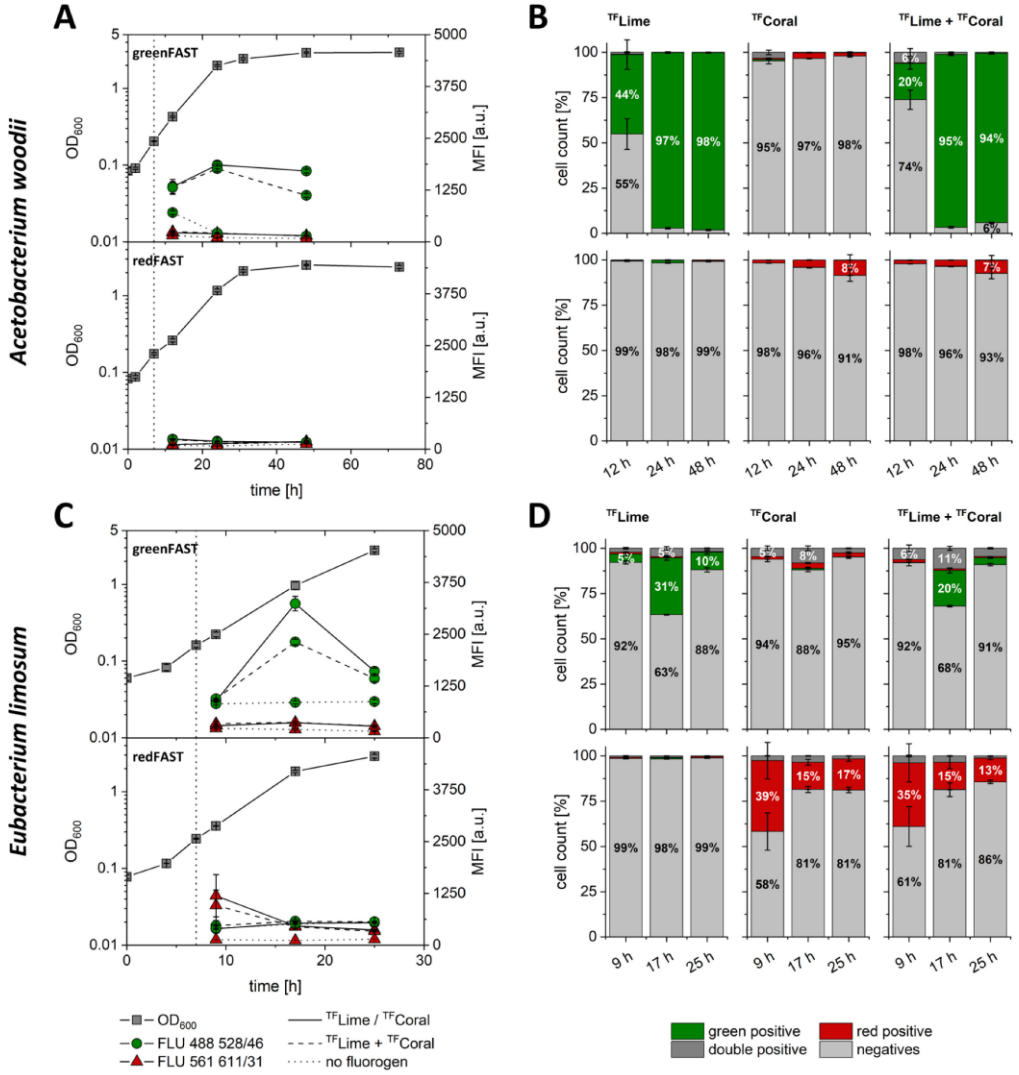

Figure 2. greenFAST and redFAST as fluorescent reporters in acetogenic anaerobes. (A) Growth, mean fluorescence intensity (MFI), and (B) number of green- or red-fluorescent cells of *A. woodii* [pMTL83251_P_{bgaL}_greenFAST] (top) and *A. woodii* [pMTL83251_P_{bgaL}_redFAST] (bottom). MFI of the whole population was determined after 12, 24, and 48 h of cultivation ($n = 3$). (C) Growth, MFI, and (D) number of green- or red-fluorescent cells of *E. limosum* [pMTL83251_P_{bgaL}_greenFAST] (top) and *E. limosum* [pMTL83251_P_{bgaL}_redFAST] (bottom). MFI of the whole population was determined after 9, 17, and 25 h of cultivation ($n = 3$). The cells were labeled using 5 μM ^{TF}Lime, 10 μM ^{TF}Coral, or a mixture of both fluorogens. Expression of the gene encoding greenFAST or redFAST was induced with 20 mM lactose after 7 h of cultivation indicated by the vertical dotted line.

fermentation.[20] The straightforward approach would be to distinguish between species regarding their physical properties such as size, shape,[21] or autofluorescence, e.g., for cyanobacteria.[22] This differentiation becomes more challenging when two metabolically engineered strains of the same species, e.g., synthetic *E. coli*–*E. coli* co-cultures, are used[23−26] or the shape and size of different bacterial species are similar. In such cases, multicolor-fluorescence reporter proteins can be combined, produced in different metabolically engineered strains, and finally used to determine the number of fluorescent cells.[11,27−30]

In this study, we aimed to establish greenFAST and redFAST as fluorescent reporter proteins in solventogens of the first and second clade (*C. acetobutylicum* and *C. saccharoperbutylacetonicum*, respectively) as well as in the acetogens *A. woodii* and *E. limosum*. Moreover, we used greenFAST- and redFAST-producing *C. acetobutylicum* and *C. saccharoperbutylacetonicum* cells in synthetic co-cultures and tracked the number of fluorescent cells during cultivation using flow cytometry. In addition, we constructed a tightly regulated, inducible two-plasmid system and evaluated the coexistence and the interaction of both plasmids in *C. saccharoperbutylacetonicum* cells regarding their green and red fluorescence at the single-cell level.

RESULTS AND DISCUSSION

Establishment of greenFAST and redFAST as Fluorescent Reporter Proteins in Solventogenic and Acetogenic Bacteria. The genes encoding the fluorescent reporter proteins greenFAST and redFAST were expressed in *C. saccharoperbutylacetonicum*, *C. acetobutylicum*, *A. woodii*, and

https://doi.org/10.1021/acssynbio.1c00554
ACS Synth. Biol. 2022, 11, 953−967

E. limosum (Figures 1 and 2). Both, greenFAST and redFAST used in this study are based on the *C. acetobutylicum* codon-optimized version of FAST.[10] The three and five additional mutations were introduced into the protein coding sequence of FAST as described by Tebo et al..[17] The mean fluorescence intensity (MFI) of greenFAST- or redFAST-producing cells of the whole population, as well as at the single-cell level, was determined in the presence of the fluorogens ^{TF}Lime, ^{TF}Coral, or a mixture of both fluorogens using flow cytometry.

greenFAST and redFAST Production in Solventogenic Anaerobes. The *C. saccharoperbutylacetonicum* strains *Cspa*-greenFAST and *Cspa*-redFAST were constructed to produce the green- or red-fluorescent reporter protein, respectively. *Cspa*-greenFAST showed bright green fluorescence when labeled with ^{TF}Lime or both fluorogens while incubation with ^{TF}Coral resulted in poor green and red fluorescence, which was comparable to autofluorescence of the cells in the absence of any fluorogen (Figure 1A). In addition to the MFI of the whole population, flow cytometry also enabled determining the number of greenFAST- and redFAST-producing cells at the single-cell level (Figure 1B). While the MFI of the whole population decreased during the early stationary phase, the number of fluorescent, greenFAST-producing cells increased from 85 to 95% in the presence of ^{TF}Lime (Figure 1B), indicating that more bacteria are fluorescent, however, fluorescence was less bright. When labeled with both fluorogens, the number of double-positive events, cells that showed both green and red fluorescence, increased to 17%. Even though the dissociation constant for greenFAST binding ^{TF}Coral (K_d = 16.2 μM) is 180 times higher compared to greenFAST binding ^{TF}Lime (K_d 0.09 μM), mislabeling might occur especially when only one of the fluorescent proteins is produced or one of them is produced in excess.[17] Up to 95% of the cells were nonfluorescent when *Cspa*-greenFAST was labeled with ^{TF}Coral (Figure 1B).

Cspa-redFAST labeled with ^{TF}Coral or both fluorogens resulted in bright red fluorescence while cells labeled with ^{TF}Lime only showed poor fluorescence comparable to autofluorescence of the cells in the absence of any fluorogen (Figure 1A). Compared to *Cspa*-greenFAST, double-positive events were reduced for *Cspa*-redFAST labeled with both fluorogens, indicating that redFAST binds ^{TF}Coral quite selectively. The selective labeling might also depend on the fluorogen concentrations.[17] The cells were labeled with a mixture of 5 μM ^{TF}Lime and 10 μM ^{TF}Coral, which might explain why greenFAST was mislabeled more frequently, as twice the amount of ^{TF}Coral was used. However, Tebo et al.[17] reported that the use of 5 μM ^{TF}Lime and 10 μM ^{TF}Coral cause labeling of 99% greenFAST and 95% redFAST when both proteins are produced in the same amount, which we aimed for in our co-culture and two-plasmid system experiments. This selective binding was confirmed on the single-cell level, since cells were red-fluorescent in the presence of ^{TF}Coral or both fluorogens, while only a negligible number of green- or double-positive events occurred (Figure 1B).

In addition, the *C. acetobutylicum* strains *Cac*-greenFAST and *Cac*-redFAST were constructed to produce greenFAST or redFAST, respectively. Compared to the bright green fluorescence of *Cspa*-greenFAST, the fluorescence of *Cac*-greenFAST was rather poor and decreased rapidly during growth until reaching values comparable to the autofluorescence of cells in the absence of any fluorogen (Figure 1C). During exponential growth, up to 76% of the cells produced the green-fluorescent reporter protein, whereas the cells were non-fluorescent in the late stationary phase (Figure 1D). When labeled with ^{TF}Coral, the cells were nonfluorescent in the exponential growth phase. However, the number of red-fluorescent cells rapidly increased during the stationary phase. Interestingly, this phenomenon also occurred when the cells were labeled with both fluorogens. In this case, *Cac*-greenFAST cells were green-fluorescent during the exponential growth phase and red-fluorescent in the late stationary phase (Figure 1C,D). The increasing red fluorescence was not only observed for *Cac*-greenFAST, but also for *Cac*-redFAST and the *C. acetobutylicum* strain harboring the empty vector (*Cac*-pMTL83251) (Figure 1C,D; Supporting Information Figure S2). Interestingly, *Cac*-redFAST showed no red fluorescence during exponential growth. Since the optical density of the *C. acetobutylicum* cultures decreased rapidly after exponential growth, cell death/lysis might be the reason for the decreasing green fluorescence intensity and might also cause the shift in red fluorescence.

greenFAST and redFAST Production in Acetogenic Anaerobes. The *A. woodii* strains *Awo*-greenFAST and *Awo*-redFAST as well as the *E. limosum* strains *Euli*-greenFAST and *Euli*-redFAST were constructed to produce greenFAST or redFAST, respectively. Respective strains harbor genes encoding greenFAST and redFAST under the control of the lactose-inducible promoter P_{bgaL} (Figure 2).

Awo-greenFAST showed green fluorescence after induction of gene expression when labeled with ^{TF}Lime or both fluorogens (Figure 2A). At the single-cell level, the number of green-fluorescent cells increased rapidly after induction of gene expression and mounted up to 98% (Figure 2B). In the early exponential growth phase up to 6% double-positive events were determined when the cells were labeled with both fluorogens. In the presence of ^{TF}Coral, MFI was in the same order of magnitude as autofluorescence in the absence of any fluorogen. *Awo*-redFAST only showed poor autofluorescence in the presence or absence of any fluorogen (Figure 2A). At the single-cell level, up to 8% fluorescent cells were determined to produce the red-fluorescent reporter protein and only during the stationary phase (Figure 2B).

Green and red MFIs were poor for *Euli*-greenFAST and *Euli*-redFAST, respectively (Figure 2C). Only up to 31% of *Euli*-greenFAST cells were green-fluorescent when labeled with ^{TF}Lime while labeling with ^{TF}Coral or both fluorogens resulted in mislabeled cells indicated by several double-positive events. In the case of *Euli*-redFAST, initially, up to 39% of cells were red-fluorescent before the number of fluorescent cells decreased rapidly (Figure 2D).

greenFAST and redFAST Are Functional in Anaerobes with Several Limitations. The fluorescent reporter proteins greenFAST and redFAST were evaluated regarding potential applications, but also their limitations in *C. saccharoperbutylacetonicum*, *C. acetobutylicum*, *A. woodii*, and *E. limosum*. The production of greenFAST caused green fluorescence in *C. saccharoperbutylacetonicum*, *C. acetobutylicum*, *A. woodii*, and *E. limosum* and is therefore suitable as a green-fluorescent reporter protein under anaerobic conditions. Nevertheless, the production of greenFAST resulted in a heterogeneous population, especially in the case of *E. limosum* and *C. acetobutylicum* (Figures 1D and 2D). Heterogeneity of bacterial populations can be caused by several factors including cell differentiation, morphogenesis, sporulation, or even differ-

https://doi.org/10.1021/acssynbio.1c00554
ACS Synth. Biol. 2022, 11, 953−967

ACS Synthetic Biology pubs.acs.org/synthbio Research Article

Table 1. Applicable Fluorescent Reporter Proteins for the Anaerobes *C. saccharoperbutylacetonicum*, *C. acetobutylicum*, *A. woodii*, and *E. limosum*

bacterial strain	reporter protein	fluorescence	application	source
C. saccharoperbutylacetonicum	greenFAST	bright green	multicolor approaches	this study
	redFAST	bright red	multicolor approaches	this study
C. acetobutylicum	PbFbFP (everglow-Pp1)	green	monitoring plasmid loss	Molitor et al. 2016[33]
	EcFbFP (everglow-Bs2)	green	promoter studies	Cheng et al. 2019[35]
	phiLOV	green	proof of functionality	Buckley et al. 2016[34]
	CreiLov	not fluorescent		Mordaka and Heap 2018[36]
	FAST	bright red or green	promoter studies, construction of fusion proteins, multicolor approaches in combination with HaloTag and SNAP-tag	Streett et al. 2019[10]
	HaloTag	orange or red	multicolor approaches in combination with FAST	Charubin et al. 2020[11]
	SNAP-tag	orange or red	multicolor approaches in combination with FAST	Charubin et al. 2020[11]
	greenFAST	poor green	proof of functionality	this study
	redFAST	not fluorescent		this study
A. woodii	greenFAST	bright green	proof of functionality	this study
	redFAST	not fluorescent		this study
E. limosum	CreiLov	green	promoter studies	Shin et al. 2019[37]
	FAST	bright red or green	construction of fusion proteins	Flaiz et al. 2021[12]
	greenFAST	poor green	proof of functionality, production resulted in a heterogeneous population	this study
	redFAST	poor red		this study

ences in gene expression.[31] A sporulating *C. acetobutylicum* culture causes an increasing forward scatter (FSC).[32] We could not determine any sporulating cells in our experiments. Still, the morphology of the *C. acetobutylicum* cells changed as both FSC and side scatter (SSC) intensity decreased while red fluorescence increased (Supporting Information Figure S1). A heterogeneous population of FAST-producing *C. acetobutylicum* cells was described before.[10] Moreover, Streett et al.[10] showed, that the MFI decreased during the stationary phase when production of FAST is controlled by the P_{thl} or a mutated super P_{thl} promoter, which matches our results for *Cac*-greenFAST. In addition, a heterogeneous population of inducible FAST-producing *E. limosum* cells was recently reported, which might be caused by the uptake mechanism of the inducer or due to plasmid instability.[12] An integration into the chromosome could help to overcome this problem. Due to this heterogeneity greenFAST and redFAST cannot be used for accurate quantification of *E. limosum* and *C. acetobutylicum* in synthetic co-cultures. Still, the number of productive cells can be determined at the single-cell level. However, greenFAST is a potent fluorescent reporter for the use in *C. saccharoperbutylacetonicum* and *A. woodii*. When greenFAST-producing cells were labeled with both fluorogens, several double-positive events were detected especially in the case of *Euli*-greenFAST, but also for *Cspa*-greenFAST and *Cac*-greenFAST, which was probably due to mislabeling. This must be considered in co-culture experiments. However, selectivity should be improved when both greenFAST and redFAST are produced in the same amount,[17] which we aimed for in co-culture experiments or when both proteins were produced in the same cell. Compared to that, the red-fluorescent protein redFAST selectively bound ^{TF}Coral even in the presence of both fluorogens. However, at this point, the use of redFAST seems to be limited for *C. saccharoperbutylacetonicum* but can be combined with greenFAST for multicolor approaches. Moreover, synthetic co-cultures with *C. saccharoperbutylacetonicum* producing redFAST combined with microbes engineered to produce greenFAST can be performed. Since the green fluorescence was rather poor in *C. acetobutylicum* and *E. limosum* in this study, the functionality of greenFAST must be evaluated for other potential co-culture partners. Besides multicolor approaches, greenFAST and redFAST have the potential to be used as reporter proteins to investigate gene expression levels, protein localization, and movement within the cell by constructing fluorescent fusion proteins, or to screen for fluorescent colonies after transformation of cells. While other fluorescent reporter proteins are not yet described for *C. saccharoperbutylacetonicum* and *A. woodii*, the use of different FbFPs is described for both *C. acetobutylicum*[33−36] and *E. limosum*.[37] Moreover, the ligand-dependent fluorescent proteins HaloTag and SNAP-tag are functional in *C. acetobutylicum* and can be considered to be used in multicolor approaches.[11] The fluorescent reporter proteins and their applications described in this study and in the literature are summarized in Table 1.

Quantification of Fluorescent Cells in Mixtures of Green- or Red-Fluorescent *C. acetobutylicum* and *C. saccharoperbutylacetonicum* Strains. The number of green- and red-fluorescent greenFAST- and redFAST-producing cells was determined in mixtures labeled with ^{TF}Lime, ^{TF}Coral, and both fluorogens. Initially, *Cspa*-greenFAST and *Cspa*-redFAST were cultivated separately until late-exponential growth phase to an OD_{600} of 4 and 3.5, respectively, washed, and adjusted to an OD_{600} of 1 in phosphate-buffered saline (PBS) and finally mixed in ratios of 20:80, 50:50, and 80:20,

https://doi.org/10.1021/acssynbio.1c00554
ACS Synth. Biol. 2022, 11, 953−967

ACS Synthetic Biology pubs.acs.org/synthbio Research Article

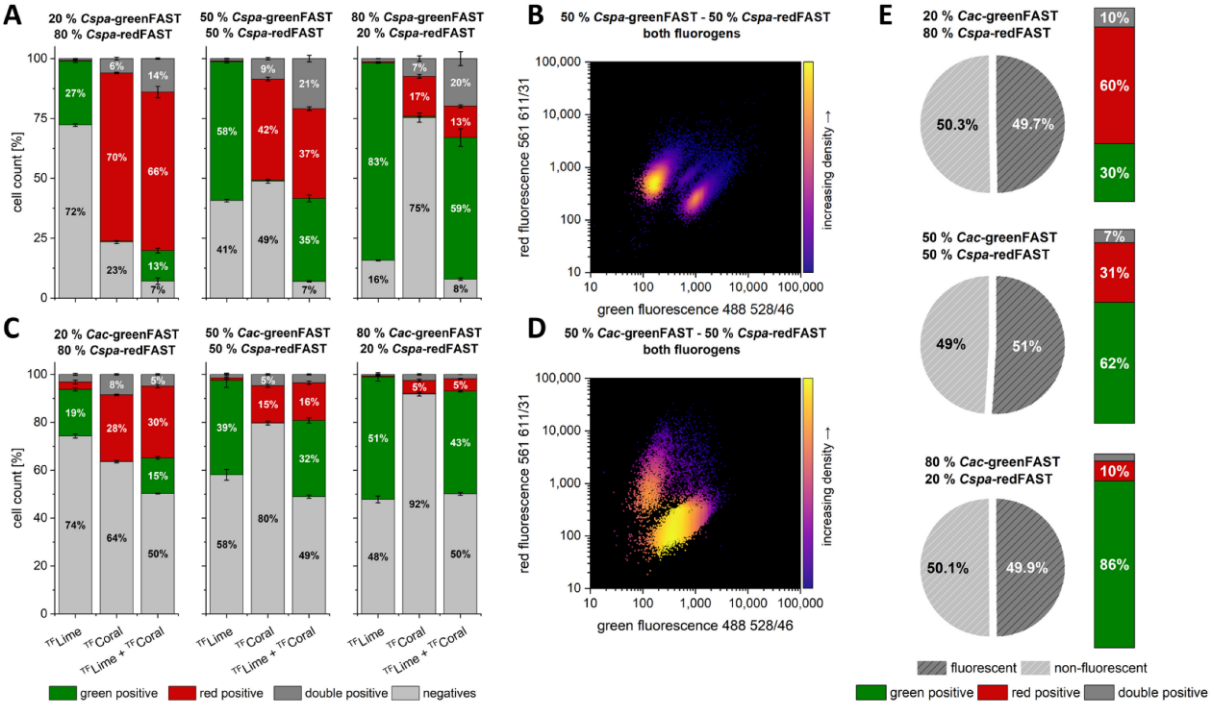

Figure 3. Fluorescence of cell mixtures of *C. saccharoperbutylacetonicum* and *C. acetobutylicum*. (A) Number of fluorescent cells of cell mixtures of separately exponentially grown *C. saccharoperbutylacetonicum* [pMTL83251_P_{thlA}_greenFAST] and *C. saccharoperbutylacetonicum* [pMTL83251_P_{thlA}_redFAST] cells labeled using 5 μM ^{TF}Lime, 10 μM ^{TF}Coral, or a mixture of both fluorogens n = 3. (B) Density plot of *C. saccharoperbutylacetonicum* [pMTL83251_P_{thlA}_greenFAST] and *C. saccharoperbutylacetonicum* [pMTL83251_P_{thlA}_redFAST] mixtures in a ratio of 50:50 and labeled using 5 μM ^{TF}Lime and 10 μM ^{TF}Coral. (C) Number of fluorescent cells of cell mixtures of separately exponentially grown *C. acetobutylicum* [pMTL83251_P_{thlA}_greenFAST] and *C. saccharoperbutylacetonicum* [pMTL83251_P_{thlA}_redFAST] cells. (D) Density plot of *C. acetobutylicum* [pMTL83251_P_{thlA}_greenFAST] and *C. saccharoperbutylacetonicum* [pMTL83251_P_{thlA}_redFAST] mixtures in a ratio of 50:50 and labeled using 5 μM ^{TF}Lime and 10 μM ^{TF}Coral. (E) Number of fluorescent and nonfluorescent *C. acetobutylicum* [pMTL83251_P_{thlA}_greenFAST] and *C. saccharoperbutylacetonicum* [pMTL83251_P_{thlA}_redFAST] cells. Fluorescent cells were further separated into green, red, and double-positive events.

respectively (Figure 3A). The cells were specifically labeled with ^{TF}Lime, which resulted in green fluorescence while only up to 0.5% red and 1.3% double-positive events were determined for the different mixtures. Red-fluorescent cells were determined when labeled with ^{TF}Coral. As shown in the above section, cells that produced greenFAST were probably mislabeled due to the excess of ^{TF}Coral since 6, 9, and 7% double-positive events were observed, respectively. Most importantly, the number of greenFAST- and redFAST-producing cells was determined simultaneously when labeled with both fluorogens. The synthetic 50:50 cell mixture labeled with both fluorogens resulted in three distinct populations when analyzed using flow cytometry (Figure 3B). Since the number of red-fluorescent cells labeled with both fluorogens was quite similar to those labeled with ^{TF}Coral alone, the finding that redFAST-producing *Cspa*-redFAST cells were labeled quite selectively was confirmed. Compared to that, the number of green-fluorescent cells was again reduced when the synthetic mixtures were labeled with both fluorogens while the number of double-positive events increased. Still, greenFAST- and redFAST-producing *C. saccharoperbutylacetonicum* cells could be detected in cell mixtures.

In a second approach, the number of green- and red-fluorescent cells was determined in synthetic mixtures composed of *Cac*-greenFAST and *Cspa*-redFAST. The cells were grown separately until mid-exponential growth phase to an OD_{600} of 3 and 2.5, respectively, washed, suspended in PBS, and mixed in the same ratios as mentioned above (Figure 3C). Green-fluorescent *Cac*-greenFAST cells were detected when labeled with ^{TF}Lime. Again, fewer green events were determined in the presence of both fluorogens while the number of double-positive events increased. The majority of the *Cspa*-redFAST cells were nonfluorescent. In the case of the 50:50 cell mixture, 16% red-positive and 32% green-positive cells were determined, also resulting in a dense nonfluorescent population containing 49% of the cells (Figure 3D). Since approximately 50% of the synthetic cell mixtures were nonfluorescent, the fluorescent cells were further separated into green-, red-, and double-positive events (Figure 3E). In general, compared to the calculated ratios, more green-fluorescent cells and less red-fluorescent cells were identified (Figure 3E). This finding indicates that more *Cspa*-redFAST cells were nonfluorescent compared to *Cac*-greenFAST cells.

The number of fluorescent cells can be determined using the different fluorescent reporter proteins. In the case of the *Cspa*-greenFAST and *Cspa*-redFAST mixture, it is even possible to quantify the number of fluorescent cells which might be an important tool to check for maintenance of a stable co-culture during fermentation. Thus, the method allows monitoring of the co-culture, but not controlling the ratios of the individual

https://doi.org/10.1021/acssynbio.1c00554
ACS Synth. Biol. 2022, 11, 953−967

ACS Synthetic Biology pubs.acs.org/synthbio Research Article

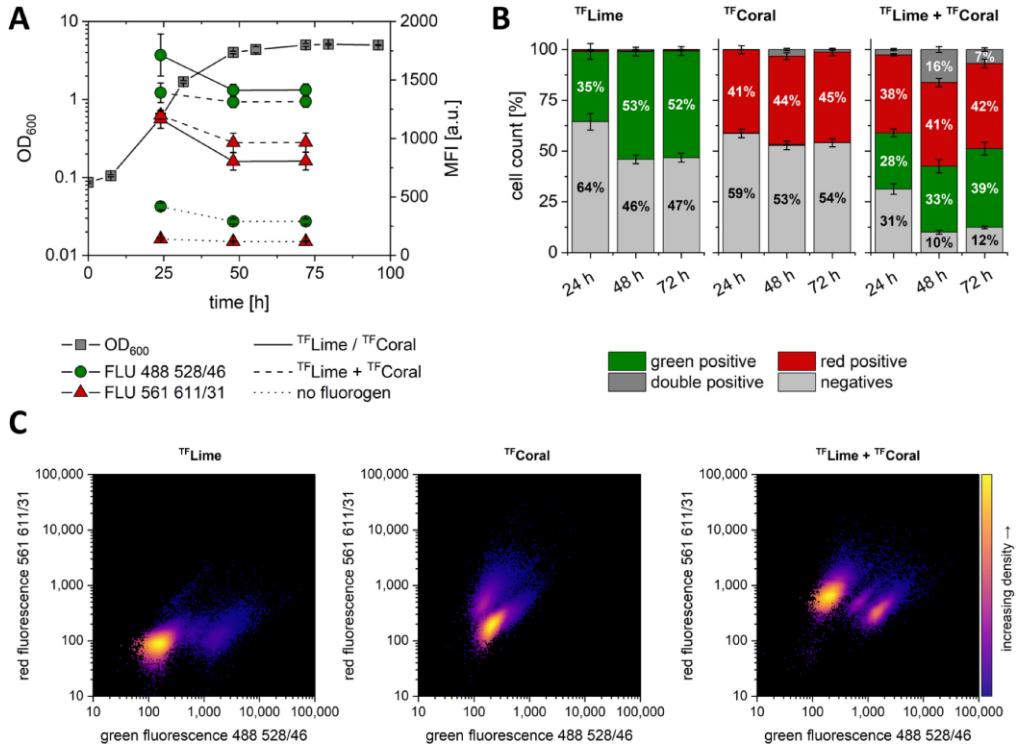

Figure 4. Synthetic *C. saccharoperbutylacetonicum* co-culture producing greenFAST and redFAST. (A) Growth and mean fluorescence intensity (MFI) of the whole population of the synthetic *C. saccharoperbutylacetonicum* [pMTL83251_P_{thlA}_greenFAST] and *C. saccharoperbutylacetonicum* [pMTL83251_P_{thlA}_redFAST] co-culture was determined after 24, 48, and 72 h of cultivation. The cells were labeled using 5 μM ^{TF}Lime, 10 μM ^{TF}Coral, or a mixture of both fluorogens (n = 3). (B) Number of green- or red-fluorescent cells of the *C. saccharoperbutylacetonicum* co-culture at the single-cell level in the presence of 5 μM ^{TF}Lime, 10 μM ^{TF}Coral, or a mixture of both fluorogens after 24, 48, and 72 h of cultivation. (C) Density plots of the synthetic *C. saccharoperbutylacetonicum* co-culture labeled using 5 μM ^{TF}Lime, 10 μM ^{TF}Coral, or a mixture of both fluorogens after 48 h of incubation.

members. Also, this quantification is limited when parts of the mixtures are nonfluorescent. In such a case, greenFAST and redFAST only indicate the number of productive cells. However, when co-cultures are designed to produce an industrially relevant product, the number of productive cells will be more important than the actual ratio of strains. The two reporters greenFAST and redFAST can therefore be used to track enzyme production during fermentation via the construction of fluorescent-tagged proteins. Fluorescent cells indicate that enzymes are indeed produced and potentially also produce the desired product while nonfluorescent cells are nonproductive. Thus, the green fluorescence of bacterium A producing product A which is then consumed by bacterium B to produce product B and resulting in red fluorescence would indicate a functional and, more importantly, productive co-culture.

Monitoring the Number of greenFAST- and redFAST-Producing Cells in Synthetic Co-cultures. *Synthetic Cspa-Cspa Co-culture.* In a first approach, a synthetic co-culture inoculated with *Cspa*-greenFAST and *Cspa*-redFAST was cultivated and the OD_{600}, the mean fluorescence intensity, and the number of greenFAST- and redFAST-producing cells were tracked during growth. Pre-cultures of both strains were cultivated separately until the exponential growth phase and used to inoculate the synthetic co-culture to a total OD_{600} of 0.1. The synthetic *C. saccharoperbutylacetonicum* co-culture reached a maximal OD_{600} of 5, while cells showed both bright green and red fluorescence during growth which proves that both *Cspa*-greenFAST and *Cspa*-redFAST were present in the co-culture. (Figure 4A). In addition, the number of greenFAST- and redFAST-producing cells was determined at the single-cell level using flow cytometry, to evaluate the strain-to-strain ratio, dynamics, and heterogeneity of the co-culture (Figure 4B). Density plots of the co-culture show a nonfluorescent and green-fluorescent population when labeled with ^{TF}Lime and a nonfluorescent and red-fluorescent population when labeled with ^{TF}Coral (Figure 4C). Since greenFAST and redFAST were produced by a comparable number of cells in the co-culture, the number of mislabeled cells and consequently double-positive events were negligible, as the thermodynamic dissociation constant of greenFAST is 180 times lower for ^{TF}Lime than for ^{TF}Coral, and in the case of redFAST, it is 9.2 times lower for ^{TF}Coral than for ^{TF}Lime.[17] Labeling with both fluorogens resulted in three distinct populations including a green- and red-fluorescent as well as a population that contained double-positive events (Figure 4C). The number of redFAST-producing, red-fluorescent cells was comparable when labeled with ^{TF}Coral or both fluorogens. However, the number of greenFAST-producing, green-fluorescent cells was lower in the presence of both fluorogens compared to those just labeled with ^{TF}Lime, while the number of double-positive events increased due to mislabeling. Nevertheless, the strain-to-strain ratio

https://doi.org/10.1021/acssynbio.1c00554
ACS Synth. Biol. 2022, 11, 953−967

ACS Synthetic Biology pubs.acs.org/synthbio Research Article

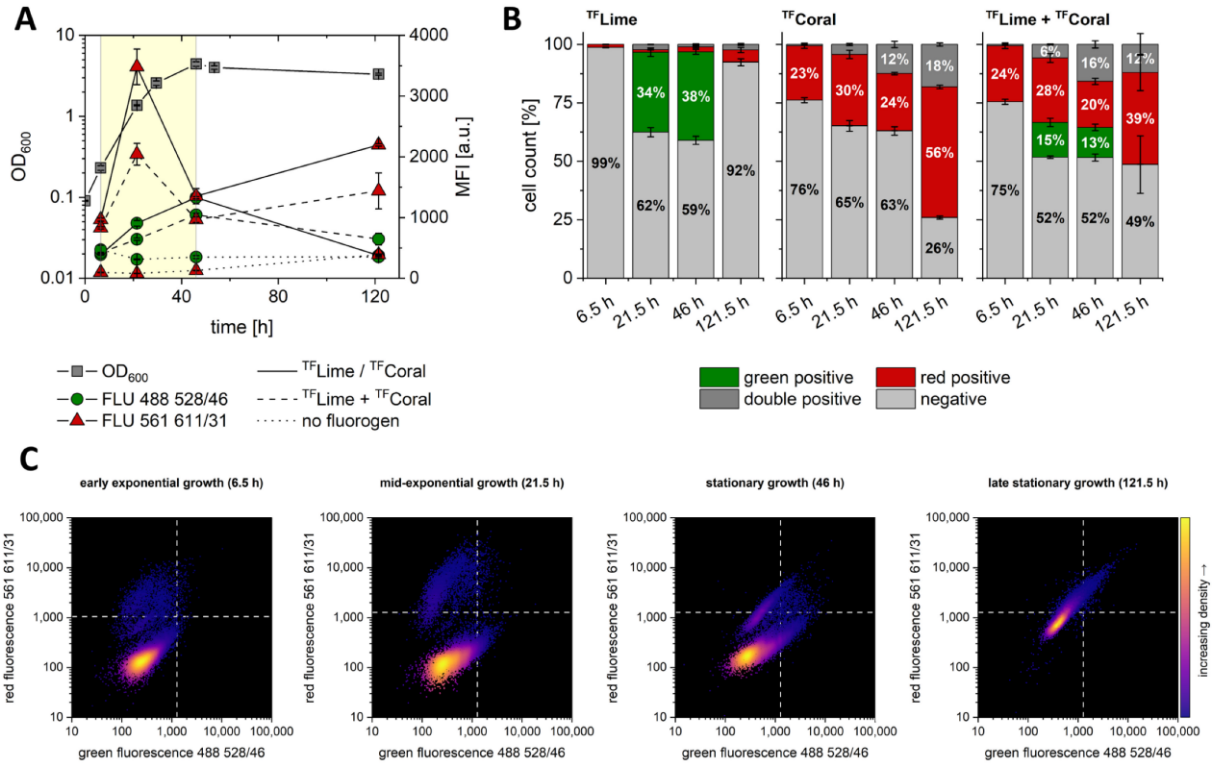

Figure 5. Synthetic *C. acetobutylicum* and *C. saccharoperbutylacetonicum* co-culture producing greenFAST and redFAST. The co-culture was inoculated to a ratio of 50 % *C. acetobutylicum* [pMTL83251_P_{thlA}_greenFAST] and 50 % *C. saccharoperbutylacetonicum* [pMTL83251_P_{thlA}_redFAST]. (A) Growth and mean fluorescence intensity (MFI) of the whole population of the synthetic *C. acetobutylicum* [pMTL83251_P_{thlA}_greenFAST] and *C. saccharoperbutylacetonicum* [pMTL83251_P_{thlA}_redFAST] co-culture was determined after 6.5, 21.5, 46, and 121.5 h of cultivation. The cells were labeled using 5 μM ^{TF}Lime, 10 μM ^{TF}Coral, or a mixture of both fluorogens. The yellow area indicates the exponential growth phase (n = 3). (B) Number of green- or red-fluorescent cells of the co-culture at the single-cell level in the presence of 5 μM ^{TF}Lime, 10 μM ^{TF}Coral, or a mixture of both fluorogens after 6.5, 21.5, 46, and 121.5 h of cultivation. (C) Density plots of the synthetic *C. saccharoperbutylacetonicum*−*C. acetobutylicum* co-culture labeled with 5 μM ^{TF}Lime and 10 μM ^{TF}Coral after 6.5, 21.5, 46, and 121.5 h of cultivation.

remained constant during fermentation while both strains were productive.

Synthetic Cac-Cspa Co-cultures. In a second approach, growth experiments with synthetic co-cultures containing *Cac*-greenFAST and *Cspa*-redFAST were performed (Figure 5, Supporting Information Figures S3 and S4). Therefore, *Cac*-greenFAST and *Cspa*-redFAST were cultivated separately in OMS medium until exponential growth phase and used to inoculate fresh OMS medium in ratios of 20:80, 80:20, and 50:50 to a total OD_{600} of 0.1. Dynamics during cultivation of the different co-cultures were tracked by determination of the MFI of the whole population, while the number of fluorescent cells was determined at the single-cell level using flow cytometry.

A bright red fluorescence of the co-culture that was inoculated to a ratio of 20% *Cac*-greenFAST and 80% *Cspa*-redFAST was detected while green fluorescence was rather poor (Supporting Information Figure S3). Up to 85% of the cells produced the red-fluorescent protein redFAST while only a negligible number of green-fluorescent cells were detected. Therefore, it can be assumed that *Cspa*-redFAST cells prevailed in the co-culture, although *Cac*-greenFAST reached growth rates 2.1 times higher compared to *Cspa*-redFAST in the monoculture experiments.

The co-culture inoculated with 80% *Cac*-greenFAST and 20% *Cspa*-redFAST, showed both green and red fluorescence during growth (Supporting Information Figure S4). During the exponential growth phase, up to 52% of the cells produced the green-fluorescent protein greenFAST, while only up to 8% of the cells were red-fluorescent. After 46 h, when the cells reached the stationary phase, the number of red-fluorescent cells increased to 36%. Two reasons for the increased red fluorescence might be possible. Either *Cspa*-redFAST started to overgrow *Cac*-greenFAST since *Cac*-greenFAST cells lyse during the stationary phase, or lysed *Cac*-greenFAST cells caused the improved red fluorescence in the presence of ^{TF}Coral as already explained for the monoculture experiments. In both initial attempts (20:80 and 80:20 mixtures), a variation of inoculation ratios, which is often used to regulate co-cultures,[38] is not possible since the major population overgrew the minor and did not enable coexistence of both strains.

Finally, a synthetic co-culture was inoculated with 50% *Cac*-greenFAST and 50% *Cspa*-redFAST (Figure 5). The MFI of the whole population labeled with ^{TF}Lime resulted in distinct green fluorescence during growth (Figure 5A). However, green-fluorescent cells were only detected during mid-exponential growth (Figure 5B). The co-culture showed bright red fluorescence during the mid-exponential and the late stationary phase when the cells were labeled with ^{TF}Coral (Figure 5A). At the single-cell level, the number of red-fluorescent cells and double-positive events increased during growth (Figure 5B). This increased red fluorescence again indicates mislabeled, lysed

https://doi.org/10.1021/acssynbio.1c00554
ACS Synth. Biol. 2022, 11, 953−967

ACS Synthetic Biology pubs.acs.org/synthbio Research Article

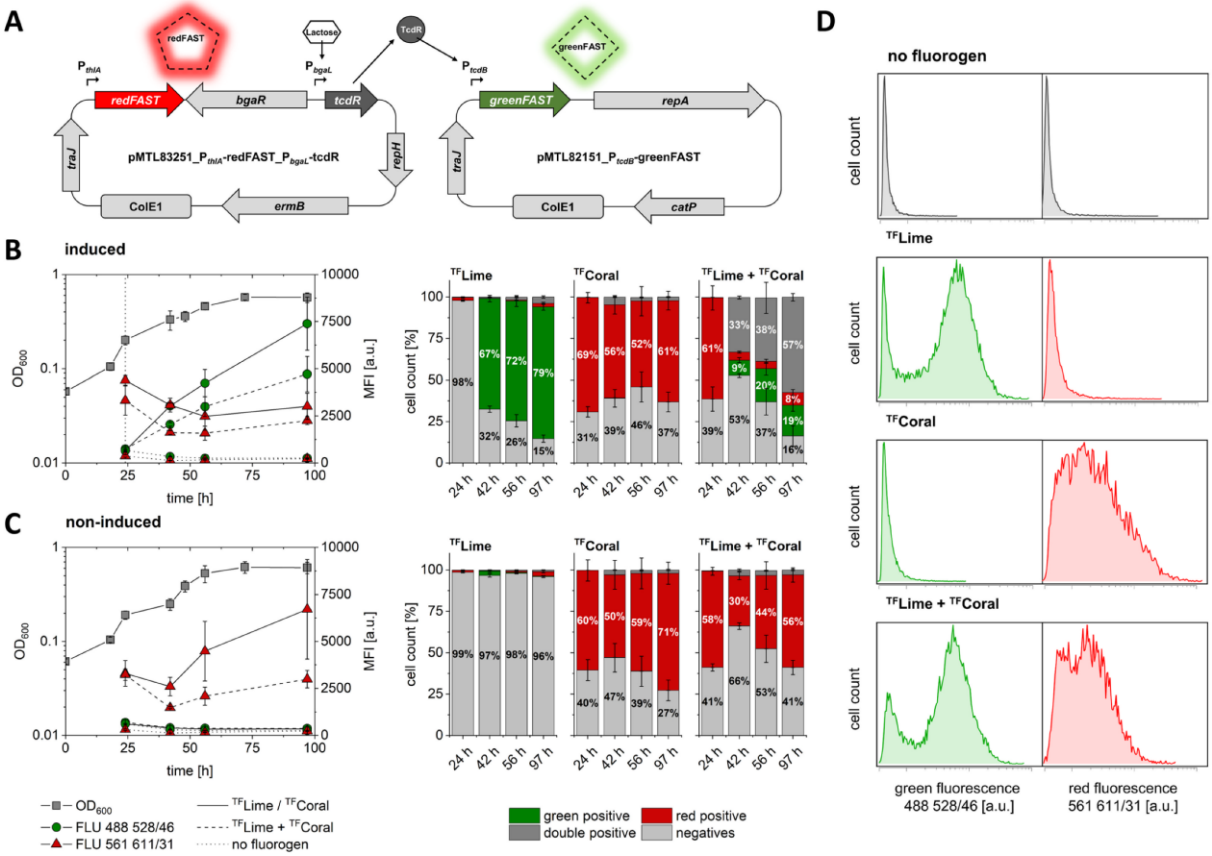

Figure 6. Production of greenFAST and redFAST by *C. saccharoperbutylacetonicum* using a tightly regulated two-plasmid system. (A) Schematic overview of pMTL83251_P_{thlA}-redFAST_P_{bgaL}-tcdR and pMTL82151_P_{tcdB}_greenFAST. The two-plasmid system was established in *C. saccharoperbutylacetonicum* and used to tightly regulate gene expression of the gene encoding greenFAST controlled by TcdR and P_{tcdB} while gene and promoter are located on different plasmids. The gene encoding redFAST was expressed constitutively controlled by P_{thlA}, while TcdR production was induced by lactose addition as *tcdR* is controlled by the *bgaR*-P_{bgaL} system. (B, C) Growth, mean fluorescence intensity (MFI), and number of fluorescent cells at the single-cell level of *C. saccharoperbutylacetonicum* [pMTL83251_P_{thlA}-redFAST_P_{bgaL}tcdR]-[pMTL82151_P_{tcdB}_greenFAST] labeled using 5 μM ^{TF}Lime, 10 μM ^{TF}Coral, or a mixture of both fluorogens. Gene expression of *tcdR* was either induced (B), indicated with the vertical dotted line, or noninduced (C). Number of fluorescent cells was determined after 24, 42, 56, and 97 h of cultivation ($n = 4$). (D) Histograms of cells with induced *tcdR* gene expression after 97 h of cultivation labeled using ^{TF}Lime, ^{TF}Coral, or a mixture of both fluorogens. The shift in green or red fluorescence is compared to histograms of cells in the absence of any fluorogen (gray).

C. acetobutylicum cells as seen in the monoculture experiments resulting in characteristic red fluorescence when labeled with ^{TF}Coral. Labeling of the co-culture using both fluorogens resulted in distinct green and red fluorescence during growth, which in both cases was less bright compared to the culture labeled with ^{TF}Lime or ^{TF}Coral alone (Figure 5A). The number of green-fluorescent cells dramatically decreased when labeled with both fluorogens, while the number of double-positive events increased. In the presence of both fluorogens, it is impossible to tell if double-positive events were caused by mislabeled *Cac*-greenFAST cells or due to red fluorescence of lysed *C. acetobutylicum* cells. The fluorescent populations of the synthetic co-culture labeled with both fluorogens are displayed in Figure 5C. In the early exponential growth phase, two distinct populations were determined consisting of 75% nonfluorescent and 24% red-fluorescent cells. While the number of red-fluorescent cells increased and slightly shifted to red fluorescence, greenFAST production started during mid-exponential growth and caused a shift of the population to green fluorescence. When growth was abandoned, the number of double-positive events increased. Finally, in the late stationary phase, the co-culture consisted of one population, which was characteristic for *C. acetobutylicum* but might also include red-fluorescent *Cspa*-redFAST cells.

Anaerobes such as *C. acetobutylicum*, *C. autoethanogenum*, *C. cellulolyticum*, *C. kluyveri*, or *C. ljungdahlii* are promising biocatalysts not only in mono- but also co-culture approaches to produce chemicals including 2,3-butanediol, isopropanol, or C_4-C_8 fatty-acids and alcohols.[21,39−41] So far, the differentiation of such strains in synthetic co-cultures is challenging since most acetogens and solventogens share a similar shape and size. Therefore, the use of fluorescent reporter proteins including FAST combined with other non-oxygen-dependent fluorescent reporter proteins, e. g. SNAP-tag or HaloTag is of great interest. Such an approach was successfully established to quantify the number of *C. acetobutylicum* and *C. ljungdahlii* in synthetic co-cultures using FAST and the HaloTag as reporters.[11,30] Still, the HaloTag and SNAP-tag have several disadvantages, especially

https://doi.org/10.1021/acssynbio.1c00554
ACS Synth. Biol. 2022, 11, 953−967

the long labeling times that might be challenging when co-culture dynamics are studied.[42] Moreover, a bilin-binding fluorescent protein was recently established as a fluorescent reporter, which is functional under anaerobic conditions[43] and might be combined with FAST for multicolor approaches. We showed that the two reporter proteins greenFAST and redFAST are suitable for use in anaerobic synthetic co-culture experiments to detect protein-producing cells as fluorescence is fast, reversible, and causes strong fluorescence. However, the use is still limited to a certain extent since redFAST was not functional in all bacteria tested.

Green- and Red-Fluorescent Cells Confirm the Functionality of the *tcdR*-P_{tcdB}-Inducible Two-Plasmid System. For the application of greenFAST and redFAST in a single host strain, we constructed a tightly regulated, inducible, two-plasmid system in *C. saccharoperbutylacetonicum* and determined the number of cells that produced both fluorescent reporters under anaerobic conditions and proved the coexistence of both plasmids during growth. The first plasmid pMTL83251_P_{thlA}_redFAST-P_{bgaL}_tcdR harbored the gene encoding for redFAST controlled by the constitutive P_{thlA} promoter and caused red fluorescence. Moreover, *tcdR* was encoded on the respective plasmid, controlled by the lactose-inducible P_{bgaL} promoter. The second plasmid termed pMTL82151_P_{tcdB}_greenFAST harbored the gene encoding greenFAST, which expression is controlled by the tightly regulated TcdR-inducible P_{tcdB} promoter. Only, when *tcdR* expression of the first plasmid is induced, the sigma factor TcdR is produced, binds P_{tcdB}, and finally induces production of the reporter protein greenFAST (Figure 6A).

The strain *Cspa* [P_{thlA}_redFAST-P_{bgaL}_tcdR][P_{tcdB}_greenFAST], which harbored both plasmids was cultivated in OMS medium with or without induction of *tcdR* gene expression (Figure 6B,C). In addition to OD_{600}, the MFI of the whole population as well as the number of fluorescent cells at the single-cell level were determined when labeled with ^{TF}Lime, ^{TF}Coral, or both fluorogens. *Cspa* [P_{thlA}_redFAST-P_{bgaL}_tcdR]-[P_{tcdB}_greenFAST] labeled with ^{TF}Coral showed distinct red fluorescence during cultivation while green fluorescence of cells labeled with ^{TF}Lime was only observed when *tcdR* expression was induced (Figure 6B,C). Besides the fact that redFAST production and the resulting red fluorescence were determined during the whole cultivation, several nonfluorescent cells were determined, indicating a heterogeneous population. In those nonfluorescent cells, the plasmid might be instable, mutated, or even lost. Still, the number of red-fluorescent cells fluctuated during cultivation since the population of cells producing redFAST was not completely separated from the population of nonfluorescent cells (Figure 6D). This was not the case for green fluorescence since two distinct populations of green-fluorescent and nonfluorescent cells were determined.

Double-positive events were recorded after induced *tcdR* expression when the cells were labeled with both fluorogens which proves the coexistence of both plasmids in the same host cell. Compared to that, noninduced cells showed solely red fluorescence (Figure 6B,C). It must be noticed, that a reduced MFI and number of fluorescent cells were determined when the cells were labeled with both fluorogens. Moreover, a small number of cells was solely red-fluorescent (<5%), while 9% of cells showed sole green fluorescence after induction of *tcdR* gene expression (Figure 6B). During the stationary phase, the number of red-fluorescent cells was still negligible (<5 and 8%), while the number of green-positive (20 and 19%) and double-positive events (38 and 57%) increased. In the case of sole red-fluorescent cells, induction of *tcdR*- or induction of greenFAST gene expression did not take place. However, since only a negligible number of sole red-fluorescent cells was determined, the induction in both cases and interaction of TcdR and the second plasmid seems quite potent. Compared to that, sole green fluorescence might indicate that redFAST production controlled by P_{thlA} stopped before greenFAST production was induced by TcdR. Most importantly, our experiments show that up to 57% of the *Cspa* [P_{thlA}_redFAST-P_{bgaL}_tcdR][P_{tcdB}_greenFAST] cells produced both greenFAST and redFAST, which resulted in double-positive events verifying the coexistence of both plasmids.

The sigma factor TcdR, is exclusively present in toxicogenic clostridia.[44] Therefore, the promoter P_{tcdB} of the toxin B gene of *C. difficile* is tightly regulated in nontoxicogenic clostridia such as *C. acetobutylicum* and *C. sporogenes*.[45] In respective strains, gene expression controlled by P_{tcdB} was only possible when *tcdR* was inserted into the genome of *C. acetobutylicum* and *C. sporogenes*. Since *C. saccharoperbutylacetonicum* does not encode *tcdR*, gene expression is also tightly regulated in our experiments. The inducible and tightly regulated P_{tcdB}-*tcdR* promoter combined with a two-plasmid system is a novel and promising tool for several applications in *C. saccharoperbutylacetonicum*.

Two-plasmid systems are a frequently used tool in molecular biology since they provide several advantages. Gene expression could be more flexible using high- and low-copy plasmids. Moreover, the transformation of cells using large plasmids often cause low transformation efficiencies and increases the probability of recombination events.[46] In anaerobes, the use of two-plasmid systems is especially of interest for CRISPR/Cas9 applications. Assembling all elements needed for CRISPR-Cas9 approaches typically results in large plasmids which upon transformation often result in low efficiencies or are not even suitable for transformation of clostridial species. Two-plasmid approaches might overcome this problem and were already successfully established for *C. autoethanogenum*,[47] *C. acetobutylicum*,[48] and *C. beijerinckii*.[49] Nevertheless, the coexistence of both plasmids in the host cell was not tracked. In *C. saccharoperbutylacetonicum*, a single-plasmid approach was used to establish the CRISPR/Cas9 genome-editing tool.[50] However, a two-plasmid approach was not yet applied. With just 378 bps, the gene sequences of greenFAST and redFAST are perfectly suited for two-plasmid systems and can be used as fluorescent reporters to evaluate the successful transformation of both plasmids by screening for cells that show both green and red fluorescence. Moreover, green and red fluorescence can be used to track the coexistence of both plasmids and as reporters to monitor plasmid curing which could become an important tool, especially in anaerobic approaches.

■ CONCLUSIONS

In this study, we established the use of the green- and red-fluorescent proteins, greenFAST and redFAST, in anaerobic bacteria for multicolor approaches. We used both reporters in combination to determine the number of protein-producing cells in synthetic *C. saccharoperbutylacetonicum* co-cultures regarding their green or red fluorescence at the single-cell level using flow cytometry. Moreover, we established an inducible, tightly regulated two-plasmid system in *C. saccharoperbutylacetonicum* and proved the coexistence of both plasmids and showed that the gene product of one plasmid, which was the TcdR sigma factor, can induce greenFAST production with its

https://doi.org/10.1021/acssynbio.1c00554
ACS Synth. Biol. 2022, 11, 953−967

ACS Synthetic Biology pubs.acs.org/synthbio Research Article

Table 2. Strains Used in This Study

bacterial strains	description	source
E. coli DH5α	*E. coli* for plasmid construction	Thermo Fisher Scientific, Inc., Waltham, MA
E. coli XL1-Blue MRF′ [pANS1]	*E. coli* for plasmid methylation	Agilent Technologies, Santa Clara, CA
C. saccharoperbutylacetonicum N1-4(HMT) DSM 14923^T	Type strain	DSMZ-German Collection of Microorganisms and Cell Cultures GmbH, Brunswick, Germany
C. acetobutylicum DSM 792^T	Type strain	DSMZ-German Collection of Microorganisms and Cell Cultures GmbH, Brunswick, Germany
E. limosum NG-6894 (B2)	ALE strain	Prof. Philippe Soucaille, INSA, University of Toulouse, Toulouse, France
A. woodii DSM 1030^T	Type strain	DSMZ-German Collection of Microorganisms and Cell Cultures GmbH, Brunswick, Germany
Cspa-greenFAST	*C. saccharoperbutylacetonicum* harboring plasmid pMTL83251_P_{thlA}_greenFAST	this work
Cspa-redFAST	*C. saccharoperbutylacetonicum* harboring plasmid pMTL83251_P_{thlA}_redFAST	this work
Cac-greenFAST	*C. acetobutylicum* harboring plasmid pMTL83251_P_{thlA}_greenFAST	this work
Cac-redFAST	*C. acetobutylicum* harboring plasmid pMTL83251_P_{thlA}_redFAST	this work
Awo-greenFAST	*A. woodii* harboring plasmid pMTL83251_P_{bgaL}_greenFAST	this work
Awo-redFAST	*A. woodii* harboring plasmid pMTL83251_P_{bgaL}_redFAST	this work
Euli-greenFAST	*E. limosum* harboring plasmid pMTL83251_P_{bgaL}_greenFAST	this work
Euli-redFAST	*E. limosum* harboring plasmid pMTL83251_P_{bgaL}_redFAST	this work
Cspa [P_{thlA}_redFAST-P_{bgaL}_tcdR] [P_{tcdB}_greenFAST]	*C. saccharoperbutylacetonicum* harboring plasmids pMTL83251_P_{thlA}_redFAST-P_{bgaL}_tcdR and pMTL82151_P_{tcdB}_greenFAST	this work

Table 3. Primers Used in This Study

primer	sequence 5′ - 3′	length [bp]
FW_FAST	atcaaaatttaggaggttaggatccatggaacacgtagcatttg	44
RV_FAST	agcttgcatgtctgcaggcctcgagtcataccctcttaacgaaaac	46
FW_FAST-PbgaL	ttaaatgtattgggagggtggatccatggaacacgtagcatttg	44
FW_PbgaL_*Sal*I	tacccggggatcctctagagtcgacgagatgaaaagtattagggc	45
RV_PbgaL-tcdR_*Sma*I	acttttgcatcccgggagtaccctcccaatacatttaaaataattatg	48
FW_PbgaL-tcdR_*Sma*I	tactcccgggatgcaaaagtctttttatgaattaattg	38
RV_tcdR_*Bam*HI	tgcaggcttcttatttttatggggatccttacaagttaaaataattttcatagtctttttttatttttttaaatg	75
FW_redFAST-tcdR	tgcaggcttcttatttttatgtcgacgagatgaaaagtattag	43
RV_redFAST-tcdR	gttcaaaaaaataatggcggcgcgcccatatgataaaaataagaagcctg	50
FW_PtcdB_*Nde*I	gaccgcggccgctgtatccatatgttaatgaatttaaagaaatatttacaatagaaatc	59
RV_PtcdB-greenFAST_*Bam*HI	ccatggatccatttttctcctttactataatatttttattg	40
FW_PtcdB-greenFAST_*Bam*HI	aggagaaaatggatccatggaacacgtag	29
RV_greenFAST_*Xho*I	agcttgcatgtctgcaggcctcgagtcataccctcttaacgaaaac	46

gene encoded on the second plasmid. The establishment of two fluorescent reporter proteins, which are functional under anaerobic conditions, improves the genetic toolbox *C. saccharoperbutylacetonicum* and opens the door for further multicolor approaches to investigate cell dynamics, gene expression, or protein localization.

METHODS

Strains and Medium. All strains used in this study are listed in Table 2. *E. coli* DH5α was used for plasmid cloning and cultivated at 37 °C in modified lysogenic broth (1% tryptone, 1% NaCl, 0.5% yeast extract)[51] supplemented with 250 μg mL^{-1} erythromycin or 15 μg mL^{-1} chloramphenicol depending on the selection marker gene used for cloning.

C. saccharoperbutylacetonicum N1-4(HMT) DSM 14923^T and *C. acetobutylicum* DSM 792^T were cultivated at 30 or 37 °C, respectively, in modified clostridial growth (CG)[52] or modified optimized synthetic (OMS) medium[53] under strictly anaerobic conditions. The CG medium consisted of 252.3 mM glucose, 5.5 mM KH_2PO_4, 4.3 mM K_2HPO_4, 15.1 mM $(NH_4)_2SO_4$, 2.9 mM $MgSO_4$, 59.2 μM $MnSO_4$, 36 μM $FeSO_4$, 17.1 mM NaCl, 15 mM asparagine, 0.5% (w/v) yeast extract, and 4.4 μM resazurin. The OMS medium consisted of 202 mM glucose, 102.5 mM MES, 15.1 mM $(NH_4)_2SO_4$, 4 mM KH_2PO_4, 2.4 mM K_2HPO_4, 0.8 mM $MgSO_4$, 162 μM $FeSO_4$, 59.5 μM $MnSO_4$, 171 μM NaCl, 68 μM $CaCl_2$, 41.3 μM Na_2MoO_4, 14.6 μM 4-aminobenzoic acid, 0.4 μM biotin, 5.9 μM thiamine-HCl, and 4.4 μM resazurin. *A. woodii* DSM 1030^T and *E. limosum* NG-6894 were cultivated at 30 or 37 °C, respectively, using modified DSM 135 medium[12] under strictly anaerobic conditions. *A. woodii* was cultivated using 44 mM fructose, while *E. limosum* was cultivated using 30 mM glucose as a carbon source.

Cultivation of Recombinant Strains. Recombinant strains were initially grown from glycerol or dimethyl sulfoxide (DMSO) stock cultures in 5 mL of CG or modified DSM 135 medium in Hungate tubes supplemented with 5 μg mL^{-1} clarithromycin. *C. saccharoperbutylacetonicum* harboring two plasmids was grown in the presence of 10 μg mL^{-1} clarithromycin and 40 μg mL^{-1} thiamphenicol. Growth experiments with recombinant *C. saccharoperbutylacetonicum* and *C. acetobutylicum* were carried out in 50 mL of OMS medium in 125 mL Müller−Krempel flasks supplemented with respective antibiotics. Growth experiments with recombinant *A. woodii* and *E. limosum* strains were performed in 50 mL of DSM

https://doi.org/10.1021/acssynbio.1c00554
ACS Synth. Biol. 2022, 11, 953−967

ACS Synthetic Biology pubs.acs.org/synthbio Research Article

Table 4. Plasmids Used in This Study

plasmids	description	source
pMTL83251	ColE1 ori$^-$, pCB102 ori$^+$, Em^r, *traJ*, *lacZ*	Heap et al. 2009[55]
pMTL82151	ColE1 ori$^-$, pBP1 ori$^+$, Cm^r, *traJ*, *lacZ*	Heap et al. 2009[55]
pANS1	p15A ori$^-$, Sp^r, *φ*3T I methyltransferase of *B. subtilis* phage *φ*3T	Böhringer, 2002[59]
pMTL83151_gusA_P_{bgaL}	pMTL83151, gusA from *E. coli*, *bgaR*-P_{bgaL} from *Clostridium perfringens*	Beck et al. 2020[60]
pMTL83251_P_{thlA}_FAST	pMTL83251, P_{thlA}, *feg*	Flaiz et al. 2021[12]
pMTL83251_P_{bgaL}_FAST	pMTL83251, *bgaR*-P_{bgaL}, *feg*	Flaiz et al. 2021[12]
pEX-A128_greenFAST	pUC ori$^-$, Amp^r, MSC, gene encoding greenFAST	Eurofins Genomics Germany GmbH, Ebersberg, Germany
pEX-A128_redFAST	pUC ori$^-$, Amp^r, MSC, gene encoding redFAST	Eurofins Genomics Germany GmbH, Ebersberg, Germany
pMTL83251_P_{thlA}_greenFAST	pMTL83251, P_{thlA}, gene encoding greenFAST	this work
pMTL83251_P_{thlA}_redFAST	pMTL83251, P_{thlA}, gene encoding redFAST	this work
pMTL83251_P_{bgaL}_greenFAST	pMTL83251, *bgaR*-P_{bgaL}, gene encoding greenFAST	this work
pMTL83251_P_{bgaL}_redFAST	pMTL83251, *bgaR*-P_{bgaL}, gene encoding redFAST	this work
pMTL83251_P_{bgaL}_tcdR	pMTL83251, *bgaR*-P_{bgaL} from *C. perfringens*, *tcdR* from *Clostridium difficile*	this work
pMTL83251_P_{thlA}_redFAST-P_{bgaL}-*tcdR*	pMTL83251, P_{thlA}, gene encoding redFAST, *bgaR*-P_{bgaL}, *tcdR*	this work
pMTL82151_P_{tcdB}-greenFAST	pMTL82151, P_{tcdB} from *C. difficile*, gene encoding greenFAST	this work

135 medium in 125 mL Müller−Krempel flasks in the presence of 5 μg mL^{-1} clarithromycin. During all growth experiments, the optical density (at 600 nm) as well as the fluorescence of the whole population and at the single-cell level was determined.

For co-culture experiments, different ratios of strains producing greenFAST and redFAST were used to inoculate the modified OMS medium to an initial optical density of 0.1. *Cspa*-greenFAST and *Cspa*-redFAST were mixed in a ratio of 50:50 depending on the optical density of the preculture. The *C. saccharoperbutylacetonicum* co-cultures were cultivated at 30 °C, and fluorescence was determined in the exponential and stationary phases (see Section 2.5). In addition, *Cac*-greenFAST and *Cspa*-redFAST were cultivated in a co-culture with ratios of 20:80, 50:50, and 80:20, respectively. The co-cultures of *C. saccharoperbutylacetonicum* and *C. acetobutylicum* were cultivated at 33 °C, and fluorescence was determined in the exponential and stationary phases (see Section 2.5).

Plasmid Construction. To establish greenFAST and redFAST in *C. saccharoperbutylacetonicum* and *C. acetobutylicum* as fluorescent reporter proteins, plasmids pMTL83251_P_{thlA}_greenFAST and pMTL83251_P_{thlA}_redFAST (Table 4) were constructed. Therefore, *feg* of pMTL83251_P_{thlA}_FAST was exchanged with the genes encoding greenFAST or redFAST. The genes encoding greenFAST or redFAST were amplified from plasmids pEX-A128_greenFAST or pEX-A128_greenFAST, respectively, using the "KAPA Hifi polymerase" (Kapa Biosystem, Sigma-Aldrich Chemie GmbH, Munich, Germany) and primers FW_FAST and RV_FAST (Table 3). All primers used in this study were synthesized by biomers.net GmbH (Ulm, Germany). Before assembly, PCR fragments were purified using the "NucleoSpin Gel and PCR clean-up kit" (Macherey-Nagel GmbH & Co. KG, Düren, Germany). Purified PCR products were cloned via *Bam*HI and *Xho*I (exclusion of *feg*) recognition sites into plasmid pMTL83251_P_{thlA}_FAST. Therefore, pMTL83251_P_{thlA}_FAST was digested with respective "Fast Digest" enzymes (Thermo Fisher Scientific, Inc., Waltham, MA) and ligated with the PCR product using the "NEBuilder Hifi DNA Assembly Cloning Kit" according to the manufacturer's protocol (New England Biolabs, Ipswich, MA).

For the establishment of greenFAST and redFAST in *A. woodii* and *E. limosum*, plasmids pMTL83251_P_{bgaL}_greenFAST and pMTL83251_P_{bgaL}_redFAST (Table 4) were constructed. Both plasmids harbor respective genes controlled by the lactose-inducible *bgaR*-P_{bgaL} promoter system of *Clostridium perfringens*.[54] The genes encoding greenFAST or redFAST were amplified from plasmids pEX-A128_greenFAST or pEX-A128_greenFAST using primers FW_FAST-PbgaL and RV_FAST (Table 3), purified, and ligated via *Bam*HI and *Xho*I recognition sites of plasmid pMTL83251_P_{bgaL}_FAST using the "NEBuilder Hifi DNA Assembly Cloning Kit".

In addition, the green- and red-fluorescent reporter proteins were used in a two-plasmid system for *C. saccharoperbutylacetonicum*, which is based on the constitutive expression of the gene encoding redFAST and the inducible expression of the gene encoding greenFAST using the inducible promoter systems *tcdR*-P_{tcdB} from *C. difficile* and *bgaR*-P_{bgaL} from *C. perfringens*. Initially, plasmid pMTL83251_P_{bgaL}_*tcdR* was constructed, which encodes the sigma factor TcdR of *C. difficile* controlled by the inducible *bgaR*-P_{bgaL} promoter system. Therefore, *tcdR* was amplified from genomic DNA of *C. difficile* DSM 27147 using primers FW_PbgaL-tcdR_*Sma*I and RV_tcdR_*Bam*HI (Table 3) while *bgaR*-P_{bgaL} was amplified from plasmid pMTL83151_gusA_P_{bgaL} using primers FW_PbgaL_*Sal*I and RV_PbgaL-tcdR_*Sma*I and the KAPA Hifi polymerase. Both PCR fragments were assembled with *Sal*I and *Nhe*I digested pMTL83251 using the "NEBuilder Hifi DNA Assembly Cloning Kit".

The two-plasmid system is composed of plasmids pMTL83251_P_{thlA}_redFAST-P_{bgaL}-*tcdR* and pMTL82151_P_{tcdB}-greenFAST. To ensure the coexistence of both plasmids in the cell, backbones were chosen to harbor different origins of replication for Gram-positive bacteria and resistance genes. Hence, pMTL82151, which encodes the Gram-positive replicon of pBP1 and the *catP* resistance gene as well as pMTL83251 encoding the replicon of pCB102 and resistance gene *ermB* were chosen as plasmid backbones.[55] For the construction of pMTL83251_P_{thlA}_redFAST-P_{bgaL}-*tcdR*, *tcdR* and promoter P_{bgaL} were amplified from plasmid pMTL83251_P_{bgaL}_tcdR using primers FW_redFAST-tcdR

https://doi.org/10.1021/acssynbio.1c00554
ACS Synth. Biol. 2022, 11, 953−967

and RV_redFAST-tcdR (Table 3) and assembled with pMTL83251_P_{thlA}_redFAST via *Sgs*I recognition site using the "NEBuilder Hifi DNA Assembly Cloning Kit". For pMTL82151_P_{tcdB}-greenFAST construction, the promoter P_{tcdB} was amplified from genomic DNA of *C. difficile* DSM 27147 using the "KAPA Hifi polymerase" and primers FW_PtcdB_*Nde*I and RV_PtcdB-greenFAST_*Bam*HI (Table 3), while the gene encoding greenFAST was amplified from plasmid pEX-A128_greenFAST using primers FW_PtcdB-greenFAST_*Bam*HI and RV_greenFAST_*Xho*I (Table 3). Both PCR products were assembled with pMTL82151 via *Xho*I and *Nde*I recognition sites using the "NEBuilder Hifi DNA Assembly Cloning Kit". Assembled plasmids were used for the transformation of chemically competent *E. coli* DH5α cells and verified via Sanger sequencing (Eurofins Genomics GmbH, Luxemburg).

Prior to the transformation of *C. acetobutylicum*, plasmids were methylated via φ3T I methyltransferase of *Bacillus subtilis* phage φ3T.[56] Therefore, electrocompetent *E. coli* XL1 Blue MRF' harboring the methylation plasmid pANS1 were transformed with respective plasmids. Methylation of plasmids was confirmed via restriction digestion using *SatI*, which is an isoschizomer of the native endonuclease *Cac*824I before the transformation of *C. acetobutylicum*. All plasmids used in this study are listed in Table 4.

Transformation. Construction of recombinant *C. saccharoperbutylacetonicum* strains was performed according to procedures described before with a few alterations.[57] For the preparation of electrocompetent *C. saccharoperbutylacetonicum* cells, 50 mL of CG medium were inoculated using an overnight-grown culture and cultivated at 30 °C, until an OD_{600} of 0.8−1.2 was reached. Then, the cells were cooled on ice, harvested in an anaerobic cabinet at 3985*g* for 10 min at 4 °C, and washed with electroporation buffer A (300 mM sucrose, 0.6 mM Na_2HPO_4, 4.3 mM NaH_2PO_4, 1 mM $MgCl_2$). Afterward, the cell pellet was suspended in 1 mL of electroporation buffer B (electroporation buffer A without $MgCl_2$) and stored on ice until electroporation. Following electroporation, the cells were regenerated in the anaerobic cabinet at 32 °C for 2−16 h. After plating, CGM agar plates were incubated at 32 °C in the anaerobic cabinet until colonies were visible. Subsequently, single colonies were picked with a canula of a syringe, flushed into fresh medium, and cultivated in 5 mL of CG medium supplemented with the proper antibiotic, until growth was visible.

Electroporation of *A. woodii*, *E. limosum*, and *C. acetobutylicum* was performed according to Leang et al.[58] with several modifications under anaerobic conditions as described before.[12] *A. woodii* was cultivated and recovered after electroporation at 30 °C in modified DSM 135 medium supplemented with 44 mM, fructose while *E. limosum* was cultivated and recovered at 37 °C in modified DSM 135 medium supplemented with 30 mM glucose. *C. acetobutylicum* was cultivated in 50 mL and recovered in 2 mL of CG medium at 37 °C. Washing and harvesting steps during the preparation of electrocompetent cells were carried out at 3500*g* for 10 min at 4 °C. Finally, the cells were suspended in 600 μL of SMP buffer and 120 μL of antifreezing buffer (40% [v/v] SMP buffer, 60% [v/v] DMSO) and immediately used for electroporation or stored in cryogenic vials at −80 °C. The transformation of electrocompetent *C. acetobutylicum* cells was performed using 2 μg of properly methylated plasmid DNA. After the electric pulse and subsequent recovery, 200 μL of cell suspension were plated on selective CGM agar plates and incubated at 37 °C in an anaerobic cabinet until colonies appeared. Single colonies were picked with canula of a syringe, flushed into fresh medium, and cultivated in 5 mL of CG medium supplemented with the proper antibiotic until growth was visible.

Fluorescence Determination (Using Flow Cytometry). MFI of the whole population as well as the number of fluorescent cells of recombinant *C. saccharoperbutylacetonicum*, *C. acetobutylicum*, *A. woodii*, and *E. limosum* strains were determined during growth using an "Amnis CellStream" flow cytometer (Luminex Corporation, Austin, TX). Culture broth of the mono- or co-cultures was harvested in the exponential and stationary phases by centrifugation at 7111*g* for 15 min at 4 °C, washed with PBS (137 mM NaCl, 2.7 mM KCl, 10 mM Na_2HPO_4, 1.8 mM KH_2PO_4), and suspended to a final OD_{600} of 1 as described before.[12] To determine the number of fluorescent cells of synthetic cell mixtures at the single-cell level, PBS-suspended cells (OD_{600} = 1) of recombinant *C. saccharoperbutylacetonicum* and *C. acetobutylicum* strains were mixed in ratios of 20:80, 50:50, and 80:20 and analyzed as described above. For analysis, at least 10 000 events of washed cells, which were diluted in PBS (end OD_{600}: 0.08) and stained with 5 μM ^{TF}Lime, 10 μM ^{TF}Coral, or 5 μM ^{TF}Lime, and 10 μM ^{TF}Coral, were recorded. Green fluorescence of the greenFAST:fluorogen complex was assessed using an excitation wavelength of 488 nm and a 528/46 nm emission filter. Red fluorescence of the redFAST:fluorogen complex was assessed using an excitation wavelength of 561 nm and a 611/31 nm emission filter. Acquired data were analyzed using the CellStream Analysis tool version 1.2.152 (Luminex Corporation, Austin, TX).

■ ASSOCIATED CONTENT

Supporting Information

The Supporting Information is available free of charge at https://pubs.acs.org/doi/10.1021/acssynbio.1c00554.

Density plots of *Cac*-redFAST during the exponential and stationary phase; growth, MFI, and number of fluorescent cells of *Cac*-pMTL83251, 20% *Cac*-greenFAST and 80% *Cspa*-redFAST synthetic co-culture, and 80% *Cac*-greenFAST and 20% *Cspa*-redFAST synthetic co-culture (PDF)

■ AUTHOR INFORMATION

Corresponding Author

Maximilian Flaiz − *Institute of Microbiology and Biotechnology, University of Ulm, 89081 Ulm, Germany*; orcid.org/0000-0003-0238-4995; Email: maximilian.flaiz@uni-ulm.de

Authors

Tina Baur − *Institute of Microbiology and Biotechnology, University of Ulm, 89081 Ulm, Germany*; orcid.org/0000-0002-4405-556X

Jana Gaibler − *Institute of Microbiology and Biotechnology, University of Ulm, 89081 Ulm, Germany*

Christian Kröly − *Institute of Microbiology and Biotechnology, University of Ulm, 89081 Ulm, Germany*

Peter Dürre − *Institute of Microbiology and Biotechnology, University of Ulm, 89081 Ulm, Germany*; orcid.org/0000-0002-5586-221X

Complete contact information is available at: https://pubs.acs.org/10.1021/acssynbio.1c00554

https://doi.org/10.1021/acssynbio.1c00554
ACS Synth. Biol. 2022, 11, 953−967

Author Contributions

M.F., T.B., and P.D. designed experiments. M.F., T.B., J.G., and C.K. performed the experiments. M.F. analyzed the data and wrote the manuscript. T.B. and P.D. participated in writing the manuscript and revised the paper. All authors read and edited the manuscript.

Notes

The authors declare no competing financial interest.

■ ACKNOWLEDGMENTS

The authors thank Philippe Soucaille (INSA, University of Toulouse, Toulouse, France) for providing the strain *E. limosum* NG-6894. Furthermore, they thank Dr. Sebastian Reich (University of Ulm, Ulm, Germany) for the support regarding flow cytometry use and data analysis. This research was funded by the European Research Area Cofund on BioTechnologies (ERACoBioTech) within the 1st Joint Call (projects BIOMETCHEM, grant 161B0609A, and BESTER, grant 161B0594A).

■ REFERENCES

(1) Birgen, C.; Dürre, P.; Preisig, H. A.; Wentzel, A. Butanol production from lignocellulosic biomass: revisiting fermentation performance indicators with exploratory data analysis. *Biotechnol. Biofuels* **2019**, *12*, No. 167.

(2) Poehlein, A.; Solano, J. D. M.; Flitsch, S. K.; Krabben, P.; Winzer, K.; Reid, S. J.; Jones, D. T.; Green, E.; Minton, N. P.; Daniel, R.; Dürre, P. Microbial solvent formation revisited by comparative genome analysis. *Biotechnol. Biofuels* **2017**, *10*, No. 58.

(3) Kosaka, T.; Nakayama, S.; Nakaya, K.; Yoshino, S.; Furukawa, K. Characterization of the sol operon in butanol-hyperproducing *Clostridium saccharoperbutylacetonicum* strain N1-4 and its degeneration mechanism. *Biosci. Biotechnol. Biochem.* **2007**, *71*, 58−68.

(4) Bengelsdorf, F. R.; Beck, M. H.; Erz, C.; Hoffmeister, S.; Karl, M. M.; Riegler, P.; Wirth, S.; Poehlein, A.; Weuster-Botz, D.; Dürre, P. Bacterial anaerobic synthesis gas (syngas) and $CO_2 + H_2$ fermentation. In *Advances in Applied Microbiology*; Elsevier, 2018; Vol. *103*, pp 143−221.

(5) Papoutsakis, E. T. Engineering solventogenic clostridia. *Curr. Opin. Biotechnol.* **2008**, *19*, 420−429.

(6) Li, S.; Huang, L.; Ke, C.; Pang, Z.; Liu, L. Pathway dissection, regulation, engineering and application: lessons learned from biobutanol production by solventogenic clostridia. *Biotechnol. Biofuels* **2020**, *13*, No. 39.

(7) Jin, S.; Bae, J.; Song, Y.; Pearcy, N.; Shin, J.; Kang, S.; Minton, N. P.; Soucaille, P.; Cho, B.-K. Synthetic biology on acetogenic bacteria for highly efficient conversion of C1 gases to biochemicals. *Int. J. Mol. Sci.* **2020**, *21*, 7639.

(8) Zimmer, M. Green fluorescent protein (GFP): Applications, structure, and related photophysical behavior. *Chem. Rev.* **2002**, *102*, 759−782.

(9) Gyulev, I. S.; Willson, B. J.; Hennessy, R. C.; Krabben, P.; Jenkinson, E. R.; Thomas, G. H. Part by part: synthetic biology parts used in solventogenic clostridia. *ACS Synth. Biol.* **2018**, *7*, 311−327.

(10) Streett, H. E.; Kalis, K. M.; Papoutsakis, E. T. A strongly fluorescing anaerobic reporter and protein-tagging system for *Clostridium* organisms based on the fluorescence-activating and absorption-shifting tag protein (FAST). *Appl. Environ. Microbiol.* **2019**, *85*, e00622−19.

(11) Charubin, K.; Streett, H.; Papoutsakis, E. T. Development of strong anaerobic fluorescent reporters for *Clostridium acetobutylicum* and *Clostridium ljungdahlii* using HaloTag and SNAP-tag proteins. *Appl. Environ. Microbiol.* **2020**, *86*, No. e01271-20.

(12) Flaiz, M.; Ludwig, G.; Bengelsdorf, F. R.; Dürre, P. Production of the biocommodities butanol and acetone from methanol with fluorescent FAST-tagged proteins using metabolically engineered strains of *Eubacterium limosum*. *Biotechnol. Biofuels* **2021**, *14*, No. 117.

(13) Plamont, M.-A.; Billon-Denis, E.; Maurin, S.; Gauron, C.; Pimenta, F. M.; Specht, C. G.; Shi, J.; Quérard, J.; Pan, B.; Rossignol, J.; Moncoq, K.; Morellet, N.; Volovitch, M.; Lescop, E.; Chen, Y.; Triller, A.; Vriz, S.; Le Saux, T.; Jullien, L.; Gautier, A. Small fluorescence-activating and absorption-shifting tag for tunable protein imaging in vivo. *Proc. Natl. Acad. Sci. U.S.A.* **2016**, *113*, 497−502.

(14) Monmeyran, A.; Thomen, P.; Jonquière, H.; Sureau, F.; Li, C.; Plamont, M.-A.; Douarche, C.; Casella, J.-F.; Gautier, A.; Henry, N. The inducible chemical-genetic fluorescent marker FAST outperforms classical fluorescent proteins in the quantitative reporting of bacterial biofilm dynamics. *Sci. Rep.* **2018**, *8*, No. 10336.

(15) Chekli, Y.; Peron-Cane, C.; Dell'Arciprete, D.; Allemand, J.-F.; Li, C.; Ghigo, J.-M.; Gautier, A.; Lebreton, A.; Desprat, N.; Beloin, C. Visualizing the dynamics of exported bacterial proteins with the chemogenetic fluorescent reporter FAST. *Sci. Rep.* **2020**, *10*, No. 15791.

(16) Li, C.; Plamont, M.-A.; Sladitschek, H. L.; Rodrigues, V.; Aujard, I.; Neveu, P.; Le Saux, T.; Jullien, L.; Gautier, A. Dynamic multicolor protein labeling in living cells. *Chem. Sci.* **2017**, *8*, 5598−5605.

(17) Tebo, A. G.; Moeyaert, B.; Thauvin, M.; Carlon-Andres, I.; Böken, D.; Volovitch, M.; Padilla-Parra, S.; Dedecker, P.; Vriz, S.; Gautier, A. Orthogonal fluorescent chemogenetic reporters for multicolor imaging. *Nat. Chem. Biol.* **2021**, *17*, 30−38.

(18) Jagmann, N.; Philipp, B. Design of synthetic microbial communities for biotechnological production processes. *J. Biotechnol.* **2014**, *184*, 209−218.

(19) Zhang, H.; Wang, X. Modular co-culture engineering, a new approach for metabolic engineering. *Metab. Eng.* **2016**, *37*, 114−121.

(20) Goers, L.; Freemont, P.; Polizzi, K. M. Co-culture systems and technologies: taking synthetic biology to the next level. *J. R. Soc. Interface* **2014**, *11*, No. 20140065.

(21) Richter, H.; Molitor, B.; Diender, M.; Sousa, D. Z.; Angenent, L. T. A narrow pH range supports butanol, hexanol, and octanol production from syngas in a continuous co-culture of *Clostridium ljungdahlii* and *Clostridium kluyveri* with in-line product extraction. *Front. Microbiol.* **2016**, *7*, 1773.

(22) Hill, E. A.; Chrisler, W. B.; Beliaev, A. S.; Bernstein, H. C. A flexible microbial co-culture platform for simultaneous utilization of methane and carbon dioxide from gas feedstocks. *Bioresour. Technol.* **2017**, *228*, 250−256.

(23) Jones, J. A.; Vernacchio, V. R.; Sinkoe, A. L.; Collins, S. M.; Ibrahim, M. H. A.; Lachance, D. M.; Hahn, J.; Koffas, M. A. G. Experimental and computational optimization of an *Escherichia coli* co-culture for the efficient production of flavonoids. *Metab. Eng.* **2016**, *35*, 55−63.

(24) Zhang, H.; Stephanopoulos, G. Co-culture engineering for microbial biosynthesis of 3-amino-benzoic acid in *Escherichia coli*. *Biotechnol. J.* **2016**, *11*, 981−987.

(25) Saini, M.; Chiang, C.-J.; Li, S.-Y.; Chao, Y.-P. Production of biobutanol from cellulose hydrolysate by the *Escherichia coli* co-culture system. *FEMS Microbiol. Lett.* **2016**, *363*, No. fnw008.

(26) Yun, J.; Zabed, H. M.; Zhang, Y.; Parvez, A.; Zhang, G.; Qi, X. Co-fermentation of glycerol and glucose by a co-culture system of engineered *Escherichia coli* strains for 1,3-propanediol production without vitamin B_{12} supplementation. *Bioresour. Technol.* **2021**, *319*, No. 124218.

(27) Miao, H.; Ratnasingam, S.; Pu, C. S.; Desai, M. M.; Sze, C. C. Dual fluorescence system for flow cytometric analysis of *Escherichia coli* transcriptional response in multi-species context. *J. Microbiol. Methods* **2009**, *76*, 109−119.

(28) Wintermute, E. H.; Silver, P. A. Emergent cooperation in microbial metabolism. *Mol. Syst. Biol.* **2010**, *6*, 407.

(29) Kusuda, M.; Shimizu, H.; Toya, Y. Reactor control system in bacterial co-culture based on fluorescent proteins using an Arduino-based home-made device. *Biotechnol. J.* **2021**, *16*, No. 2100169.

(30) Charubin, K.; Modla, S.; Caplan, J. L.; Papoutsakis, E. T. Interspecies microbial fusion and large-scale exchange of cytoplasmic proteins and RNA in a syntrophic *Clostridium* coculture. *mBio* **2020**, *11*, e02030−20.

https://doi.org/10.1021/acssynbio.1c00554
ACS Synth. Biol. 2022, 11, 953−967

(31) Tracy, B. P.; Gaida, S. M.; Papoutsakis, E. T. Flow cytometry for bacteria: enabling metabolic engineering, synthetic biology and the elucidation of complex phenotypes. *Curr. Opin. Biotechnol.* **2010**, *21*, 85−99.
(32) Tracy, B. P.; Gaida, S. M.; Papoutsakis, E. T. Development and application of flow-cytometric techniques for analyzing and sorting endospore-forming Clostridia. *Appl. Environ. Microbiol.* **2008**, *74*, 7497−7506.
(33) Molitor, B.; Kirchner, K.; Henrich, A. W.; Schmitz, S.; Rosenbaum, M. A. Expanding the molecular toolkit for the homoacetogen *Clostridium ljungdahlii*. *Sci. Rep.* **2016**, *6*, No. 31518.
(34) Buckley, A. M.; Jukes, C.; Candlish, D.; Irvine, J. J.; Spencer, J.; Fagan, R. P.; Roe, A. J.; Christie, J. M.; Fairweather, N. F.; Douce, G. R. Lighting up *Clostridium difficile*: reporting gene expression using fluorescent Lov domains. *Sci. Rep.* **2016**, *6*, No. 23463.
(35) Cheng, C.; Lin, M.; Jiang, W.; Zhao, J.; Li, W.; Yang, S.-T. Development of an in vivo fluorescence based gene expression reporter system for *Clostridium tyrobutyricum*. *J. Biotechnol.* **2019**, *305*, 18−22.
(36) Mordaka, P. M.; Heap, J. T. Stringency of synthetic promoter sequences in *Clostridium* revealed and circumvented by tuning promoter library mutation rates. *ACS Synth. Biol.* **2018**, *7*, 672−681.
(37) Shin, J.; Kang, S.; Song, Y.; Jin, S.; Lee, J. S.; Lee, J.-K.; Kim, D. R.; Kim, S. C.; Cho, S.; Cho, B.-K. Genome engineering of *Eubacterium limosum* using expanded genetic tools and the CRISPR-Cas9 system. *ACS Synth. Biol.* **2019**, *8*, 2059−2068.
(38) Wen, Z.; Wu, M.; Lin, Y.; Yang, L.; Lin, J.; Cen, P. Artificial symbiosis for acetone-butanol-ethanol (ABE) fermentation from alkali extracted deshelled corn cobs by co-culture of *Clostridium beijerinckii* and *Clostridium cellulovorans*. *Microb. Cell Factories* **2014**, *13*, No. 92.
(39) Charubin, K.; Papoutsakis, E. T. Direct cell-to-cell exchange of matter in a synthetic *Clostridium* syntrophy enables CO_2 fixation, superior metabolite yields, and an expanded metabolic space. *Metab. Eng.* **2019**, *52*, 9−19.
(40) Salimi, F.; Mahadevan, R. Characterizing metabolic interactions in a clostridial co-culture for consolidated bioprocessing. *BMC Biotechnol.* **2013**, *13*, No. 95.
(41) Diender, M.; Stams, A. J. M.; Sousa, D. Z. Production of medium-chain fatty acids and higher alcohols by a synthetic co-culture grown on carbon monoxide or syngas. *Biotechnol. Biofuels* **2016**, *9*, No. 82.
(42) Streett, H.; Charubin, K.; Papoutsakis, E. T. Anaerobic fluorescent reporters for cell identification, microbial cell biology and high-throughput screening of microbiota and genomic libraries. *Curr. Opin. Biotechnol.* **2021**, *71*, 151−163.
(43) Chia, H. E.; Koebke, K. J.; Rangarajan, A. A.; Koropatkin, N. M.; Marsh, E. N. G.; Biteen, J. S. New orange ligand-dependent fluorescent reporter for anaerobic imaging. *ACS Chem. Biol.* **2021**, *16*, 2109−2115.
(44) Minton, N. P.; Ehsaan, M.; Humphreys, C. M.; Little, G. T.; Baker, J.; Henstra, A. M.; Liew, F.; Kelly, M. L.; Sheng, L.; Schwarz, K.; Zhang, Y. A roadmap for gene system development in *Clostridium*. *Anaerobe* **2016**, *41*, 104−112.
(45) Zhang, Y.; Grosse-Honebrink, A.; Minton, N. P. A universal mariner transposon system for forward genetic studies in the genus *Clostridium*. *PLoS One* **2015**, *10*, No. e0122411.
(46) Harth, G.; Masleša-Galić, S.; Horwitz, M. A. A two-plasmid system for stable, selective-pressure-independent expression of multiple extracellular proteins in mycobacteria. *Microbiology* **2004**, *150*, 2143−2151.
(47) Nagaraju, S.; Davies, N. K.; Walker, D. J. F.; Köpke, M.; Simpson, S. D. Genome editing of *Clostridium autoethanogenum* using CRISPR/Cas9. *Biotechnol. Biofuels* **2016**, *9*, No. 219.
(48) Wasels, F.; Jean-Marie, J.; Collas, F.; López-Contreras, A. M.; Lopes Ferreira, N. A two-plasmid inducible CRISPR/Cas9 genome editing tool for *Clostridium acetobutylicum*. *J. Microbiol. Methods* **2017**, *140*, 5−11.
(49) Diallo, M.; Hocq, R.; Collas, F.; Chartier, G.; Wasels, F.; Wijaya, H. S.; Werten, M. W. T.; Wolbert, E. J. H.; Kengen, S. W. M.; van der Oost, J.; Ferreira, N. L.; López-Contreras, A. M. Adaptation and application of a two-plasmid inducible CRISPR-Cas9 system in *Clostridium beijerinckii*. *Methods* **2020**, *172*, 51−60.
(50) Wang, S.; Dong, S.; Wang, P.; Tao, Y.; Wang, Y. Genome editing in *Clostridium saccharoperbutylacetonicum* N1-4 with the CRISPR-Cas9 system. *Appl. Environ. Microbiol.* **2017**, *83*, No. e00233-17.
(51) Bertani, G. Studies on lysogenesis I: the mode of phage liberation by lysogenic *Escherichia coli*. *J. Bacteriol.* **1951**, *62*, 293−300.
(52) Roos, J. W.; McLaughlin, J. K.; Papoutsakis, E. T. The effect of pH on nitrogen supply, cell lysis, and solvent production in fermentations of *Clostridium acetobutylicum*. *Biotechnol. Bioeng.* **1985**, *27*, 681−694.
(53) Standfest, T. Optimierung und alternative Substrate in der ABE-Fermentation mit *Clostridium acetobutylicum*. Ph. D. thesis, University of Ulm: Ulm, Germany, 2013.
(54) Hartman, A. H.; Liu, H.; Melville, S. B. Construction and characterization of a lactose-inducible promoter system for controlled gene expression in *Clostridium perfringens*. *Appl. Environ. Microbiol.* **2011**, *77*, 471−478.
(55) Heap, J. T.; Pennington, O. J.; Cartman, S. T.; Minton, N. P. A modular system for *Clostridium* shuttle plasmids. *J. Microbiol. Methods* **2009**, *78*, 79−85.
(56) Mermelstein, L. D.; Papoutsakis, E. T. *In vivo* methylation in *Escherichia coli* by the *Bacillus subtilis* phage *φ*3T I methyltransferase to protect plasmids from restriction upon transformation of *Clostridium acetobutylicum* ATCC 824. *Appl. Environ. Microbiol.* **1993**, *59*, 1077−1081.
(57) Wirth, S.; Dürre, P. Investigation of putative genes for the production of medium-chained acids and alcohols in autotrophic acetogenic bacteria. *Metab. Eng.* **2021**, *66*, 296−307.
(58) Leang, C.; Ueki, T.; Nevin, K. P.; Lovley, D. R. A genetic system for *Clostridium ljungdahlii*: a chassis for autotrophic production of biocommodities and a model homoacetogen. *Appl. Environ. Microbiol.* **2013**, *79*, 1102−1109.
(59) Böhringer, M. Molekularbiologische und enzymatische Untersuchungen zur Regulation des Gens der Acetacetat-Decarboxylase von *Chlostridium acetobutylicum*. Ph. D. thesis, University of Ulm: Ulm, Germany, 2002.
(60) Beck, M. H.; Flaiz, M.; Bengelsdorf, F. R.; Dürre, P. Induced heterologous expression of the arginine deiminase pathway promotes growth advantages in the strict anaerobe *Acetobacterium woodii*. *Appl. Microbiol. Biotechnol.* **2020**, *104*, 687−699.

https://doi.org/10.1021/acssynbio.1c00554
ACS Synth. Biol. 2022, 11, 953−967

2.4 *Caproicibacter fermentans* gen. nov., sp. nov., a new caproate-producing bacterium and emended description of the genus *Caproiciproducens.*

Flaiz, M.; Baur, T.; Brahner, S.; Poehlein, A.; Daniel, R.; Bengelsdorf, F. R. *Caproicibacter fermentans* gen. nov., sp. nov., a new caproate-producing bacterium and emended description of the genus *Caproiciproducens*. *Int. J. Syst. Evol. Microbiol.* ***2020***, *70*, 4269–4279. https://doi.org/10.1099/ijsem.0.004283

Rights and permissions

Reprinted under author rights.

The original article can be accessed via https://doi.org/10.1099/ijsem.0.004283

INTERNATIONAL JOURNAL OF SYSTEMATIC AND EVOLUTIONARY MICROBIOLOGY

TAXONOMIC DESCRIPTION
Flaiz *et al.*, *Int. J. Syst. Evol. Microbiol.*
DOI 10.1099/ijsem.0.004283

MICROBIOLOGY SOCIETY

Caproicibacter fermentans gen. nov., sp. nov., a new caproate-producing bacterium and emended description of the genus *Caproiciproducens*

Maximilian Flaiz[1], Tina Baur[1], Sven Brahner[1], Anja Poehlein[2], Rolf Daniel[2] and Frank R. Bengelsdorf[1,*]

Abstract

A strictly anaerobic bacterial strain designated EA1^T was isolated from an enrichment culture inoculated with biogas reactor content. Cells of strain EA1^T are spore-forming rods (1–3×0.4–0.8 µm) and stain Gram-negative, albeit they possess a Gram-positive type of cell-wall ultrastructure. Growth of strain EA1^T was observed at 30 and 37 °C and within a pH range of pH 5–9. The major components recovered in the fatty acid fraction were $C_{14:0}$, $C_{16:0}$, $C_{16:0}$ DMA (dimethyl acetal) and $C_{16:1}$ $\omega 7c$. Strain EA1^T fermented several mono- and disaccharides. Metabolic end products from fructose were acetate, butyrate, caproate and lactate. Furthermore, ethanol, CO_2 and H_2 were identified as products. The genome consists of a chromosome (3.9 Mbp) with 3797 predicted protein-encoding genes and a G+C content of 51.25 mol%. Phylogenetic analysis based on 16S rRNA gene sequences indicated that strain EA1^T represents a novel taxon within the family *Oscillospiraceae*. The most closely related type strains of EA1^T, based on 16S rRNA gene sequence identity, are *Caproiciproducens galactitolivorans* BS-1^T (94.9 %), [*Clostridium*] *leptum* DSM 753^T (93.8 %), [*Clostridium*] *sporosphaeroides* DSM 1294^T (91.7 %) and *Ruminococcus bromii* ATCC 27255^T (91.0 %). Further phenotypic characteristics of strain EA1^T differentiate it from related, validly described bacterial species. Strain EA1^T represents a novel genus and novel species within the family *Oscillospiraceae*. The proposed name is *Caproicibacter fermentans* gen. nov., sp. nov. The type strain is EA1^T (DSM 107079^T=JCM 33110^T).

At present, only a limited number of bacterial species have been reported to be capable of caproate formation through chain elongation via reverse β-oxidation (for a review see [1]). For example, caproate is produced by *Clostridium kluyveri* [2] from acetate and ethanol, by *Caproiciproducens galactitolivorans* [3], by *Megasphaera elsdenii* [4, 5] as well as *Megasphaera cerevisiae* [6] from sugars. A strain referred to as '*Ruminococcaceae* bacterium CPB6' uses lactate [7] whereas *Eubacterium limosum* [8, 9] and *Clostridium carboxidivorans* [10, 11] can use C1-compounds such as methanol or carbon monoxide to produce caproate. Caproate fermentation has been known ever since the discovery of *C. kluyveri* enriched by H. A. Barker in 1937 in Delft, the Netherlands [12]. The initial substrate for growth of caproate-producing bacteria can vary, but it is accepted that chain elongation starts with the central intermediate acetyl-coenzyme A (CoA) as demonstrated for butyrate formation in *C. kluyveri* [13]. In a first cycle, two molecules of acetyl-CoA are condensed via a thiolase (Thl) forming acetoacetyl-CoA. Subsequently, acetoacetyl-CoA is converted to 3-hydroxybutyryl-CoA by a respective dehydrogenase (Hbd) and 3-hydroxybutyryl-CoA is then dehydrated to crotonyl-CoA via a crotonase (Crt). Afterwards, the enzyme complex formed by a butyryl-CoA dehydrogenase and electron-transferring flavoproteins A and B (Bcd-EtfAB) catalyses the crotonyl-CoA-dependent reduction of ferredoxin (E0′=−420 mV) with NADH forming butyryl-CoA (electron bifurcation [13]). In a second cycle of reverse β-oxidation, caproate formation is assumed to be based on further CoA-thioester intermediates and direct use of acetyl-CoA for acyl-chain elongation [14]. Butyryl-CoA is elongated with acetyl-CoA by the action of a thiolase and results in 3-ketohexanoyl-CoA, which is subsequently converted to hexanoyl-CoA in two further steps. Presumably, a second electron-bifurcating reaction is involved that requires

Author affiliations: [1]Institut für Mikrobiologie und Biotechnologie, Universität Ulm, Albert-Einstein-Allee 11, 89081 Ulm, Germany; [2]Genomic and Applied Microbiology & Göttingen Genomics Laboratory, Georg-August University Göttingen, Grisebachstr. 8, D-37077 Göttingen, Germany.
***Correspondence:** Frank R. Bengelsdorf, frank.bengelsdorf@uni-ulm.de
Keywords: strictly anaerobic; Gram-stain-negative; spore-forming; *Caproiciproducens*.
Abbreviations: AAI, average amino acid identity; ANI, average nucleotide identity; YTF, yeast extract–tryptone–fructose.
The whole-genome shotgun project has been deposited at DDBJ/ENA/GenBank under the accession number VWXL00000000. The version described in this paper is version VWXL01000000. Raw data have been deposited at the NCBI SRA database under the accession number SRS5758927. Accession number for the 16S rRNA gene sequence of strain EA1^T is MN851263.

004283 © 2020 The Authors

trans-2-hexanoyl-CoA and NADH to form hexanoyl-CoA whereby ferredoxin is reduced. The enzymes for the second cycle have not been described but are assumed to act in a way similar to the enzymes necessary for butyryl-CoA formation. The Rnf (*Rhodobacter n*itrogen *f*ixation) complex, present in caproate-producing bacteria [13, 15–20], generates an electrochemical potential ($\Delta\mu H^+$ or $\Delta\mu Na^+$) from oxidation of reduced ferredoxin and reduction of oxidized NAD [21]. Subsequently, the electrochemical potential drives an F_0F_1-ATP synthase (ATPase) to form ATP by electron transport phosphorylation [22]. Furthermore, it is assumed that butyrate- and caproate-producing bacteria convert acetate or butyrate from their environment to acetyl-CoA or butyryl-CoA to avoid acidosis. Thus, bacteria maintain a pH high enough to prevent immediate toxic concentration of undissociated acids.

Caproate is an industrially relevant C6-compound with a wide range of applications [14]. It is used as basic commodity for the chemical industry, as an additive in animal feed for poultry and pigs, as a flavour additive in the food industry, as an antimicrobial agent in the pharmaceutical industry and as a possible precursor in the production of biofuels. Currently, caproate is mainly produced from fossil-based n-hexanol [23].

ISOLATION AND ECOLOGY

Strain EA1^T was isolated under anaerobic conditions from an anaerobic enrichment culture (reactor microbiome) producing organic acids such as acetate, butyrate and caproate. This 1.6 l enrichment culture was set up using 320 ml inoculum from a full-scale anaerobic biogas plant (Ströbele-Beck GbR Ulm, Germany) supplied with 31 g corn silage as feedstock, 350 mM ethanol as an additional electron donor, 500 mM sodium 2-bromoethanesulfonate (BES) to inhibit methanogenic archaea and incubated anaerobically at 37 °C for 50 days. Content of this enrichment culture was diluted (10^{-3}) and 1 ml was used to inoculate 50 ml Tanner mod2 medium at pH 6 in order to obtain bacterial mixed cultures in 125 ml Müller–Krempel bottles. The Tanner mod2 medium is based on a medium published by Tanner *et al.* [24] and contained 95.6 mM MOPS (3-(*N*-morpholino) propanesulfonic acid), 2.9 mM L-cysteine-HCl·H_2O, 0.05 % (wt/vol) yeast extract, 1 % (vol/vol) trace metal solution, 1 % (vol/vol) vitamin solution, 2.5 % (vol/vol) SL-9 mineral solution and 0.1 % (vol/vol) resazurin. The trace metal solution contained: 80 g l^{-1} NaCl, 100 g l^{-1} NH_4Cl, 10 g l^{-1} KCl, 10 g l^{-1} KH_2PO_4, 20 g l^{-1} $MgSO_4{\cdot}7H_2O$ and 4 g l^{-1} $CaCl_2{\cdot}2H_2O$. The vitamin solution [24] contained: 10 mg l^{-1} pyridoxine-HCl, 5 mg l^{-1} thiamine–HCl·$2H_2O$, 5 mg l^{-1} riboflavin, 5 mg l^{-1} calcium D-(+)-pantothenate, 5 mg l^{-1} lipoic acid, 5 mg l^{-1} 4-aminobenzoic acid, 5 mg l^{-1} nicotinic acid, 5 mg l^{-1} vitamin B12, 2 mg l^{-1} biotin, 2 mg l^{-1} folic acid and 10 mg l^{-1} MESNA (2-mercaptoethanesulfonic acid sodium salt). The SL-9 mineral solution [24] contained: 2 g l^{-1} nitrilotriacetic acid, 1 g l^{-1} $MnSO_4{\cdot}H_2O$, 0.8 g l^{-1} $Fe(SO_4)_3(NH_4)_2{\cdot}6H_2O$, 0.2 g l^{-1} $CoCl_2{\cdot}6H_2O$, 1 mg l^{-1} $ZnSO_4{\cdot}7H_2O$, 20 mg l^{-1} $CuCl_2{\cdot}2H_2O$, 20 mg l^{-1} $NiCl_2{\cdot}6\ H_2O$, 20 mg l^{-1} $Na_2MoO_4{\cdot}2H_2O$, 20 mg l^{-1} $Na_2SeO_4{\cdot}5H_2O$ and 20 mg l^{-1} $Na_2WO_4{\cdot}2H_2O$. One mixed culture was supplied with ethanol (350 mM) and acetate (102 mM) and cultivated anaerobically at 37 °C with a H_2+CO_2 (67 % H_2+33 % CO_2) gas atmosphere. This mixed culture was monitored for growth (optical density OD_{600}) and formation of metabolic end products, which were analysed by HPLC using an 1260 Infinity LC apparatus (Agilent Technologies). After confirmation of growth and product formation of the mixed culture, 1 ml cell suspension was diluted (10^{-1}–10^{-3}) and 0.2 ml of each dilution was plated on modified YTF (yeast extract–tryptone–fructose [25]) agar plates and incubated at 37 °C in an anaerobic chamber containing a N_2+H_2 (95 % N_2+5 % H_2) gas atmosphere. The modified YTF agar plates (pH 7) contained 1 % (wt/vol) yeast extract, 1.6 % (wt/vol) tryptone, 68.5 mM NaCl, 27.8 mM fructose, 5.7 mM L-cysteine–HCl·H_2O, 3.7 mM NH_4Cl, 0.2 % (vol/vol) vitamin solution, 0.2 % (vol/vol) SL-9 mineral solution and 0.1 % (vol/vol) resazurin. Colony-forming units were re-streaked on fresh anaerobic agar plates to obtain pure cultures. Strains were subsequently transferred under anaerobic conditions and maintained for further use, using the Hungate technique in either Tanner mod2 medium or modified YTF medium.

In general, similar anaerobic enrichment cultures have been studied in detail as biotechnological production platforms for medium-chain carboxylates such as n-caproate and n-caprylate [1]. Open cultures of microbial consortia ferment organic biomass or organic wastes into valuable biochemicals that can be extracted. Meanwhile, a variety of different types of reactors and feedstock combinations have been tested [26–30]. Interestingly, phylogenetic analyses of the respective reactor microbiomes often revealed the presence of bacteria related to a strain termed '*Ruminococcaceae* bacterium CPB6' and the bacterial species *Cp. galactitolivorans* [27–30]. Both bacteria belong to the family *Oscillospiraceae* [31] with very few related strains available as pure cultures.

PHYLOGENY

The 16S rRNA gene sequence of strain EA1^T was analysed using reference sequences retrieved from GenBank [32] or the Ribosomal Database Project [33]. Phylogenetic tree reconstruction was done using MAFFT (Multiple Alignment using Fast Fourier Transform [34]) and MrBayes version 3.2.1 [35]. In the reconstructed phylogenetic tree shown in Fig. 1, the closest relatives of strain EA1^T are *Clostridium* sp. W14A [36], *Clostridium* sp. MB2-A37 [37], *Cp. galactitolivorans* BS-1^T [3] and '*Ruminococcaceae* bacterium CPB6' [19]. *Cp. galactitolivorans* BS-1^T is the only relative of strain EA1^T for which its name has been validly published [3]. Moreover, the 16S rRNA gene sequence similarities for strain EA1^T were determined by pairwise alignments for more distinctly related species with valid names. This resulted in 16S rRNA gene similarity values of 94.9 % for *Cp. galactitolivorans* BS-1^T, 93.8 % for [*Clostridium*] *leptum* DSM 753^T, 91.7 % for [*Clostridium*] *sporosphaeroides* DSM 1294^T and 91.0 % for *R. bromii* ATCC 27255^T. The highest 16S rRNA gene sequence similarity of 99 % was achieved to a strain termed *Clostridium* sp. W14A.

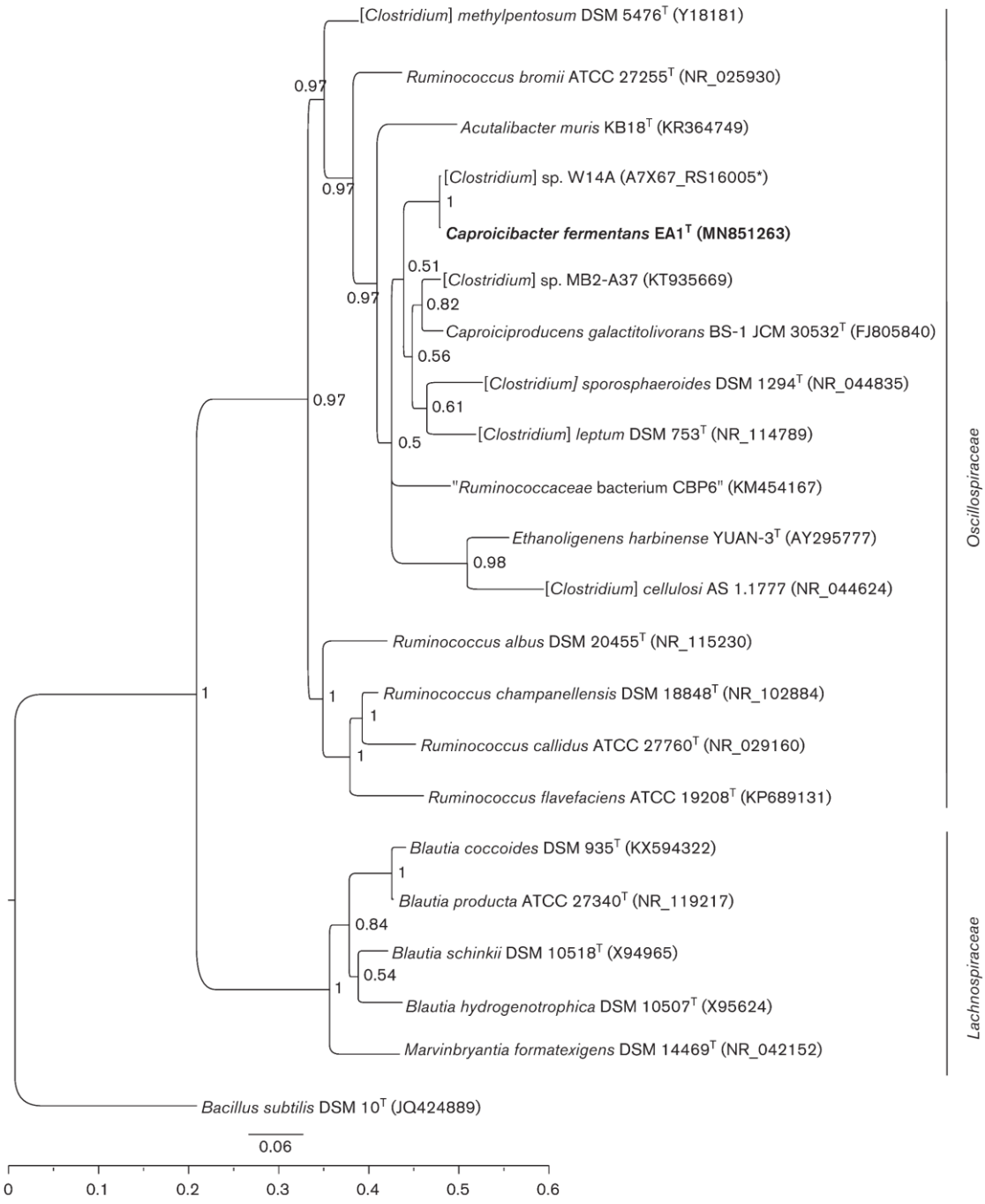

Fig. 1. Phylogenetic tree based on 16S rRNA gene sequences for classification of strain EA1^T and related bacterial strains. The phylogenetic tree was rooted to *Bacillus subtilis* DSM 10^T. GenBank accession numbers of the 16S rRNA gene sequences are given in parentheses. Estimation is based on Bayesian inference and an MAFFT alignment. The bar shows the expected changes per site resulting in different branch lengths. Numbers indicate posterior probabilities for each of the individual clades of the tree. *16S rRNA gene LocusTag number of the respective genome sequence (MBSV00000000). Square brackets ([ ]) around a genus indicate that the name awaits appropriate action by the research community to be transferred to another genus.

Strain W14A has neither been deposited in a culture collection nor has a species name been validly published for this strain. The genome sequence is available at the IMG/JGI database (https://img.jgi.doe.gov) and a short description was published by Ransom-Jones and McDonald [36].

Yarza *et al.* [38] stated that a sequence identity of 94.5 % or lower for two 16S rRNA genes is strong evidence for distinct genera. The sequence identity of 94.9 % for strain EA1^T and *Cp. galactitolivorans* BS-1^T is already close to this cut-off value. However, morphological and physiological differences between both strains provide further insights to justify the description of strain EA1^T as a new genus within the bacterial family of *Oscillospiraceae*.

GENOME FEATURES

Genome sequencing

Genomic DNA of strain EA1^T was extracted using the MasterPure Gram Positive DNA Purification kit as recommended by the manufacturer (Biozym). Quality of isolated DNA was initially checked by agarose gel electrophoresis and validated on an Agilent Bioanalyzer 2100 using an Agilent DNA 12000 kit as recommended by the manufacturer (Agilent Technologies). Concentration and purity of the isolated DNA was first checked with a NanoDrop ND-1000 (PeqLab Biotechnologie GmbH) and concentration was determined using the Qubit dsDNA HS Assay kit as recommended by the manufacturer (Life Technologies GmbH). Illumina sequencing libraries were prepared using the Nextera XT DNA Sample Preparation kit and subsequently sequenced on a MiSeq system with the reagent kit v3 with 600 cycles as recommended by the manufacturer (Illumina). Quality filtering of the 40420078 raw reads using Trimmomatic version 0.39 [39] resulted in 4078054 paired-end reads with an average read length of 301 bp. The assembly was performed with the SPAdes genome assembler software version 3.13.1 [40]. The assembly resulted in 113 contigs (>500 bp) and an average coverage of 240-fold. The assembly was validated and the read coverage was determined with QualiMap version 2.2.1 [41]. The Prokka software tool was used for automatic annotation and identification of rRNA and tRNA genes [42].

The genome of strain EA1^T consists of a circular chromosome (3.9 Mb) with an overall G+C content of 51.25 mol%. The draft genome sequence contained five rRNA genes (3×5S rRNA, 1×16S rRNA and 1×23S rRNA), 49 tRNA genes, 2615 protein-encoding genes with a predicted function and 1182 genes coding for hypothetical proteins. The analysis of the genome revealed that strain EA1^T harbours genes encoding the *bcs* operon (butyryl-CoA synthesis) [43]. The *bcs* operon, as it is present in *Clostridium acetobutylicum*, consists of the genes *crt*, *bcd*, *etfB*, *etfA* and *hbd* encoding the enzymes Crt [EC 4.2.1.17], Bcd-EtfAB [EC 1.3.8.1] and Hbd [EC 1.1.1.157], respectively. In strain EA1^T, the gene encoding the thiolase [EC 2.3.1.9], which condenses two acetyl-CoA to one acetoacetyl-CoA, is also present in the corresponding gene cluster. Genes encoding proteins required for sporulation such as spore coat proteins, various spore maturation proteins, spore membrane proteins (sporulation integral membrane proteins) and a spore protease are present in the genome of strain EA1^T. Moreover, the genome comprises a complete gene cluster encoding the Rnf complex. This protein complex functions as a ferredoxin:NAD$^+$ oxidoreductase [EC 1.18.1.3] [44], which oxidizes reduced ferredoxin (Fd^{2-}) and thereby yields NADH. An ion gradient generated by H^+ or Na^+ crossing the cytoplasmic membrane [45] drives an ATPase for ATP production. Seedorf *et al.* [13] assumed that *C. kluyveri* generates Fd^{2-} via crotonyl-CoA reduction, which is then used for the regeneration of NADH via the Rnf complex. Most likely, the Rnf complex in strain EA1^T also functions as a ferredoxin:NAD$^+$ oxidoreductase to oxidize Fd^{2-} gained from the activity of the pyruvate:ferredoxin oxidoreductase or the Bcd-EtfAB complex. Complete gene clusters required for the synthesis of cytochromes or quinones are not present in the genome.

Strain EA1^T harbours a gene cluster similar to the *lct* operon, which encodes enzymes that are responsible for lactate uptake and utilization as described for *Acetobacterium woodii* [46]. The organization of genes of that specific cluster varies compared to the *lct* operon of *A. woodii* but matches perfectly with a corresponding gene cluster present in '*Ruminococcaceae* bacterium CPB6' [19]. Strain CPB6 was shown to utilize lactate (45.1 g l^{-1}) and produce high caproate titers (16.6 g l^{-1}) with a productivity of 0.2 g l^{-1} h^{-1} [7]. However, under the conditions tested, strain EA1^T was not able to grow with lactate as a substrate.

An average nucleotide identity (ANI) analysis of genome sequences was performed for related strains using the IMG/ER system [47]. Pairwise ANI values ranged between 67.8 % and 71.6 % for the stains *Cp. galactitolivorans* BS-1^T (71.6 %), [*Clostridium*] *leptum* DSM 753^T (70.3 %), [*Clostridium*] *sporosphaeroides* DSM 1294^T (71.5 %), *R. bromii* ATCC 27255^T (67.8 %) and strain CPB6 (70.2 %). An ANI value of 99 % was recorded for *Clostridium* sp. W14A confirming the results from the 16S rRNA gene analysis. Additionally, the average amino acid identity (AAI) was calculated using the AAI-profiler software tool [48]. Pairwise AAI values compared to strain EA1^T revealed 98.5 % for strain W14A, 65.3 % for strain CPB6, 69.4 % for *Cp. galactitolivorans* BS-1^T and 64.8 % for [*Clostridium*] *leptum* DSM 753^T. [*Clostridium*] *sporosphaeroides* DSM 1294^T and *R. bromii* ATCC 27255^T were not included in the analysis since respective data were not available in the UniProt database [49].

CELL MORPHOLOGY AND PHYSIOLOGY

Morphological features

Gram-staining was carried out as previously described [50]. Cells of strain EA1^T were visualized using a Zeiss light microscope, a Hitachi S-5200 scanning electron microscope and a JEOL JEM-1400 transmission electron microscope. Gram-staining of strain EA1^T was performed in comparison to the Gram-stain-positive bacterium *Corynebacterium glutamicum*

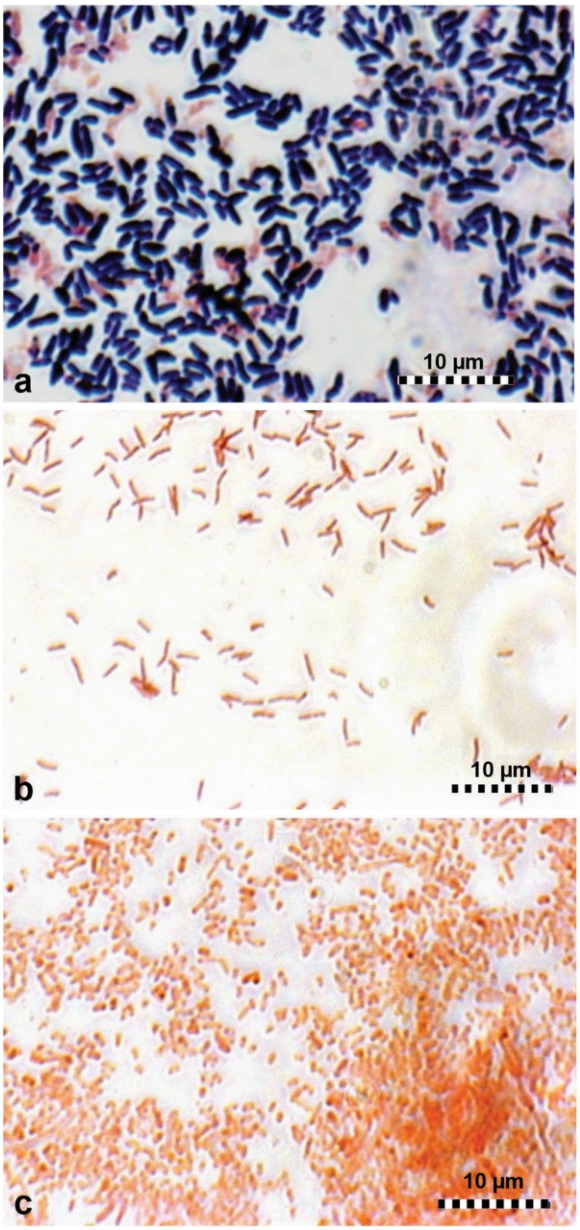

Fig. 2. Microscopy images showing Gram-stained cells of *Corynebacterium glutamicum* DSM 1933 (a) strain EA1^T (b) and *Escherichia coli* XL1-Blue (c).

DSM 1933 and the Gram-stain-negative bacterium *Escherichia coli* strain XL1-Blue. Strain EA1^T clearly stained Gram-negative as shown in Fig. 2. Motility of EA1^T and BS-1^T cells was investigated using a Zeiss light microscope and sealed imaging dishes (µ-Dish 35 mm, high, ibidi GmbH). Dishes were filled with cell suspension in an anaerobic chamber under a N_2+H_2 (95 %+5 %) gas atmosphere. Beforehand,

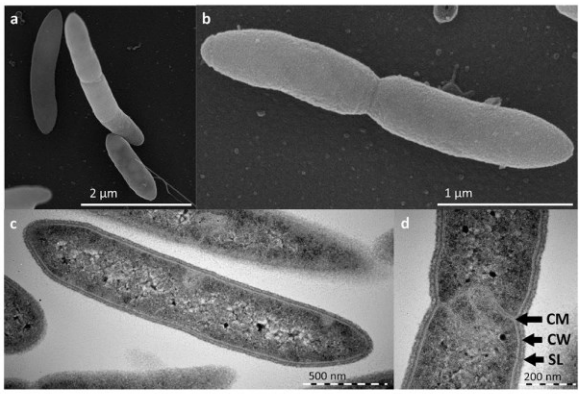

Fig. 3. Microscopy images showing cells of strain EA1^T. Scanning electron microscopy images using a 20000-fold (a) and 45000-fold (b) magnification. Transmission electron microscopy images using 50000-fold (c) and 185000-fold (d) magnification. CM, cytoplasmic membrane; CW, cell wall; SL, surface layer.

cells were cultivated in Hungate tubes containing Tanner mod2 medium for 18 h. Cells of BS-1^T showed clear motility, while cells of EA1^T cells did not. The rod-shaped EA1^T cells showed a length of 1–3 µm and a width of 0.4–0.8 µm. The shape and length of the cells was confirmed using scanning electron microscopy (Fig. 3a, b). Moreover, transmission electron microscopy images showed a typical Gram-positive type of cell-wall ultrastructure (Fig. 3c, d). In Fig. 3d, the cytoplasmic membrane, the densely stained cell wall and an additional surface layer are indicated by arrows. In bacteria that clearly stain Gram-positive, the thickness of cell walls ranges between 30 and 50 nm [51]. It has been speculated by Cheng and Costerton [51] that a minimum cell wall thickness is required to retain the Gram-stain-complex during decoloration. Several other bacteria have been described that stain Gram-negative and possess a Gram-positive cell-wall structure, e.g. *Butyrivibrio fibrisolvens* strain D1 [51], *Clostridium polysaccharolyticum* ATCC 33142^T [52], *Lachnoclostridium phytofermentans* ATCC 700394^T, *Cellulosilyticum lentocellum* NCIMB 11756^T and *Clostridium populeti* ATCC 35295^T [53].

Growth characteristics and analytical procedures

Growth of strain EA1^T was examined in Tanner mod2 medium at different temperatures and pH values. The tested temperatures were 25, 30, 37, 45 and 55 °C and the initial pH values of the media were set to pH 5, 6, 7, 8 and 9, respectively. Growth of strain EA1^T was observed between 30 and 37 °C and not below 25 or above 45 °C. The initial pH value of the medium that allowed growth of strain EA1^T ranged between pH 5 and 9. The growth rates (µ) of cells grown at 37 °C were determined and accounted for µ=0.1 at pH 5, µ=0.11 at pH 6, µ=0.12 at pH 7 and µ=0.05 at pH 8. Thus, the optimal pH for growth was pH 7. Subsequently, growth experiments to determine the substrate spectrum of strain EA1^T and BS-1^T were performed at 37 °C and pH 7 in Tanner mod2. Strain

EA1^T showed growth (≥ 2.5 doublings of cell mass) using the substrates cellobiose, fructose, galactose, glucosamine, glucose, mannitol, mannose, starch and sucrose. Furthermore, a slight increase of biomass (≤2 doublings of cell mass) was observed using the substrates arabinose, galactitol, sorbitol and xylose. Strain EA1^T was not able to utilize the substrates fumarate, lactate, malate, succinate, ethanol, methanol, glycerol, alanine, alanine and glycine in combination, glutamate, glycine, ribose and xylitol. Substrates were added to a final concentration of 20 mM besides alanine, ethanol, methanol, glutamate and glycine, where just 10 mM were used.

Metabolic end products of strain EA1^T were analysed via GC (Clarus 600, PerkinElmer) and HPLC. Fructose, acetate and lactate were quantified using an HPLC equipped with a refraction index detector and a diode array detector. The prepared samples (20 µl) were analysed using the CS-Organic-Acid Resin (40×8 mm) pre-column and CS-Organic-Acid Resin (150×8 mm) column packed with polystyrene divinylbenzene copolymer. Column temperature was set to 40 °C. As the mobile phase, 5 mM H_2SO_4 at a constant flow rate of 0.7 ml min^{-1} was applied. Ethanol, butyrate and caproate were analysed using a GC equipped with a flame ionization detector operating at 300 °C. Prepared samples were injected at 225 °C into an Elite-FFAP (0.32 mm×30 m) column packed with nitroterephthalic acid modified polyethylene glycol. The carrier gas consisted of H_2 and a flow rate of 2.25 ml min^{-1} was applied. The GC temperature profile was set to 90 °C for 2 min, 90 °C - 250 °C by 40 °C min^{-1} and 250 °C for 1 min. H_2 and CO_2 were analysed using GC (Arnel Engineered Solutions Clarus 580 GC, PerkinElmer) equipped with a thermal conductivity detector operating at 200 °C. Headspace gas samples were injected using a 2.5 ml injection syringe (SGE Analytical Science) into a stainless steel packed column (320 µm×50 m; Cat. No. NR022501). Argon was used as carrier gas with a flow rate of 50 ml min^{-1}. Injected gases were analysed for 11 min at 60 °C. Fermentation, oxidation/reduction (O/R) and proton balances of supplied carbon and detected metabolic products were calculated according to Gottschalk [54].

The fermentation balance of strain EA1^T was determined using 19 mM fructose as substrate. The strain produced 3 mM acetate, 0.5 mM butyrate, 3 mM caproate, 24 mM lactate and 1 mM ethanol as well as 8 mM CO_2 and 5 mM H_2 as metabolic products. The corresponding fermentation balance (mol/100 mol substrate) accounted for 91.5 % carbon recovered in those products (Table 1). The remaining 8.5 % carbon must have been used for biomass formation. The ratio of oxidized and reduced fermentation products (oxidation/reduction balance, O/R mol/100 mol) accounted for 0.95. The ratio of available protons (H^+) compared to detected protons accounted for 1.09 (Table 1). All ratios are close to one and consequently the fermentation balance can be considered as even.

Sporulation of strains EA1^T and BS-1^T was tested according to Bahl *et al.* [55]. The 'vegetative medium' was inoculated and incubated for at least 1 week at 37 °C. Subsequently, cells and spores were concentrated by centrifugation, the supernatant was removed, the cells were aliquoted in glycerol suspensions (20 % (wt/vol)) and finally stored at −80 °C. Subsequently, the spore suspension was heated at 80 °C for 15 min and transferred to Tanner mod2 medium. Cells of strain EA1^T recovered from spores within 7 days at 37 °C, while cells of strain BS-1^T did not.

Cellular fatty acid composition

Freeze-dried cells were prepared for the analysis of fatty acids. The cell suspension (200 ml) of strain EA1^T was harvested and washed twice with 15 ml 0.8 % (wt/vol) saline. Pellets were dissolved in 2 ml saline and the respective glass vials

Table 1. Carbon recovery, O/R balance and balance of available protons of fermentation products of strain EA1^T

Carbon recovered: 549/600×100=91.5 %; O/R balance: 84/88=0.95; balance of available protons H^+ 2400/2204=1.09. The values for O/R and proton balance are different because the carbon recovery impacts the balance of available protons but not the O/R balance (O/R value of fructose=0).

			O/R balance		Balance of available protons	
Substrate/ products	**Mol/100 mol substrate**	**Mol carbon**	**O/R value**	**O/R mol/100 mol**	**Available H^+**	**Available H^+ mol/100 mol**
Fructose	100	600	0	0	24	2400
Acetate	16	32	0	0	8	128
Butyrate	3	12	−2	−6	20	60
Caproate	11	66	−4	−44	32	352
Lactate	129	387	0	0	12	1548
Ethanol	5	10	−2	−10	12	60
CO_2	42	42	+2	+84	0	0
H_2	28	0	−1	−28	2	56
Total		549		−88		2204
				+84		

were sealed with cotton wool plugs (dentist's size 2, Hartmann AG). Cells in glass vials were frozen using liquid nitrogen and placed into a pre-chilled cooling block at −80 °C. Afterwards, the vials were placed into the lyophilisator (Alpha 1-4LOC-1M, Martin Christ Gefriertrocknungsanlagen GmbH) for primary drying. A vacuum (0.01 mbar) was applied at a temperature of −54 °C for 30 h. For secondary drying, the wool plug was exchanged with a rubber stopper and placed onto a manifold (Martin Christ Gefriertrocknungsanlagen GmbH), which was placed onto the lyophilisator Alpha 1–4 LD plus (Martin Christ Gefriertrocknungsanlagen GmbH), then vacuum was applied (0.001 mbar) for about 12 h. Fatty acid analyses were carried out by the Identification Service of the DSMZ, Brunswick, Germany.

The major components in the cellular fatty acid fraction of EA1^T cells grown using fructose were $C_{14:0}$ (23.1 %), $C_{16:0}$ (13.2 %), $C_{16:0}$ DMA (17.0 %) and $C_{16:1}$ *ω7c* (11.7 %). The presence of dimethyl acetals in the fatty acid fraction is indicative of the presence of plasmalogens in the lipids of this organism. The fatty acid composition of strain EA1^T is clearly different from *Cp. galactitolivorans* BS-1^T and [*Clostridium*] *sporosphaeroides* DSM 1294^T (Table 2). Especially the major cellular fatty acid $C_{14:0}$ of strain EA1^T with 23.1 % clearly differs from *Cp. galactitolivorans* BS-1^T (3.2 %) and [*Clostridium*] *sporosphaeroides* DSM 1294^T (4.5 %). Depending on the reaction conditions, cleavage of the plasmalogens can lead to the formation of both the corresponding dimethyl acetals and aldehydes (i.e. $C_{16:0}$ DMA and $C_{16:0}$ aldehyde) and when evaluating their presence, these two derivatives should be considered to have originated from a single plasmalogen. $C_{16:0}$ dimethyl acetals/aldehydes are one of the major components in the fatty acid fraction in both *Cp. galactitolivorans* BS-1^T (36.2 %) and [*Clostridium*] *sporosphaeroides* DSM 1294^T (38.5 %), but in strain EA1^T, this comprises only 20.0 %. Some fatty acids, such as $C_{16:1}$ ω5*c*, $C_{16:1}$ ω7*c* or $C_{16:1}$ ω7*c* DMA are unique for strain EA1^T (Table 2). The presence of 18:1 ω7*c* derivatives of fatty acids and plasmalogens in strain EA1^T vs 18:1 ω9*c* and 18:1 ω11*c* derivatives of fatty acids and plasmalogens in *Cp. galactitolivorans* BS-1^T also indicates, that enzymes with different specificities for the positions of unsaturation are present in these two organisms.

Distinguishing characteristics

Results of 16S rRNA gene sequence comparisons and phylogenetic tree reconstruction already indicate that strain EA1^T represents a novel taxon within the family *Oscillospiraceae* [31]. Furthermore, strain EA1^T differs from *Cp. galactitolivorans* BS-1^T with respect to the following phenotypic features. Strain EA1^T stained Gram-negative whereas strain BS-1^T stained Gram-positive [3]. Strain EA1^T is able to sporulate and regrow from spores but strain BS-1^T is not. Strain EA1^T was not able to grow at 45 °C but strain BS-1^T is able to do so. Moreover, the genome of strain EA1^T accounts for 3.9 Mbp whereas the genome of strain BS-1^T comprises 2.57 Mbp [20]. Differences in the quantitative and qualitative amounts of both fatty acids (as their methyl esters) and the dimethyl acetal/aldehyde derivates of lipid plasmalogens also indicate clear phenotypic differences at the level of these compounds.

Table 3 summarizes the main phenotypic features of the closely related type strains [*Clostridium*] *leptum* DSM 753^T, [*Clostridium*] *sporosphaeroides* DSM 1294^T and *R. bromii* ATCC 27255^T. All strains show phenotypic differences compared to strain EA1^T. In summary, the phenotypic and genotypic characteristics suggest that strain EA1^T represents a novel genus within the family *Oscillospiraceae*, when compared to closely related type strains (Table 3).

DESCRIPTON OF *CAPROICIBACTER* GEN. NOV.

Caproicibacter (Ca.pro.i.ci.bac'ter. N.L. neut. n. *acidum caproicum* caproic acid; N.L. masc. n. *bacter* a rod; N.L. masc. n. *Caproicibacter* a rod-shaped organism that produces caproate).

Cells are strictly anaerobic, caproate-producing, spore-forming and possess a Gram-positive type of cell-wall structure. Carbohydrate utilization includes but is not limited to arabinose, cellobiose, fructose, galactose, glucose, mannose, starch, sucrose, xylose, glucosamine, galactitol, mannitol and sorbitol. The major metabolic end products are acetate, butyrate, caproate and lactate, as well as CO_2 and H_2. The major components of the cellular fatty acid fraction are $C_{14:0}$, $C_{16:0}$ DMA/aldehyde, $C_{16:0}$ and $C_{16:1}$ *ω7c*. Phylogenetically, the genus represents a distinct lineage in the family *Oscillospiraceae*. The type species is *Caproicibacter fermentans*.

DESCRIPTON OF *CAPROICIBACTER FERMENTANS* SP. NOV.

Caproicibacter fermentans (fer.men´tans. L. part. adj. *fermentans* fermenting).

Cells are strictly anaerobic, Gram-stain-negative, spore-forming, non-motile and caproate-producing. Colonies growing on modified YTF agar plates are punctiform, circular and white. Cells are 1.3–3.3 µm long and 0.4–0.8 µm wide. Growth of cells occurs in a temperature range of 30–37 °C with a growth optimum at 37 °C. Furthermore, cell growth occurs in a pH range of pH 5–9 with an optimum at pH 7. Organic acids are produced from sugars including arabinose, cellobiose, fructose, galactose, glucose, mannose, starch, sucrose, xylose, the sugar alcohols galactitol, mannitol and sorbitol as well as from the amino sugar glucosamine. No cell growth occurs using the substrates ribose, fumarate, succinate, malate, lactate, glycerol, ethanol, methanol, alanine, glutamate, glycine, galactitol and xylitol. Fermentative end products from growth on fructose are acetate, butyrate, caproate and lactate, as well as CO_2 and H_2. The genome harbours genes encoding the *bcs* operon and genes encoding lactate dehydrogenases. Furthermore, genes encoding spore coat proteins, spore maturation proteins, spore membrane proteins and a spore protease are present. A complete gene cluster encoding the Rnf complex and a gene cluster similar to the *lct* operon (lactate uptake and utilization) is present in the genome. The major components of the cellular fatty acid fraction, when cells grown using fructose, are $C_{14:0}$, $C_{16:0}$, $C_{16:0}$ DMA/aldeyhde and $C_{16:1}$ *ω7c*. The type strain of

Table 2. Fatty acid analysis of strain EA1^T and the two closely related strains *Cp. galactitolivorans* BS-1^T and [*Clostridium*] *sporosphaeroides* DSM 1294^T

Strains: 1, EA1^T; 2, *Cp. galactitolivorans* BS-1^T; 3, [*Clostridium*] *sporosphaeroides* DSM 1294^T. Strain EA1^T cells were cultivated for 3 days at 37 °C in Tanner mod2 medium. Values are percentages of total fatty acids. –, Not detected; DMA, dimethyl acetal. Major components are indicated with bold text. Data for *Cp. galactitolivorans* BS-1^T and [*Clostridium*] *sporosphaeroides* DSM 1294^T were obtained from Kim *et al.* [3].

Fatty acid	1	2	3
Straight-chain:			
$C_{12:0}$	–	–	4.3
$C_{13:0}$	–	–	1
$C_{14:0}$	**23.1**	3.2	4.5
$C_{16:0}$	**13.2**	3.1	1.9
$C_{14:0}$ DMA	8.2	5.4	8.9
$C_{16:0}$ DMA	**17.0**	**22.1**	**35.9**
$C_{18:0}$ DMA	–	4.0	2.5
$C_{16:0}$ aldehyde	3.0	**14.1**	**22.6**
$C_{18:0}$ aldehyde	–	3.1	1.8
Branched-chain:			
anteiso-$C_{17:0}$	–	5.9	–
Unsaturated:			
$C_{16:1}$ $\omega5c$	8.0	–	–
$C_{16:1}$ $\omega7c$	**11.7**	–	–
$C_{16:1}$ $\omega9c$	–	–	1.2
$C_{18:1}$ $\omega9c$	–	1.1	–
$C_{16:1}$ $\omega7c$ DMA	5.0	–	–
$C_{18:1}$ $\omega7c$ DMA	1.6	–	–
$C_{18:1}$ $\omega9c$ DMA	–	7.6	–
$C_{18:1}$ $\omega11c$ DMA	–	4.6	–
$C_{18:2}$ $\omega9c$ $\omega12c$	–	1.1	1.4
Summed features:*			
1	1.3	2.5	4.3
5	–	2.4	4.7
7	–	5.6	–
8	–	3.5	–
10	1.1	–	–
11	–	**10.0**	1.1

*Groups of fatty acids that could not be separated by gas chromatography using the MIDI Sherlock system are summarized under the term summed features. Summed feature 1 contained $C_{13:1}$ $\omega2c$ and/or $C_{14:0}$ aldehyde. Summed feature 5 contained $C_{15:0}$ DMA and/or $C_{14:0}$ 3OH. Summed feature 7 contained $C_{17:2}$ $\omega2c$ and/or $C_{17:1}$ $\omega8c$. Summed feature 8 contained $C_{17:1}$ $\omega8c$ and/or $C_{17:2}$. Summed feature 10 contained $C_{18:1}$ $\omega7c$/$\omega9t$/$\omega12t$ and/or unknown ECL 17.834. Summed feature 11 contained iso-$C_{17:0}$ 3OH and/or $C_{18:2}$ DMA.

Table 3. Comparison of genotypic and phenotypic characteristics of strain EA1^T and most closely related type strains

Strains: 1, EA1^T; 2, *Cp. galactitolivorans* BS-1^T [3]; 3, [*Clostridium*] *sporosphaeroides* DSM 1294^T [56, 57]; 4, [*Clostridium*] *leptum* DSM 753^T [58]; 5, *R. bromii* ATCC 27255^T [59]. +, Positive; –, negative; (+), products were not always detected.

Characteristics	1	2	3	4	5
Cell shape	Rod	Rod	Rod	Rod	Coccus
Cell size:					
Length (µm)	1.3–3.3	0.4–2.0	1.8–8.0	1.3–2.8	0.7–1.1
Width (µm)	0.4–0.8	0.3–0.5	0.5–0.6	0.6–0.8	0.7–1.1
Spore formation	+	–	+	+	–
Gram-staining	–	+	+	+	+
Motility	–	+	–	–	–
Metabolic end products:					
Acetate	+	+	+	+	+
Propionate	–	–	+	–	(+)
Butyrate	+	+	+	–	–
Caproate	+	+	–	–	–
Lactate	+	+	–	(+)	(+)
Ethanol	+	+	–	+	+
G+C content (mol%)	51.25	50.00	53.54	51.00	40.00
Genome size (Mbp)	3.90	2.57	3.18	3.27	2.25
Optimum temperature for growth (°C)	37	40	37–45	37	37

Caproicibacter fermentans is strain EA1^T (DSM 107079^T, JCM 33110^T).

EMENDED DESCRIPTION OF *CAPROICIPRODUCENS* KIM *ET AL.* 2015

The description is as given by Kim *et al.* [3] with the following modifications. Cells are motile and produce lactate as a major metabolic product. These insights were obtained by performing experiments using cells of *Cp. galactitolivorans* BS-1^T and the media and analytics as described above.

EMENDED DESCRIPTION OF *CAPROICIPRODUCENS GALACTITOLIVORANS* KIM *ET AL.* 2015

The description is as given by Kim *et al.* [3] with the following modifications. Cells are motile and produce lactate as a major metabolic product in addition to the known products (acetate, butyrate, caproate and H_2). The genome of strain BS-1^T contains genes encoding the *bcs* operon, genes encoding lactate dehydrogenases and a complete gene cluster encoding the Rnf complex [20]. Approximately one third of the components in the fatty acid fraction comprises dimethyl acetals/aldehydes ($C_{16:0}$ DMA/aldehyde dominate), while a smaller proportion of the fraction comprises unsaturated derivatives with the double bonds located at the ω9*c* or ω11*c* positions. This indicates that different enzymes are involved in the production of these compounds.

Funding information
This study was funded by the Institute of Microbiology and Biotechnology (Ulm University) and the Genomic and Applied Microbiology and Göttingen Genomics Laboratory (Georg-August University Göttingen).

Acknowledgements
We thank Kathleen Gollnow, Frauke-Dorothee Meyer, and Christian Kröly for the technical support and Paul Walther from the Zentrale Einrichtung Elektronenmikroskopie of Ulm University for his support. A special thanks goes to Dr. Brian J. Tindall for his excellent advice regarding the fatty acid analysis, the taxonomic descriptions, and his further valuable input to our manuscript.

Author contributions
M.F., T.B., S.B. and A.P. performed investigations, data curation, formal analysis and validation. M.F. wrote the original draft of the manuscript. M.F., T.B., A.P., R.D. and F.R.B. reviewed and edited the manuscript. R.D. contributed to funding acquisition and F.R.B. was responsible for conceptualization, supervision and funding acquisition.

Conflicts of interest
The authors declare that there are no conflicts of interest.

References

1. Angenent LT, Richter H, Buckel W, Spirito CM, Steinbusch KJJ *et al.* Chain elongation with reactor microbiomes: open-culture

biotechnology to produce biochemicals. *Environ Sci Technol* 2016;50:2796–2810.

2. **Weimer PJ**, **Stevenson DM**. Isolation, characterization, and quantification of *Clostridium kluyveri* from the bovine rumen. *Appl Microbiol Biotechnol* 2012;94:461–466.
3. **Kim B-C**, **Seung Jeon B**, **Kim S**, **Kim H**, **Um Y** *et al*. *Caproiciproducens galactitolivorans* gen. nov., sp. nov., a bacterium capable of producing caproic acid from galactitol, isolated from a wastewater treatment plant. *Int J Syst Evol Microbiol* 2015;65:4902–4908.
4. **Choi K**, **Jeon BS**, **Kim B-C**, **Oh M-K**, **Um Y** *et al*. In situ biphasic extractive fermentation for hexanoic acid production from sucrose by *Megasphaera elsdenii* NCIMB 702410. *Appl Biochem Biotechnol* 2013;171:1094–1107.
5. **Elsden SR**, **Lewis D**. The production of fatty acids by a Gram-negative coccus. *Biochem J* 1953;55:183–189.
6. **Engelmann U**, **Weiss N**. *Megasphaera cerevisiae* sp. nov.: a new Gram-negative obligately anaerobic coccus isolated from spoiled beer. *Syst Appl Microbiol* 1985;6:287–290.
7. **Zhu X**, **Zhou Y**, **Wang Y**, **Wu T**, **Li X** *et al*. Production of high-concentration n-caproic acid from lactate through fermentation using a newly isolated *Ruminococcaceae* bacterium CPB6. *Biotechnol Biofuels* 2017;10:102.
8. **Genthner BR**, **Davis CL**, **Bryant MP**. Features of rumen and sewage sludge strains of *Eubacterium limosum*, a methanol- and H_2-CO_2-utilizing species. *Appl Environ Microbiol* 1981;42:12–19.
9. **Lindley ND**, **Loubiere P**, **Pacaud S**, **Mariotto C**, **Goma G**. Novel products of the acidogenic fermentation of methanol during growth of *Eubacterium limosum* in the presence of high concentrations of organic acids. *Microbiology* 1987;133:3557–3563.
10. **Phillips JR**, **Atiyeh HK**, **Tanner RS**, **Torres JR**, **Saxena J** *et al*. Butanol and hexanol production in *Clostridium carboxidivorans* syngas fermentation: medium development and culture techniques. *Bioresour Technol* 2015;190:114–121.
11. **Ramió-Pujol S**, **Ganigué R**, **Bañeras L**, **Colprim J**. Incubation at 25 °C prevents acid crash and enhances alcohol production in *Clostridium carboxidivorans* P7. *Bioresour Technol* 2015;192:296–303.
12. **Barker HA**. The production of caproic and butyric acids by the methane fermentation of ethyl alcohol. *Archiv. Mikrobiol.* 1937;8:415–421.
13. **Seedorf H**, **Fricke WF**, **Veith B**, **Bruggemann H**, **Liesegang H** *et al*. The genome of *Clostridium kluyveri*, a strict anaerobe with unique metabolic features. *Proc Natl Acad Sci U S A* 2008;105:2128–2133.
14. **Cavalcante WdeA**, **Leitão RC**, **Gehring TA**, **Angenent LT**, **Santaella ST**. Anaerobic fermentation for n-caproic acid production: a review. *Process Biochemistry* 2017;54:106–119.
15. **Marx H**, **Graf AB**, **Tatto NE**, **Thallinger GG**, **Mattanovich D** *et al*. Genome sequence of the ruminal bacterium *Megasphaera elsdenii*. *J Bacteriol* 2011;193:5578–5579.
16. **Kutumbaka KK**, **Pasmowitz J**, **Mategko J**, **Reyes D**, **Friedrich A** *et al*. Draf!Genome Sequence of the Beer Spoilage Bacterium *Megasphaera cerevisiae* Strain PA^{T}1^T. *Genome Announc* 2015;3:e01045–15.
17. **Song Y**, **Cho B-K**. Draft genome sequence of chemolithoautotrophic acetogenic butanol-producing *Eubacterium limosum* ATCC 8486. *Genome Announc* 2015;3:e01564–14.
18. **Bruant G**, **Lévesque M-J**, **Peter C**, **Guiot SR**, **Masson L**. Genomic analysis of carbon monoxide utilization and butanol production by *Clostridium carboxidivorans* strain P7T. *PLoS One* 2010;5:e13033.
19. **Tao Y**, **Zhu X**, **Wang H**, **Wang Y**, **Li X** *et al*. Complete genome sequence of *Ruminococcaceae* bacterium CPB6: a newly isolated culture for efficient N -caproic acid production from lactate. *J Biotechnol* 2017;259:91–94.
20. **Bengelsdorf FR**, **Poehlein A**, **Daniel R**, **Dürre P**. Genome sequence of the caproic acid-producing bacterium *Caproiciproducens galactitolivorans* BS-1^T (JCM 30532). *Microbiol Resour Announc* 2019;8:e00346–19.
21. **Hackmann TJ**, **Firkins JL**. Electron transport phosphorylation in rumen butyrivibrios: unprecedented ATP yield for glucose fermentation to butyrate. *Front Microbiol* 2015;6:622.
22. **Buckel W**, **Thauer RK**. Energy conservation via electron bifurcating ferredoxin reduction and proton/Na+ translocating ferredoxin oxidation. *Biochim Biophys Acta BBA - Bioenerg* 1827;2013:94–113.
23. **Wasewar KL**, **Shende DZ**. Reactive extraction of caproic acid using tri- *n* -butyl phosphate in hexanol, octanol, and decanol. *J Chem Eng Data* 2011;56:288–297.
24. **Tanner RS**. Cultivation of bacteria and fungi. In: Hurst CJ, Lipson DA, Garland JL, Stetzenbach LD, Mills AL ***et al***. (editors). *Manual of Environmental Microbiology*, 3rd ed. Washington, DC: American Society of Microbiology; 2007. pp. pp69–78.
25. **Leang C**, **Ueki T**, **Nevin KP**, **Lovley DR**. A genetic system for *Clostridium ljungdahlii*: a chassis for autotrophic production of biocommodities and a model homoacetogen. *Appl Environ Microbiol* 2013;79:1102–1109.
26. **Grootscholten TIM**, **Strik DPBTB**, **Steinbusch KJJ**, **Buisman CJN**, **Hamelers HVM**. Two-Stage medium chain fatty acid (MCFA) production from municipal solid waste and ethanol. *Appl Energy* 2014;116:223–229.
27. **Zhu X**, **Tao Y**, **Liang C**, **Li X**, **Wei N** *et al*. The synthesis of n-caproate from lactate: a new efficient process for medium-chain carboxylates production. *Sci Rep* 2015;5:14360.
28. **Kucek LA**, **Nguyen M**, **Angenent LT**. Conversion of L-lactate into n-caproate by a continuously fed reactor microbiome. *Water Res* 2016;93:163–171.
29. **Marone A**, **Trably E**, **Carrère H**, **Prompsy P**, **Guillon F** *et al*. Enhancement of corn stover conversion to carboxylates by extrusion and biotic triggers in solid-state fermentation. *Appl Microbiol Biotechnol* 2019;103:489–503.
30. **Nzeteu CO**, **Trego AC**, **Abram F**, **O'Flaherty V**. Reproducible, high-yielding, biological caproate production from food waste using a single-phase anaerobic reactor system. *Biotechnol Biofuels* 2018;11:108.
31. **Tindall BJ**. The names *Hungateiclostridium* Zhang *et al*. 2018, *Hungateiclostridium thermocellum* (Viljoen *et al*. 1926) Zhang *et al*. 2018, *Hungateiclostridium cellulolyticum* (Patel *et al*. 1980) Zhang *et al*. 2018, *Hungateiclostridium aldrichii* (Yang *et al*. 1990) Zhang *et al*. 2018, *Hungateiclostridium alkalicellulosi* (Zhilina *et al*. 2006) Zhang *et al*. 2018, *Hungateiclostridium clariflavum* (Shiratori *et al*. 2009) Zhang *et al*. 2018, *Hungateiclostridium straminisolvens* (Kato *et al*. 2004) Zhang *et al*. 2018 and *Hungateiclostridium saccincola* (Koeck *et al*. 2016) Zhang *et al*. 2018 contravene rule 51b of the International Code of Nomenclature of prokaryotes and require replacement names in the genus *Acetivibrio* Patel *et al*. 1980. *Int J Syst Evol Microbiol* 2019;69:3927–3932.
32. **Agarwala R**, **Barrett T**, **Beck J**, **Benson DA** *et al*, **NCBI Resource Coordinators**. Database resources of the National center for biotechnology information. *Nucleic Acids Res* 2018;46:8–13.
33. **Cole JR**, **Wang Q**, **Fish JA**, **Chai B**, **McGarrell DM** *et al*. Ribosomal database project: data and tools for high throughput rRNA analysis. *Nucleic Acids Res* 2014;42:633–642.
34. **Katoh K**, **Toh H**. Recent developments in the MAFFT multiple sequence alignment program. *Brief Bioinform* 2008;9:286–298.
35. **Ronquist F**, **Teslenko M**, **van der Mark P**, **Ayres DL**, **Darling A** *et al*. MrBayes 3.2: efficient Bayesian phylogenetic inference and model choice across a large model space. *Syst Biol* 2012;61:539–542.
36. **Ransom-Jones E**, **McDonald JE**. Draft genome sequence of *Clostridium* sp. strain W14A isolated from a cellulose-degrading biofilm in a landfill leachate microcosm. *Genome Announc* 2016;4:e00985–16.
37. **Rinland ME**, **Gómez MA**. Isolation and characterization of onion degrading bacteria from onion waste produced in South Buenos Aires Province, Argentina. *World J Microbiol Biotechnol* 2015;31:487–497.
38. **Yarza P**, **Yilmaz P**, **Pruesse E**, **Glöckner FO**, **Ludwig W** *et al*. Uniting the classification of cultured and uncultured bacteria

and archaea using 16S rRNA gene sequences. *Nat Rev Microbiol* 2014;12:635–645.

39. **Bolger AM**, **Lohse M**, **Usadel B**. Trimmomatic: a flexible trimmer for illumina sequence data. *Bioinformatics* 2014;30:2114–2120.
40. **Bankevich A**, **Nurk S**, **Antipov D**, **Gurevich AA**, **Dvorkin M** *et al*. SPAdes: a new genome assembly algorithm and its applications to single-cell sequencing. *J Comput Biol* 2012;19:455–477.
41. **García-Alcalde F**, **Okonechnikov K**, **Carbonell J**, **Cruz LM**, **Götz S** *et al*. Qualimap: evaluating next-generation sequencing alignment data. *Bioinformatics* 2012;28:2678–2679.
42. **Seemann T**. Prokka: rapid prokaryotic genome annotation. *Bioinformatics* 2014;30:2068–2069.
43. **Boynton ZL**, **Bennet GN**, **Rudolph FB**. Cloning, sequencing, and expression of clustered genes encoding beta-hydroxybutyryl-coenzyme A (CoA) dehydrogenase, crotonase, and butyryl-CoA dehydrogenase from *Clostridium acetobutylicum* ATCC 824. *J Bacteriol* 1996;178:3015–3024.
44. **Westphal L**, **Wiechmann A**, **Baker J**, **Minton NP**, **Müller V**. The Rnf Complex Is an Energy-Coupled Transhydrogenase Essential To Reversibly Link Cellular NADH and Ferredoxin Pools in the Acetogen *Acetobacterium woodii*. *J Bacteriol* 2018;200:e00357–18.
45. **Schuchmann K**, **Müller V**. Autotrophy at the thermodynamic limit of life: a model for energy conservation in acetogenic bacteria. *Nat Rev Microbiol* 2014;12:809–821.
46. **Weghoff MC**, **Bertsch J**, **Müller V**. A novel mode of lactate metabolism in strictly anaerobic bacteria. *Environ Microbiol* 2015;17:670–677.
47. **Chen I-MA**, **Chu K**, **Palaniappan K**, **Pillay M**, **Ratner A** *et al*. IMG/M v.5.0: an integrated data management and comparative analysis system for microbial genomes and microbiomes. *Nucleic Acids Res* 2019;47:D666–D677.
48. **Medlar AJ**, **Törönen P**, **Holm L**. AAI-profiler: fast proteome-wide exploratory analysis reveals taxonomic identity, misclassification and contamination. *Nucleic Acids Res* 2018;46:W479–W485.
49. **The UniProt Consortium**. UniProt: a worldwide hub of protein knowledge. *Nucleic Acids Res* 2019;47:D506–D515.
50. **Simbert RM**, **Krieg NR**. Phenotypic characterization. In: Gerhardt P, Murray RGM, Wood WA, Krieg NR (editors). *Methods for General and Molecular Bacteriology*, 2nd ed. Washington, DC: American Society for Microbiology; 1994. pp. 607–654.
51. **Cheng KJ**, **Costerton JW**. Ultrastructure of *Butyrivibrio fibrisolvens*: a Gram-positive bacterium. *J Bacteriol* 1977;129:1506–1512.
52. **Van Gylswyk NO**, **Morris EJ**, **Els HJ**. Sporulation and cell wall structure of *Clostridium polysaccharolyticum* comb.nov. (formerly *Fusobacterium polysaccharolyticum*). *Microbiology* 1980;121:491–493.
53. **Warnick TA**, **Methé BA**, **Leschine SB**. *Clostridium phytofermentans* sp. nov., a cellulolytic mesophile from forest soil. *Int J Syst Evol Microbiol* 2002;52:1155–1160.
54. **Gottschalk G**. Bacterial Fermentation. In: Gottschalk G (editor). *Bacterial Metabolism*, 2nd ed. New York, NY: Springer New York; 1986. pp. 210–280.
55. **Bahl H**, **Andersch W**, **Gottschalk G**. Continuous production of acetone and butanol by *Clostridium acetobutylicum* in a two-stage phosphate limited chemostat. *European J Appl Microbiol Biotechnol* 1982;15:201–205.
56. **Chen S**, **Dong X**. *Acetanaerobacterium elongatum* gen. nov., sp. nov., from paper mill waste water. *Int J Syst Evol Microbiol* 2004;54:2257–2262.
57. **Cato EP**, **George WL**, **Finegold SM**. Genus *Clostridium*. In: Sneath PHA, Mair NS, Sharpe ME, Holt JG (editors). *Bergey's Manual of Systematic Bacteriology, 1986*, 2. Baltimore: Williams & Wilkins. pp. 1141–1200.
58. **Moore WEC**, **Johnson JL**, **Holdeman LV**. Emendation of *Bacteroidaceae* and *Butyrivibrio* and descriptions of *Desulfomonas* gen. nov. and ten new species in the genera *Desulfomonas*, *Butyrivibrio*, *Eubacterium*, *Clostridium*, and *Ruminococcus*. *Int J Syst Bacteriol* 1976;26:238–252.
59. **Moore WEC**, **Cato EP**, **Holdeman LV**. *Ruminococcus bromii* sp. nov. and emendation of the description of *Ruminococcus sijpestein*Sijpestein. *Int J Syst Bacteriol* 1972;22:78–80.

Five reasons to publish your next article with a Microbiology Society journal

1. The Microbiology Society is a not-for-profit organization.
2. We offer fast and rigorous peer review – average time to first decision is 4–6 weeks.
3. Our journals have a global readership with subscriptions held in research institutions around the world.
4. 80% of our authors rate our submission process as 'excellent' or 'very good'.
5. Your article will be published on an interactive journal platform with advanced metrics.

Find out more and submit your article at microbiologyresearch.org.

3. Summary

Acetogens have the potential to become biocatalysts for the production of high-value chemicals from C1 carbon sources at industrial scale.[3,17,37] However, growth rates and productivities are low for most acetogens, and the product spectrum is limited. Thus, the development of new molecular tools for acetogens to overcome these hurdles has been part of recent research.[26] So far, multiple genetic engineering tools and synthetic pathways for recombinant production of biocommodities are established, however, other elementary tools are not.[106] Therefore, this thesis focused on expanding the molecular toolbox of acetogenic, but also solventogenic anaerobes by implementing pathways to recombinantly produce biocommodities, improving ATP supply, and establishing strong fluorescent reporter proteins.

In the first part of this thesis, the limited ATP supply during the autotrophic growth of the acetogen *A. woodii*, which harbors a well-established molecular toolbox, was addressed. Supplementation of arginine and exploitation of the arginine deiminase (ADI) pathway can improve ATP supply, which in consequence boosts growth and finally might help to overcome energetic barriers.[48] Therefore, the ADI pathway was established in *A. woodii* to improve autotrophic growth on H_2 + CO_2. The results obtained during this study are described in the attached publication "Induced heterologous expression of the arginine deiminase pathway promotes growth advantages in the strict anaerobe *Acetobacterium woodii*." Initially, genes of the ADI pathway of *C. autoethanogenum* were expressed in *A. woodii* controlled by the constitutive P_{ptaack} and the inducible P_{tet} promoter. The strain *A. woodii* [pMTL83151_P_{tet}_Boost] consumed arginine, which was supplemented as a surrogate for yeast extract and ammonia as the sole nitrogen source, and produced ornithine, but only when genes encoding the ADI pathway were expressed under both heterotrophic and autotrophic conditions. While heterotrophic cultivation boosted the growth of *A. woodii* cells, autotrophic growth did not. However, since the production of ornithine corresponds to ATP production, the assumption can be made that the genes of the ADI pathway are expressed and respective enzymes are functional in *A. woodii* under both conditions tested to provide additional energy. Interestingly, results of this study showed that expression of genes encoding the ADI pathway enabled growth on an arginine-supplemented defined medium. Constitutive expression of the ADI pathway genes using *A. woodii* [pMTL83151_P_{ptaack}_Boost] resulted in rapid arginine consumption and accumulation of ornithine and the intermediate of the ADI pathway citrulline during heterotrophic growth, while cells did not grow under

autotrophic growth conditions. These results demonstrated that strong constitutive expression could result in the accumulation of intermediates of the pathway and can negatively influence growth. Still, the recombinant expression of the ADI pathway genes improved ATP supply in the acetogen *A. woodii*, which was presented for the first time in this study. In conclusion, the establishment of the ADI pathway as a new molecular tool and the supplementation of arginine as a nitrogen source has the potential to overcome energetic barriers emerging during the recombinant production of value-added chemicals during autotrophic growth and is presumably applicable in multiple acetogens.

In the second part of the thesis, the molecular toolbox of the acetogen *E. limosum* should be expanded. So far, the recombinant production of the biocommodities butanol and acetone was achieved with various acetogens from C1 gases, however, was not yet reported from the industrially auspicious C1 carbon source methanol.[108,109,118,124,128] Therefore, a potent methanol-utilizing and genetically accessible acetogen is needed. Both demands are fulfilled by *E. limosum*, which was used in this study to produce both butanol as well as acetone from methanol.[62,112] In addition, FAST was established as a strong fluorescent reporter protein and used to construct fluorescent fusion proteins to track the production during growth. All results are presented in the attached manuscript "Production of the biocommodities butanol and acetone from methanol with fluorescent FAST-tagged proteins using metabolically engineered strains of *E. limosum.*" Butyrate, the precursor of butanol, was naturally produced by *E. limosum* from various C1 carbon sources, although the chosen substrate highly influenced the amount produced. The cultivation using methanol resulted in improved growth rates when compared to cultivation with the C1 gases H_2 + CO_2 or syngas, but also shifted the acetate:butyrate ratio in favor of butyrate. This shift confirmed the finding that methanol utilization via the WLP provides NAD(P)H, which in consequence is used by the NAD(P)H-dependent enzymes 3-hydroxybutyryl-CoA dehydrogenase (Hbd) and crotonase (Crt) of the *bcs* operon to produce butyrate. The further conversion of butyrate to butanol was achieved by heterologous expression of the gene encoding the bifunctional aldehyde/alcohol dehydrogenase (AdhE2) from the solventogen and natural butanol producer *C. acetobutylicum*, using the inducible *bgaR*-P_{bgaL} promoter system. The metabolically engineered *E. limosum* [pMTL83251_P_{bgaL}_AdhE2] strain produced up to 0.6 mM butanol and traces of ethanol from methanol. In addition, the heterologous AdhE2 production was tracked during cultivation by constructing fluorescent fusion proteins. Therefore, the functionality of

FAST for use in anoxic environments had to be proven. Hence, the FAST-encoding gene (*feg*) was expressed in a plasmid-based manner, controlled by the P_{bgaL} promoter of *C. perfringens* in *E. limosum*. Labeling of cells using ^{TF}Lime resulted in bright green fluorescence, which was determined using fluorescent microplate reader, fluorescence microscopy, and flow cytometry. Besides the green fluorescence of ^{TF}Lime-labeled cells, metabolically engineered *E. limosum* cells labeled with ^{TF}Coral resulted in bright red fluorescence. Subsequently, the fluorescence of this newly established reporter protein was further improved by expressing *feg* controlled by the constitutive P_{thlA} promoter of *C. acetobutylicum* and by constructing a tandemerized FAST version, tdFAST2, which was codon-optimized for *E. limosum*. In this study, the functionality of FAST was described for the first time in the acetogen *E. limosum*. In order to monitor AdhE2 protein production during growth, the enzyme was FAST-tagged at the C- or N-terminal end. Respective FAST-tagged AdhE2 fusion proteins were produced from methanol using *E. limosum* [pMTL83251_P_{bgaL}_C-FAST-AdhE2] and *E. limosum* [pMTL83251_P_{bgaL}_N-FAST-AdhE2] in a plasmid-based manner. The metabolically engineered *E. limosum* cells showed bright fluorescence during cultivation and produced 0.4 mM and 0.6 mM butanol, respectively, when genes encoding the C-terminally and N-terminally tagged AdhE2 fusion protein were expressed.

Furthermore, acetone production from methanol was achieved by establishing the acetone production operon (APO) of *C. acetobutylicum*, which includes the genes *thlA*, *ctfA/B*, and *adc* (encoding thiolase, acetoacetyl-CoA:acetate/butyrate-CoA transferase, and acetoacetate decarboxylase, respectively) controlled by the constitutive P_{thlA} promoter in *E. limosum*. The respective metabolically engineered strain *E. limosum* [pMTL83251_P_{thlA}_act] that expressed genes of the APO produced 0.3 mM acetone from methanol. In addition, the enzyme production of the APO was successfully monitored using the fluorescent reporter protein FAST. Therefore, the last enzyme of the APO, which is the acetoacetate decarboxylase (Adc), was FAST-tagged at the C- or N-terminal end, respective genes were expressed together with the remaining genes of the APO in *E. limosum*, and the fluorescence intensity of cells producing the fluorescent fusion proteins measured. *E. limosum* [pMTL83251_P_{thlA}_C-FAST-Adc] produced 1.6 mM acetone from methanol while bright green fluorescence was determined. In comparison, the production of the N-terminally tagged fusion protein only resulted in traces of acetone while fluorescence was poor.

The use of methanol as a carbon source is an attractive alternative to commonly used C1 gases and perfectly suited to produce high-value products. For the first time, metabolically engineered *E. limosum* strains were used as biocatalyst for the production of the industrially relevant biocommodities butanol and acetone from methanol. Moreover, the establishment of FAST as fluorescent reporter protein improved the molecular toolbox of *E. limosum*. The presented study showed that FAST can be used as fluorescent tag to monitor protein production under anaerobic conditions. Moreover, it was proven that the fusion proteins were produced by *E. limosum*, were still functional, and the productivity was not negatively affected, dependent on which end the protein was tagged at. The establishment of FAST serves as a basis for various applications in anaerobes as reporter protein and might be suited for multicolor approaches.

Such multicolor approaches are challenging in anaerobes due to the lack of fluorescent reporter proteins that are functional under anaerobic conditions.[26,169] Thus, establishing orthogonal fluorescent reporter proteins to enable multicolor approaches is of great interest, especially for monitoring intracellular dynamics or dynamics of anaerobic bacterial co-cultures.[183] The third part of the thesis focused on the realization of multicolor approaches in both solventogenic and acetogenic anaerobes, by making use of the mutated FAST variant greenFAST and redFAST.[181] Both reporter proteins were established to monitor the dynamics in synthetic co-cultures and investigate the intracellular interaction of a tightly regulated two-plasmid system. All findings are described in detail in the attached manuscript "Establishment of green- and red-fluorescent reporter proteins based on the fluorescence-activating and absorption-shifting tag for the use in acetogenic and solventogenic anaerobes." The plasmid-based production of greenFAST by the solventogens *C. saccharoperbutylacetonicum* and *C. acetobutylicum* and the acetogens *A. woodii* and *E. limosum* resulted in bright green fluorescence. Thus, this study showed that greenFAST is suited as an anaerobic fluorescent reporter protein. Still, several limitations occurred. While up to 95 % and 98 % of *C. saccharoperbutylacetonicum* and *A. woodii* cells produced greenFAST, respectively, the population of greenFAST-producing *C. acetobutylicum* and *E. limosum* cells was heterogeneous. In addition, *C. acetobutylicum* cells showed distinct red fluorescence in the stationary phase, presumably due to cell lysis, making the application of redFAST challenging. So far, redFAST seems to be limited for use in *C. saccharoperbutylacetonicum*. Metabolically engineered *C. saccharoperbutylacetonicum*

cells producing redFAST in a plasmid-based manner showed distinct red fluorescence and up to 89 % of cells produced the red fluorescent reporter. Hence, the orthogonal fluorescence of greenFAST and redFAST can be combined in *C. saccharoperbutylacetonicum* for multicolor approaches. In the case of *C. acetobutylicum*, the production of redFAST did not result in red fluorescent cells, while both acetogens *A. woodii* and *E. limosum* only showed poor red fluorescence.

In this study, the dynamics of a synthetic *C. saccharoperbutylacetonicum* co-culture was investigated regarding the number of greenFAST- and redFAST-producing cells. The combination of both reporter proteins to quantify the number of cells present in a co-culture was shown for the first time. During the exponential and stationary phase, the number of green- and red-fluorescent cells was stable, and both strains were productive. This finding opens the door to producing industrially relevant products using recombinant *C. saccharoperbutylacetonicum* strains in stable synthetic co-cultures. In addition, the co-cultivation of redFAST-producing *C. saccharoperbutylacetonicum* and greenFAST-producing *C. acetobutylicum* strains revealed that both cells are fluorescent and productive in the exponential and early stationary phase. However, in the late stationary phase, red autofluorescence of lysed *C. acetobutylicum* cells outweighs the fluorescence signal of redFAST, making further conclusions about co-culture dynamics impossible. Moreover, it was shown that when batch experiments are inoculated with one strain in excess, only this one prevails while the other is suppressed. Furthermore, the orthogonal fluorescence of greenFAST and redFAST was used to investigate intracellular dynamics in *C. saccharoperbutylacetonicum*. Therefore, the functionality of the inducible tightly regulated two-plasmid system based on the *tcdR*-P_{tcdB} promoter system of toxicogenic clostridia was shown. The co-existence of both plasmids was proven by the red fluorescence of cells, which was due to constitutive production of redFAST controlled by P_{thlA} and the green fluorescence of greenFAST controlled by the TcdR inducible P_{tcdB} promoter. Double-positive events only occurred after induction of *tcdR* expression controlled by P_{bgaL}. Since non-induced cells were sole red fluorescent, it has been shown that the two-plasmid system is indeed tightly regulated. Hence, this study showed the co-existence and interaction of both plasmids. This system can serve as the basis to evaluate the successful transformation of two-plasmids, to monitor plasmid curing, or in CRISPR-Cas9 approaches where a tight regulation is indispensable.

The presented study showed that the application of greenFAST and redFAST improves the molecular toolbox of *C. saccharoperbutylacetonicum* and facilitates two-color approaches. For the first time, multicolor approaches using fluorescent reporter proteins were applied for this solventogen. However, the use of redFAST as a reporter is so far limited for the use in *C. saccharoperbutylacetonicum*, as fluorescence of the other examined anaerobes was poor. Still, redFAST-producing *C. saccharoperbutylacetonicum* strains can be combined with greenFAST-producing microbes in synthetic co-cultures. However, the functionality of greenFAST must be further evaluated for potential co-culture partners.

Bacterial co-cultures are often used as a biotechnological production platform to produce medium-chain carboxylic acids. One of such carboxylic acids is hexanoate, which can be produced via chain elongation.[101] In the fourth part of this thesis, the isolation, and characterization of a new hexanoate producing bacterium from an anaerobic digester is described. The valid description of this new hexanoate-producing anaerobe is part of the attached manuscript "*Caproicibacter fermentans* gen. nov., sp. nov., a new caproate-producing bacterium and emended description of the genus *Caproiciproducens.*" Strain EA1^T was isolated from an anaerobic digester inoculated with a biogas plant sample. The isolated strain is a strict anaerobe, non-motile, rod-shaped, spore-forming, Gram-negative bacteria, which possesses a Gram-positive cell-wall structure. Most importantly, strain EA1^T produces acetate, butyrate, lactate, ethanol, and considerable large amounts of hexanoate from fructose. Genome analysis revealed that the genome of EA1^T consists of a circular chromosome of 3.9 Mb and a G+C content of 51.25 mol% and harbors all genes of the *bcs* operon. The gene products of the *bcs* operon might be involved in the conversion of acetyl-CoA to both butyrate and hexanoate in strain EA1^T. The major components of the cellular fatty acid fraction were $C_{14:0}$ (23.1 %), $C_{16:0}$ (13.2 %), $C_{16:0}$ dimethyl acetal (DMA) (17.0 %), and $C_{16:1}$ ω7c (11.7 %) and are considerably different from the closely related strains *Caproiciproducens galactitolivorans* BS-1 and *Ruminococcaceae* bacterium CBP6, which are both capable to produce hexanoate. Summarized, phenotypic and genotypic characteristics indicate that strain EA1^T represents a novel genus in the family *Oscillospiraceae* and was termed *Caproicibacter fermentans* (DSM 107079^T, JCM 33110^T). This study showed that *Cb. fermentans* is a novel anaerobe and a potent hexanoate producer. The presented results form the basis for further investigations, including synthetic biology approaches and the feasibility of the described strain as an industrially relevant hexanoate producer.

4. Literature

(1) Horowitz, C. A. Paris Agreement. *Int. Leg. Mater.* ***2016***, *55*, 740–755. https://doi.org/10.1017/S0020782900004253.

(2) International Energy Agency. Net zero by 2050: a roadmap for the global energy sector; OECD, ***2021***. https://doi.org/10.1787/c8328405-en.

(3) Dürre, P.; Eikmanns, B. J. C1-carbon sources for chemical and fuel production by microbial gas fermentation. *Curr. Opin. Biotechnol.* ***2015***, *35*, 63–72. https://doi.org/10.1016/j.copbio.2015.03.008.

(4) Tracy, B. P.; Jones, S. W.; Fast, A. G.; Indurthi, D. C.; Papoutsakis, E. T. Clostridia: the importance of their exceptional substrate and metabolite diversity for biofuel and biorefinery applications. *Curr. Opin. Biotechnol.* ***2012***, *23*, 364–381. https://doi.org/10.1016/j.copbio.2011.10.008.

(5) Schiel-Bengelsdorf, B.; Montoya, J.; Linder, S.; Dürre, P. Butanol fermentation. *Environ. Technol.* ***2013***, *34*, 1691–1710. https://doi.org/10.1080/09593330.2013.827746.

(6) Poehlein, A.; Solano, J. D. M.; Flitsch, S. K.; Krabben, P.; Winzer, K.; Reid, S. J.; Jones, D. T.; Green, E.; Minton, N. P.; Daniel, R.; Dürre, P. Microbial solvent formation revisited by comparative genome analysis. *Biotechnol. Biofuels* ***2017***, *10*, 58. https://doi.org/10.1186/s13068-017-0742-z.

(7) Boynton, Z. L.; Bennet, G. N.; Rudolph, F. B. Cloning, sequencing, and expression of clustered genes encoding β-hydroxybutyryl-coenzyme A (CoA) dehydrogenase, crotonase, and butyryl-CoA dehydrogenase from *Clostridium acetobutylicum* ATCC 824. *J. Bacteriol.* ***1996***, *178*, 3015–3024. https://doi.org/10.1128/jb.178.11.3015-3024.1996.

(8) Fischer, R. J.; Helms, J.; Dürre, P. Cloning, sequencing, and molecular analysis of the *sol* operon of *Clostridium acetobutylicum*, a chromosomal locus involved in solventogenesis. *J. Bacteriol.* ***1993***, *175*, 6959–6969. https://doi.org/10.1128/jb.175.21.6959-6969.1993.

(9) Kosaka, T.; Nakayama, S.; Nakaya, K.; Yoshino, S.; Furukawa, K. Characterization of the *sol* operon in butanol-hyperproducing *Clostridium saccharoperbutylacetonicum* strain N1-4 and its degeneration mechanism. *Biosci. Biotechnol. Biochem.* ***2007***, *71*, 58–68. https://doi.org/10.1271/bbb.60370.

(10) Dürre, P. New insights and novel developments in clostridial acetone/butanol/isopropanol fermentation. *Appl. Microbiol. Biotechnol.* ***1998***, *49*, 639–648. https://doi.org/10.1007/s002530051226.

(11) Dürre, P. Fermentative butanol production: bulk chemical and biofuel. *Ann. N. Y. Acad. Sci.* ***2008***, *1125*, 353–362. https://doi.org/10.1196/annals.1419.009.

(12) Papoutsakis, E. T. Engineering solventogenic clostridia. *Curr. Opin. Biotechnol.* ***2008***, *19*, 420–429. https://doi.org/10.1016/j.copbio.2008.08.003.

(13) Birgen, C.; Dürre, P.; Preisig, H. A.; Wentzel, A. Butanol production from lignocellulosic biomass: revisiting fermentation performance indicators with exploratory data

analysis. *Biotechnol. Biofuels* ***2019***, *12*, 167. https://doi.org/10.1186/s13068-019-1508-6.

(14) Li, S.; Huang, L.; Ke, C.; Pang, Z.; Liu, L. Pathway dissection, regulation, engineering and application: lessons learned from biobutanol production by solventogenic clostridia. *Biotechnol. Biofuels* ***2020***, 13, 39. https://doi.org/10.1186/s13068-020-01674-3.

(15) Bharathiraja, B.; Jayamuthunagai, J.; Sudharsanaa, T.; Bharghavi, A.; Praveenkumar, R.; Chakravarthy, M.; Yuvaraj, D. Biobutanol - an impending biofuel for future: a review on upstream and downstream processing tecniques. *Renew. Sustain. Energy Rev.* ***2017***, 68, 788–807. https://doi.org/10.1016/j.rser.2016.10.017.

(16) Gottumukkala, L. D.; Haigh, K.; Görgens, J. Trends and advances in conversion of lignocellulosic biomass to biobutanol: microbes, bioprocesses and industrial viability. *Renew. Sustain. Energy Rev.* ***2017***, *76*, 963–973. https://doi.org/10.1016/j.rser.2017.03.030.

(17) Bengelsdorf, F. R.; Beck, M. H.; Erz, C.; Hoffmeister, S.; Karl, M. M.; Riegler, P.; Wirth, S.; Poehlein, A.; Weuster-Botz, D.; Dürre, P. Bacterial anaerobic synthesis gas (syngas) and CO_2 + H_2 fermentation. In *Advances in Applied Microbiology*; Elsevier, ***2018***; Vol. 103, pp 143–221. https://doi.org/10.1016/bs.aambs.2018.01.002.

(18) Thieme, N.; Panitz, J. C.; Held, C.; Lewandowski, B.; Schwarz, W. H.; Liebl, W.; Zverlov, V. Milling byproducts are an economically viable substrate for butanol production using clostridial ABE fermentation. *Appl. Microbiol. Biotechnol.* ***2020***, *104*, 8679–8689. https://doi.org/10.1007/s00253-020-10882-8.

(19) Kim, B.-C.; Seung Jeon, B.; Kim, S.; Kim, H.; Um, Y.; Sang, B.-I. *Caproiciproducens galactitolivorans* gen. nov., sp. nov., a bacterium capable of producing caproic acid from galactitol, isolated from a wastewater treatment plant. *Int. J. Syst. Evol. Microbiol.* ***2015***, *65*, 4902–4908. https://doi.org/10.1099/ijsem.0.000665.

(20) Zhu, X.; Zhou, Y.; Wang, Y.; Wu, T.; Li, X.; Li, D.; Tao, Y. Production of high-concentration n-caproic acid from lactate through fermentation using a newly isolated *Ruminococcaceae* bacterium CPB6. *Biotechnol. Biofuels* ***2017***, *10*, 102. https://doi.org/10.1186/s13068-017-0788-y.

(21) Jeon, B. S.; Kim, S.; Sang, B.-I. *Megasphaera hexanoica* sp. nov., a medium-chain carboxylic acid-producing bacterium isolated from a cow rumen. *Int. J. Syst. Evol. Microbiol.* ***2017***, *67*, 2114–2120. https://doi.org/10.1099/ijsem.0.001888.

(22) Wood, J. C.; Marcellin, E.; Plan, M. R.; Virdis, B. High methanol-to-formate ratios induce butanol production in *Eubacterium limosum*. *Microb. Biotechnol.* ***2021***, *0*, 1–8. https://doi.org/10.1111/1751-7915.13963.

(23) Keis, S.; Shaheen, R.; Jones, D. T. Emended descriptions of *Clostridium acetobutylicum* and *Clostridium beijerinckii*, and descriptions of *Clostridium saccharoperbutylacetonicum* sp. nov. and *Clostridium saccharobutylicum* sp. nov. *Int. J. Syst. Evol. Microbiol.* ***2001***, *51*, 2095–2103. https://doi.org/10.1099/00207713-51-6-2095.

(24) Thauer, R. K.; Jungermann, K.; Henninger, H.; Wenning, J.; Decker, K. The energy metabolism of *Clostridium kluyveri*. *Eur. J. Biochem.* ***1968***, *4*, 173–180. https://doi.org/10.1111/j.1432-1033.1968.tb00189.x.

(25) Buschhorn, H.; Dürre, P.; Gottschalk, G. Production and utilization of ethanol by the homoacetogen *Acetobacterium woodii*. *Appl. Environ. Microbiol.* ***1989***, *55*, 1835–1840. https://doi.org/10.1128/aem.55.7.1835-1840.1989.

(26) Jin, S.; Bae, J.; Song, Y.; Pearcy, N.; Shin, J.; Kang, S.; Minton, N. P.; Soucaille, P.; Cho, B.-K. Synthetic biology on acetogenic bacteria for highly efficient conversion of C1 gases to biochemicals. *Int. J. Mol. Sci.* ***2020***, *21*, 7639. https://doi.org/10.3390/ijms21207639.

(27) Flüchter, S.; Follonier, S.; Schiel-Bengelsdorf, B.; Bengelsdorf, F. R.; Zinn, M.; Dürre, P. Anaerobic production of poly(3-hydroxybutyrate) and its precursor 3-hydroxybutyrate from synthesis gas by autotrophic clostridia. *Biomacromolecules* ***2019***, *20*, 3271–3282. https://doi.org/10.1021/acs.biomac.9b00342.

(28) Wang, X.; Qin, J.; Ma, C.; Wang, J.; Wang, X.; Xu, S.; Feng, J.; Chen, K.; Ouyang, P. Methanol assimilation with CO_2 reduction in *Butyribacterium methylotrophicum* and development of genetic toolkits for its engineering. *ACS Sustain. Chem. Eng.* ***2021***, *9*, 12079–12090. https://doi.org/10.1021/acssuschemeng.1c02365.

(29) Liu, Y.; Li, J.; Du, G.; Chen, J.; Liu, L. Metabolic engineering of *Bacillus subtilis* fueled by systems biology: recent advances and future directions. *Biotechnol. Adv.* ***2017***, *35*, 20–30. https://doi.org/10.1016/j.biotechadv.2016.11.003.

(30) Charubin, K.; Bennett, R. K.; Fast, A. G.; Papoutsakis, E. T. Engineering *Clostridium* organisms as microbial cell-factories: challenges & opportunities. *Metab. Eng.* ***2018***, *50*, 173–191. https://doi.org/10.1016/j.ymben.2018.07.012.

(31) Li, A.; Wen, Z.; Fang, D.; Lu, M.; Ma, Y.; Xie, Q.; Jin, M. Developing *Clostridium diolis* as a biorefinery chassis by genetic manipulation. *Bioresour. Technol.* ***2020***, *305*, 123066. https://doi.org/10.1016/j.biortech.2020.123066.

(32) Hellinger, E. *Clostridium aurantibutyricum* (n.sp.): a pink butyric acid *Clostridium*. *J. Gen. Microbiol.* ***1947***, *1*, 203–210. https://doi.org/10.1099/00221287-1-2-203.

(33) Drake, H. L.; Gößner, A. S.; Daniel, S. L. Old acetogens, new light. *Ann. N. Y. Acad. Sci.* ***2008***, *1125*, 100–128. https://doi.org/10.1196/annals.1419.016.

(34) Drake, H. L.; Küsel, K.; Matthies, C. Ecological consequences of the phylogenetic and physiological diversities of acetogens. *Antonie Van Leeuwenhoek* ***2002***, *81*, 203–213. https://doi.org/10.1023/A:1020514617738.

(35) Molitor, B.; Richter, H.; Martin, M. E.; Jensen, R. O.; Juminaga, A.; Mihalcea, C.; Angenent, L. T. Carbon recovery by fermentation of CO-rich off gases - turning steel mills into biorefineries. *Bioresour. Technol.* ***2016***, *215*, 386–396. https://doi.org/10.1016/j.biortech.2016.03.094.

(36) Swalec, C.; Shearer, C. Pedal to the metal: no time to delay decarbonizing the global steel sector. Global Energy Monitor, San Francisco, CA, ***2021***. https://globalenergymonitor.org/report/pedal-to-the-metal-no-time-for-delay-in-decarbonizing-global-steel-sector/ (called January 2022)

(37) Köpke, M.; Simpson, S. D. Pollution to products: recycling of 'above ground' carbon by gas fermentation. *Curr. Opin. Biotechnol.* ***2020***, *65*, 180–189. https://doi.org/10.1016/j.copbio.2020.02.017.

(38) Heffernan, J. K.; Valgepea, K.; de Souza Pinto Lemgruber, R.; Casini, I.; Plan, M.; Tappel, R.; Simpson, S. D.; Köpke, M.; Nielsen, L. K.; Marcellin, E. Enhancing CO_2-valorization using *Clostridium autoethanogenum* for sustainable fuel and chemicals production. *Front. Bioeng. Biotechnol.* ***2020***, *8*, 204. https://doi.org/10.3389/fbioe.2020.00204.

(39) Karlson, B.; Bellavitis, C.; France, N. Commercializing LanzaTech, from waste to fuel: an effectuation case. *J. Manag. Organ.* ***2021***, *27*, 175–196. https://doi.org/10.1017/jmo.2017.83.

(40) Simpson, S.; Abdalla, T.; Brown, S.; Canter, C.; Conrado, R.; Daniell, J.; Dassanayake, A.; Gao, A.; Jensen, R.; Köpke, M.; Leang, C.; Liew, F.; Nagaraju, S.; Nogle, R.; Tappel, R.; Tran, L.; Charania, P.; Engle, N.; Giannone, R.; Hettich, R.; Klingeman, D.; Poudel, S.; Tschaplinski, T.; Yang, Z. Development of a sustainable green chemistry platform for production of acetone and downstream drop-in fuel and commodity products directly from biomass syngas via a novel energy conserving route in engineered acetogenic bacteria. Lanzatech, Inc., Skokie, IL, ***2019***. https://doi.org/10.2172/1599328.

(41) Nesbitt, E. R. Using waste carbon feedstocks to produce chemicals. *Ind. Biotechnol.* ***2020***, *16*, 147–163. https://doi.org/10.1089/ind.2020.29217.ern.

(42) Fuchs, G. Alternative pathways of carbon dioxide fixation: insights into the early evolution of life? *Annu. Rev. Microbiol.* ***2011***, *65*, 631–658. https://doi.org/10.1146/annurev-micro-090110-102801.

(43) Sánchez-Andrea, I.; Guedes, I. A.; Hornung, B.; Boeren, S.; Lawson, C. E.; Sousa, D. Z.; Bar-Even, A.; Claassens, N. J.; Stams, A. J. M. The reductive glycine pathway allows autotrophic growth of *Desulfovibrio desulfuricans*. *Nat. Commun.* ***2020***, *11*, 5090. https://doi.org/10.1038/s41467-020-18906-7.

(44) Ragsdale, S. W.; Pierce, E. Acetogenesis and the Wood–Ljungdahl pathway of CO_2 fixation. *Biochim. Biophys. Acta BBA - Proteins Proteomics* ***2008***, *1784*, 1873–1898. https://doi.org/10.1016/j.bbapap.2008.08.012.

(45) Schuchmann, K.; Müller, V. Autotrophy at the thermodynamic limit of life: a model for energy conservation in acetogenic bacteria. *Nat. Rev. Microbiol.* ***2014***, *12*, 809–821. https://doi.org/10.1038/nrmicro3365.

(46) Bertsch, J.; Müller, V. Bioenergetic constraints for conversion of syngas to biofuels in acetogenic bacteria. *Biotechnol. Biofuels* ***2015***, *8*, 210. https://doi.org/10.1186/s13068-015-0393-x.

(47) de Souza Pinto Lemgruber, R.; Valgepea, K.; Tappel, R.; Behrendorff, J. B.; Palfreyman, R. W.; Plan, M.; Hodson, M. P.; Simpson, S. D.; Nielsen, L. K.; Köpke, M.; Marcellin, E. Systems-level engineering and characterisation of *Clostridium autoethanogenum* through heterologous production of poly-3-hydroxybutyrate (PHB). *Metab. Eng.* ***2019***, *53*, 14–23. https://doi.org/10.1016/j.ymben.2019.01.003.

(48) Valgepea, K.; Loi, K. Q.; Behrendorff, J. B.; Lemgruber, R. de S. P.; Plan, M.; Hodson, M. P.; Köpke, M.; Nielsen, L. K.; Marcellin, E. Arginine deiminase pathway provides ATP

and boosts growth of the gas-fermenting acetogen *Clostridium autoethanogenum*. *Metab. Eng.* ***2017***, *41*, 202–211. https://doi.org/10.1016/j.ymben.2017.04.007.

(49) Emerson, D. F.; Woolston, B. M.; Liu, N.; Donnelly, M.; Currie, D. H.; Stephanopoulos, G. Enhancing hydrogen-dependent growth of and carbon dioxide fixation by *Clostridium ljungdahlii* through nitrate supplementation. *Biotechnol. Bioeng.* ***2019***, *116*, 294–306. https://doi.org/10.1002/bit.26847.

(50) Thauer, R. K.; Jungermann, K.; Decker, K. Energy conservation in chemotrophic anaerobic bacteria. *Bacteriol. Rev.* ***1977***, *41*, 100–180. https://doi.org/10.1128/br.41.1.100-180.1977.

(51) Zúñiga, M. Evolution of arginine deiminase (ADI) pathway genes. *Mol. Phylogenet. Evol.* ***2002***, *25*, 429–444. https://doi.org/10.1016/S1055-7903(02)00277-4.

(52) Vander Wauven, C.; Piérard, A.; Kley-Raymann, M.; Haas, D. *Pseudomonas aeruginosa* mutants affected in anaerobic growth on arginine: evidence for a four-gene cluster encoding the arginine deiminase pathway. *J. Bacteriol.* ***1984***, *160*, 928–934. https://doi.org/10.1128/jb.160.3.928-934.1984.

(53) Noens, E. E. E.; Lolkema, J. S. Convergent evolution of the arginine deiminase pathway: the ArcD and ArcE arginine/ornithine exchangers. *MicrobiologyOpen* ***2017***, *6*, e00412. https://doi.org/10.1002/mbo3.412.

(54) Acharya, B.; Roy, P.; Dutta, A. Review of syngas fermentation processes for bioethanol. *Biofuels* ***2014***, *5*, 551–564. https://doi.org/10.1080/17597269.2014.1002996.

(55) Bertau, M., Offermanns, H., Plass, L., Schmidt, F., Wernicke, H.-J. Methanol: the basic chemical and energy feedstock of the future; Springer, ***2014***; Vol. 1. https://doi.org/10.1007/978-3-642-39709-7.

(56) Sheldon, D. Methanol production - a technical history. *Johns. Matthey Technol. Rev.* ***2017***, *61*, 172–182. https://doi.org/10.1595/205651317X695622.

(57) Dalena, F.; Senatore, A.; Marino, A.; Gordano, A.; Basile, M.; Basile, A. Methanol production and applications: an overview. In *Methanol*; Elsevier, ***2018***; pp 3–28. https://doi.org/10.1016/B978-0-444-63903-5.00001-7.

(58) Acquarola, C.; Ao, M.; Bhatelia, T.; Prakash, B.; Faka, S.; Pareek, V.; Shah, M. T. Simulations and optimization of a reduced CO_2 emission process for methanol production using syngas from bi-reforming. *Energy Fuels* ***2021***, *35*, 8844–8856. https://doi.org/10.1021/acs.energyfuels.1c00227.

(59) Irena and methanol institute. Innovation outlook: renewable methanol. International Renewable Energy Agency, Abu Dhabi, ***2021***. https://www.irena.org/publications/2021/Jan/Innovation-Outlook-Renewable-Methanol (called January 2022)

(60) Zeikus, J. G.; Lynd, L. H.; Thompson, T. E.; Krzycki, J. A.; Weimer, P. J.; Hegge, P. W. Isolation and characterization of a new, methylotrophic, acidogenic anaerobe, the Marburg strain. *Curr. Microbiol.* ***1980***, *3*, 381–386. https://doi.org/10.1007/BF02601907.

(61) Bache, R.; Pfennig, N. Selective isolation of *Acetobacterium woodii* on methoxylated aromatic acids and determination of growth yields. *Arch. Microbiol.* ***1981***, *130*, 255–261. https://doi.org/10.1007/BF00459530.

(62) Genthner, B. R.; Davis, C. L.; Bryant, M. P. Features of rumen and sewage sludge strains of *Eubacterium limosum*, a methanol- and H_2-CO_2-utilizing species. *Appl. Environ. Microbiol.* ***1981***, *42*, 12–19. https://doi.org/10.1128/aem.42.1.12-19.1981.

(63) Daniel, S. L.; Hsu, T.; Dean, S. I.; Drake, H. L. Characterization of the H_2- and CO-dependent chemolithotrophic potentials of the acetogens *Clostridium thermoaceticum* and *Acetogenium kivui*. *J. Bacteriol.* ***1990***, *172*, 4464–4471. https://doi.org/10.1128/jb.172.8.4464-4471.1990.

(64) Das, A.; Fu, Z.-Q.; Tempel, W.; Liu, Z.-J.; Chang, J.; Chen, L.; Lee, D.; Zhou, W.; Xu, H.; Shaw, N.; Rose, J. P.; Ljungdahl, L. G.; Wang, B.-C. Characterization of a corrinoid protein involved in the C1 metabolism of strict anaerobic bacterium *Moorella thermoacetica*. *Proteins Struct. Funct. Bioinforma.* ***2007***, *67*, 167–176. https://doi.org/10.1002/prot.21094.

(65) Pierce, E.; Xie, G.; Barabote, R. D.; Saunders, E.; Han, C. S.; Detter, J. C.; Richardson, P.; Brettin, T. S.; Das, A.; Ljungdahl, L. G.; Ragsdale, S. W. The complete genome sequence of *Moorella thermoacetica* (f. *Clostridium thermoaceticum*). *Environ. Microbiol.* ***2008***, *10*, 2550–2573. https://doi.org/10.1111/j.1462-2920.2008.01679.x.

(66) Visser, M.; Pieterse, M. M.; Pinkse, M. W. H.; Nijsse, B.; Verhaert, P. D. E. M.; de Vos, W. M.; Schaap, P. J.; Stams, A. J. M. Unravelling the one-carbon metabolism of the acetogen *Sporomusa* strain An4 by genome and proteome analysis. *Environ. Microbiol.* ***2016***, *18*, 2843–2855. https://doi.org/10.1111/1462-2920.12973.

(67) Kremp, F.; Poehlein, A.; Daniel, R.; Müller, V. Methanol metabolism in the acetogenic bacterium *Acetobacterium woodii*. *Environ. Microbiol.* ***2018***, *20*, 4369–4384. https://doi.org/10.1111/1462-2920.14356.

(68) Kremp, F.; Müller, V. Methanol and methyl group conversion in acetogenic bacteria: biochemistry, physiology and application. *FEMS Microbiol. Rev.* ***2021***, *45*, fuaa040. https://doi.org/10.1093/femsre/fuaa040.

(69) Claassens, N. J.; Cotton, C. A. R.; Kopljar, D.; Bar-Even, A. Making quantitative sense of electromicrobial production. *Nat. Catal.* ***2019***, *2*, 437–447. https://doi.org/10.1038/s41929-019-0272-0.

(70) Cotton, C. A.; Claassens, N. J.; Benito-Vaquerizo, S.; Bar-Even, A. Renewable methanol and formate as microbial feedstocks. *Curr. Opin. Biotechnol.* ***2020***, *62*, 168–180. https://doi.org/10.1016/j.copbio.2019.10.002.

(71) Barker, H. A.; Haas, V. *Butyribacterium*, a new genus of Gram-positive, non-sporulating anaerobic bacteria of intestinal origin. *J. Bacteriol.* ***1944***, *47*, 301–305. https://doi.org/10.1128/jb.47.3.301-305.1944.

(72) Jeong, J.; Bertsch, J.; Hess, V.; Choi, S.; Choi, I.-G.; Chang, I. S.; Müller, V. Energy conservation model based on genomic and experimental analyses of a carbon monoxide-utilizing, butyrate-forming acetogen, *Eubacterium limosum* KIST612. *Appl. Environ. Microbiol.* ***2015***, *81*, 4782–4790. https://doi.org/10.1128/AEM.00675-15.

(73) Pacaud, S.; Loubière, P.; Goma, G.; Lindley, N. D. Organic acid production during methylotrophic growth of *Eubacterium limosum* B2: displacement towards increased butyric acid yields by supplementing with acetate. *Appl. Microbiol. Biotechnol.* ***1986***, *23*, 330–335. https://doi.org/10.1007/BF00257028.

(74) Litty, D.; Müller, V. Butyrate production in the acetogen *Eubacterium limosum* is dependent on the carbon and energy source. *Microb. Biotechnol.* ***2021***, *14*, 2686–2692. https://doi.org/10.1111/1751-7915.13779.

(75) Pacaud, S.; Loubière, P.; Goma, G. Methanol metabolism by *Eubacterium limosum* B2: effects of pH and carbon dioxide on growth and organic acid production. *Curr. Microbiol.* ***1985***, *12*, 245–250. https://doi.org/10.1007/BF01567972.

(76) Loubière, P.; Lindley, N. D. The use of acetate as an additional co-substrate improves methylotrophic growth of the acetogenic anaerobe *Eubacterium limosum* when CO_2 fixation is rate-limiting. *J. Gen. Microbiol.* ***1991***, *137*, 2247–2251. https://doi.org/10.1099/00221287-137-9-2247.

(77) Song, Y.; Cho, B.-K. Draft genome sequence of chemolithoautotrophic acetogenic butanol-producing *Eubacterium limosum* ATCC 8486. *Genome Announc.* ***2015***, *3*, e01564-14. https://doi.org/10.1128/genomeA.01564-14.

(78) Song, Y.; Shin, J.; Jeong, Y.; Jin, S.; Lee, J.-K.; Kim, D. R.; Kim, S. C.; Cho, S.; Cho, B.-K. Determination of the genome and primary transcriptome of syngas fermenting *Eubacterium limosum* ATCC 8486. *Sci. Rep.* ***2017***, *7*, 13694. https://doi.org/10.1038/s41598-017-14123-3.

(79) Lindley, N. D.; Loubiere, P.; Pacaud, S.; Mariotto, C.; Goma, G. Novel products of the acidogenic fermentation of methanol during growth of *Eubacterium limosum* in the presence of high concentrations of organic acids. *Microbiology* ***1987***, *133*, 3557–3563. https://doi.org/10.1099/00221287-133-12-3557.

(80) Dietrich, H. M.; Kremp, F.; Öppinger, C.; Ribaric, L.; Müller, V. Biochemistry of methanol-dependent acetogenesis in *Eubacterium callanderi* KIST612. *Environ. Microbiol.* ***2021***, *23*, 4505–4517. https://doi.org/10.1111/1462-2920.15643.

(81) Mechichi, T.; Labat, M.; Woo, T. H. S.; Thomas, P.; Garcia, J.-L.; Patel, B. K. C. *Eubacterium aggregans* sp. nov., a new homoacetogenic bacterium from olive mill wastewater treatment digestor. *Anaerobe* ***1998***, *4*, 283–291. https://doi.org/10.1006/anae.1998.0179.

(82) Liou, J. S.-C.; Balkwill, D. L.; Drake, G. R.; Tanner, R. S. *Clostridium carboxidivorans* sp. nov., a solvent-producing clostridium isolated from an agricultural settling lagoon, and reclassification of the acetogen *Clostridium scatologenes* strain SL1 as *Clostridium drakei* sp. nov. *Int. J. Syst. Evol. Microbiol.* ***2005***, *55*, 2085–2091. https://doi.org/10.1099/ijs.0.63482-0.

(83) Wirth, S.; Dürre, P. Investigation of putative genes for the production of medium-chained acids and alcohols in autotrophic acetogenic bacteria. *Metab. Eng.* ***2021***, *66*, 296–307. https://doi.org/10.1016/j.ymben.2021.04.010.

(84) Grethlein, A. J.; Worden, R. M.; Jain, M. K.; Datta, R. Evidence for production of n-butanol from carbon monoxide by *Butyribacterium methylotrophicum*. *J. Ferment. Bioeng.* ***1991***, *72*, 58–60. https://doi.org/10.1016/0922-338X(91)90147-9.

(85) Shen, G.-J.; Shieh, J.-S.; Grethlein, A. J.; Jain, M. K.; Zeikus, J. G. Biochemical basis for carbon monoxide tolerance and butanol production by *Butyribacterium methylotrophicum*. *Appl. Microbiol. Biotechnol.* ***1999***, *51*, 827–832. https://doi.org/10.1007/s002530051469.

(86) Fernández-Naveira, Á.; Abubackar, H. N.; Veiga, M. C.; Kennes, C. Efficient butanol-ethanol (B-E) production from carbon monoxide fermentation by *Clostridium carboxidivorans*. *Appl. Microbiol. Biotechnol.* ***2016***, *100*, 3361–3370. https://doi.org/10.1007/s00253-015-7238-1.

(87) Köpke, M.; Mihalcea, C.; Liew, F.; Tizard, J. H.; Ali, M. S.; Conolly, J. J.; Al-Sinawi, B.; Simpson, S. D. 2,3-butanediol production by acetogenic bacteria, an alternative route to chemical synthesis, using industrial waste gas. *Appl. Environ. Microbiol.* ***2011***, *77*, 5467–5475. https://doi.org/10.1128/AEM.00355-11.

(88) Köpke, M.; Mihalcea, C.; Bromley, J. C.; Simpson, S. D. Fermentative production of ethanol from carbon monoxide. *Curr. Opin. Biotechnol.* ***2011***, *22*, 320–325. https://doi.org/10.1016/j.copbio.2011.01.005.

(89) Zahn, J. A.; Saxena, J. Ethanologenic *Clostridium* species, *Clostridium coskatii*. US 8143037 B2. Washington, DC: U.S. Patent and Trademark Office ***2012***.

(90) Richter, H.; Molitor, B.; Wei, H.; Chen, W.; Aristilde, L.; Angenent, L. T. Ethanol production in syngas-fermenting *Clostridium ljungdahlii* is controlled by thermodynamics rather than by enzyme expression. *Energy Environ. Sci.* ***2016***, *9*, 2392–2399. https://doi.org/10.1039/C6EE01108J.

(91) Liew, F.; Henstra, A. M.; Köpke, M.; Winzer, K.; Simpson, S. D.; Minton, N. P. Metabolic engineering of *Clostridium autoethanogenum* for selective alcohol production. *Metab. Eng.* ***2017***, *40*, 104–114. https://doi.org/10.1016/j.ymben.2017.01.007.

(92) Mahamkali, V.; Valgepea, K.; de Souza Pinto Lemgruber, R.; Plan, M.; Tappel, R.; Köpke, M.; Simpson, S. D.; Nielsen, L. K.; Marcellin, E. Redox controls metabolic robustness in the gas-fermenting acetogen *Clostridium autoethanogenum*. *Proc. Natl. Acad. Sci. USA* ***2020***, *117*, 13168–13175. https://doi.org/10.1073/pnas.1919531117.

(93) Cavalcante, W. de A.; Leitão, R. C.; Gehring, T. A.; Angenent, L. T.; Santaella, S. T. Anaerobic fermentation for n-caproic acid production: a review. *Process Biochem.* ***2017***, *54*, 106–119. https://doi.org/10.1016/j.procbio.2016.12.024.

(94) Seedorf, H.; Fricke, W. F.; Veith, B.; Bruggemann, H.; Liesegang, H.; Strittmatter, A.; Miethke, M.; Buckel, W.; Hinderberger, J.; Li, F.; Hagemeier, C.; Thauer, R. K.; Gottschalk, G. The genome of *Clostridium kluyveri*, a strict anaerobe with unique metabolic features. *Proc. Natl. Acad. Sci. USA* ***2008***, *105*, 2128–2133. https://doi.org/10.1073/pnas.0711093105.

(95) Choi, K.; Jeon, B. S.; Kim, B.-C.; Oh, M.-K.; Um, Y.; Sang, B.-I. *In situ* biphasic extractive fermentation for hexanoic acid production from sucrose by *Megasphaera elsdenii*

NCIMB 702410. *Appl. Biochem. Biotechnol.* ***2013***, *171*, 1094–1107. https://doi.org/10.1007/s12010-013-0310-3.

(96) Engelmann, U.; Weiss, N. *Megasphaera cerevisiae* sp. nov.: a new Gram-negative obligately anaerobic coccus isolated from spoiled beer. *Syst. Appl. Microbiol.* ***1985***, *6*, 287–290. https://doi.org/10.1016/S0723-2020(85)80033-3.

(97) Chen, W. S.; Ye, Y.; Steinbusch, K. J. J.; Strik, D. P. B. T. B.; Buisman, C. J. N. Methanol as an alternative electron donor in chain elongation for butyrate and caproate formation. *Biomass Bioenergy* ***2016***, *93*, 201–208. https://doi.org/10.1016/j.biombioe.2016.07.008.

(98) Candry, P.; Ganigué, R. Chain elongators, friends, and foes. *Curr. Opin. Biotechnol.* ***2021***, *67*, 99–110. https://doi.org/10.1016/j.copbio.2021.01.005.

(99) Phillips, J. R.; Atiyeh, H. K.; Tanner, R. S.; Torres, J. R.; Saxena, J.; Wilkins, M. R.; Huhnke, R. L. Butanol and hexanol production in *Clostridium carboxidivorans* syngas fermentation: medium development and culture techniques. *Bioresour. Technol.* ***2015***, *190*, 114–121. https://doi.org/10.1016/j.biortech.2015.04.043.

(100) Van Eerten-Jansen, M. C. A. A.; Ter Heijne, A.; Grootscholten, T. I. M.; Steinbusch, K. J. J.; Sleutels, T. H. J. A.; Hamelers, H. V. M.; Buisman, C. J. N. Bioelectrochemical production of caproate and caprylate from acetate by mixed cultures. *ACS Sustain. Chem. Eng.* ***2013***, *1*, 513–518. https://doi.org/10.1021/sc300168z.

(101) Angenent, L. T.; Richter, H.; Buckel, W.; Spirito, C. M.; Steinbusch, K. J. J.; Plugge, C. M.; Strik, D. P. B. T. B.; Grootscholten, T. I. M.; Buisman, C. J. N.; Hamelers, H. V. M. Chain elongation with reactor microbiomes: open-culture biotechnology to produce biochemicals. *Environ. Sci. Technol.* ***2016***, *50*, 2796–2810. https://doi.org/10.1021/acs.est.5b04847.

(102) Steinbusch, K. J. J.; Hamelers, H. V. M.; Plugge, C. M.; Buisman, C. J. N. Biological formation of caproate and caprylate from acetate: fuel and chemical production from low grade biomass. *Energy Env. Sci* ***2011***, *4*, 216–224. https://doi.org/10.1039/C0EE00282H.

(103) Agler, M. T.; Spirito, C. M.; Usack, J. G.; Werner, J. J.; Angenent, L. T. Chain elongation with reactor microbiomes: upgrading dilute ethanol to medium-chain carboxylates. *Energy Environ. Sci.* ***2012***, *5*, 8189-8192. https://doi.org/10.1039/c2ee22101b.

(104) Zhang, F.; Ding, J.; Zhang, Y.; Chen, M.; Ding, Z.-W.; van Loosdrecht, M. C. M.; Zeng, R. J. Fatty acids production from hydrogen and carbon dioxide by mixed culture in the membrane biofilm reactor. *Water Res.* ***2013***, *47*, 6122–6129. https://doi.org/10.1016/j.watres.2013.07.033.

(105) Roghair, M.; Hoogstad, T.; Strik, D. P. B. T. B.; Plugge, C. M.; Timmers, P. H. A.; Weusthuis, R. A.; Bruins, M. E.; Buisman, C. J. N. Controlling ethanol use in chain elongation by CO_2 loading rate. *Environ. Sci. Technol.* ***2018***, *52*, 1496–1505. https://doi.org/10.1021/acs.est.7b04904.

(106) Bourgade, B.; Minton, N. P.; Islam, M. A. Genetic and metabolic engineering challenges of C1-gas fermenting acetogenic chassis organisms. *FEMS Microbiol. Rev.* ***2021***, *45*, fuab008. https://doi.org/10.1093/femsre/fuab008.

(107) Strätz, M.; Sauer, U.; Kuhn, A.; Dürre, P. Plasmid transfer into the homoacetogen *Acetobacterium woodii* by electroporation and conjugation. *Appl. Environ. Microbiol.* ***1994***, *60*, 1033–1037. https://doi.org/10.1128/aem.60.3.1033-1037.1994.

(108) Köpke, M.; Held, C.; Hujer, S.; Liesegang, H.; Wiezer, A.; Wollherr, A.; Ehrenreich, A.; Liebl, W.; Gottschalk, G.; Dürre, P. *Clostridium ljungdahlii* represents a microbial production platform based on syngas. *Proc. Natl. Acad. Sci. USA* ***2010***, *107*, 13087–13092. https://doi.org/10.1073/pnas.1004716107.

(109) Köpke, M.; Liew, F. Recombinant microorganism and methods of production thereof. US 2011/0236941 A1. Washington, DC: U.S. Patent and Trademark Office ***2011***.

(110) Leang, C.; Ueki, T.; Nevin, K. P.; Lovley, D. R. A genetic system for *Clostridium ljungdahlii*: a chassis for autotrophic production of biocommodities and a model homoacetogen. *Appl. Environ. Microbiol.* ***2013***, *79*, 1102–1109. https://doi.org/10.1128/AEM.02891-12.

(111) Kita, A.; Iwasaki, Y.; Sakai, S.; Okuto, S.; Takaoka, K.; Suzuki, T.; Yano, S.; Sawayama, S.; Tajima, T.; Kato, J.; Nishio, N.; Murakami, K.; Nakashimada, Y. Development of genetic transformation and heterologous expression system in carboxydotrophic thermophilic acetogen *Moorella thermoacetica*. *J. Biosci. Bioeng.* ***2013***, *115*, 347–352. https://doi.org/10.1016/j.jbiosc.2012.10.013.

(112) Shin, J.; Kang, S.; Song, Y.; Jin, S.; Lee, J. S.; Lee, J.-K.; Kim, D. R.; Kim, S. C.; Cho, S.; Cho, B.-K. Genome engineering of *Eubacterium limosum* using expanded genetic tools and the CRISPR-Cas9 system. *ACS Synth. Biol.* ***2019***, *8*, 2059–2068. https://doi.org/10.1021/acssynbio.9b00150.

(113) Jeong, J.; Kim, J.-Y.; Park, B.; Choi, I.-G.; Chang, I. S. Genetic engineering system for syngas-utilizing acetogen, *Eubacterium limosum* KIST612. *Bioresour. Technol. Rep.* ***2020***, *11*, 100452. https://doi.org/10.1016/j.biteb.2020.100452.

(114) Mock, J.; Zheng, Y.; Mueller, A. P.; Ly, S.; Tran, L.; Segovia, S.; Nagaraju, S.; Köpke, M.; Dürre, P.; Thauer, R. K. Energy conservation associated with ethanol formation from H_2 and CO_2 in *Clostridium autoethanogenum* involving electron bifurcation. *J. Bacteriol.* ***2015***, *197*, 2965–2980. https://doi.org/10.1128/JB.00399-15.

(115) Cheng, C.; Li, W.; Lin, M.; Yang, S.-T. Metabolic engineering of *Clostridium carboxidivorans* for enhanced ethanol and butanol production from syngas and glucose. *Bioresour. Technol.* ***2019***, *284*, 415–423. https://doi.org/10.1016/j.biortech.2019.03.145.

(116) Basen, M.; Geiger, I.; Henke, L.; Müller, V. A genetic system for the thermophilic acetogenic bacterium *Thermoanaerobacter kivui*. *Appl. Environ. Microbiol.* ***2018***, *84*, e02210-17. https://doi.org/10.1128/AEM.02210-17.

(117) Heap, J. T.; Pennington, O. J.; Cartman, S. T.; Minton, N. P. A modular system for *Clostridium* shuttle plasmids. *J. Microbiol. Methods* ***2009***, *78*, 79–85. https://doi.org/10.1016/j.mimet.2009.05.004.

(118) Hoffmeister, S.; Gerdom, M.; Bengelsdorf, F. R.; Linder, S.; Flüchter, S.; Öztürk, H.; Blümke, W.; May, A.; Fischer, R.-J.; Bahl, H.; Dürre, P. Acetone production with

metabolically engineered strains of *Acetobacterium woodii*. *Metab. Eng.* ***2016***, *36*, 37–47. https://doi.org/10.1016/j.ymben.2016.03.001.

(119) Woolston, B. M.; Emerson, D. F.; Currie, D. H.; Stephanopoulos, G. Rediverting carbon flux in *Clostridium ljungdahlii* using CRISPR interference (CRISPRi). *Metab. Eng.* ***2018***, *48*, 243–253. https://doi.org/10.1016/j.ymben.2018.06.006.

(120) Annan, F. J.; Al-Sinawi, B.; Humphreys, C. M.; Norman, R.; Winzer, K.; Köpke, M.; Simpson, S. D.; Minton, N. P.; Henstra, A. M. Engineering of vitamin prototrophy in *Clostridium ljungdahlii* and *Clostridium autoethanogenum*. *Appl. Microbiol. Biotechnol.* ***2019***, *103*, 4633–4648. https://doi.org/10.1007/s00253-019-09763-6.

(121) Minton, N. P.; Ehsaan, M.; Humphreys, C. M.; Little, G. T.; Baker, J.; Henstra, A. M.; Liew, F.; Kelly, M. L.; Sheng, L.; Schwarz, K.; Zhang, Y. A roadmap for gene system development in *Clostridium*. *Anaerobe* ***2016***, *41*, 104–112. https://doi.org/10.1016/j.anaerobe.2016.05.011.

(122) Huang, H.; Chai, C.; Li, N.; Rowe, P.; Minton, N. P.; Yang, S.; Jiang, W.; Gu, Y. CRISPR/Cas9-based efficient genome editing in *Clostridium ljungdahlii*, an autotrophic gas-fermenting bacterium. *ACS Synth. Biol.* ***2016***, *5*, 1355–1361. https://doi.org/10.1021/acssynbio.6b00044.

(123) Nagaraju, S.; Davies, N. K.; Walker, D. J. F.; Köpke, M.; Simpson, S. D. Genome editing of *Clostridium autoethanogenum* using CRISPR/Cas9. *Biotechnol. Biofuels* ***2016***, *9*, 219. https://doi.org/10.1186/s13068-016-0638-3.

(124) Banerjee, A.; Leang, C.; Ueki, T.; Nevin, K. P.; Lovley, D. R. Lactose-inducible system for metabolic engineering of *Clostridium ljungdahlii*. *Appl. Environ. Microbiol.* ***2014***, *80*, 2410–2416. https://doi.org/10.1128/AEM.03666-13.

(125) Schobert, H. H.; Song, C. Chemicals and materials from coal in the 21st century. *Fuel* ***2002***, *81*, 15–32. https://doi.org/10.1016/S0016-2361(00)00203-9.

(126) Schmidt, R. J. Industrial catalytic processes—phenol production. *Appl. Catal. Gen.* ***2005***, *280*, 89–103. https://doi.org/10.1016/j.apcata.2004.08.030.

(127) Bengelsdorf, F. R.; Poehlein, A.; Linder, S.; Erz, C.; Hummel, T.; Hoffmeister, S.; Daniel, R.; Dürre, P. Industrial acetogenic biocatalysts: a comparative metabolic and genomic analysis. *Front. Microbiol.* ***2016***, *7*, 1036. https://doi.org/10.3389/fmicb.2016.01036.

(128) Jones, S. W.; Fast, A. G.; Carlson, E. D.; Wiedel, C. A.; Au, J.; Antoniewicz, M. R.; Papoutsakis, E. T.; Tracy, B. P. CO_2 fixation by anaerobic non-photosynthetic mixotrophy for improved carbon conversion. *Nat. Commun.* ***2016***, *7*, 12800. https://doi.org/10.1038/ncomms12800.

(129) Diner, B. A.; Fan, J.; Scotcher, M. C.; Wells, D. H.; Whited, G. M. Synthesis of heterologous mevalonic acid pathway enzymes in *Clostridium ljungdahlii* for the conversion of fructose and of syngas to mevalonate and isoprene. *Appl. Environ. Microbiol.* ***2018***, *84*, e01723-17. https://doi.org/10.1128/AEM.01723-17.

(130) Weitz, S.; Hermann, M.; Linder, S.; Bengelsdorf, F. R.; Takors, R.; Dürre, P. Isobutanol production by autotrophic acetogenic bacteria. *Front. Bioeng. Biotechnol.* ***2021***, 9, 657253. https://doi.org/10.3389/fbioe.2021.657253.

(131) Shimomura, O.; Johnson, F. H.; Saiga, Y. Extraction, purification and properties of aequorin, a bioluminescent protein from the luminous hydromedusan, *Aequorea*. *J. Cell. Comp. Physiol.* ***1962***, *59*, 223–239. https://doi.org/10.1002/jcp.1030590302.

(132) Chalfie, M.; Tu, Y.; Euskirchen, G.; Ward, W. W.; Prasher, D. C. Green fluorescent protein as a marker for gene expression. *Science* ***1994***, *263*, 802–805. https://doi.org/10.1126/science.8303295.

(133) Chudakov, D. M.; Lukyanov, S.; Lukyanov, K. A. Fluorescent proteins as a toolkit for *in vivo* imaging. *Trends Biotechnol.* ***2005***, *23*, 605–613. https://doi.org/10.1016/j.tibtech.2005.10.005.

(134) Southward, C. M.; Surette, M. G. The dynamic microbe: green fluorescent protein brings bacteria to light: monitoring microbial dynamics with GFP. *Mol. Microbiol.* ***2002***, *45*, 1191–1196. https://doi.org/10.1046/j.1365-2958.2002.03089.x.

(135) Bloemberg, G. V.; O'Toole, G. A.; Lugtenberg, B. J.; Kolter, R. Green fluorescent protein as a marker for *Pseudomonas* spp. *Appl. Environ. Microbiol.* ***1997***, *63*, 4543–4551. https://doi.org/10.1128/aem.63.11.4543-4551.1997.

(136) Pande, S.; Shitut, S.; Freund, L.; Westermann, M.; Bertels, F.; Colesie, C.; Bischofs, I. B.; Kost, C. Metabolic cross-feeding via intercellular nanotubes among bacteria. *Nat. Commun.* ***2015***, *6*, 6238. https://doi.org/10.1038/ncomms7238.

(137) Benomar, S.; Ranava, D.; Cárdenas, M. L.; Trably, E.; Rafrafi, Y.; Ducret, A.; Hamelin, J.; Lojou, E.; Steyer, J.-P.; Giudici-Orticoni, M.-T. Nutritional stress induces exchange of cell material and energetic coupling between bacterial species. *Nat. Commun.* ***2015***, *6*, 6283. https://doi.org/10.1038/ncomms7283.

(138) Li, C.; Tebo, A.; Gautier, A. Fluorogenic labeling strategies for biological imaging. *Int. J. Mol. Sci.* ***2017***, *18*, 1473. https://doi.org/10.3390/ijms18071473.

(139) Magliery, T. J.; Wilson, C. G. M.; Pan, W.; Mishler, D.; Ghosh, I.; Hamilton, A. D.; Regan, L. Detecting protein−protein interactions with a green fluorescent protein fragment reassembly trap: scope and mechanism. *J. Am. Chem. Soc.* ***2005***, *127*, 146–157. https://doi.org/10.1021/ja046699g.

(140) Ciruela, F. Fluorescence-based methods in the study of protein–protein interactions in living cells. *Curr. Opin. Biotechnol.* ***2008***, *19*, 338–343. https://doi.org/10.1016/j.copbio.2008.06.003.

(141) Day, R. N.; Davidson, M. W. The fluorescent protein palette: tools for cellular imaging. *Chem. Soc. Rev.* ***2009***, *38*, 2887. https://doi.org/10.1039/b901966a.

(142) Shaner, N. C.; Campbell, R. E.; Steinbach, P. A.; Giepmans, B. N. G.; Palmer, A. E.; Tsien, R. Y. Improved monomeric red, orange and yellow fluorescent proteins derived from *Discosoma* sp. red fluorescent protein. *Nat. Biotechnol.* ***2004***, *22*, 1567–1572. https://doi.org/10.1038/nbt1037.

(143) Zhang, C.; Xing, X.-H.; Lou, K. Rapid detection of a gfp-marked *Enterobacter aerogenes* under anaerobic conditions by aerobic fluorescence recovery. *FEMS Microbiol. Lett.* ***2005***, *249*, 211–218. https://doi.org/10.1016/j.femsle.2005.05.051.

(144) Tracy, B. P.; Gaida, S. M.; Papoutsakis, E. T. Flow cytometry for bacteria: enabling metabolic engineering, synthetic biology and the elucidation of complex phenotypes. *Curr. Opin. Biotechnol.* ***2010***, *21*, 85–99. https://doi.org/10.1016/j.copbio.2010.02.006.

(145) Hartman, A. H.; Liu, H.; Melville, S. B. Construction and characterization of a lactose-inducible promoter system for controlled gene expression in *Clostridium perfringens*. *Appl. Environ. Microbiol.* ***2011***, *77*, 471–478. https://doi.org/10.1128/AEM.01536-10.

(146) Ransom, E. M.; Williams, K. B.; Weiss, D. S.; Ellermeier, C. D. Identification and characterization of a gene cluster required for proper rod shape, cell division, and pathogenesis in *Clostridium difficile*. *J. Bacteriol.* ***2014***, *196*, 2290–2300. https://doi.org/10.1128/JB.00038-14.

(147) Ransom, E. M.; Ellermeier, C. D.; Weiss, D. S. Use of mCherry red fluorescent protein for studies of protein localization and gene expression in *Clostridium difficile*. *Appl. Environ. Microbiol.* ***2015***, *81*, 1652–1660. https://doi.org/10.1128/AEM.03446-14.

(148) Drepper, T.; Eggert, T.; Circolone, F.; Heck, A.; Krauß, U.; Guterl, J.-K.; Wendorff, M.; Losi, A.; Gärtner, W.; Jaeger, K.-E. Reporter proteins for *in vivo* fluorescence without oxygen. *Nat. Biotechnol.* ***2007***, *25*, 443–445. https://doi.org/10.1038/nbt1293.

(149) Chapman, S.; Faulkner, C.; Kaiserli, E.; Garcia-Mata, C.; Savenkov, E. I.; Roberts, A. G.; Oparka, K. J.; Christie, J. M. The photoreversible fluorescent protein iLOV outperforms GFP as a reporter of plant virus infection. *Proc. Natl. Acad. Sci. USA* ***2008***, *105*, 20038–20043. https://doi.org/10.1073/pnas.0807551105.

(150) Christie, J. M.; Hitomi, K.; Arvai, A. S.; Hartfield, K. A.; Mettlen, M.; Pratt, A. J.; Tainer, J. A.; Getzoff, E. D. Structural tuning of the fluorescent protein iLOV for improved photostability. *J. Biol. Chem.* ***2012***, *287*, 22295–22304. https://doi.org/10.1074/jbc.M111.318881.

(151) Mukherjee, A.; Weyant, K. B.; Agrawal, U.; Walker, J.; Cann, I. K. O.; Schroeder, C. M. Engineering and characterization of new LOV-based fluorescent proteins from *Chlamydomonas reinhardtii* and *Vaucheria frigida*. *ACS Synth. Biol.* ***2015***, *4*, 371–377. https://doi.org/10.1021/sb500237x.

(152) Buckley, A. M.; Petersen, J.; Roe, A. J.; Douce, G. R.; Christie, J. M. LOV-Based reporters for fluorescence imaging. *Curr. Opin. Chem. Biol.* ***2015***, *27*, 39–45. https://doi.org/10.1016/j.cbpa.2015.05.011.

(153) Li, Y.; Xu, T.; Tschaplinski, T. J.; Engle, N. L.; Yang, Y.; Graham, D. E.; He, Z.; Zhou, J. Improvement of cellulose catabolism in *Clostridium cellulolyticum* by sporulation abolishment and carbon alleviation. *Biotechnol. Biofuels* ***2014***, *7*, 25. https://doi.org/10.1186/1754-6834-7-25.

(154) Teng, L.; Wang, K.; Xu, J.; Xu, C. Flavin mononucleotide (FMN)-based fluorescent protein (FbFP) as reporter for promoter screening in *Clostridium cellulolyticum*. *J. Microbiol. Methods* ***2015***, *119*, 37–43. https://doi.org/10.1016/j.mimet.2015.09.018.

(155) Cheng, C.; Lin, M.; Jiang, W.; Zhao, J.; Li, W.; Yang, S.-T. Development of an *in vivo* fluorescence based gene expression reporter system for *Clostridium tyrobutyricum*. *J. Biotechnol.* ***2019***, *305*, 18–22. https://doi.org/10.1016/j.jbiotec.2019.08.019.

(156) Seo, S.-O.; Lu, T.; Jin, Y.-S.; Blaschek, H. P. Development of an oxygen-independent flavin mononucleotide-based fluorescent reporter system in *Clostridium beijerinckii* and its potential applications. *J. Biotechnol.* ***2018***, *265*, 119–126. https://doi.org/10.1016/j.jbiotec.2017.11.003.

(157) Bruder, M. R.; Pyne, M. E.; Moo-Young, M.; Chung, D. A.; Chou, C. P. Extending CRISPR-Cas9 technology from genome editing to transcriptional engineering in the genus *Clostridium*. *Appl. Environ. Microbiol.* ***2016***, *82*, 6109–6119. https://doi.org/10.1128/AEM.02128-16.

(158) Molitor, B.; Kirchner, K.; Henrich, A. W.; Schmitz, S.; Rosenbaum, M. A. Expanding the molecular toolkit for the homoacetogen *Clostridium ljungdahlii*. *Sci. Rep.* ***2016***, *6*, 31518. https://doi.org/10.1038/srep31518.

(159) Buckley, A. M.; Jukes, C.; Candlish, D.; Irvine, J. J.; Spencer, J.; Fagan, R. P.; Roe, A. J.; Christie, J. M.; Fairweather, N. F.; Douce, G. R. Lighting up *Clostridium difficile*: reporting gene expression using fluorescent Lov domains. *Sci. Rep.* ***2016***, *6*, 23463. https://doi.org/10.1038/srep23463.

(160) Mordaka, P. M.; Heap, J. T. Stringency of synthetic promoter sequences in *Clostridium* revealed and circumvented by tuning promoter library mutation rates. *ACS Synth. Biol.* ***2018***, *7*, 672–681. https://doi.org/10.1021/acssynbio.7b00398.

(161) Surre, J.; Saint-Ruf, C.; Collin, V.; Orenga, S.; Ramjeet, M.; Matic, I. Strong increase in the autofluorescence of cells signals struggle for survival. *Sci. Rep.* ***2018***, *8*, 12088. https://doi.org/10.1038/s41598-018-30623-2.

(162) Gyulev, I. S.; Willson, B. J.; Hennessy, R. C.; Krabben, P.; Jenkinson, E. R.; Thomas, G. H. Part by part: synthetic biology parts used in solventogenic clostridia. *ACS Synth. Biol.* ***2018***, *7*, 311–327. https://doi.org/10.1021/acssynbio.7b00327.

(163) Los, G. V.; Encell, L. P.; McDougall, M. G.; Hartzell, D. D.; Karassina, N.; Zimprich, C.; Wood, M. G.; Learish, R.; Ohana, R. F.; Urh, M.; Simpson, D.; Mendez, J.; Zimmerman, K.; Otto, P.; Vidugiris, G.; Zhu, J.; Darzins, A.; Klaubert, D. H.; Bulleit, R. F.; Wood, K. V. HaloTag: a novel protein labeling technology for cell imaging and protein analysis. *ACS Chem. Biol.* ***2008***, *3*, 373–382. https://doi.org/10.1021/cb800025k.

(164) Keppler, A.; Gendreizig, S.; Gronemeyer, T.; Pick, H.; Vogel, H.; Johnsson, K. A General Method for the covalent labeling of fusion proteins with small molecules *in vivo*. *Nat. Biotechnol.* ***2003***, *21*, 86–89. https://doi.org/10.1038/nbt765.

(165) Gautier, A.; Juillerat, A.; Heinis, C.; Corrêa, I. R.; Kindermann, M.; Beaufils, F.; Johnsson, K. An engineered protein tag for multiprotein labeling in living cells. *Chem. Biol.* ***2008***, *15*, 128–136. https://doi.org/10.1016/j.chembiol.2008.01.007.

(166) Cassona, C. P.; Pereira, F.; Serrano, M.; Henriques, A. O. A fluorescent reporter for single cell analysis of gene expression in *Clostridium difficile*. In *Clostridium difficile. Methods in Molecular Biology*; Springer, ***2016***; Vol. 1476, pp 69–90. https://doi.org/10.1007/978-1-4939-6361-4_6.

(167) Pereira, F. C.; Saujet, L.; Tomé, A. R.; Serrano, M.; Monot, M.; Couture-Tosi, E.; Martin-Verstraete, I.; Dupuy, B.; Henriques, A. O. The spore differentiation pathway in the

enteric pathogen *Clostridium difficile*. *PLoS Genet.* ***2013***, *9*, e1003782. https://doi.org/10.1371/journal.pgen.1003782.

(168) Serrano, M.; Crawshaw, A. D.; Dembek, M.; Monteiro, J. M.; Pereira, F. C.; Pinho, M. G.; Fairweather, N. F.; Salgado, P. S.; Henriques, A. O. The SpoIIQ-SpoIIIAH complex of *Clostridium difficile* controls forespore engulfment and late stages of gene expression and spore morphogenesis. *Mol. Microbiol.* ***2016***, *100*, 204–228. https://doi.org/10.1111/mmi.13311.

(169) Charubin, K.; Streett, H.; Papoutsakis, E. T. Development of strong anaerobic fluorescent reporters for *Clostridium acetobutylicum* and *Clostridium ljungdahlii* using HaloTag and SNAP-tag proteins. *Appl. Environ. Microbiol.* ***2020***, *86*, e01271-20. https://doi.org/10.1128/AEM.01271-20.

(170) Streett, H.; Charubin, K.; Papoutsakis, E. T. Anaerobic fluorescent reporters for cell identification, microbial cell biology and high-throughput screening of microbiota and genomic libraries. *Curr. Opin. Biotechnol.* ***2021***, *71*, 151–163. https://doi.org/10.1016/j.copbio.2021.07.005.

(171) Hinner, M. J.; Johnsson, K. How to obtain labeled proteins and what to do with them. *Curr. Opin. Biotechnol.* ***2010***, *21*, 766–776. https://doi.org/10.1016/j.copbio.2010.09.011.

(172) Chia, H. E.; Zuo, T.; Koropatkin, N. M.; Marsh, E. N. G.; Biteen, J. S. Imaging living obligate anaerobic bacteria with bilin-binding fluorescent proteins. *Curr. Res. Microb. Sci.* ***2020***, *1*, 1–6. https://doi.org/10.1016/j.crmicr.2020.04.001.

(173) Chia, H. E.; Koebke, K. J.; Rangarajan, A. A.; Koropatkin, N. M.; Marsh, E. N. G.; Biteen, J. S. New orange ligand-dependent fluorescent reporter for anaerobic imaging. *ACS Chem. Biol.* ***2021***, *16*, 2109-2115. https://doi.org/10.1021/acschembio.1c00391.

(174) Plamont, M.-A.; Billon-Denis, E.; Maurin, S.; Gauron, C.; Pimenta, F. M.; Specht, C. G.; Shi, J.; Quérard, J.; Pan, B.; Rossignol, J.; Moncoq, K.; Morellet, N.; Volovitch, M.; Lescop, E.; Chen, Y.; Triller, A.; Vriz, S.; Le Saux, T.; Jullien, L.; Gautier, A. Small fluorescence-activating and absorption-shifting tag for tunable protein imaging *in vivo*. *Proc. Natl. Acad. Sci. USA* ***2016***, *113*, 497–502. https://doi.org/10.1073/pnas.1513094113.

(175) Li, C.; Plamont, M.-A.; Sladitschek, H. L.; Rodrigues, V.; Aujard, I.; Neveu, P.; Le Saux, T.; Jullien, L.; Gautier, A. Dynamic multicolor protein labeling in living cells. *Chem. Sci.* ***2017***, *8*, 5598–5605. https://doi.org/10.1039/C7SC01364G.

(176) Benaissa, H.; Ounoughi, K.; Aujard, I.; Fischer, E.; Goïame, R.; Nguyen, J.; Tebo, A. G.; Li, C.; Le Saux, T.; Bertolin, G.; Tramier, M.; Danglot, L.; Pietrancosta, N.; Morin, X.; Jullien, L.; Gautier, A. Engineering of a fluorescent chemogenetic reporter with tunable color for advanced live-cell imaging. *Nat. Commun.* ***2021***, *12*, 6989. https://doi.org/10.1038/s41467-021-27334-0.

(177) Li, C.; Mourton, A.; Plamont, M.-A.; Rodrigues, V.; Aujard, I.; Volovitch, M.; Le Saux, T.; Perez, F.; Vriz, S.; Jullien, L.; Joliot, A.; Gautier, A. Fluorogenic probing of membrane protein trafficking. *Bioconjug. Chem.* ***2018***, *29*, 1823–1828. https://doi.org/10.1021/acs.bioconjchem.8b00180.

(178) Chekli, Y.; Peron-Cane, C.; Dell'Arciprete, D.; Allemand, J.-F.; Li, C.; Ghigo, J.-M.; Gautier, A.; Lebreton, A.; Desprat, N.; Beloin, C. Visualizing the dynamics of exported bacterial proteins with the chemogenetic fluorescent reporter FAST. *Sci. Rep.* ***2020***, *10*, 15791. https://doi.org/10.1038/s41598-020-72498-2.

(179) Tebo, A. G.; Pimenta, F. M.; Zhang, Y.; Gautier, A. Improved chemical-genetic fluorescent markers for live cell microscopy. *Biochemistry* ***2018***, *57*, 5648–5653. https://doi.org/10.1021/acs.biochem.8b00649.

(180) Tebo, A. G.; Gautier, A. A split fluorescent reporter with rapid and reversible complementation. *Nat. Commun.* ***2019***, *10*, 2822. https://doi.org/10.1038/s41467-019-10855-0.

(181) Tebo, A. G.; Moeyaert, B.; Thauvin, M.; Carlon-Andres, I.; Böken, D.; Volovitch, M.; Padilla-Parra, S.; Dedecker, P.; Vriz, S.; Gautier, A. Orthogonal fluorescent chemogenetic reporters for multicolor imaging. *Nat. Chem. Biol.* ***2021***, *17*, 30–38. https://doi.org/10.1038/s41589-020-0611-0.

(182) Streett, H. E.; Kalis, K. M.; Papoutsakis, E. T. A strongly fluorescing anaerobic reporter and protein-tagging system for *Clostridium* organisms based on the fluorescence-activating and absorption-shifting tag protein (FAST). *Appl. Environ. Microbiol.* ***2019***, *85*, e00622-19. https://doi.org/10.1128/AEM.00622-19.

(183) Charubin, K.; Modla, S.; Caplan, J. L.; Papoutsakis, E. T. Interspecies microbial fusion and large-scale exchange of cytoplasmic proteins and RNA in a syntrophic *Clostridium* coculture. *mBio* ***2020***, *11*, *e02030-20*. https://doi.org/10.1128/mBio.02030-20.

5. Abbreviations

A.: *Acetobacterium*

ABE: acetone-butanol-ethanol

AcK: acetate kinase

Adc: acetoacetate decarboxylase

AdhE: bifunctional aldehyde/alcohol dehydrogenase

ADI: arginine deiminase

ADP: adenosine diphosphate

Aor: aldehyde:ferredoxin oxidoreductase

APO: acetone production operon

ArcD: arginine:ornithin antiporter

ATP: adenosine triphosphate

B.: *Butyribacterium*

BASF: Badische Anilin- & Sodafabrik

BBFP: Bilin-binding fluorescent protein

Bcd: butyryl-CoA dehydrogenase

bcs: butyryl-CoA synthesis

Buk: butyrate kinase

C.: *Clostridium*

Cb.: *Caproicibacter*

CFP: cyan fluorescent protein

CK: carbamate kinase

CO: carbon monoxide

CO_2: carbon dioxide

CoA: coenzyme A

CODH/ACS: CO dehydrogenase/acetyl-CoA synthase

CoFeSP: corrinoid iron-sulfur protein

Cp.: *Caproicidiproducens*

CRISPR: clustered regularly interspaced short palindromic repeats

CRISPRi: CRISPR interference

Crt: crotonase

CtfA/B: acetoacetyl-CoA:acetate/butyrate-CoA transferase

DMA: dimethyl acetal

DNA: desoxyribonucleic acid

DSMZ: German Collection of Microorganisms and Cell Cultures GmbH

E.: *Eubacterium*

e.g.: *exempli gratia* (for example)

Ech: energy-converting hydrogenase

Etf: electron transfer flavoproteins

Fak: fatty acid kinase

FAST: fluorescence-activating and absorption-shifting tag

FbFP: flavin mononucleotide-based fluorescent protein

Fd/Fd^{2-}: ferredoxin

feg: FAST encoding gene

FMN: flavin mononucleotide

FP: fluorescent protein

GFP: green fluorescent protein

H_2: hydrogen

Hbd: 3-hydroxybutyryl-CoA dehydrogenase

HBR: 4-hydroxybenzylidene-rhodanine

HBR-3,5DM: 4-hydroxy-3,5-dimethylbenzylidene-rhodanine

HBR-3,5DOM: 4-hydroxy-3,5-dimethoxybenzylidene-rhodanine

hcs: hexanoyl-CoA synthesis

HMBR: 4-hydroxy-3-methylbenzylidene-rhodanine

ICI: Imperial Chemical Industries

JCM: Japan Collection of Microorganisms

LOV: light oxygen voltage

M.: *Morella*

MtaABC: methanol:THF-methyltransferase system

NAD^+: nicotinamide adenine dinucleotide (oxidized)

NADH: nicotinamide adenine dinucleotide (reduced)

$NADP^+$: nicotinamide adenine dinucleotide phosphate (oxidized)

NADPH: nicotinamide adenine dinucleotide phosphate (reduced)

NCBI: National Center for Biotechnology Information

OTC: ornithine transcarbamoylase

PAGE: polyacrylamide gel electrophoresis

pFAST: promiscuous FAST

PilB: type IV pilus-associated ATPase

Pta: phosphotransacetylase

Ptb: phosphotransbutyrylase

Ptf: phosphotransferase

Rnf: *Rhodobacter* nitrogen fixation

rRNA: ribosomal ribonucleic acid

SDS: sodium dodecyl sulfate

sp.: *species*

spp.: *species pluralis*

syngas: synthesis gas

^{T}: type strain

T.: *Thermoanaerobacter*

THF: tetrahydrofolate

Thl: thiolase

WLP: Wood-Ljungdahl pathway

YFP: yellow fluorescent protein

6. Publications

6.1 Chronological list of publications

Flaiz, M.; Baur, T.; Brahner, S.; Poehlein, A.; Daniel, R.; Bengelsdorf, F. R. *Caproicibacter fermentans* gen. nov., sp. nov., a new caproate-producing bacterium and emended description of the genus *Caproiciproducens*. *Int. J. Syst. Evol. Microbiol.* ***2020***, *70*, 4269–4279.

Beck, M. H.; **Flaiz, M.;** Bengelsdorf, F. R.; Dürre, P. Induced heterologous expression of the arginine deiminase pathway promotes growth advantages in the strict anaerobe *Acetobacterium woodii*. *Appl. Microbiol. Biotechnol.* ***2020***, *104*, 687–699.

Flaiz, M.; Ludwig, G.; Bengelsdorf, F. R.; Dürre, P. Production of the biocommodities butanol and acetone from methanol with fluorescent FAST-tagged proteins using metabolically engineered strains of *Eubacterium limosum*. *Biotechnol. Biofuels* ***2021***, *14*, 117.

Flaiz, M.; Baur, T.; Gaibler, J.; Kröly, C.; Dürre, P. Establishment of green- and red-fluorescent reporter proteins based on the fluorescence-activating and absorption-shifting tag for the use in acetogenic and solventogenic anaerobes. *ACS Synth. Biol.* ***2022****, 11,* 953-967.

6.2 Personal contribution to the scientific publications

My contribution to the publication "*Caproicibacter fermentans* gen. nov., sp. nov., a new caproate-producing bacterium and emended description of the genus *Caproiciproducens*" includes isolation and phylogenetic characterization of *Caproicibacter fermentans*. Moreover, I determined growth characteristics, analyzed the cellular fatty acid composition, and deposited *Cb. fermentans* at the Leibniz Institute DSMZ - German Collection of Microorganisms and Cell Cultures GmbH (DSMZ, Braunschweig, Germany) and the Japan Collection of Microorganisms (JCM, Tsukuba, Japan). I prepared most of the manuscript and participated in revising the manuscript during revision process.

My contribution to the publication "Induced heterologous expression of the arginine deiminase pathway promotes growth advantages in the strict anaerobe *Acetobacterium woodii*" includes construction and performance of autotrophic growth experiments of recombinant *A. woodii* strains expressing the arginine deiminase pathway genes.

My contribution to the publication "Production of the biocommodities butanol and acetone from methanol with fluorescent FAST-tagged proteins using metabolically engineered strains of *Eubacterium limosum*" includes the performance of all presented experiments (except for

construction and analyzation of butanol-producing *Eubacterium limosum* strains, performed by Gideon Ludwig). In addition, I evaluated all recorded data, created all tables and figures, prepared, and submitted the manuscript. I revised the manuscript during revision process.

My contribution to the submitted manuscript “Establishment of green- and red-fluorescent reporter proteins based on the fluorescence-activating and absorption-shifting tag for the use in acetogenic and solventogenic anaerobes” includes the conduction of growth experiments and fluorescence determination using flow cytometry. Strains were constructed in cooperation with Tina Baur and Jana Gaibler. In addition, I evaluated all recorded data, created all tables and figures, prepared, and submitted the manuscript. I revised the manuscript during revision process.

6.3 Scientific contributions on conferences

Poster contributions

Flaiz, M.; Beck, M. H.; Bengelsdorf, F.R.; Dürre, P. Arginine deiminase pathway in *Acetobacterium woodii*. ***2018***. Clostridium XV. Munich, Freising, Germany.

Flaiz, M.; Bengelsdorf, F.R.; Dürre, P. Heterologous expression of genes for 1,4-butanediol production with the acetogen *Eubacterium limosum*. ***2019***. C1-net. Nottingham, United Kingdom.

Flaiz, M.; Bengelsdorf, F.R.; Dürre, P. Heterologous production of 1,4-butanediol using the acetogen *Eubacterium limosum*. ***2019***. VAAM. Mainz, Germany.

Flaiz, M.; Gaibler J.; Ludwig, G.; Bengelsdorf, F.R.; Dürre, P. Observation of fluorescent FAST-tagged protein production during growth of the strictly anaerobic acetogen *Eubacterium limosum*. ***2020***. CC-net. Nottingham, United Kingdom.

Oral presentations

Flaiz, M.; Beck, M. H.; Bengelsdorf, F.R.; Dürre, P. Arginine deiminase pathway in *Acetobacterium woodii*. ***2018***. VAAM. Wolfsburg, Germany.

Flaiz, M.; Gaibler, J.; Bengelsdorf, F.R.; Dürre, P. Observation of fluorescent FAST-tagged protein production during growth of the strict anaerobic acetogen *Eubacterium limosum*. ***2020***. VAAM. Leipzig, Germany.

Flaiz, M.; Bengelsdorf, F.R.; Dürre, P. Light up acetogens: acetone production with fluorescent *Eubacterium limosum* strains cultivated using the C1-carbon source methanol. ***2021.*** CC-net. Nottingham, United Kingdom.

7. Appendix

7.1 Acknowledgements

[Acknowledgements have been removed for privacy reasons]

7.2 Curriculum vitae

[Curriculum vitae has been removed for privacy reasons]

7.3 Declaration of independent scientific work

I hereby declare that the present thesis is the result of my own work. All sources of literature used for the achievement of this thesis have been mentioned in the text and the list of literature. In addition, I assure that the present work has not been submitted in full or in part elsewhere with the aim of obtaining an academic degree. All existing copies of the present thesis are identical regarding their form and content.

Ulm, January 2022

Maximilian Flaiz